Charged particle optics :

Principles and applications

Florent Houdellier
CEMES-CNRS, 29 rue Jeanne Marvig 31055 Toulouse
et DGP-INSA,135 avenue de Rangueil 31400 Toulouse

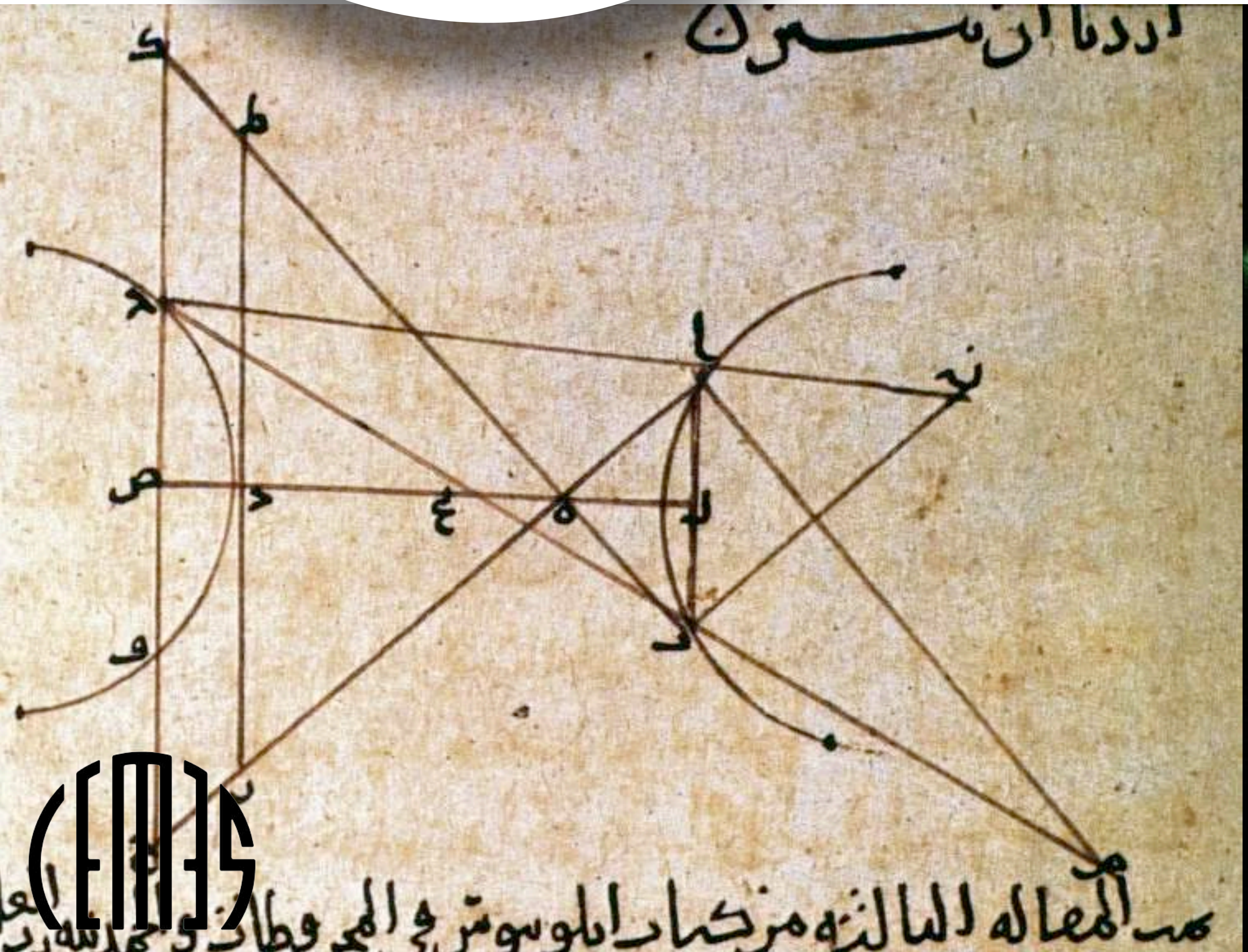

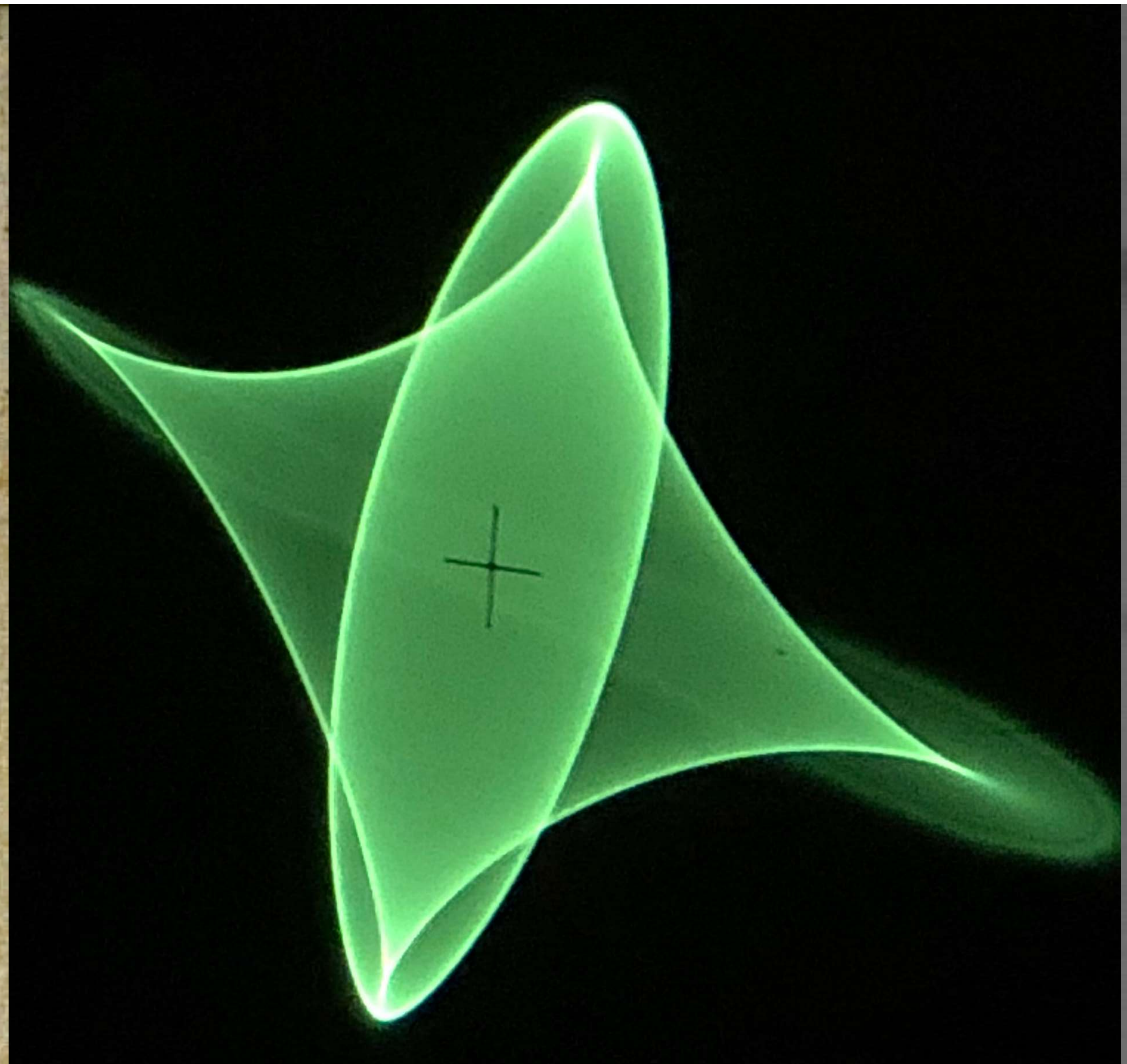

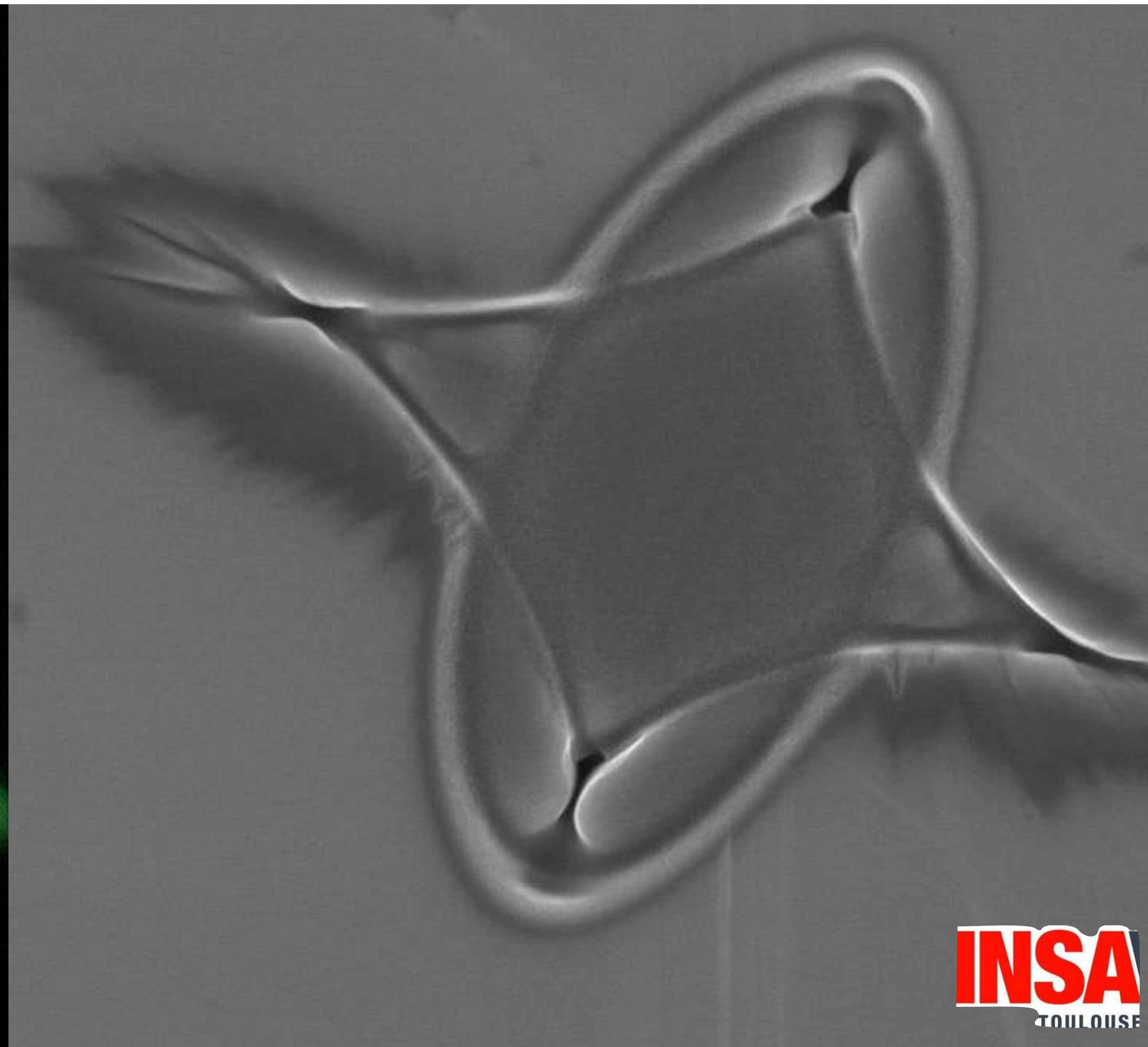

What is geometrical optics ? What is an image ?

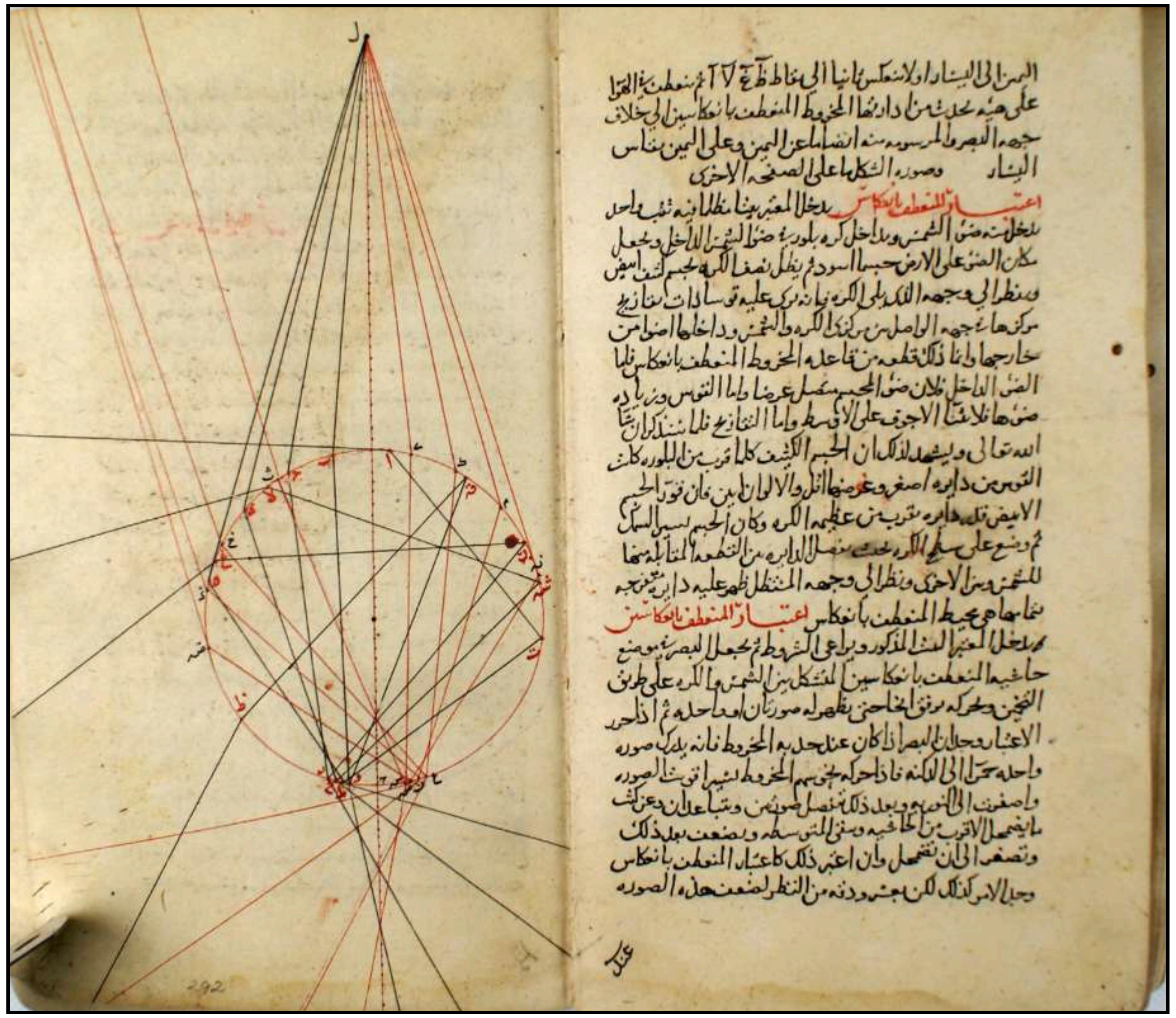

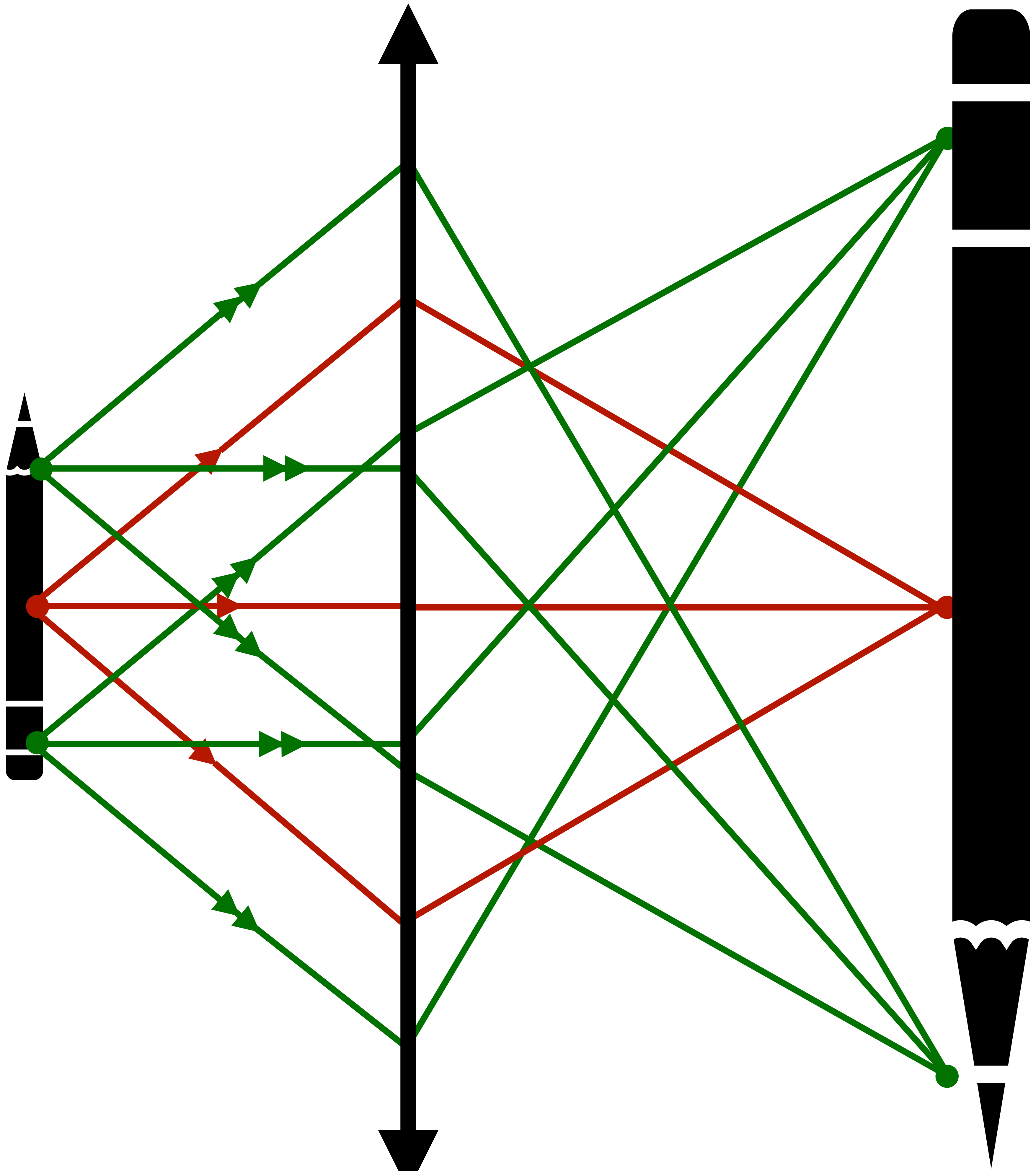

Fermat and the principle of least time : a « causa sive ratio » for the refraction

- **Pierre de Fermat (1601-m. 1665)**
  « Synthèse pour les réfractions » (1662)

*« Je reconnais premièrement avec vous la vérité de ce principe, <u>**que la nature agit toujours par les voies les plus courtes**</u>. Vous en déduisez très bien l'égalité des angles de réflexion et d'incidence »*

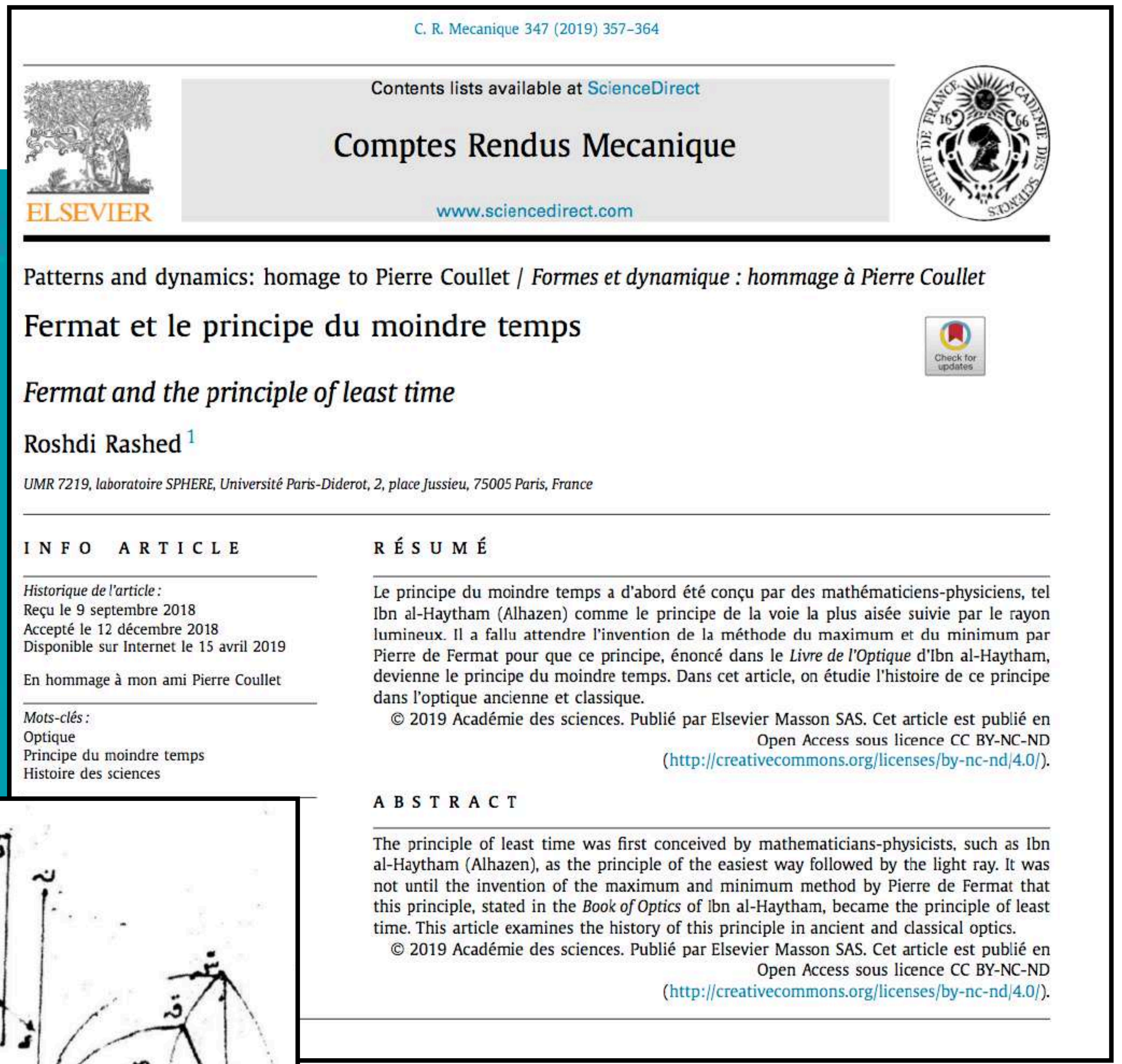
C. R. Mecanique 347 (2019) 357–364

Contents lists available at ScienceDirect

Comptes Rendus Mecanique

www.sciencedirect.com

Patterns and dynamics: homage to Pierre Coullet / *Formes et dynamique : hommage à Pierre Coullet*

Fermat et le principe du moindre temps

Fermat and the principle of least time

Roshdi Rashed[1]

UMR 7219, laboratoire SPHERE, Université Paris-Diderot, 2, place Jussieu, 75005 Paris, France

INFO ARTICLE

Historique de l'article :
Reçu le 9 septembre 2018
Accepté le 12 décembre 2018
Disponible sur Internet le 15 avril 2019

En hommage à mon ami Pierre Coullet

Mots-clés :
Optique
Principe du moindre temps
Histoire des sciences

RÉSUMÉ

Le principe du moindre temps a d'abord été conçu par des mathématiciens-physiciens, tel Ibn al-Haytham (Alhazen) comme le principe de la voie la plus aisée suivie par le rayon lumineux. Il a fallu attendre l'invention de la méthode du maximum et du minimum par Pierre de Fermat pour que ce principe, énoncé dans le *Livre de l'Optique* d'Ibn al-Haytham, devienne le principe du moindre temps. Dans cet article, on étudie l'histoire de ce principe dans l'optique ancienne et classique.
© 2019 Académie des sciences. Publié par Elsevier Masson SAS. Cet article est publié en Open Access sous licence CC BY-NC-ND (http://creativecommons.org/licenses/by-nc-nd/4.0/).

ABSTRACT

The principle of least time was first conceived by mathematicians-physicists, such as Ibn al-Haytham (Alhazen), as the principle of the easiest way followed by the light ray. It was not until the invention of the maximum and minimum method by Pierre de Fermat that this principle, stated in the *Book of Optics* of Ibn al-Haytham, became the principle of least time. This article examines the history of this principle in ancient and classical optics.
© 2019 Académie des sciences. Publié par Elsevier Masson SAS. Cet article est publié en Open Access sous licence CC BY-NC-ND (http://creativecommons.org/licenses/by-nc-nd/4.0/).

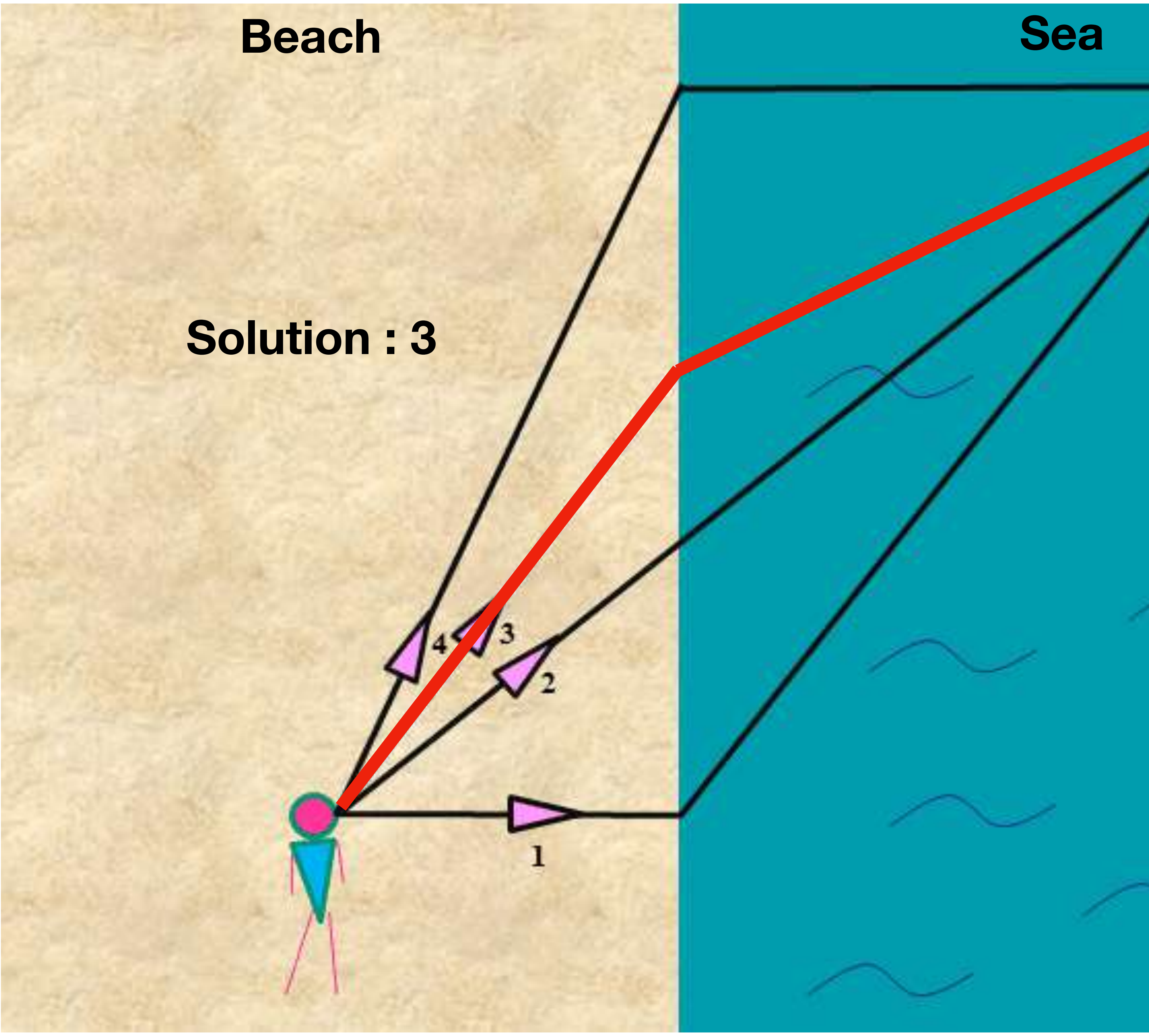

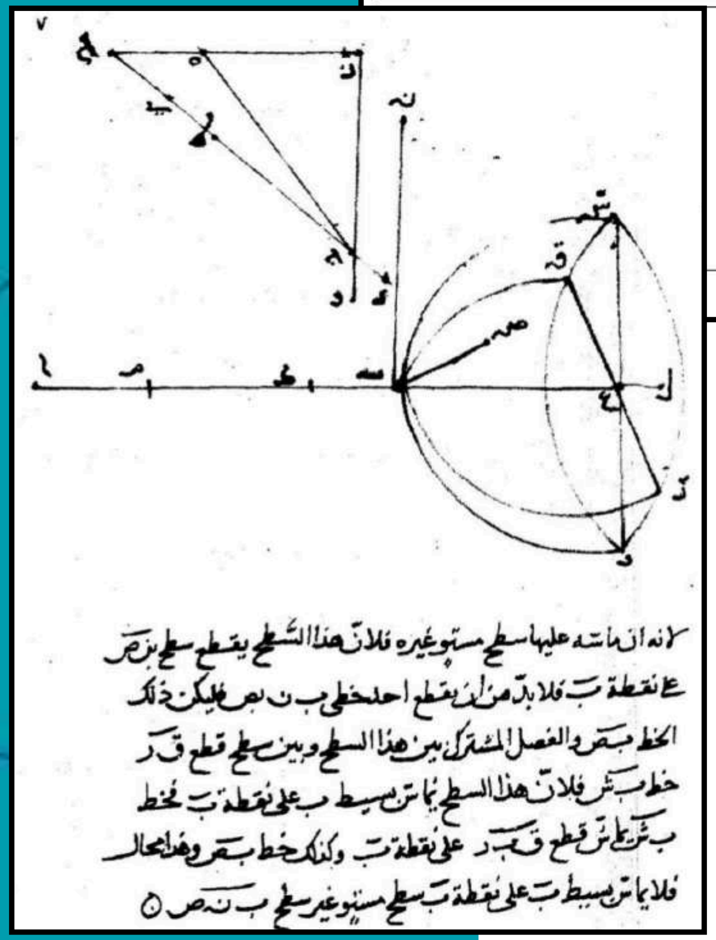

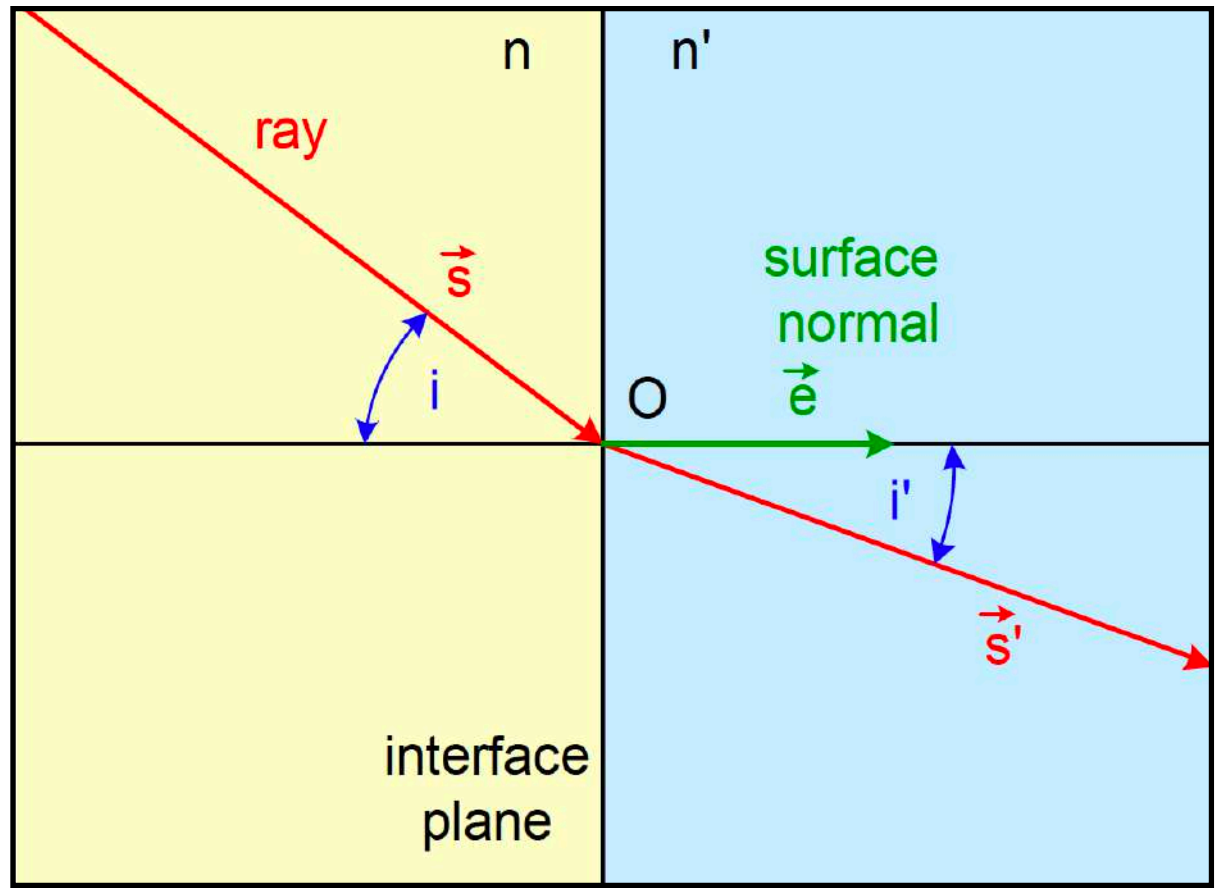

$$\frac{\sin(i)}{\sin(i')} = \frac{n'}{n}$$

The idea behind the concept of Hamilton's characteristic function

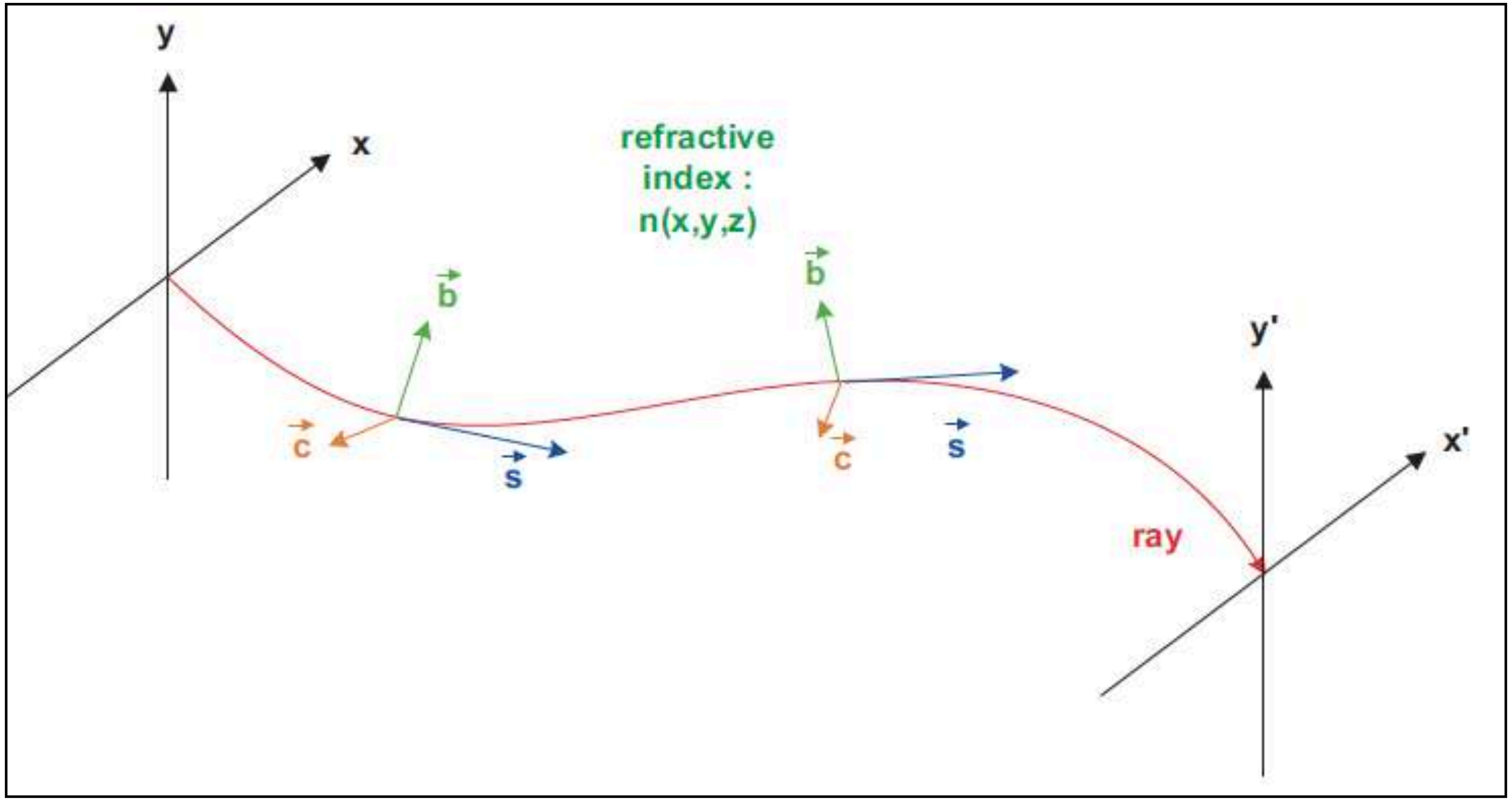

$$\boxed{\delta L = \delta \int_{P_1}^{P_2} n(x,y,z)ds = 0}$$

➡

$$\boxed{L = \int_A^B \left(n(x,y,z)\sqrt{1 + x'^2 + y'^2} \right) dz}$$

1

Principle of optics

Foundations of geometrical optics (introduction)
: Eikonal functions and aberration series

Fermat's principle : consequences

In optics time is the function that must be minimized.

Linked to the optical path length L given by :

$$L = n_1 d_1 + n_2 d_2 + n_3 d_3 + \dots$$

➡ From A to B all lengths L are the same

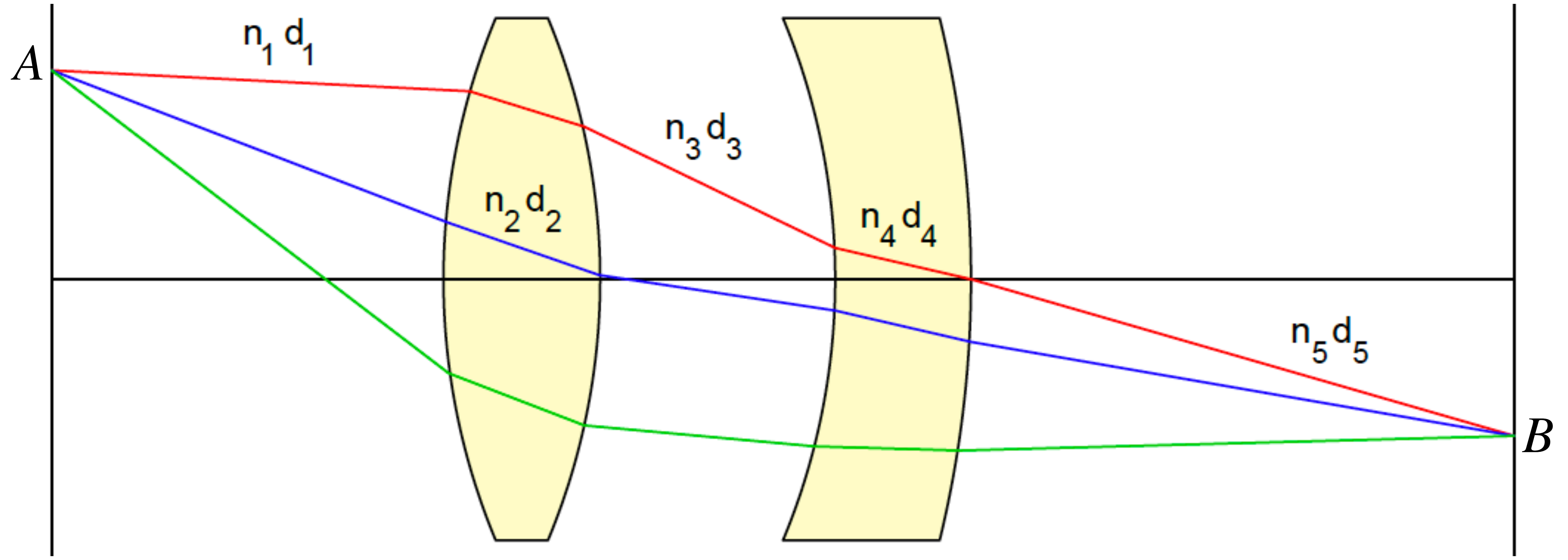

https://phet.colorado.edu/sims/html/bending-light/latest/bending-light_all.html?locale=es

➡ What is geometrical optics? How do we make high-performance instruments ?

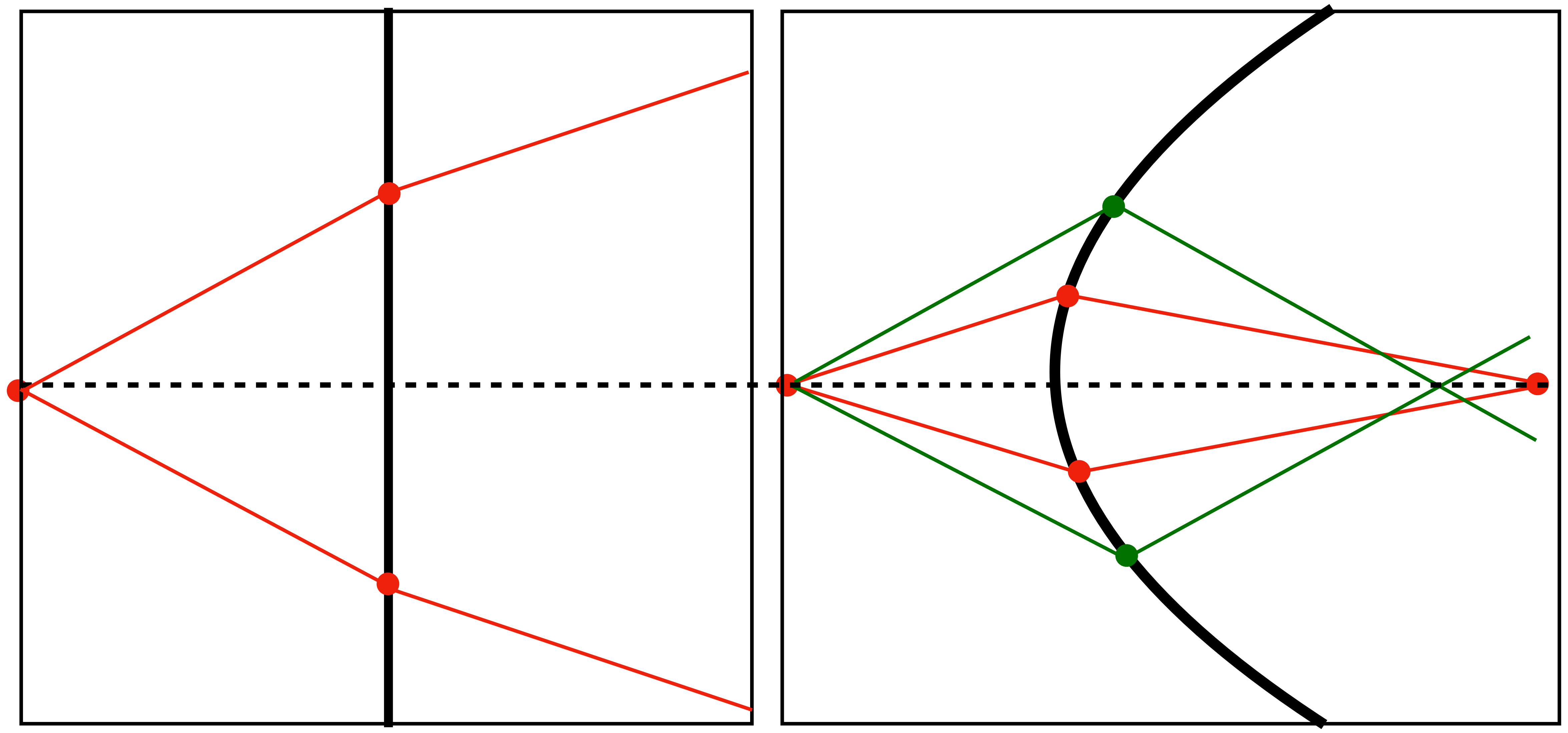

Sum of various polynomial functions :

$$L = \boxed{L^0} + \boxed{L^2} + \boxed{L^4} + \dots$$

Axe optique **Paraxial** **Aberrations**

Shape to remove L_4

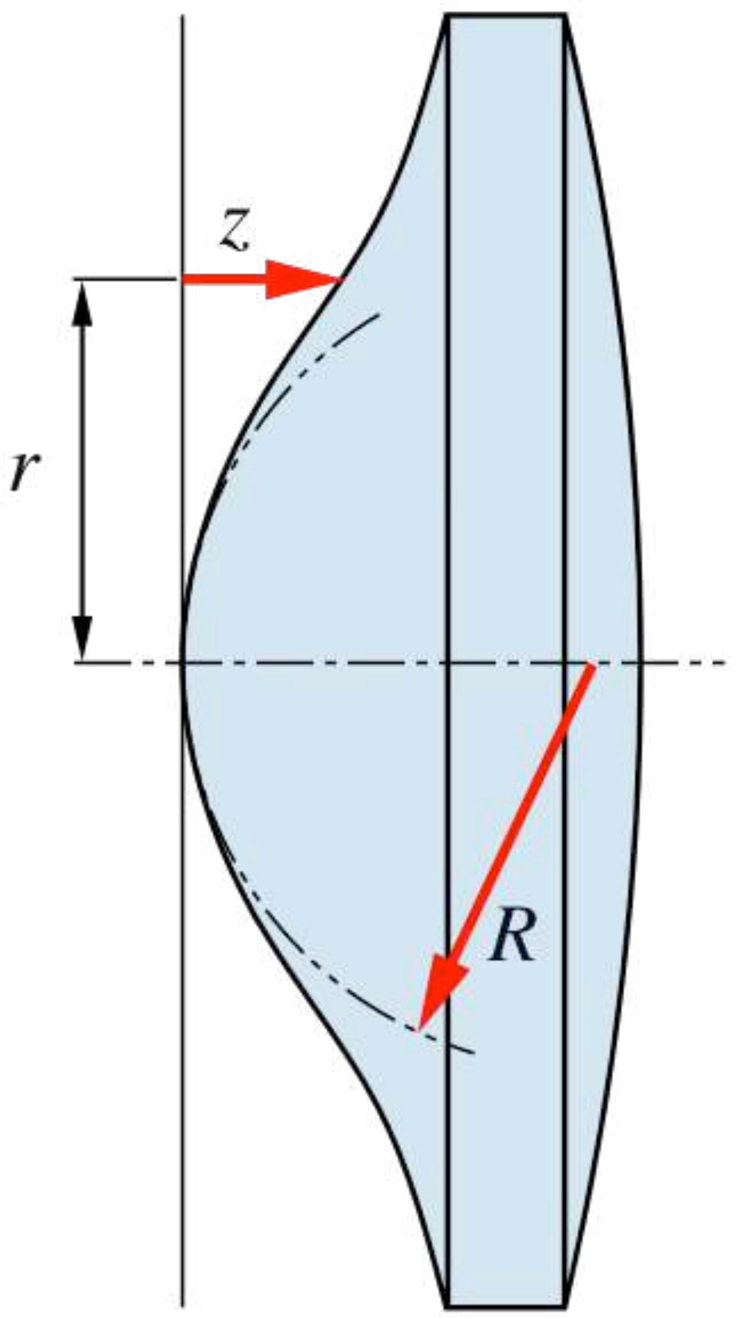

Development of modern mathematical geometrical optics

by way of introduction to the optical method … what is a serie expansion ? Why is it the « multi-purpose » tool of all physicists ?

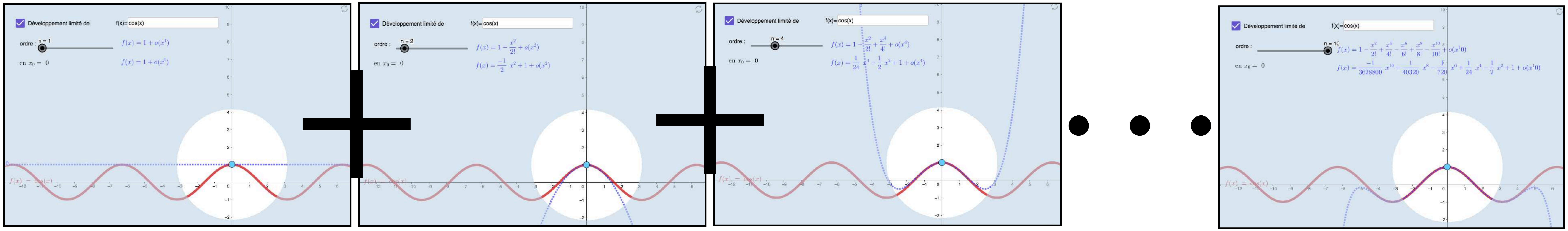

- **Johann Carl Friedrich Gauß (1777-m. 1855)**
  « Dioptrische Untersuchungen (1856) »

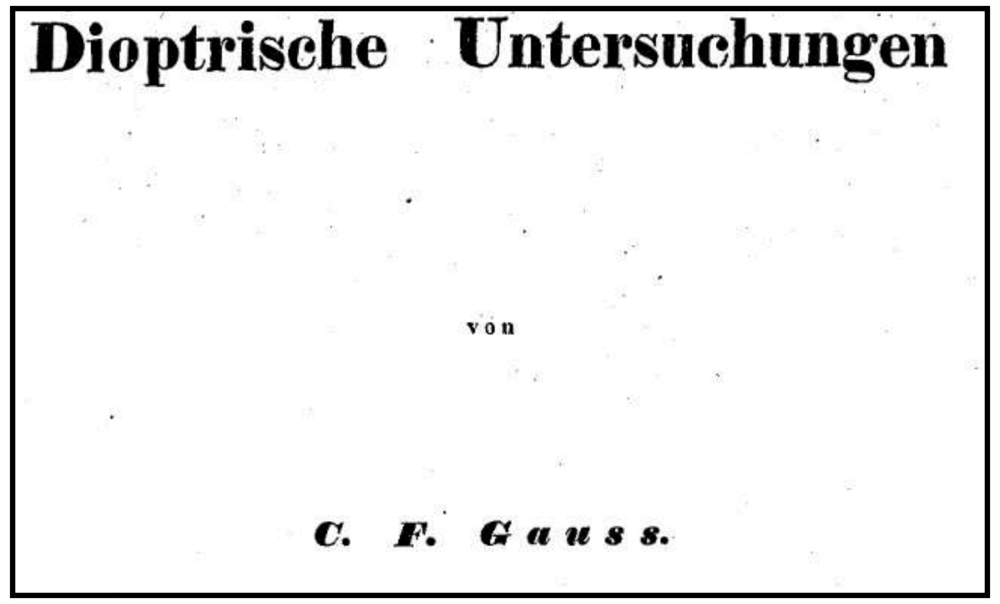
Dioptrische Untersuchungen

von

C. F. Gauss.

Definition of the stigmatic imaging condition:
linear approximation of the optical length

$$L = \boxed{L^0} + \boxed{L^2}$$

Axe optique **Paraxial**

Geometrically a **perfect imaging process** is defined by :
The optical length any curve in the object space is equal to the optical length of it's image
It corresponds to a ***linear transformation***

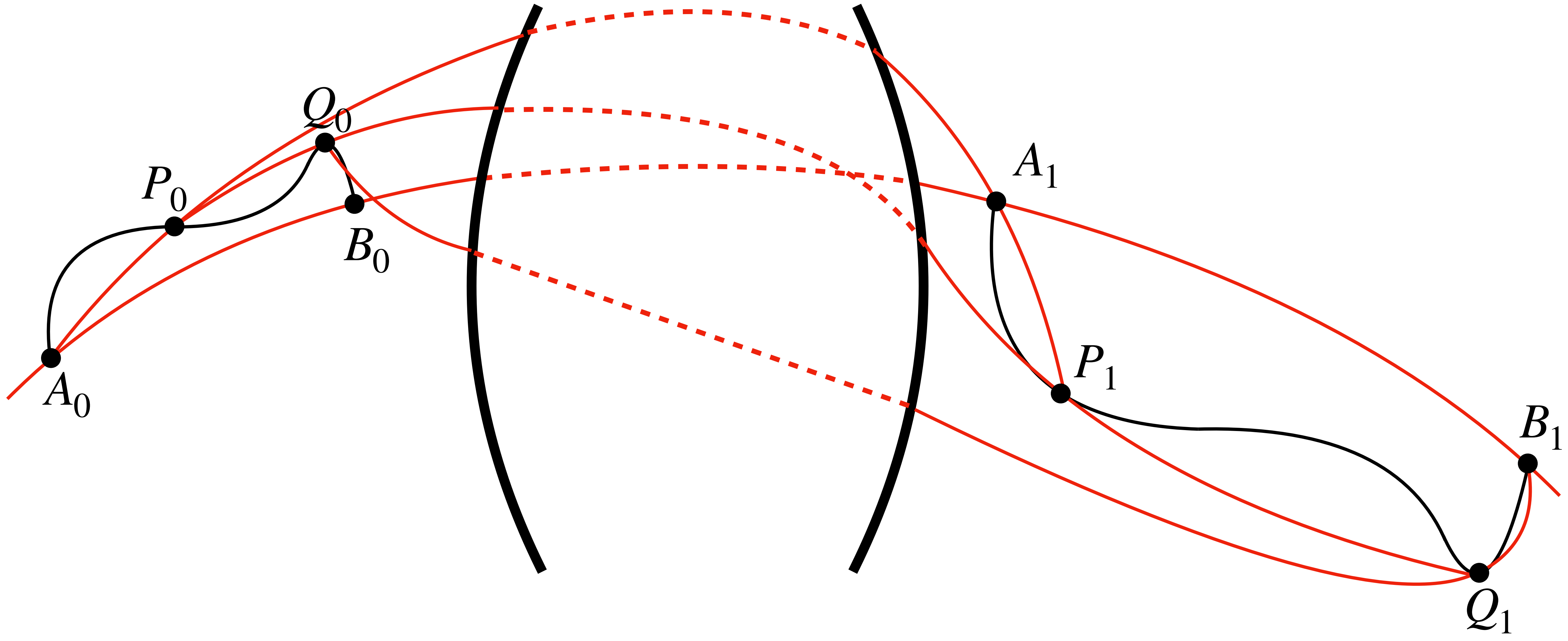

The paraxial approximation

$$L_A = L_A^{(0)} + L_A^{(2)}$$

$$\frac{\partial L_A^{(2)}}{\partial s'_y} = -n' y'_{para} \sim A(z)u_y + B$$

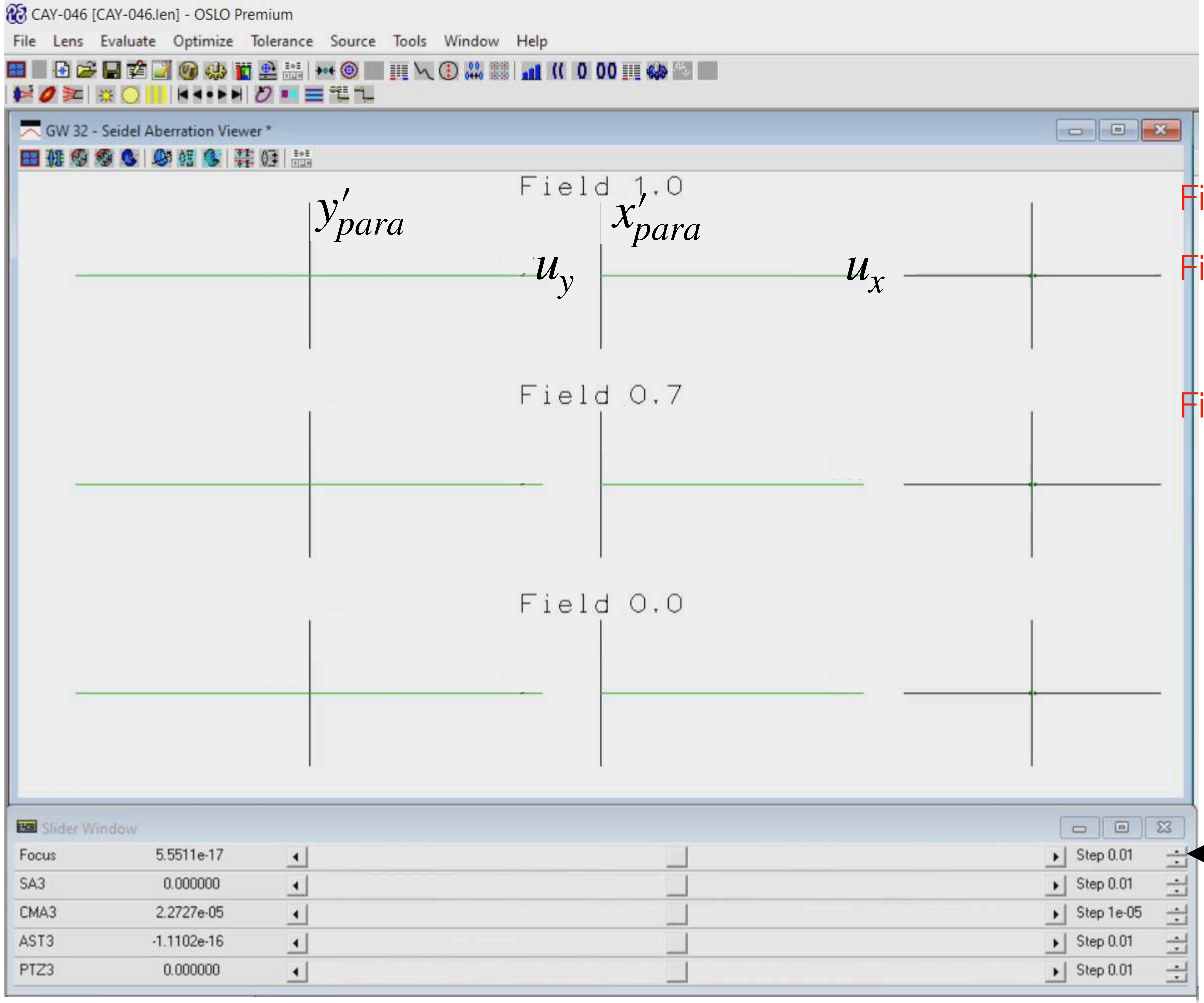

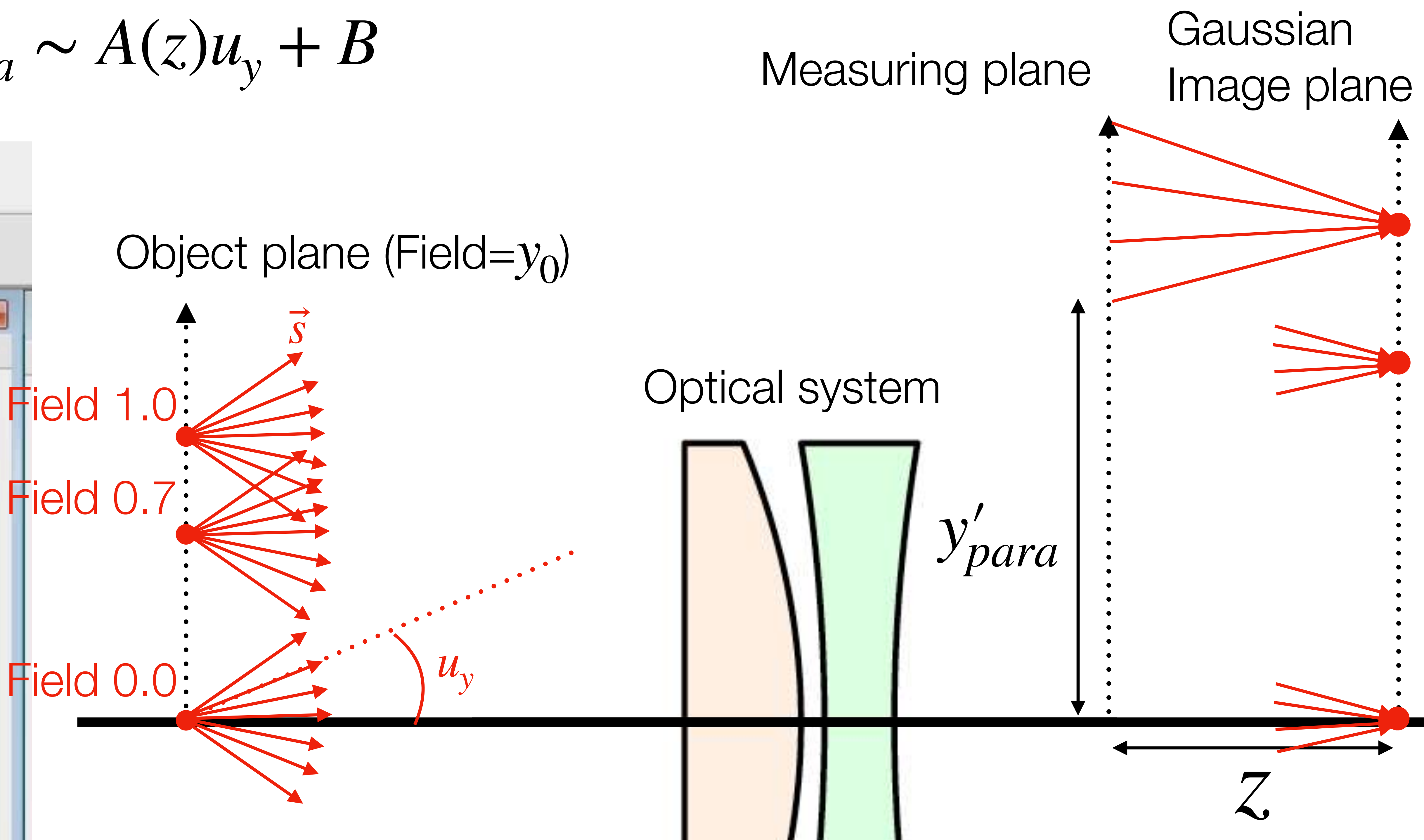

Change z, ray position changes linearly wrt to the starting angle (i.e. $s_y \sim u_y$)

Description of the optical system under the paraxial approximation : the cardinal planes

- P : principal planes
- S : intersection surfaces/optical axis
- F : focal planes
- f : focal distances
- r : radii of curvature of surfaces
- d : thickness SS'
- n : refraction index

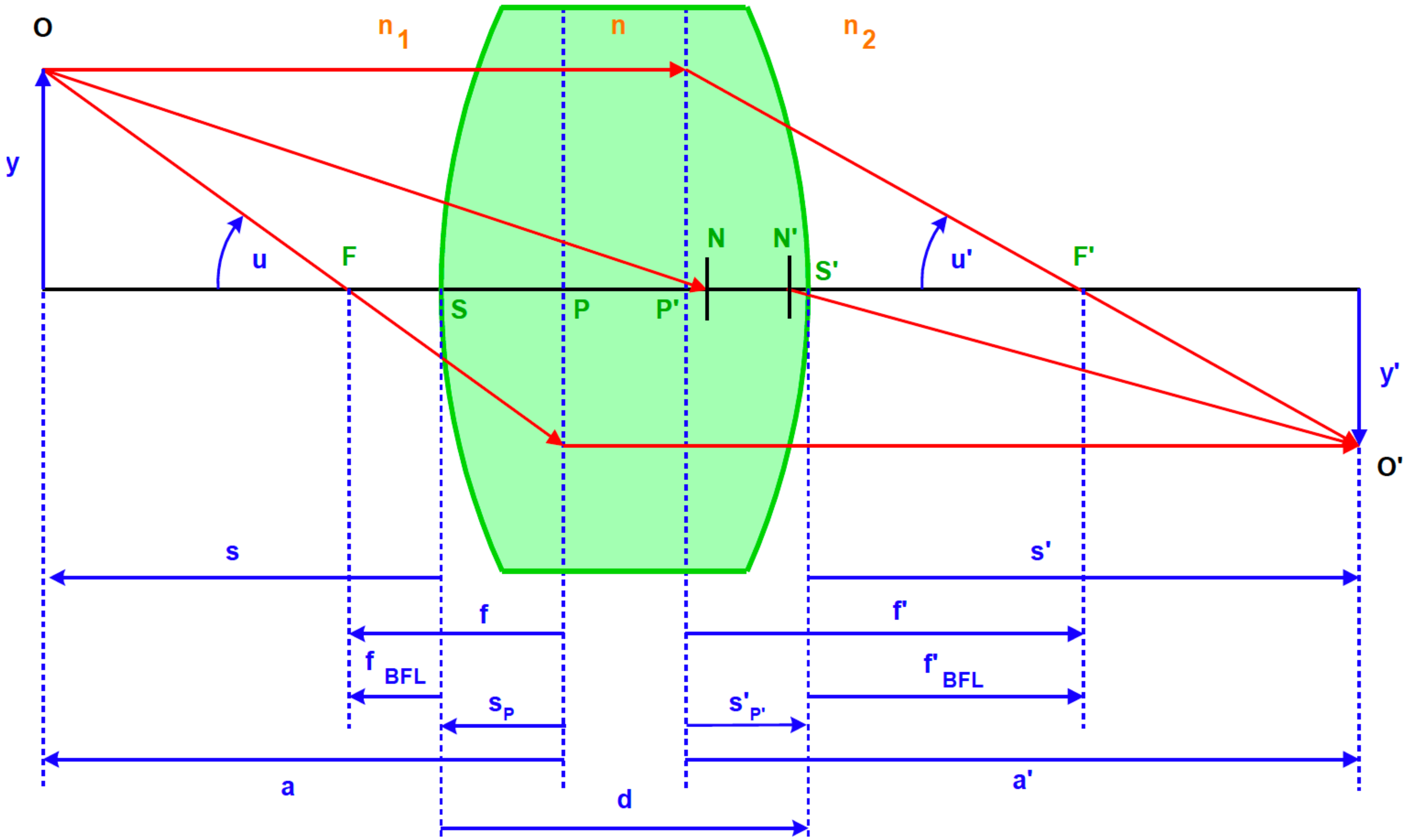

Description of the optical system under the paraxial approximation : the fundamental rays

➡ The **marginal ray** defines the maximum aperture angle. Intersection with optic axis : defines the **Gaussian image planes**

➡ The **principal ray** defines the maximum field. Intersection with optic axis : defines the **pupil planes**

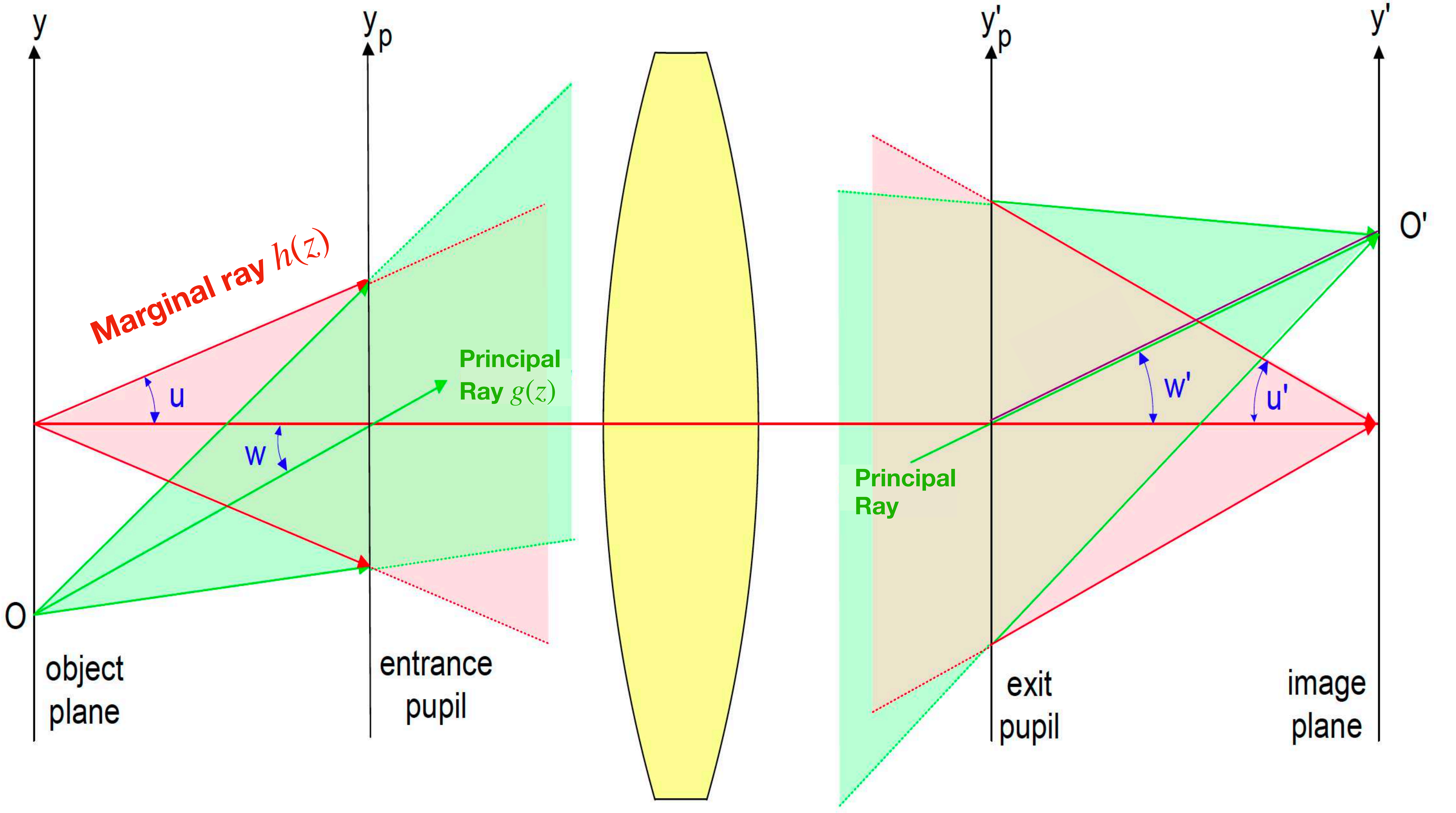

➡ Under paraxial approximation, any ray (define by it's angle α and field height y) can be written using linear combinaison between marginal (aperture) and principal (field) rays :

$$u(z) = \alpha h(z) + y g(z)$$

Mathematical optics and the design of high-performance instruments

- **Karl Siegmund Schwarzschild (1873-m. 1916)**

  « Untersuchungen zur geometrischen (1905) »

Astronomische Mittheilungen
der
Königlichen Sternwarte zu Göttingen.
Neunter Theil.
Herausgegeben von
K. Schwarzschild,
Direktor der Sternwarte.

Untersuchungen
zur geometrischen Optik. I.
Einleitung in die Fehlertheorie optischer Instrumente
auf Grund des Eikonalbegriffs.
Von
K. Schwarzschild.
Mit 6 Figuren im Text.
(Aus den Abhandlungen der Königl. Gesellschaft der Wissenschaften zu Göttingen.
Mathematisch-physikalische Klasse. Neue Folge. Band IV. No. 1.)
Göttingen 1905.

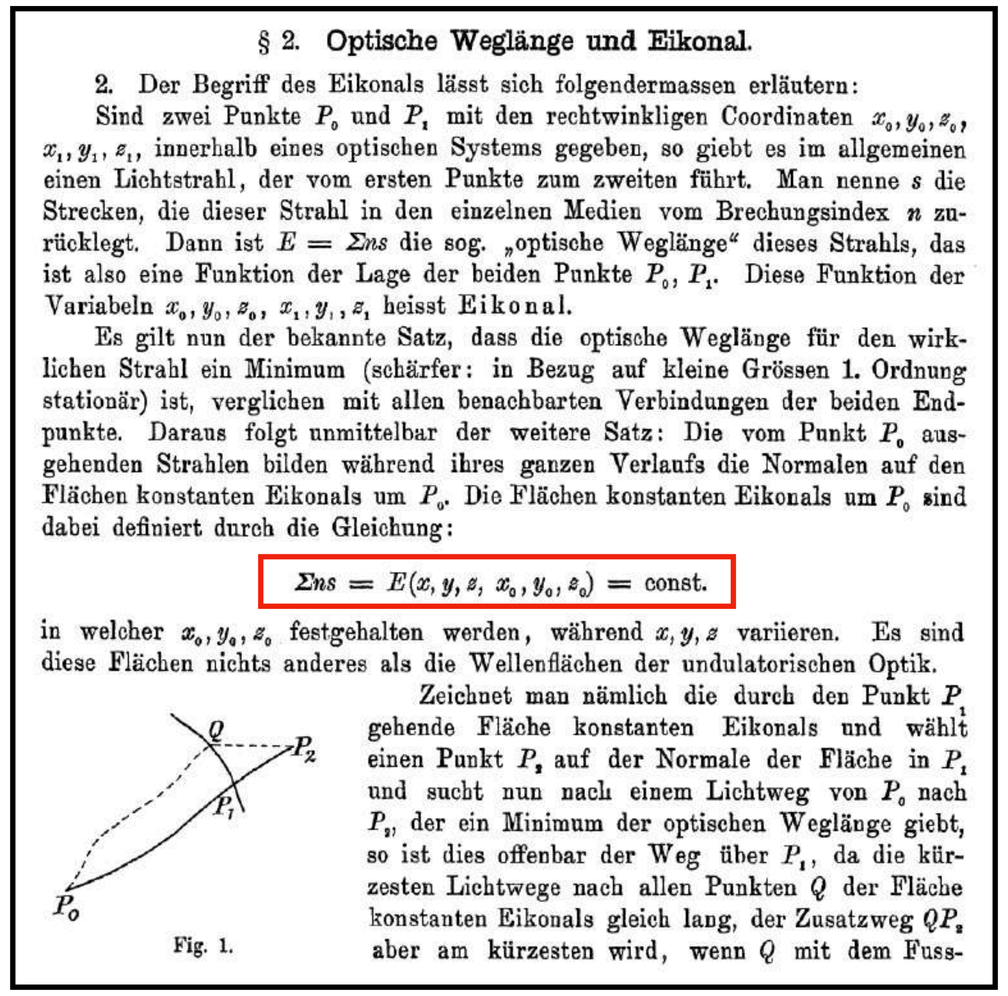

§ 2. Optische Weglänge und Eikonal.

2. Der Begriff des Eikonals lässt sich folgendermassen erläutern: Sind zwei Punkte P_0 und P_1 mit den rechtwinkligen Coordinaten x_0, y_0, z_0, x_1, y_1, z_1, innerhalb eines optischen Systems gegeben, so giebt es im allgemeinen einen Lichtstrahl, der vom ersten Punkte zum zweiten führt. Man nenne s die Strecken, die dieser Strahl in den einzelnen Medien vom Brechungsindex n zurücklegt. Dann ist $E = \Sigma ns$ die sog. „optische Weglänge" dieses Strahls, das ist also eine Funktion der Lage der beiden Punkte P_0, P_1. Diese Funktion der Variabeln x_0, y_0, z_0, x_1, y_1, z_1 heisst Eikonal.

Es gilt nun der bekannte Satz, dass die optische Weglänge für den wirklichen Strahl ein Minimum (schärfer: in Bezug auf kleine Grössen 1. Ordnung stationär) ist, verglichen mit allen benachbarten Verbindungen der beiden Endpunkte. Daraus folgt unmittelbar der weitere Satz: Die vom Punkt P_0 ausgehenden Strahlen bilden während ihres ganzen Verlaufs die Normalen auf den Flächen konstanten Eikonals um P_0. Die Flächen konstanten Eikonals um P_0 sind dabei definiert durch die Gleichung:

$$\boxed{\Sigma ns = E(x, y, z, x_0, y_0, z_0) = \text{const.}}$$

in welcher x_0, y_0, z_0 festgehalten werden, während x, y, z variieren. Es sind diese Flächen nichts anderes als die Wellenflächen der undulatorischen Optik.

Zeichnet man nämlich die durch den Punkt P_1 gehende Fläche konstanten Eikonals und wählt einen Punkt P_2 auf der Normale der Fläche in P_1 und sucht nun nach einem Lichtweg von P_0 nach P_2, der ein Minimum der optischen Weglänge giebt, so ist dies offenbar der Weg über P_1, da die kürzesten Lichtwege nach allen Punkten Q der Fläche konstanten Eikonals gleich lang, der Zusatzweg QP_2 aber am kürzesten wird, wenn Q mit dem Fuss-

Fig. 1.

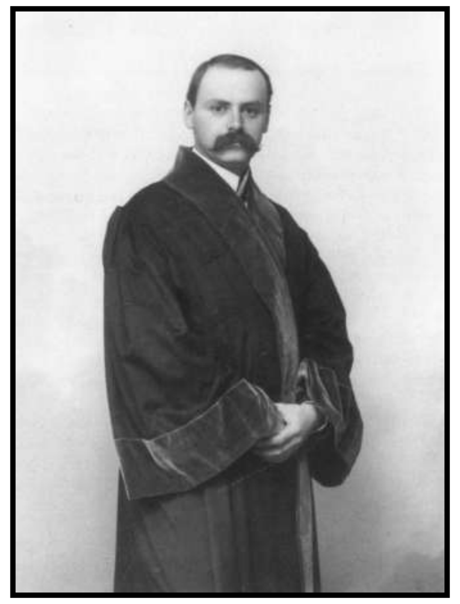

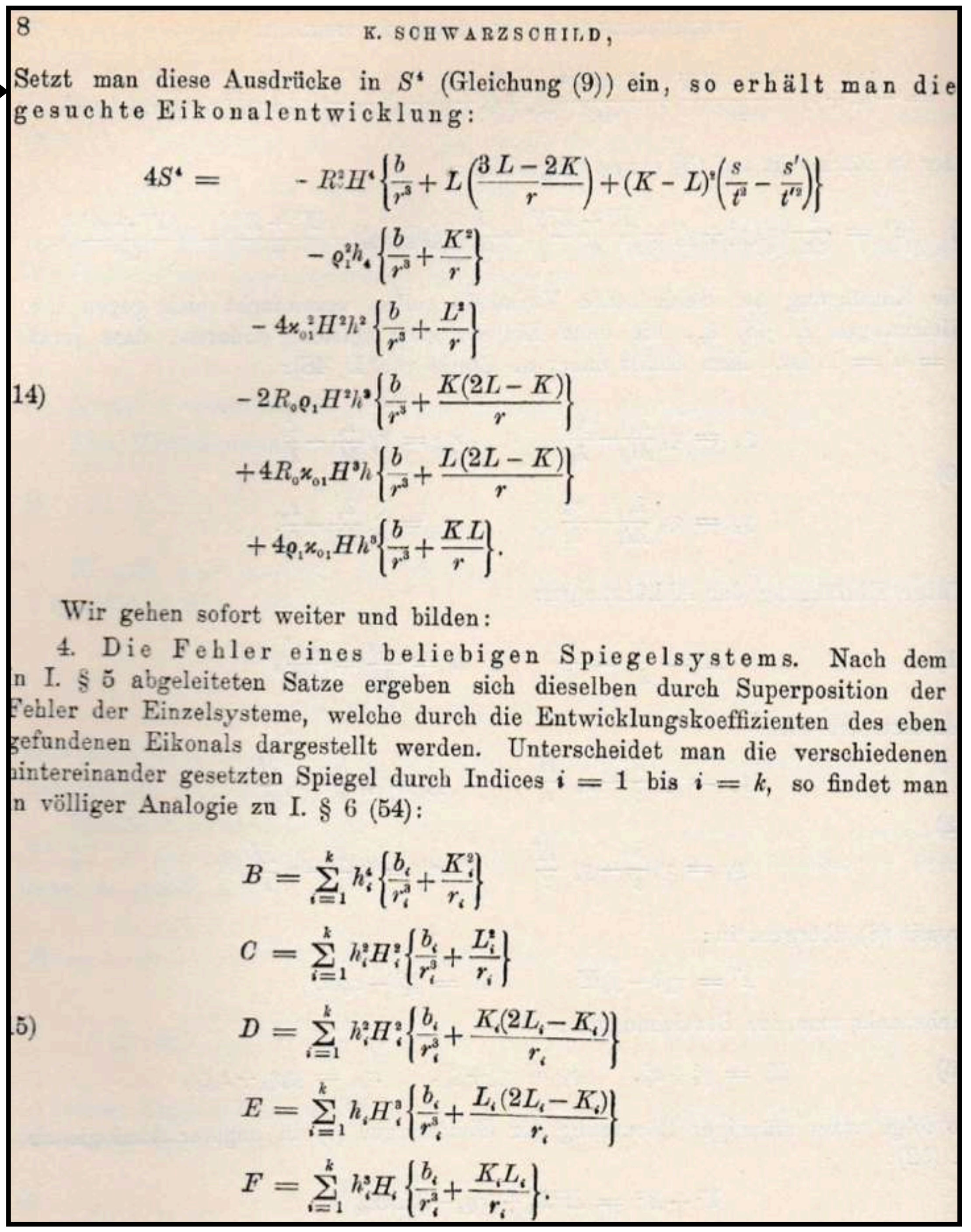

8 K. SCHWARZSCHILD,

Setzt man diese Ausdrücke in S^4 (Gleichung (9)) ein, so erhält man die gesuchte Eikonalentwicklung:

$$
\begin{aligned}
(14)\quad 4S^4 = & -R^2H^4\left\{\frac{b}{r^3}+L\left(\frac{3L-2K}{r}\right)+(K-L)^2\left(\frac{s}{t^2}-\frac{s'}{t'^2}\right)\right\}\\
& -\varrho_0^4h_0^4\left\{\frac{b}{r^3}+\frac{K^2}{r}\right\}\\
& -4\varkappa_{01}^2H^2h^2\left\{\frac{b}{r^3}+\frac{L^2}{r}\right\}\\
& -2R_0\varrho_0H^2h^2\left\{\frac{b}{r^3}+\frac{K(2L-K)}{r}\right\}\\
& +4R_0\varkappa_{01}H^3h\left\{\frac{b}{r^3}+\frac{L(2L-K)}{r}\right\}\\
& +4\varrho_0\varkappa_{01}Hh^3\left\{\frac{b}{r^3}+\frac{KL}{r}\right\}.
\end{aligned}
$$

Wir gehen sofort weiter und bilden:

4. Die Fehler eines beliebigen Spiegelsystems. Nach dem in I. § 5 abgeleiteten Satze ergeben sich dieselben durch Superposition der Fehler der Einzelsysteme, welche durch die Entwicklungskoeffizienten des eben gefundenen Eikonals dargestellt werden. Unterscheidet man die verschiedenen hintereinander gesetzten Spiegel durch Indices $i = 1$ bis $i = k$, so findet man in völliger Analogie zu I. § 6 (54):

$$
\begin{aligned}
& B = \sum_1^k h_i^4\left\{\frac{b_i}{r_i^3}+\frac{K_i^2}{r_i}\right\}\\
& C = \sum_1^k h_i^2H_i^2\left\{\frac{b_i}{r_i^3}+\frac{L_i^2}{r_i}\right\}\\
(15)\quad & D = \sum_1^k h_i^2H_i^2\left\{\frac{b_i}{r_i^3}+\frac{K_i(2L_i-K_i)}{r_i}\right\}\\
& E = \sum_1^k h_iH_i^3\left\{\frac{b_i}{r_i^3}+\frac{L_i(2L_i-K_i)}{r_i}\right\}\\
& F = \sum_1^k h_i^3H_i\left\{\frac{b_i}{r_i^3}+\frac{K_iL_i}{r_i}\right\}.
\end{aligned}
$$

Developed a Hamiltonian approach
to the calculation of Seidel aberrations.
He builds on Bruns' work and develops
his own characteristic function (or eikonal).

- **Heinrich Bruns (1848-m. 1919)**

  « Das Eikonal (1895) »

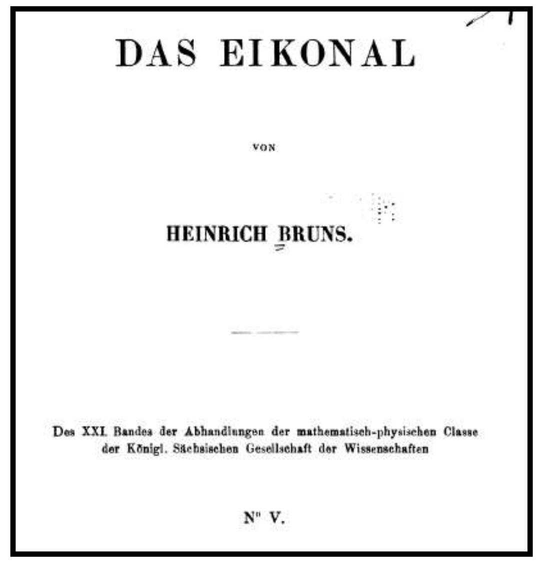

DAS EIKONAL
VON
HEINRICH BRUNS.
Des XXI. Bandes der Abhandlungen der mathematisch-physischen Classe
der Königl. Sächsischen Gesellschaft der Wissenschaften
Nº V.

- **Philipp Ludwig von Seidel (1821-m. 1896)**

  « Über die Entwicklung der Glieder 3ter Ordnung welche den Weg eines ausserhalb der Ebene der Axe gelegene Lichtstrahles durch ein System brechender Medien bestimmen (1856) »

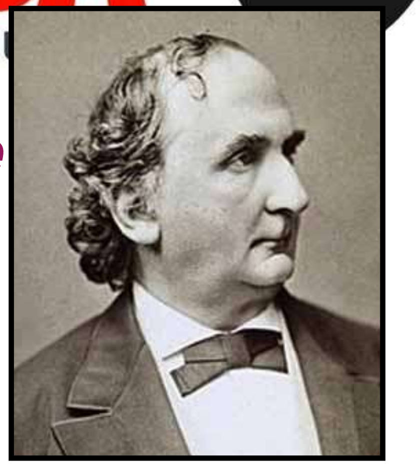

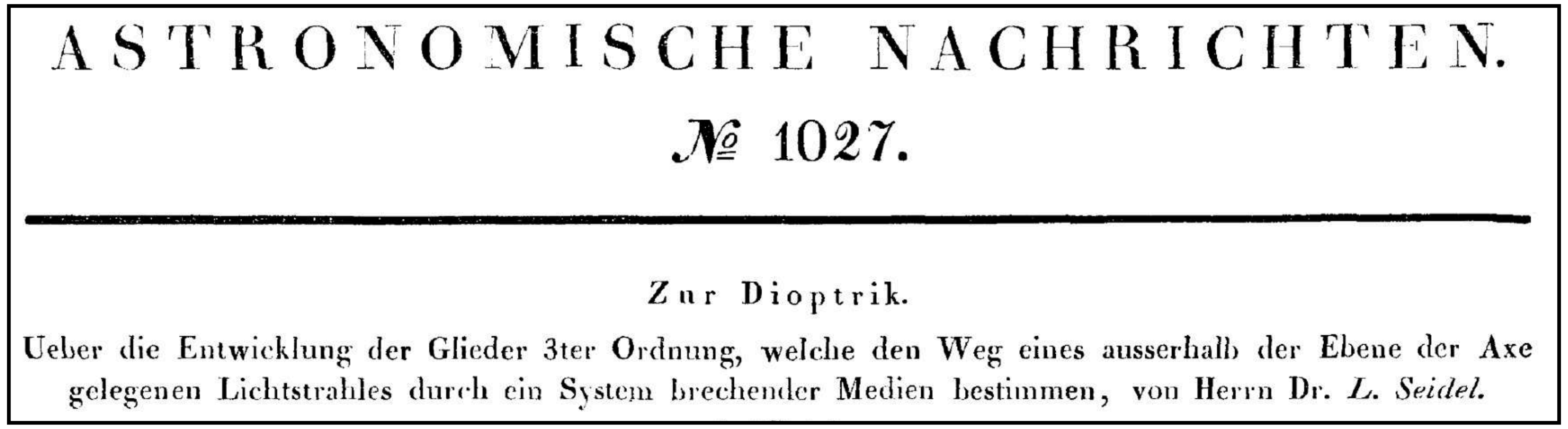

ASTRONOMISCHE NACHRICHTEN.
№ 1027.

Zur Dioptrik.

Ueber die Entwicklung der Glieder 3ter Ordnung, welche den Weg eines ausserhalb der Ebene der Axe gelegenen Lichtstrahles durch ein System brechender Medien bestimmen, von Herrn Dr. *L. Seidel.*

Perturbations of Gaussian optics :

5 primary geometrical aberrations L^4 and 2 chromatics $L^2(\lambda)$

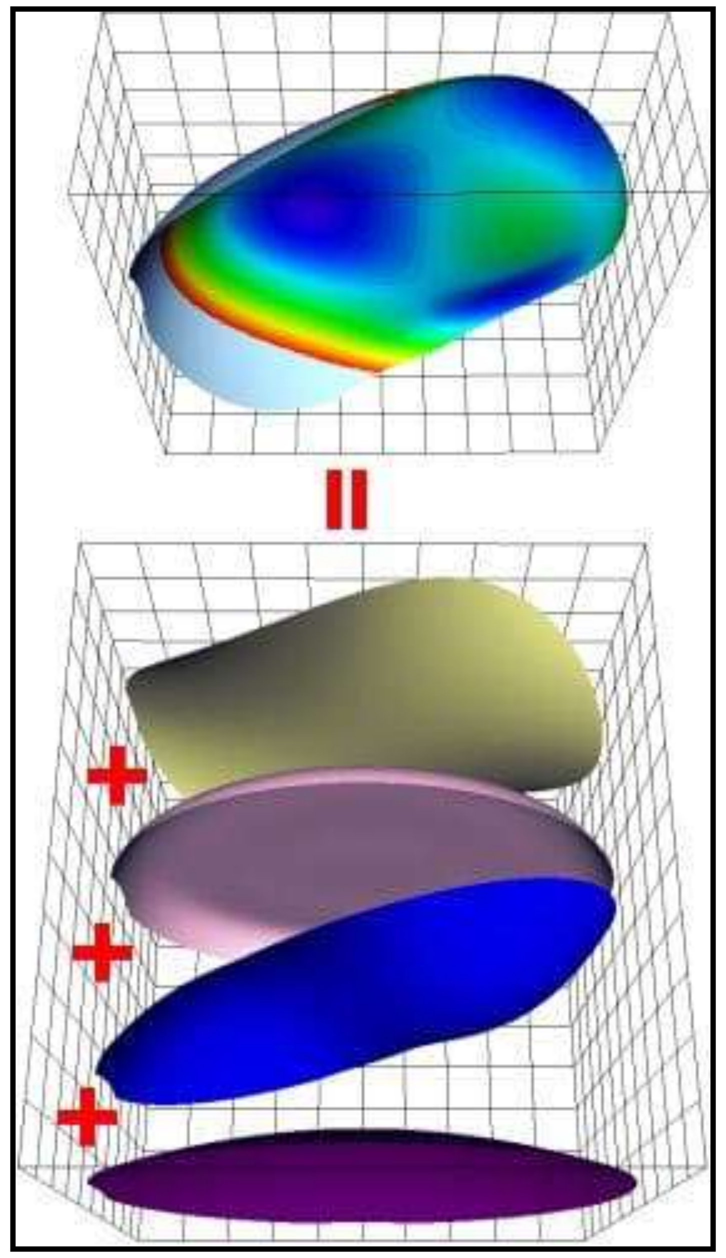

Primary aberrations or Seidel aberrations

$$y' = m\,.\,y + \Delta y' = -\frac{1}{n'}\frac{\partial L_A}{\partial s'_y}$$

$$\Delta y' = -\frac{1}{n'}\frac{\partial L_A^{(4)}}{\partial s'_y}$$

$$L_A^{(4)}(s_x, s_y, s'_x, s'_y) \propto As_x^4 + Bs_y^4 + Cs_x^2 s_y^2 + Ds_x^2 s_y^2 + \dots$$

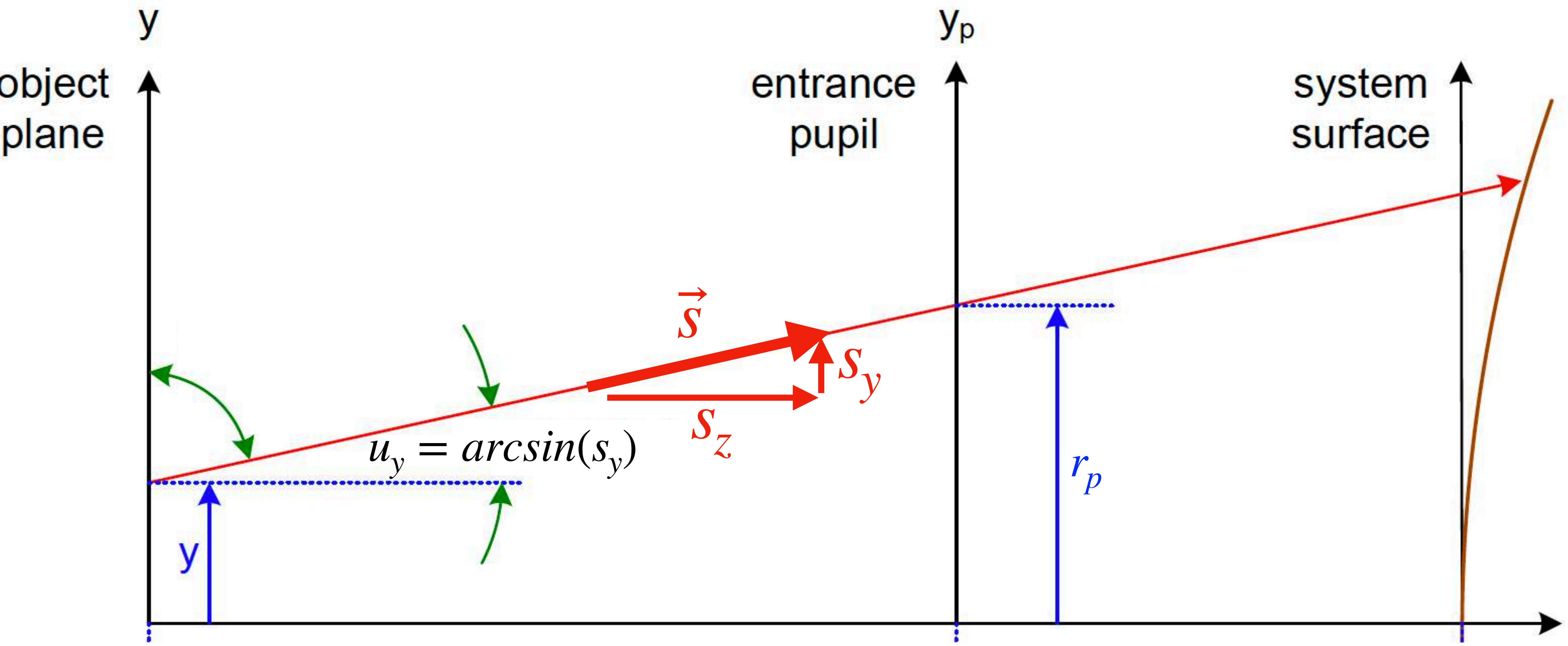

➡change of variables $s_x, s_y, s'_x, s'_y \rightarrow \boxed{x, y,} \boxed{u_x, u_y}$ (**field**, **aperture**)

➡or $s_x, s_y, s'_x, s'_y \rightarrow \boxed{x, y,} \boxed{r_p, \theta}$ (**field**, **aperture**)

$$L_A^{(4)}(x, y, r_p, \theta) \propto \boxed{Sr_p^4} + \boxed{Cr_p^3 y cos(\theta)} + \boxed{Pr_p^2 y^2} + \boxed{Ay^2 r_p^2 cos^2(\theta)} + \boxed{Dy^4}$$

$(L_A^{(4)})_{sph}$ $(L_A^{(4)})_{cma}$ $(L_A^{(4)})_{ptz}$ $(L_A^{(4)})_{astg}$ $(L_A^{(4)})_{dist}$

Seidel aberrations : primary (third order) spherical aberration

$$\Delta y'_{sph} = -\frac{1}{n'}\frac{\partial (L_A^{(4)})_{sph}}{\partial s'_y} \sim S u_y^3$$

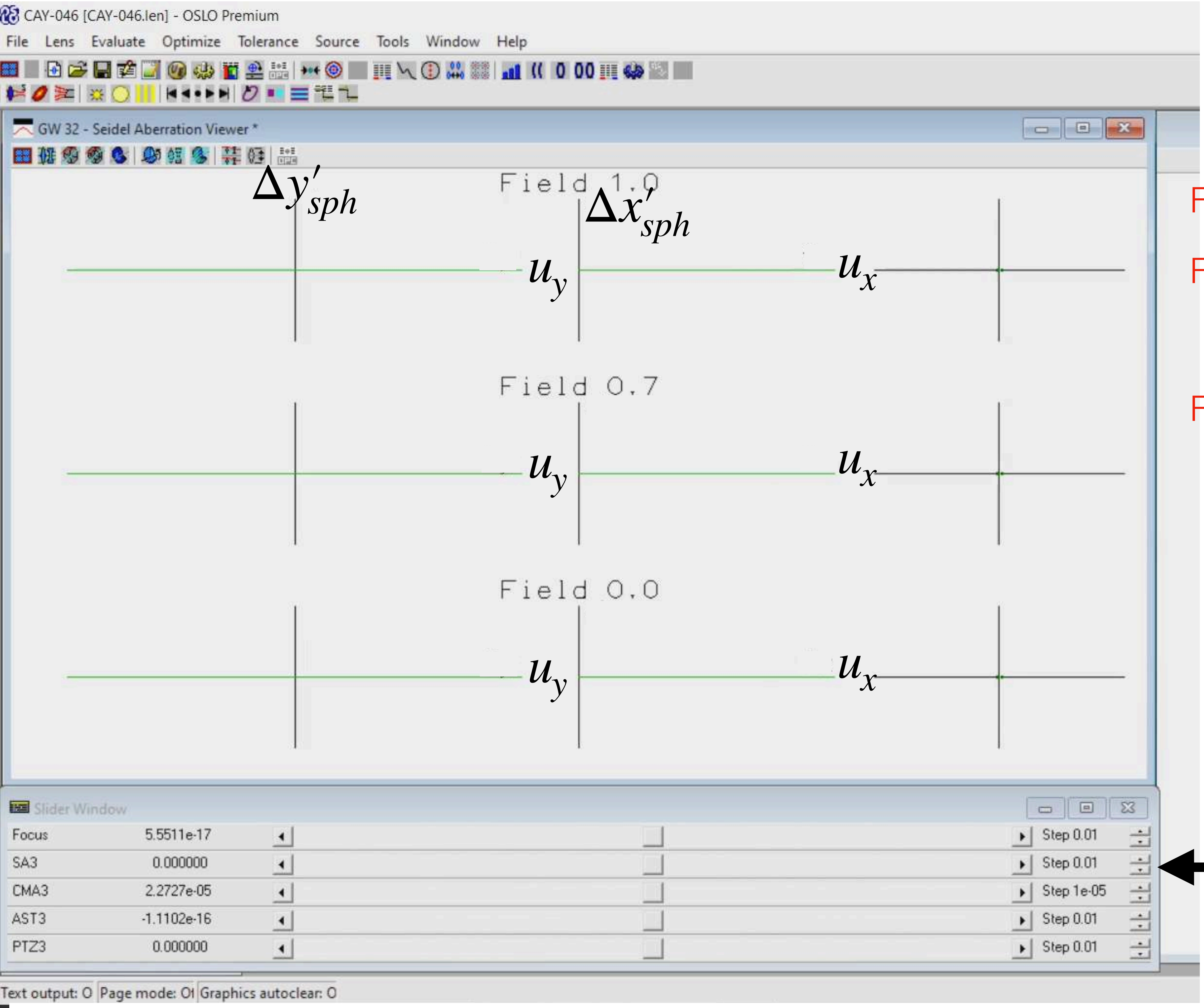

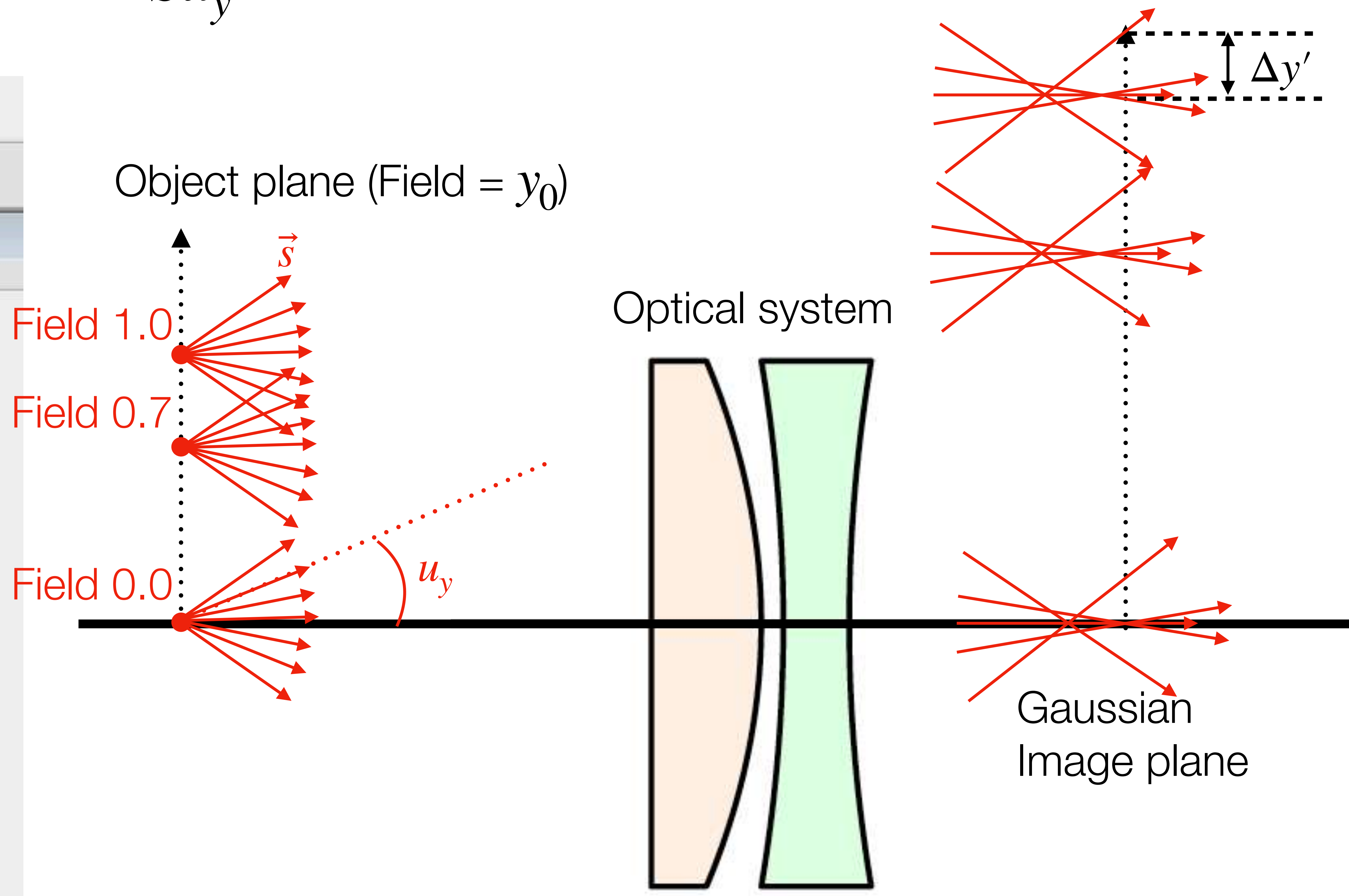

In the Gaussian plane, change Spherical aberration contribution

Seidel aberrations : primary coma aberration

$$\Delta y'_{cma} = -\frac{1}{n'}\frac{\partial (L_A^{(4)})_{cma}}{\partial s'_y} \sim C u_y^2 y_0^1$$

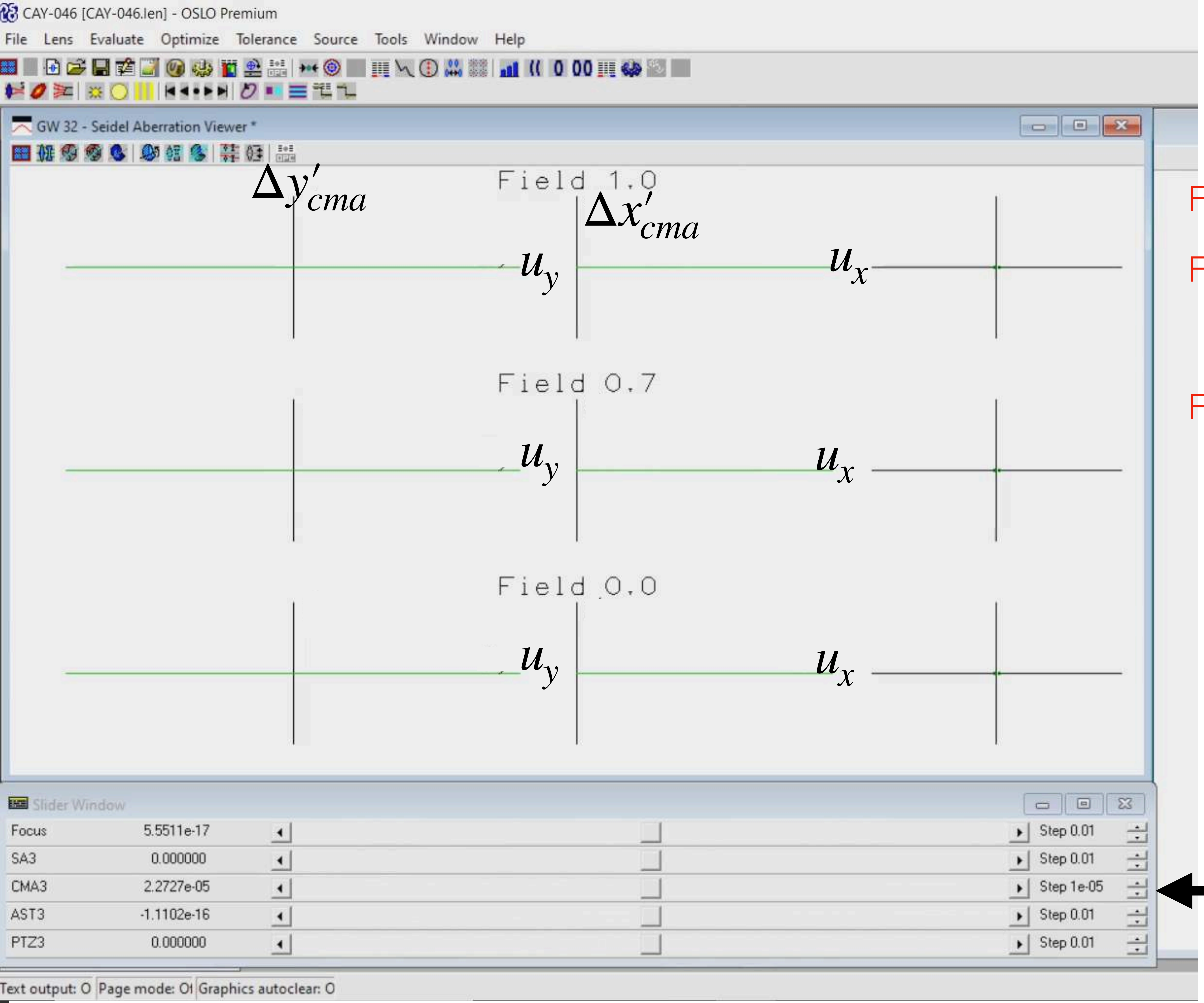

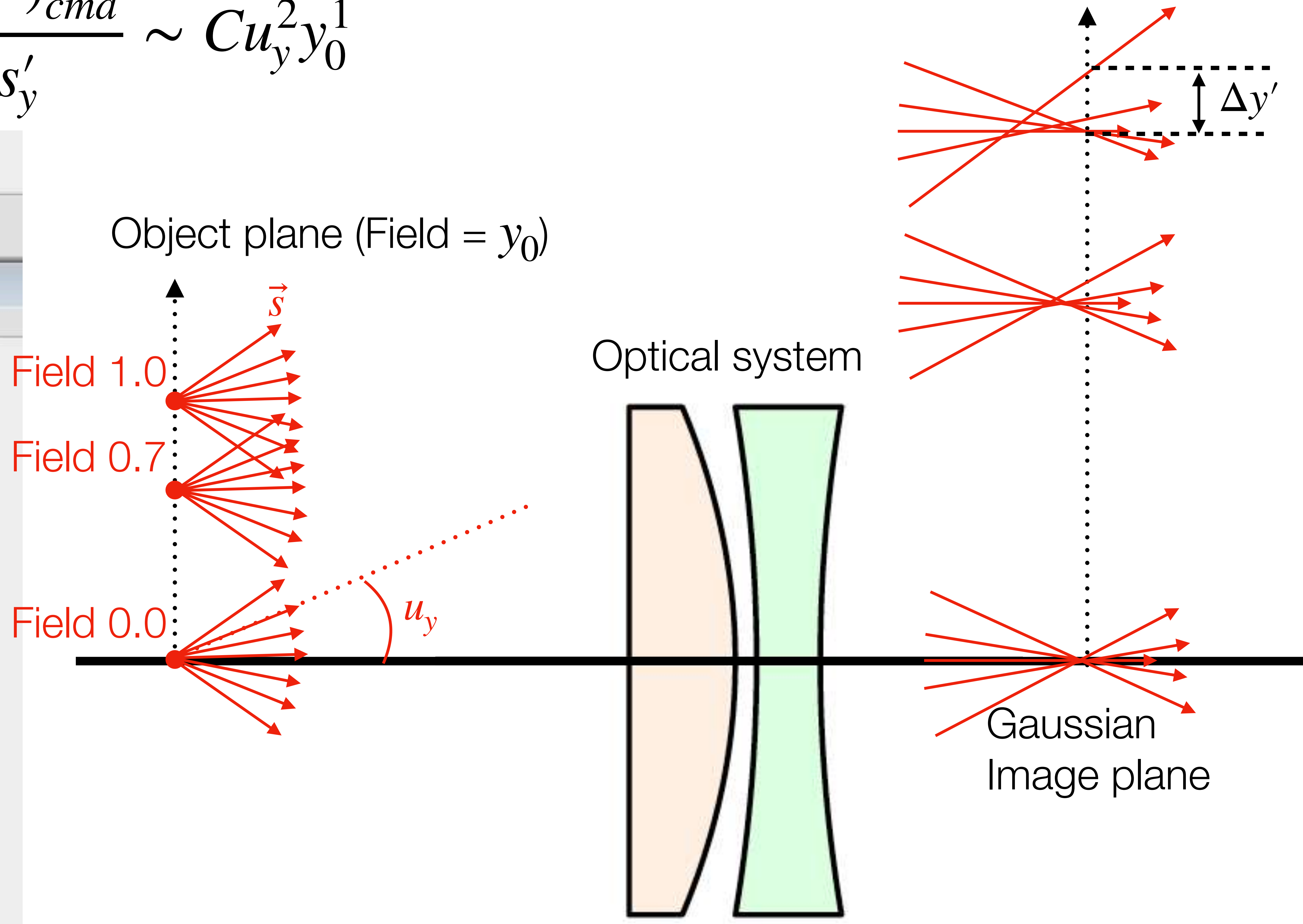

In the Gaussian plane, change Coma aberration contribution

Seidel aberrations : primary field curvature aberration (Petzval curvature)

$$\Delta y'_{ptz} = -\frac{1}{n'}\frac{\partial (L_A^{(4)})_{ptz}}{\partial s'_y} \sim P u_y^1 y_0^2$$

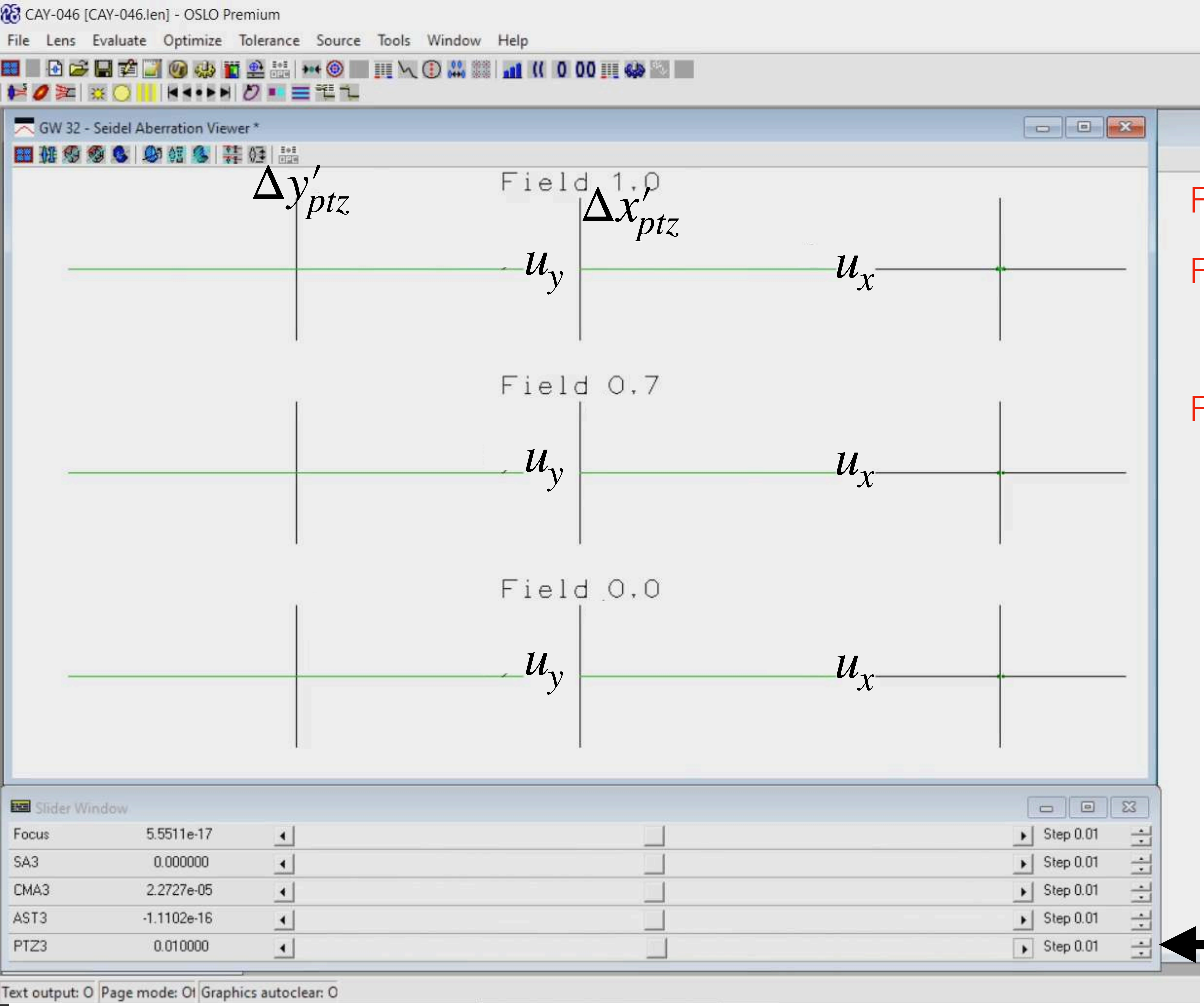

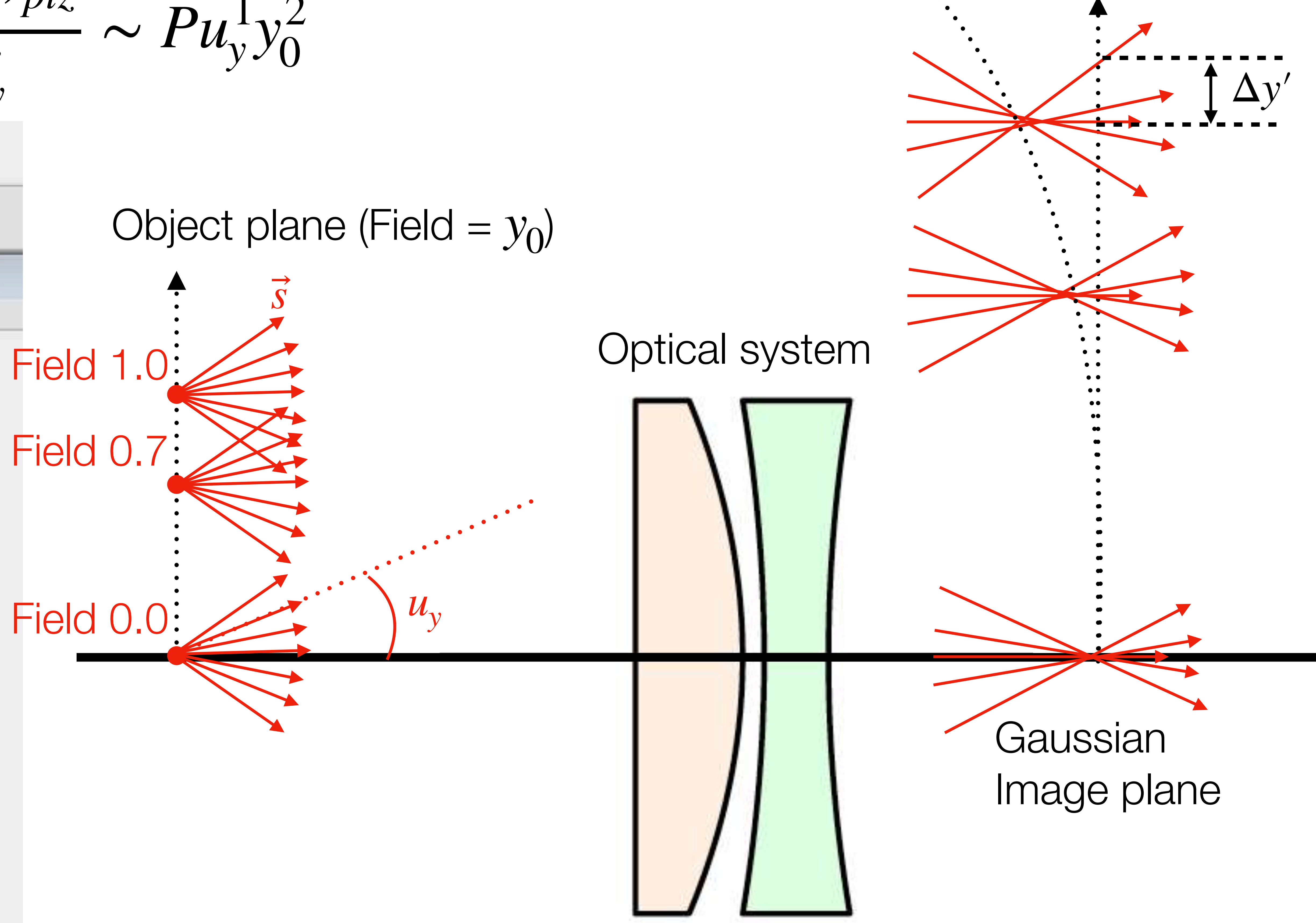

In the Gaussian plane, change field curvature aberration contribution

Seidel aberrations : primary field astigmatism aberration

$$\Delta y'_{ast} = -\frac{1}{n'}\frac{\partial (L_A^{(4)})_{ast}}{\partial s'_y} \sim A(u_y^1 x_0^2 + u_x^1 x_0 y_0)$$

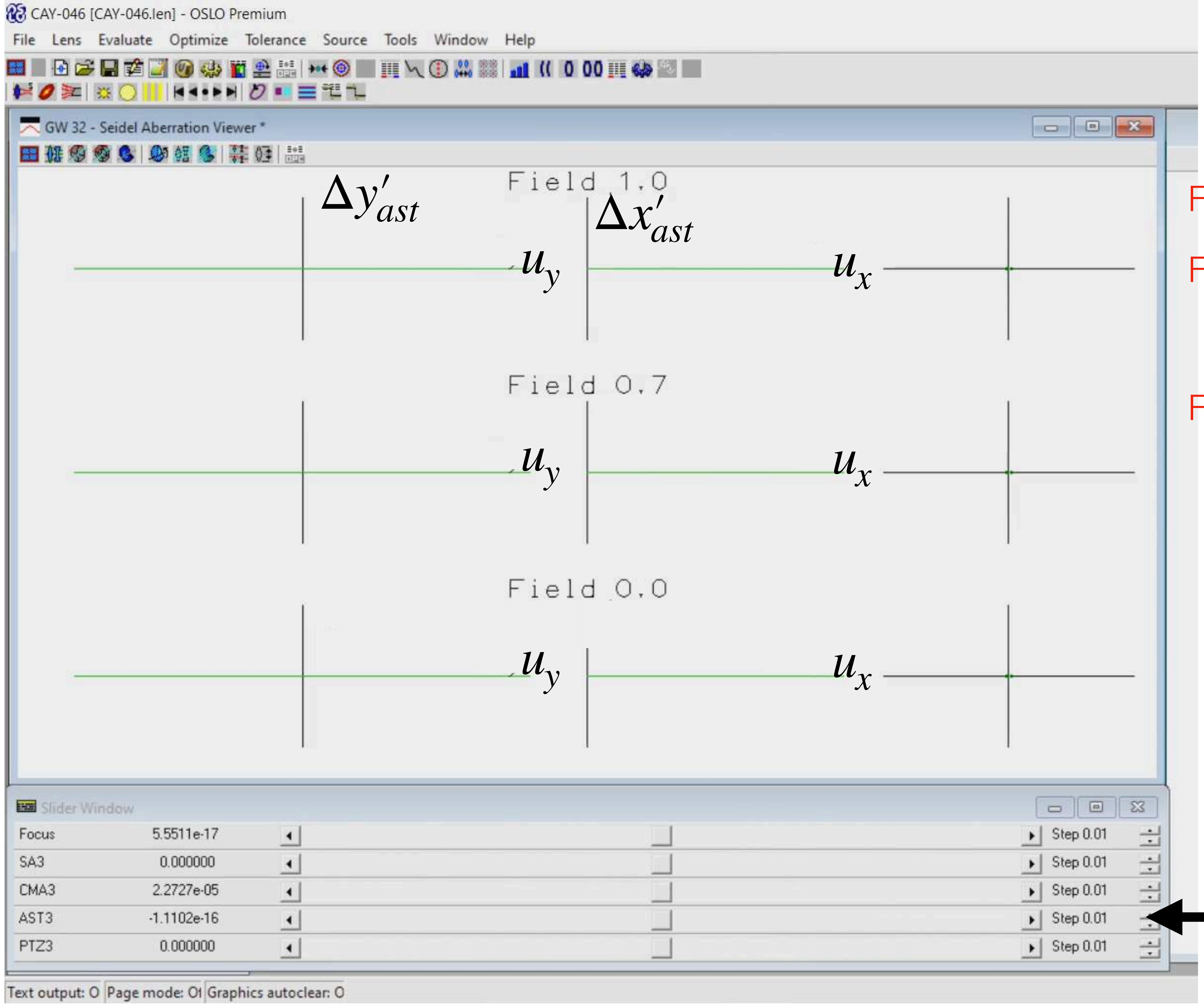

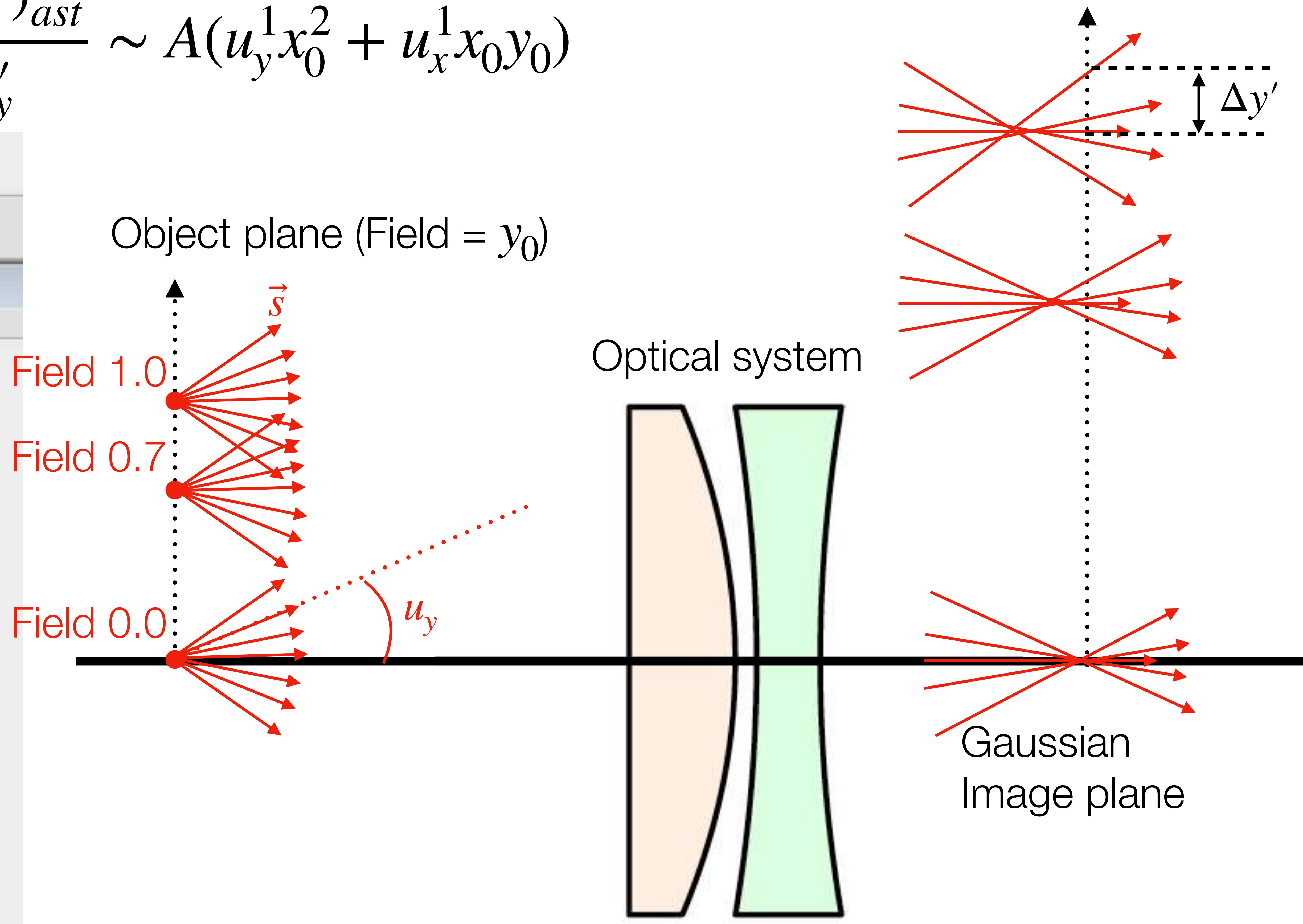

In the Gaussian plane, change field astigmatism aberration contribution

Seidel aberrations : primary distorsion aberration

$$\Delta y'_{dist} = -\frac{1}{n'}\frac{\partial (L_A^{(4)})_{dist}}{\partial s'_y} \sim D y_0^3$$

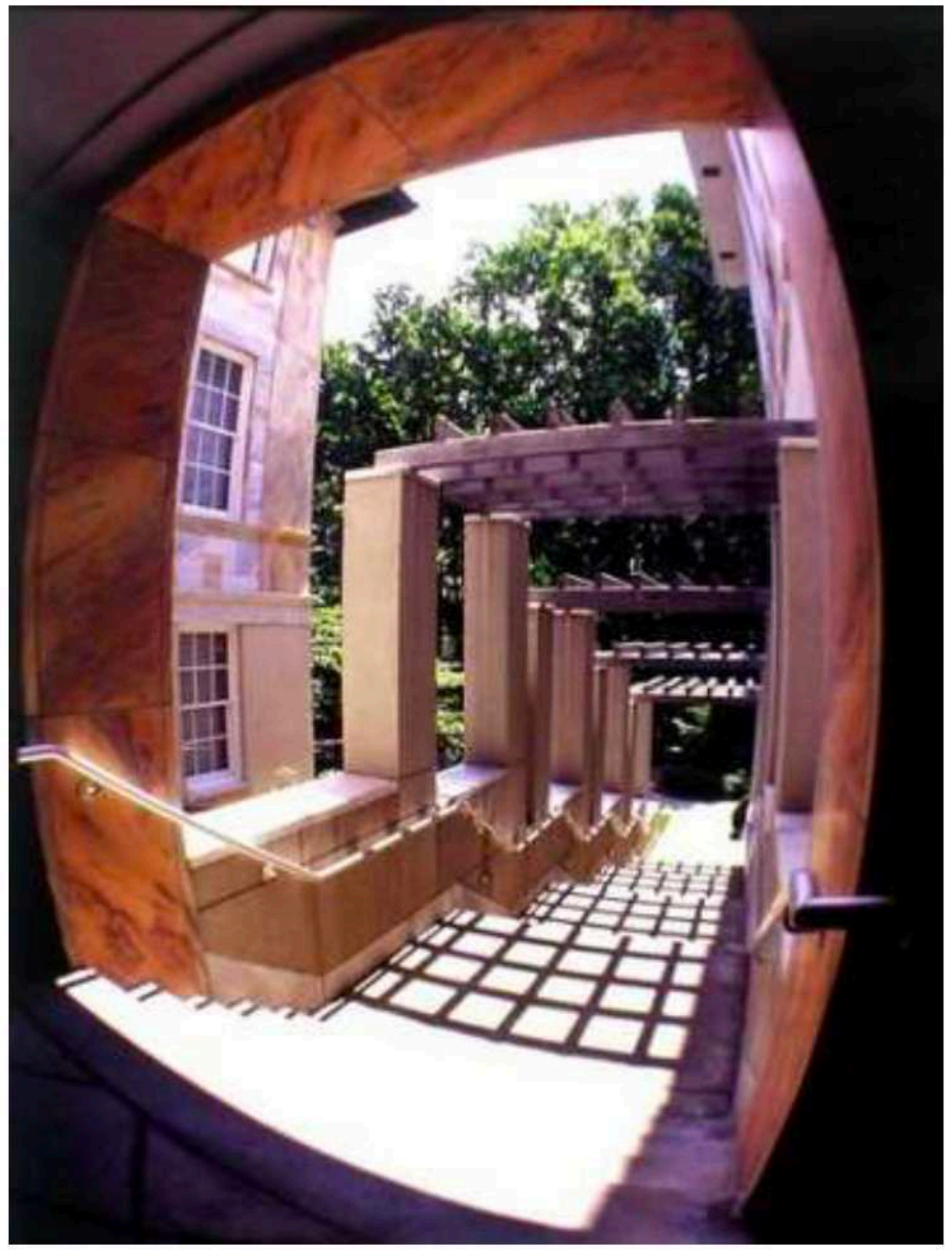

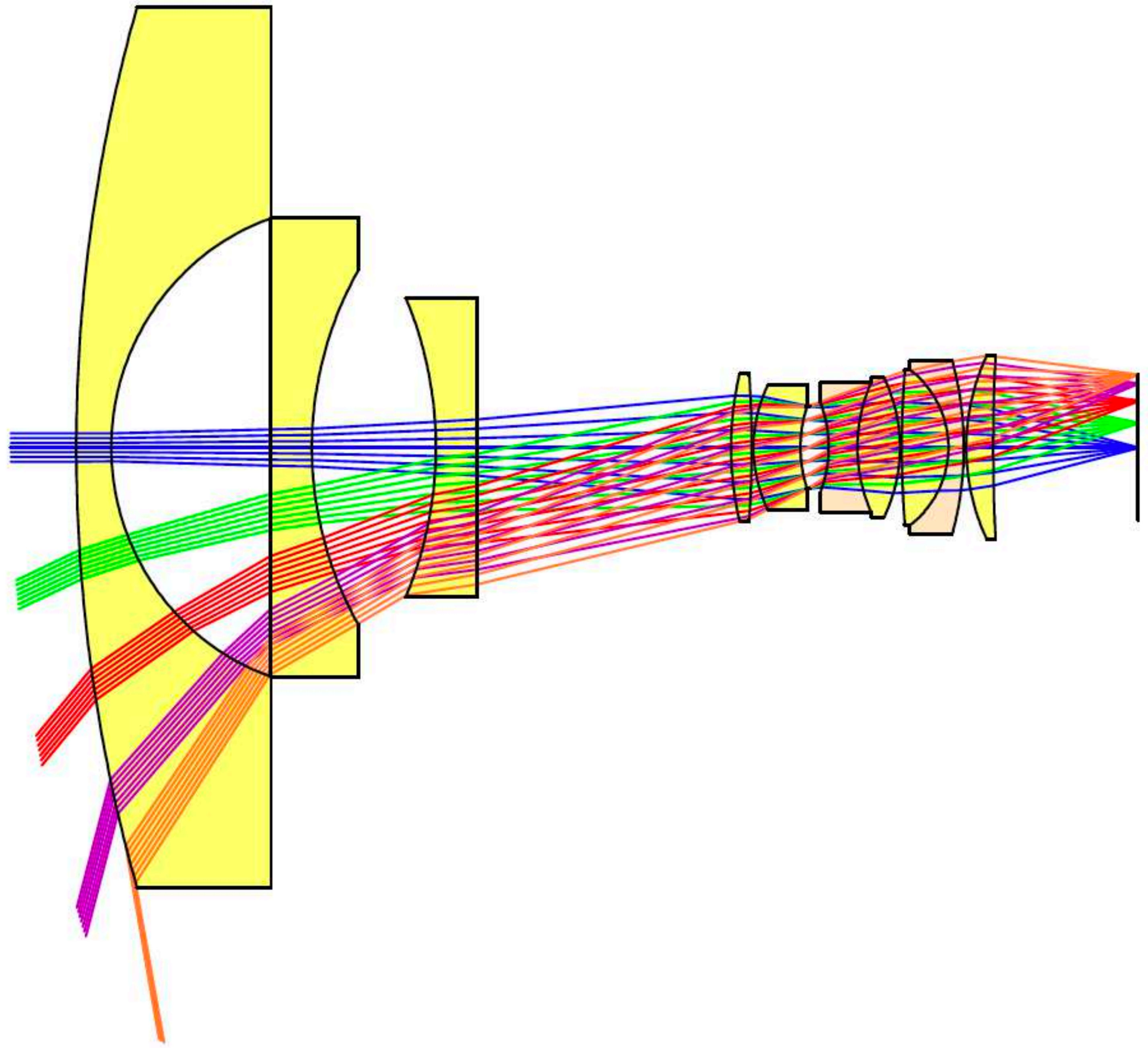

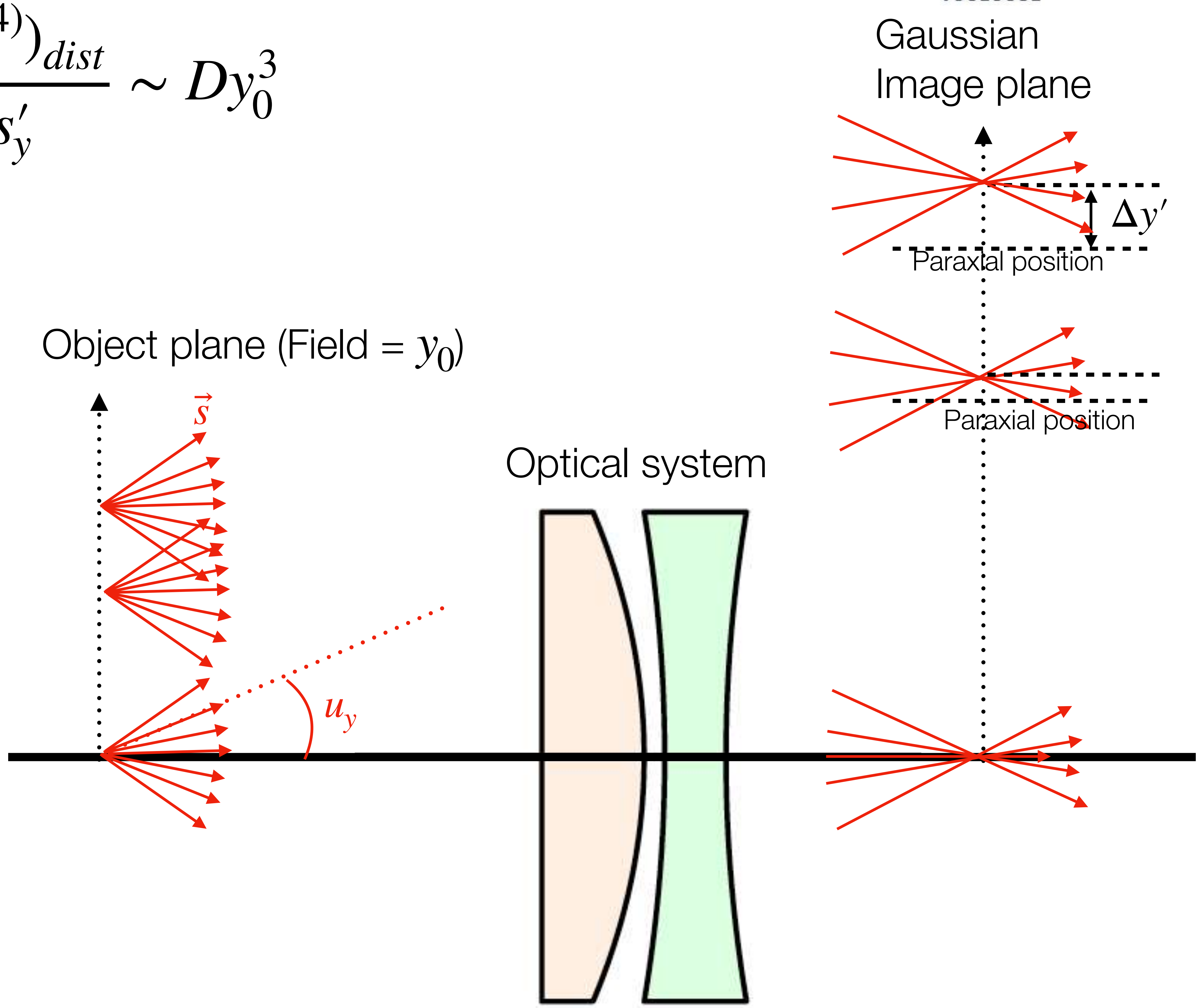

Aberrations series expansion

➡ Representation using a 2-dimensional Taylor series expansion: **field of view** y and **aperture angle** u_y **or pupil plane coordinate** (r, θ)

➡ The sum of the exponents must be constant according to the order of the aberration considered

Primary aberrations
Seidel aberrations

Paraxial (linear)

Secondary aberrations

			Field y →					
			Spherical	**Coma**	**Astigmatism**			
			y^0	y^1	y^2	y^3	y^4	y^5
Aperture r ↓	**Distortion**	r^0		$y \cos\theta$ Tilt		$y^3 \cos\theta$ Distortion primary		$y^5 \cos\theta$ Distortion secondary
		r^1	r^1 Defocus		$y^2 r^1 \cos^2\theta$, $y^2 r^1$ Astig./Curvat.		$y^4 r^1 \cos^2\theta$, $y^4 r^1$	
		r^2		$y r^2 \cos\theta$ Coma primary		$y^3 r^2 \cos^3\theta$, $y^3 r^2 \cos\theta$		
		r^3	r^3 Spherical primary		$y^2 r^3 \cos^2\theta$, $y^2 r^3$			
		r^4		$y r^4 \cos\theta$ Coma secondary				
		r^5	r^5 Spherical secondary					

Going back to the quasi-real situation (paraxial + Seidel aberrations) …

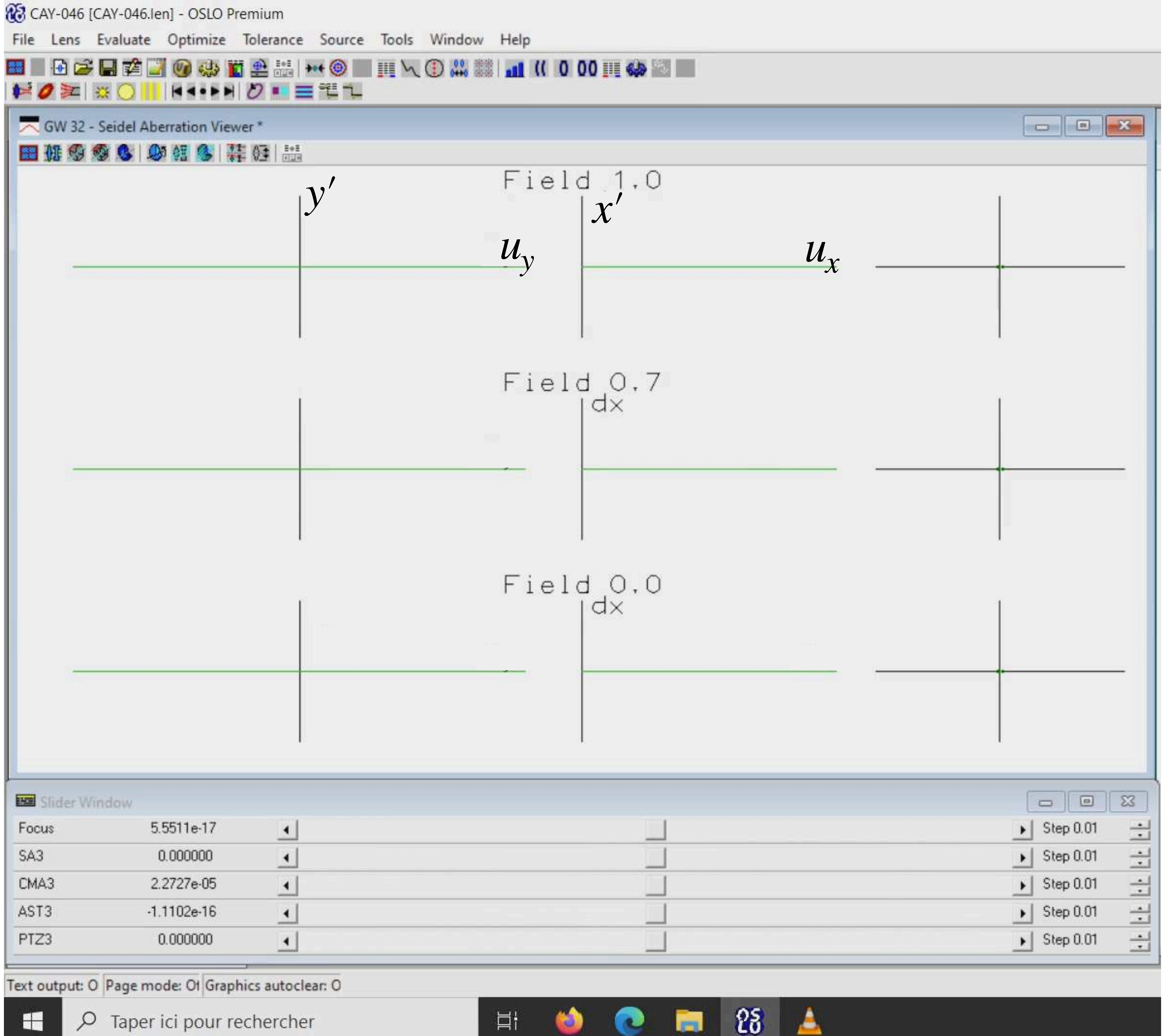

$$y' = y_{para} + \Delta y' = -\frac{1}{n'}\frac{\partial L_A}{\partial s'_y}$$

Various kind of aberrations representations

Pupil plane $(u_x, u_y) \rightarrow (x_p, y_p) \rightarrow (r_p, \theta)$

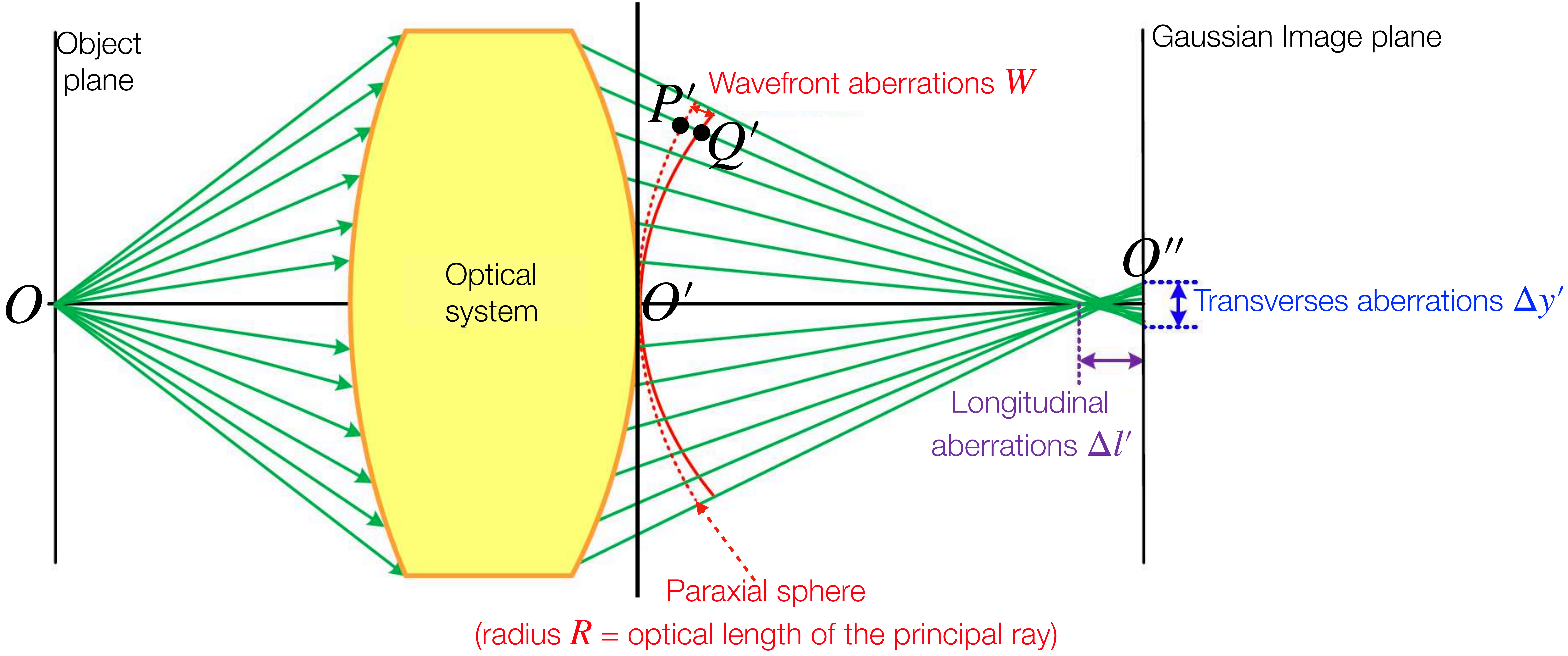

Wavefront aberrations W = differences between radius of Principal ray wavefront and the real wavefront in the pupil plane :

$$W = L_{P'Q'} = L_{OQ'} - L_{OP'} \approx L_A - L_A^{(2)} = L_A^{(4)}$$

Transverse aberrations $\Delta y'$ are then simply derived from wavefront aberration by differentiate it relatively to pupil coordinate (i.e. the aperture angles)

$$\Delta y' = -R \, . \frac{\partial W(x_p, y_p)}{\partial y_p}$$

Seidel primary aberrations : wavefront vs transverse aberrations

A

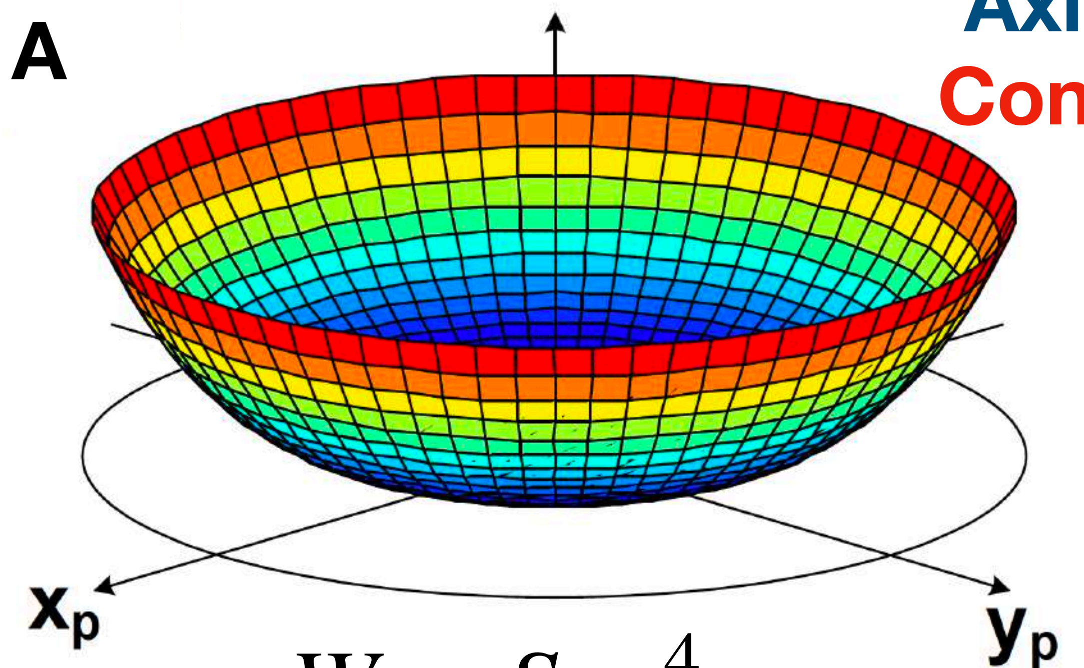

Axis
Const

$$W = S\,.\,r_p^4$$

$$\Delta y' = S\,.\,r_p^3 cos(\varphi_p)$$

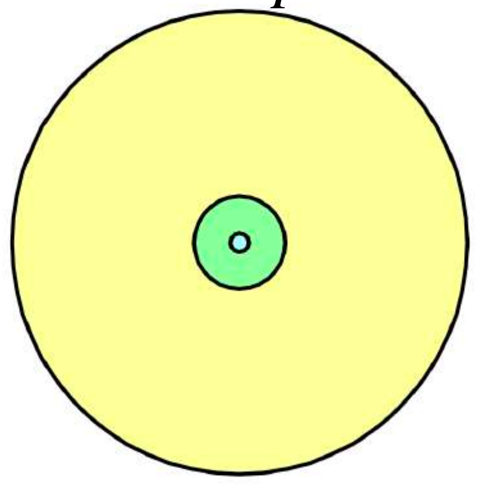

Point
Const

$$\Delta x' = S\,.\,r_p^3 sin(\varphi_p)$$

B

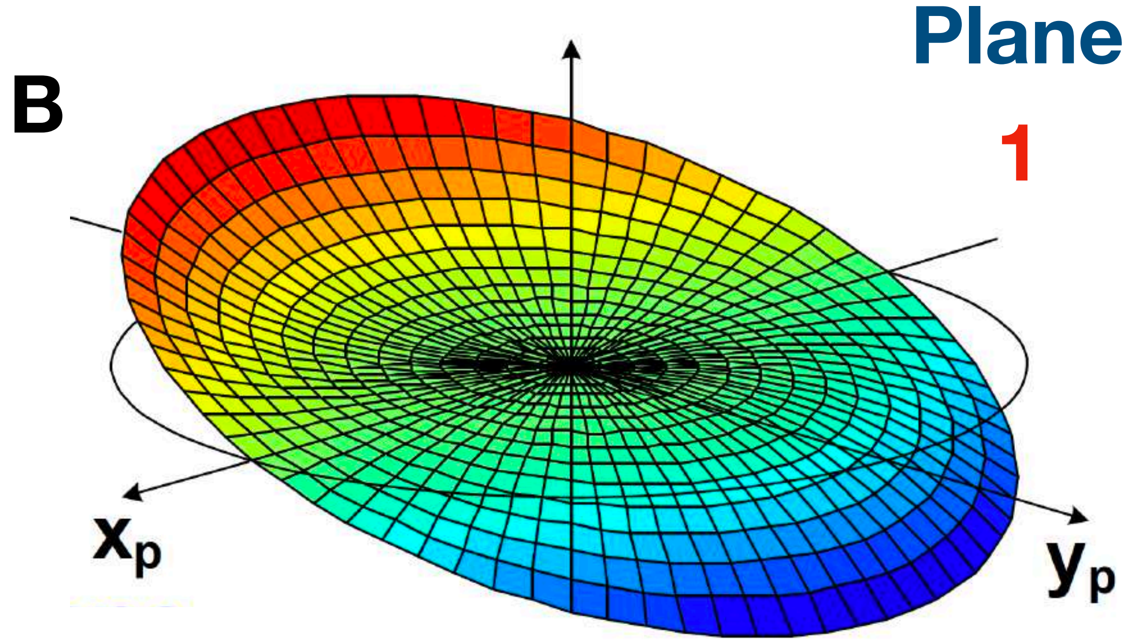

Plane
1

$$W = C\,.\,y r_p^3 cos(\varphi_p)$$

$$\Delta y' = C\,.\,y\,.\,r_p^2(2 + cos(2\varphi_p))$$

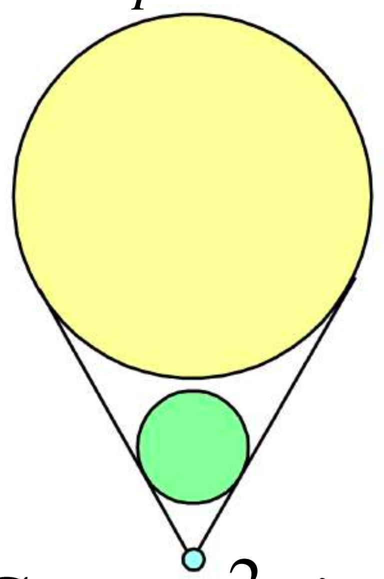

Line
2

$$\Delta x' = C\,.\,y\,.\,r_p^2 sin(2\varphi_p)$$

C

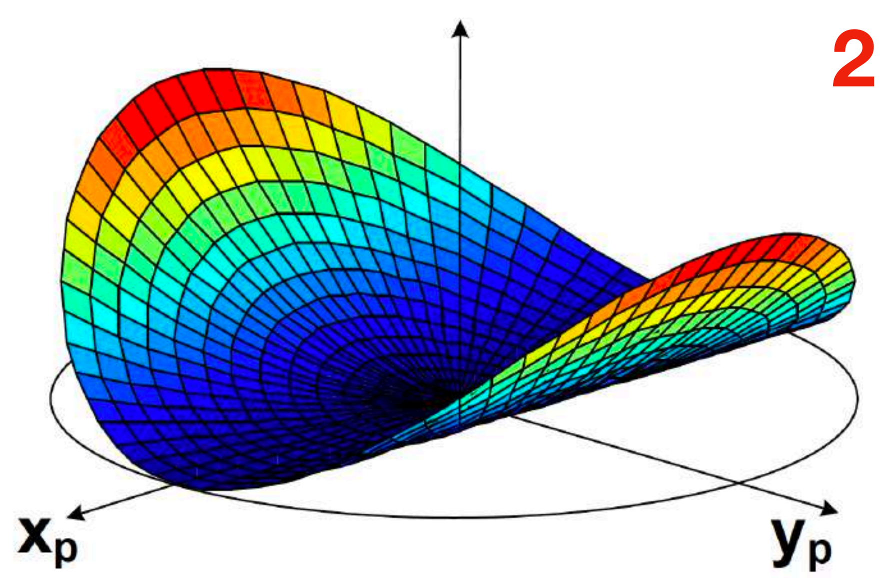

Two planes
2

$$W = A\,.\,y^2\,.\,r_p^2 cos^2(\varphi_p)$$

$$\Delta y' = A\,.\,y^2\,.\,r_p cos(\varphi_p)$$

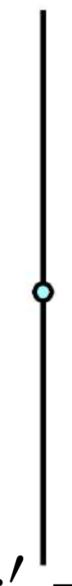

2 lines
1

$$\Delta x' = 0$$

D

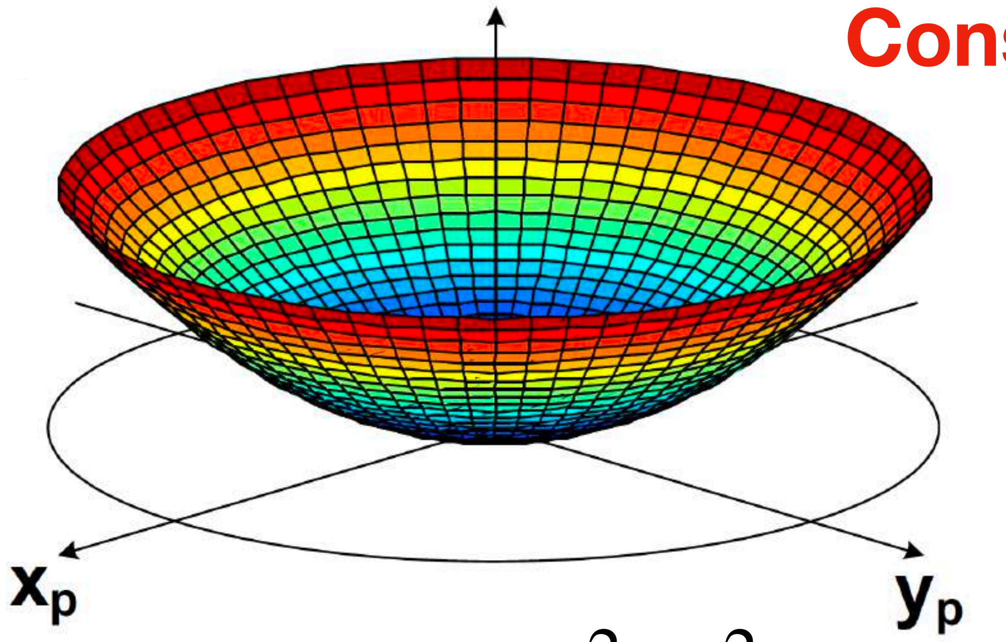

Axis
Const

$$W = P\,.\,y^2\,.\,r_p^2$$

$$\Delta y' = P\,.\,y^2\,.\,r_p cos(\varphi_p)$$

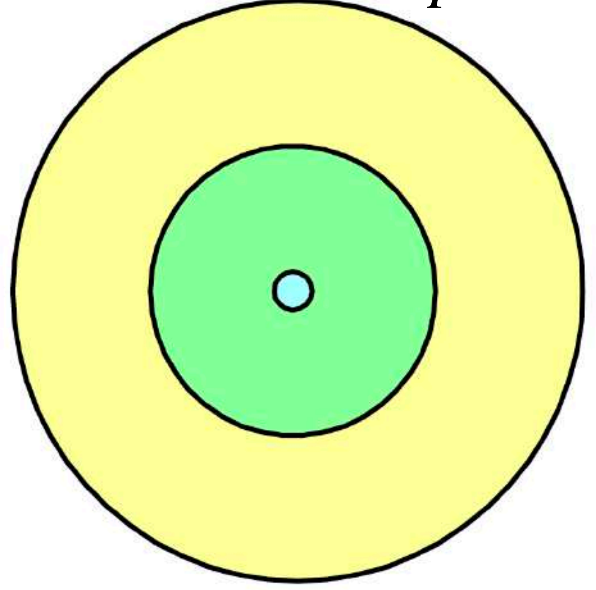

Point
1

$$\Delta x' = P\,.\,y^2\,.\,r_p sin(\varphi_p)$$

E

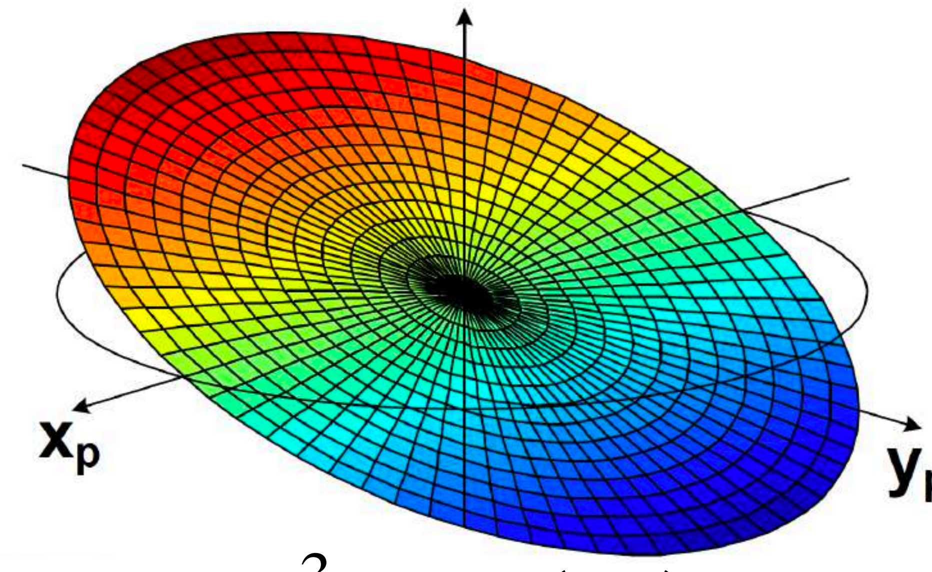

One plane
1

$$W = D\,.\,y^3 r_p cos(\varphi_p)$$

$$\Delta y' = D\,.\,y^3$$

Line
Const

$$\Delta x = 0$$

A. Spherical aberration
B.Coma
C.Astigmatism
D.Petzval curvature
E.Distorsion

Symmetry with respect to ....

Periodicity ...

Mathematical optics and the design of high-performance instruments

- **Ernst Karl Abbe (1840-m. 1905)**

  « Beiträge zur Theorie des Mikroskops und der mikroskopischen Wahrnehmung (1873) »

Resolution limit
for optical instruments

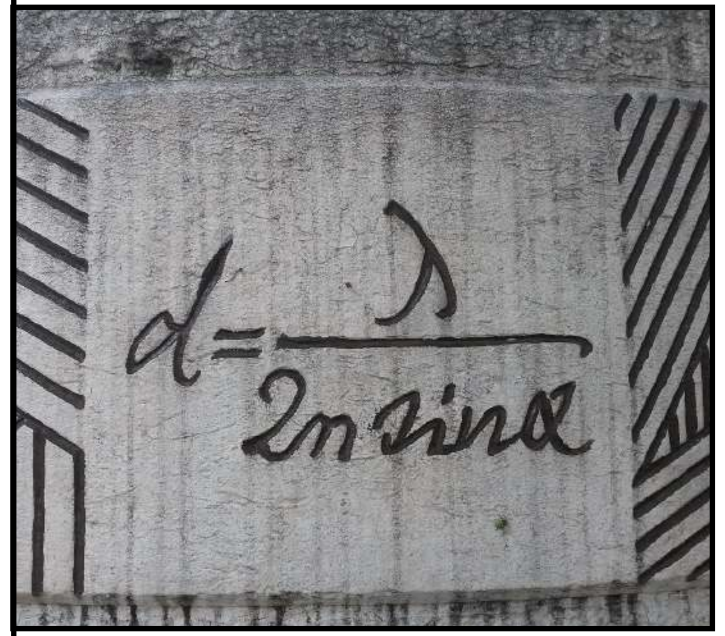

Development of corrected optics

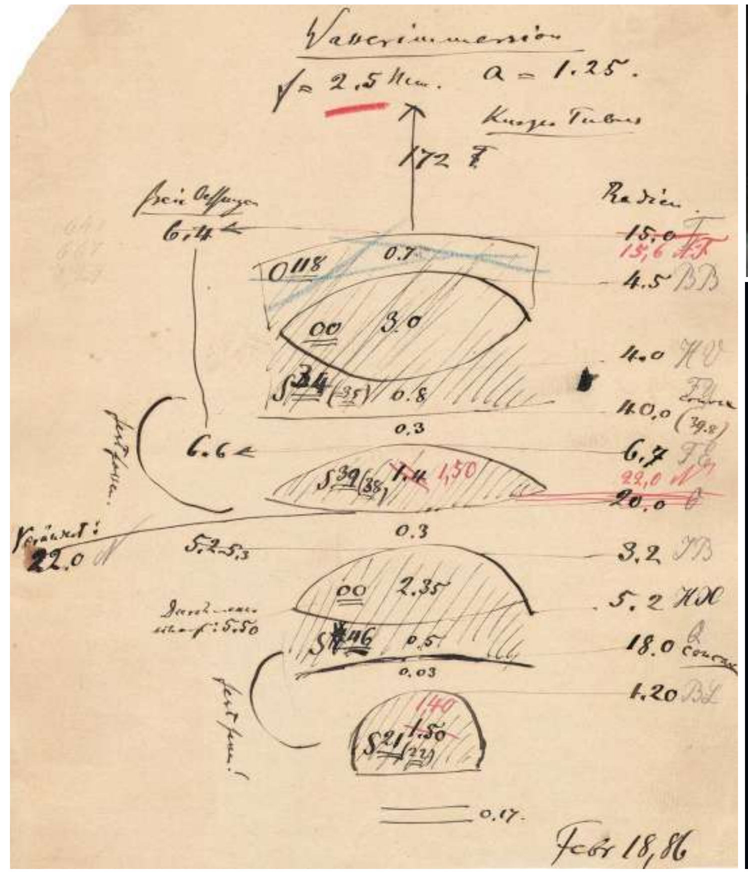

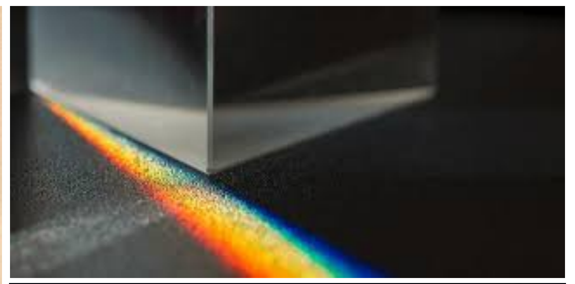

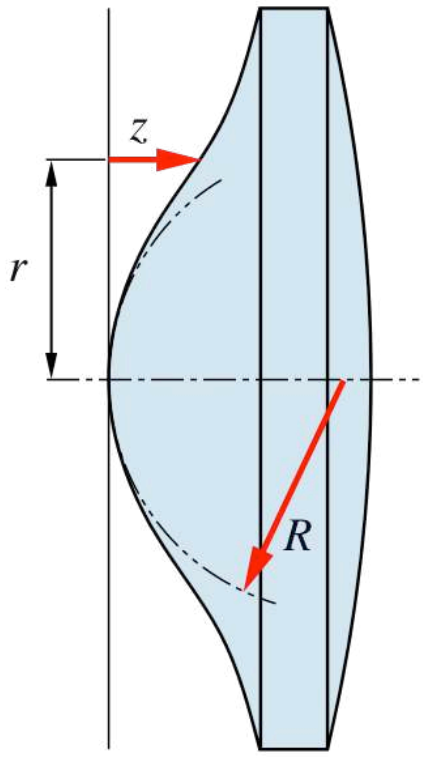

- **Carl Friedrich Zeiss (1816-m. 1888)**

  « Zeiss company » : collaboration with Abbe

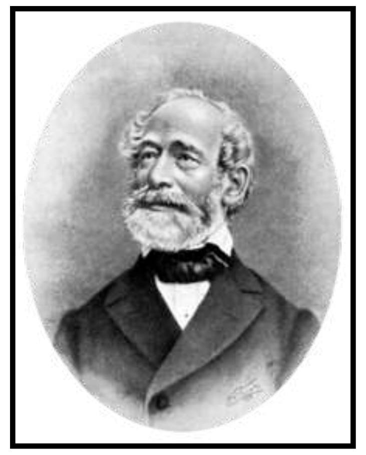

Zeiss microscope (1879)
with Abbe optics

New illumination system
developed by Abbe

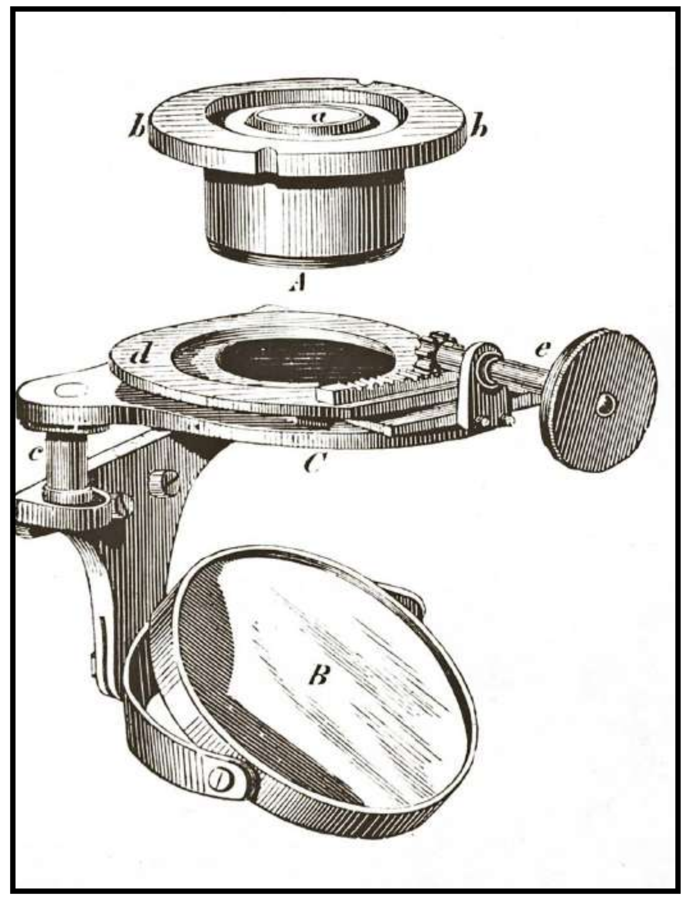

Today: example of a smartphone lens

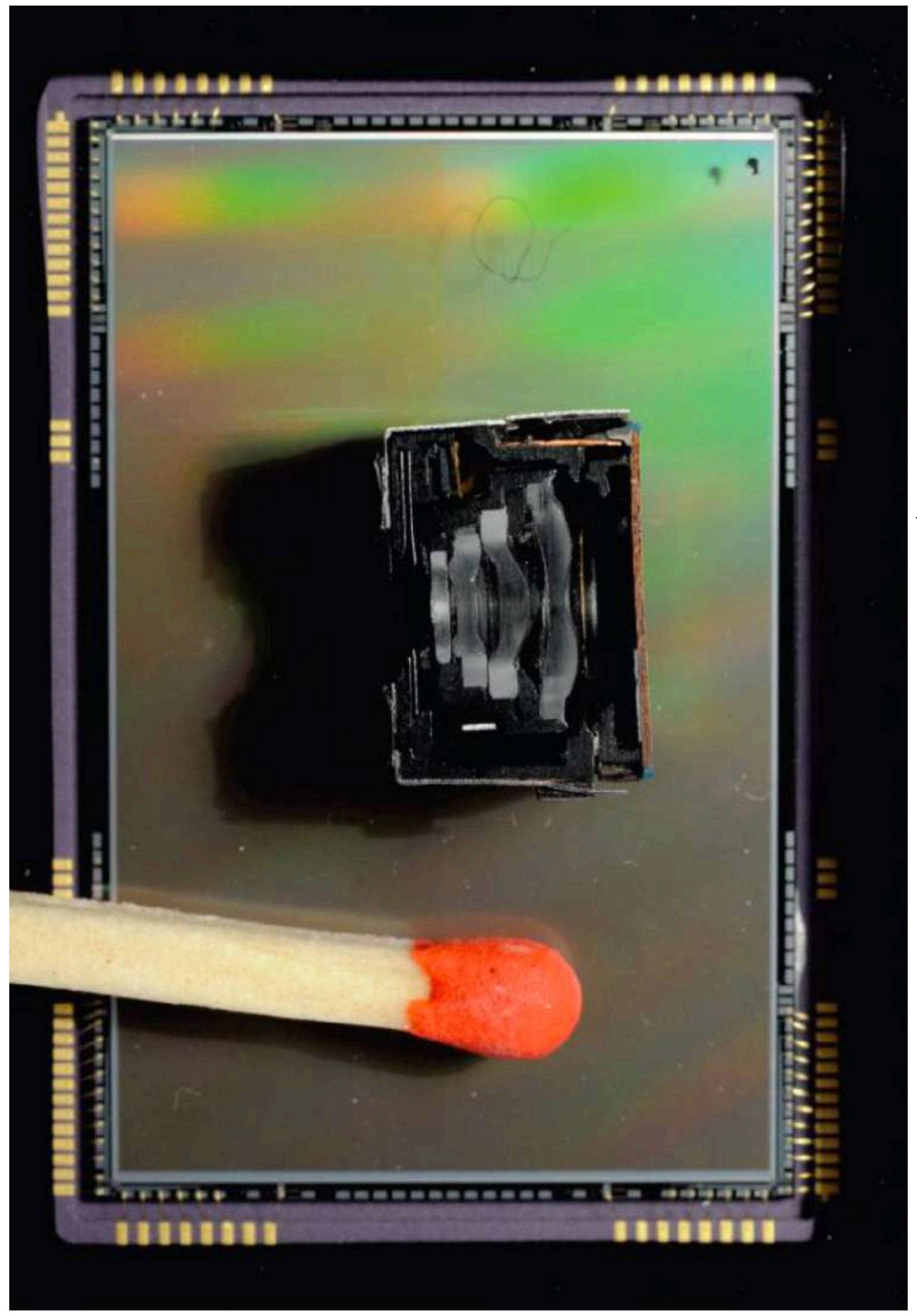

Spots diagram
(square size $30\mu m$)

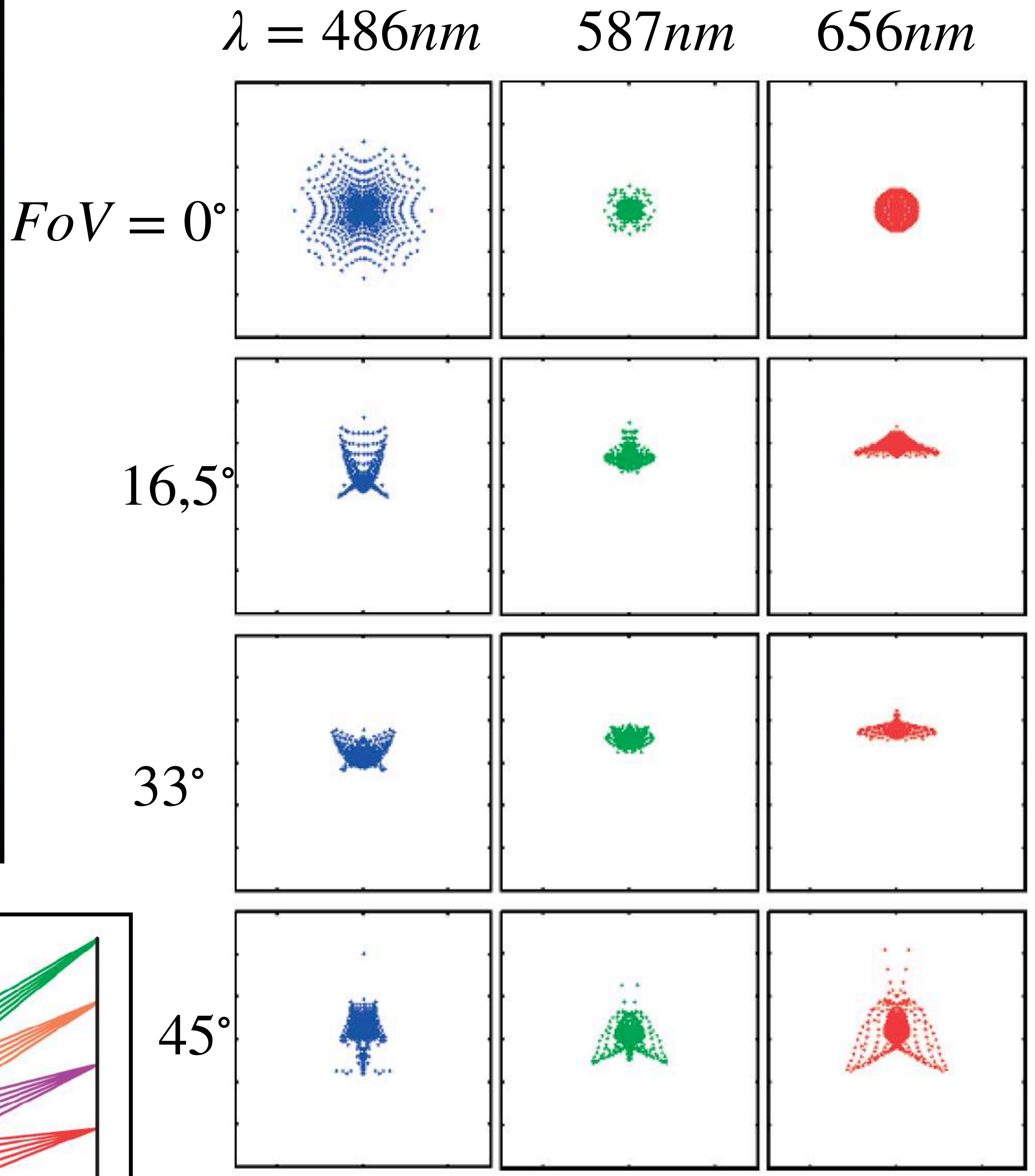

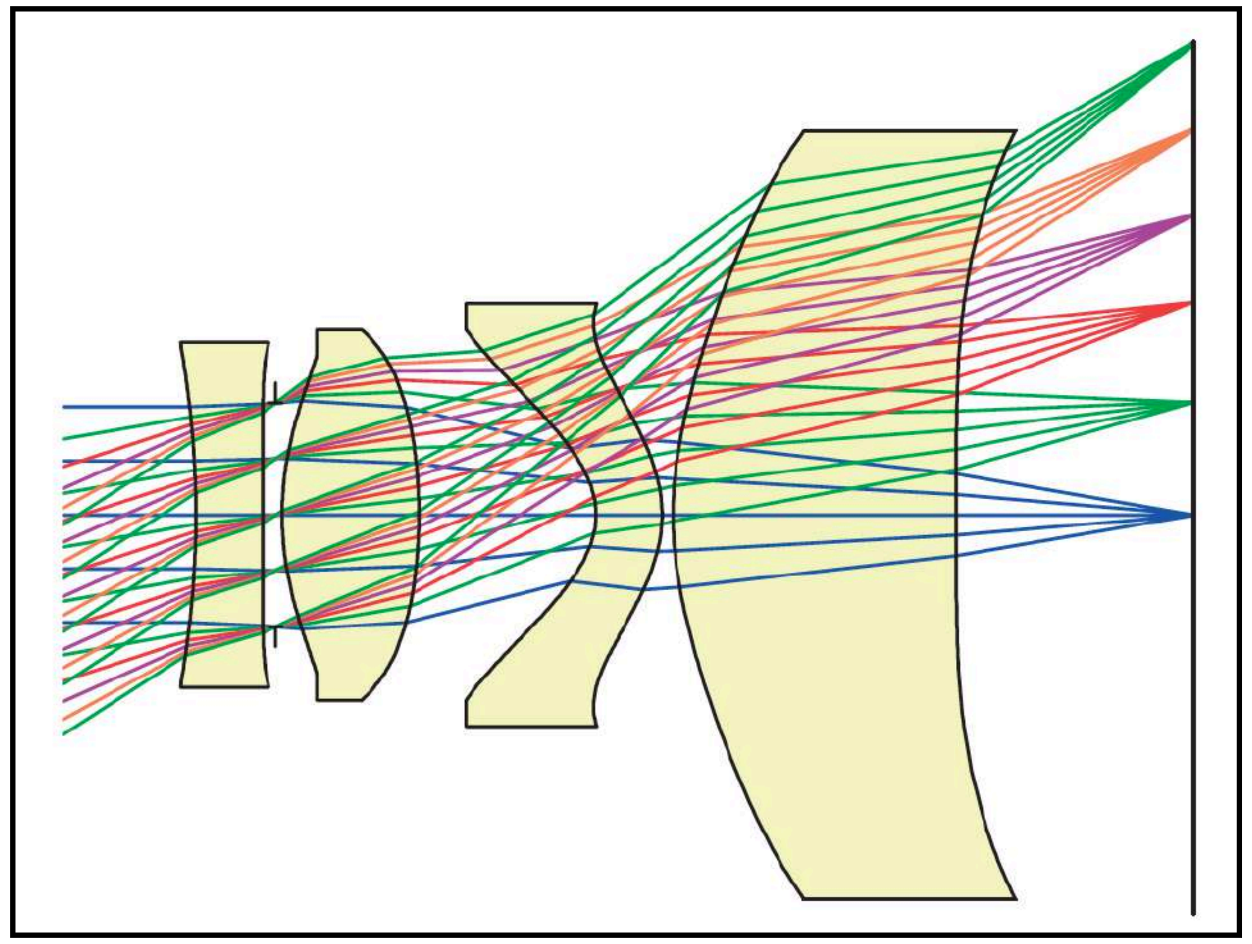

Corrected microscopy: how far can we go?

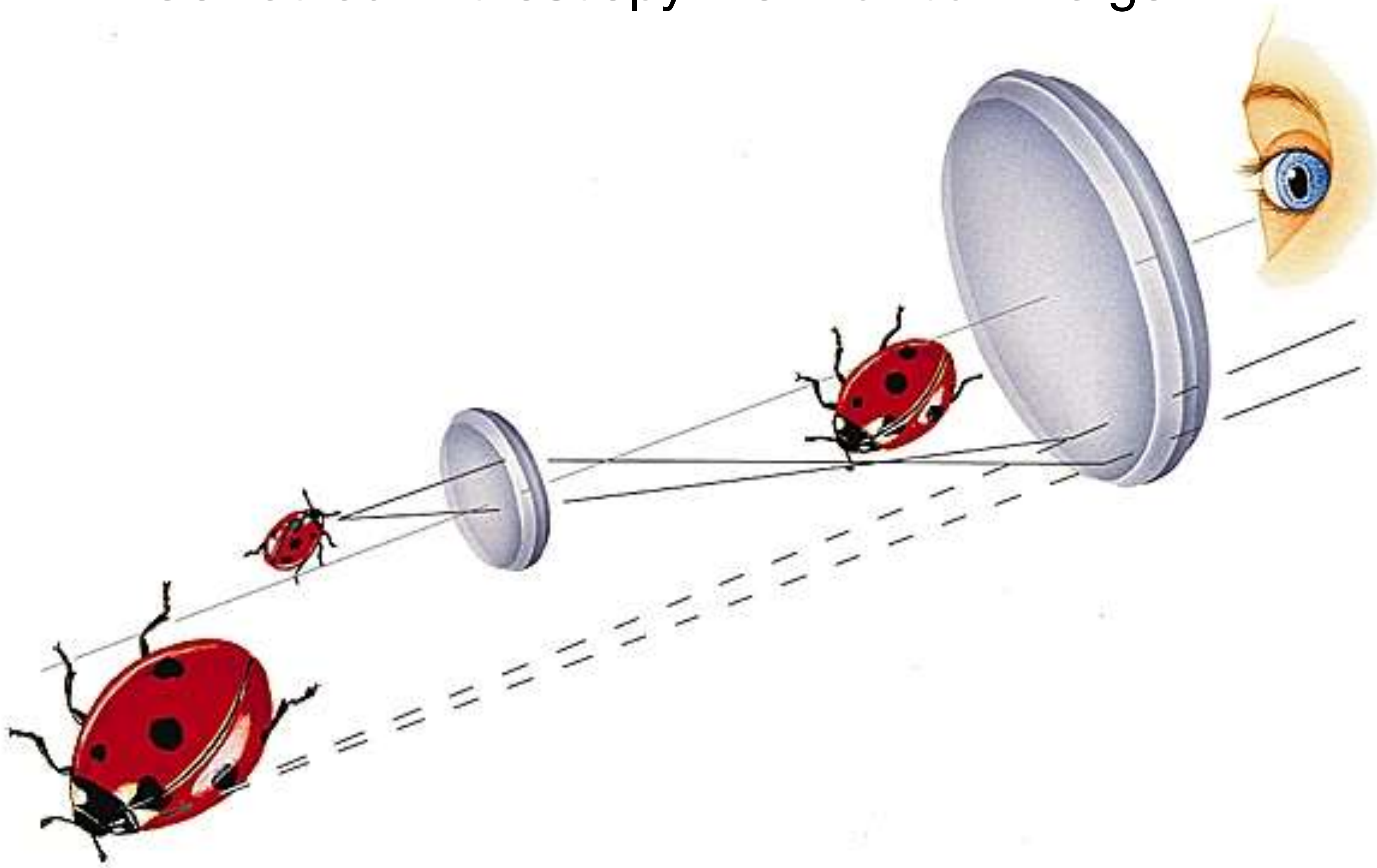

After a while, the points on the object are no longer points in the image ...

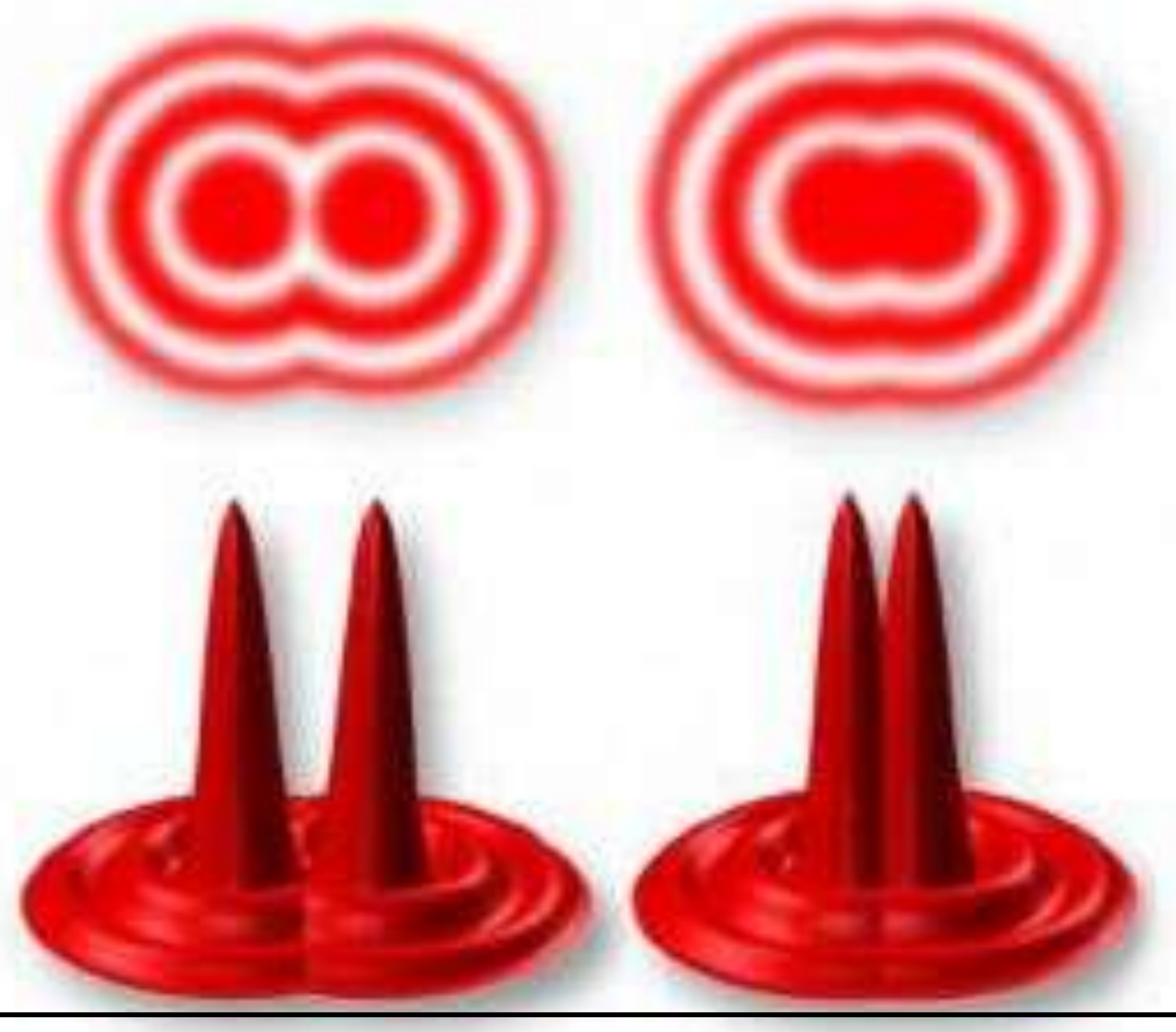

Why ? And how does this affect the resolution?

Here is a 'resolution test' object

Point spread function due to diffraction

Final image of the object

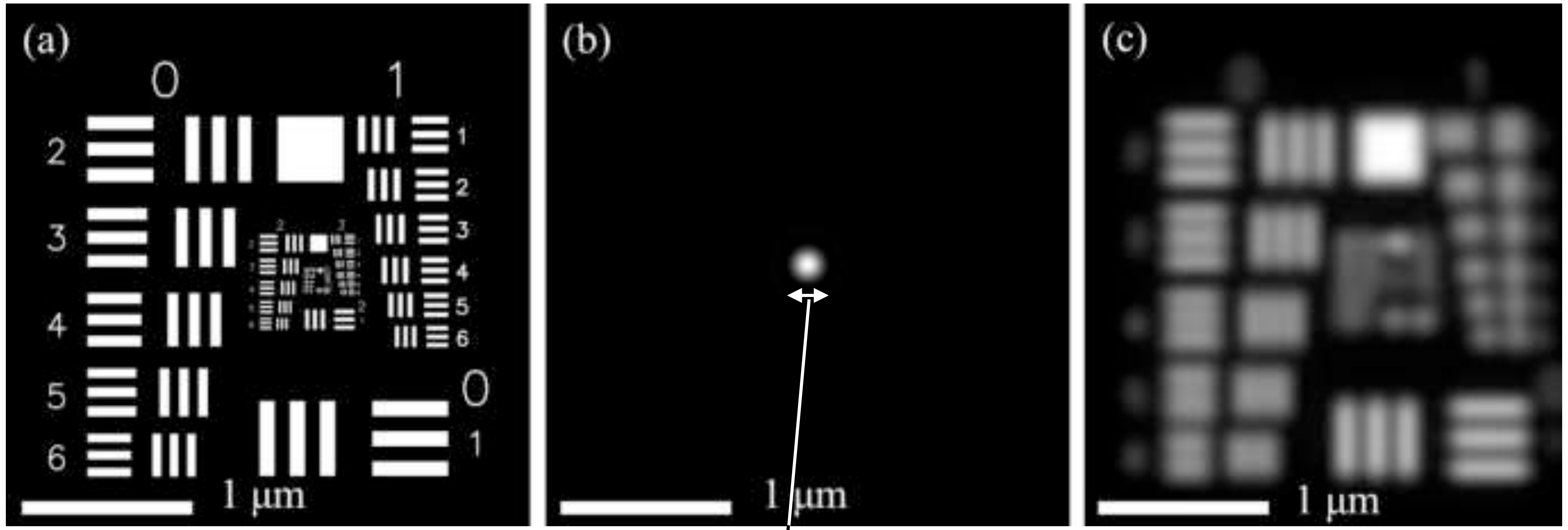

Abbe's formula : $\boxed{\Delta x = k \,.\, \dfrac{\lambda}{NA}}$

2 Introduction to Variational mechanics

General history, introduction to main concepts and application to charged particles in static electromagnetic fields

The revolution of the principle of least action: variational mechanics

- **Joseph Louis de Lagrange (1736-m. 1813)**

First part of the history :

« Application de la méthode dans le mémoire précédent à la solution de différents problèmes de la dynamique » (1744)

APPLICATION DE LA MÉTHODE
EXPOSÉE DANS LE MÉMOIRE PRÉCÉDENT
À LA SOLUTION DE
DIFFÉRENTS PROBLÈMES DE DYNAMIQUE.

(*Miscellanea Taurinensia*, t. II, 1760-1761.)

Second part of the history :

« Recherche sur la libération de la Lune» (1780)

THÉORIE
DE LA LIBRATION DE LA LUNE,
ET
DES AUTRES PHÉNOMÈNES QUI DÉPENDENT DE LA FIGURE NON SPHÉRIQUE
DE CETTE PLANÈTE.

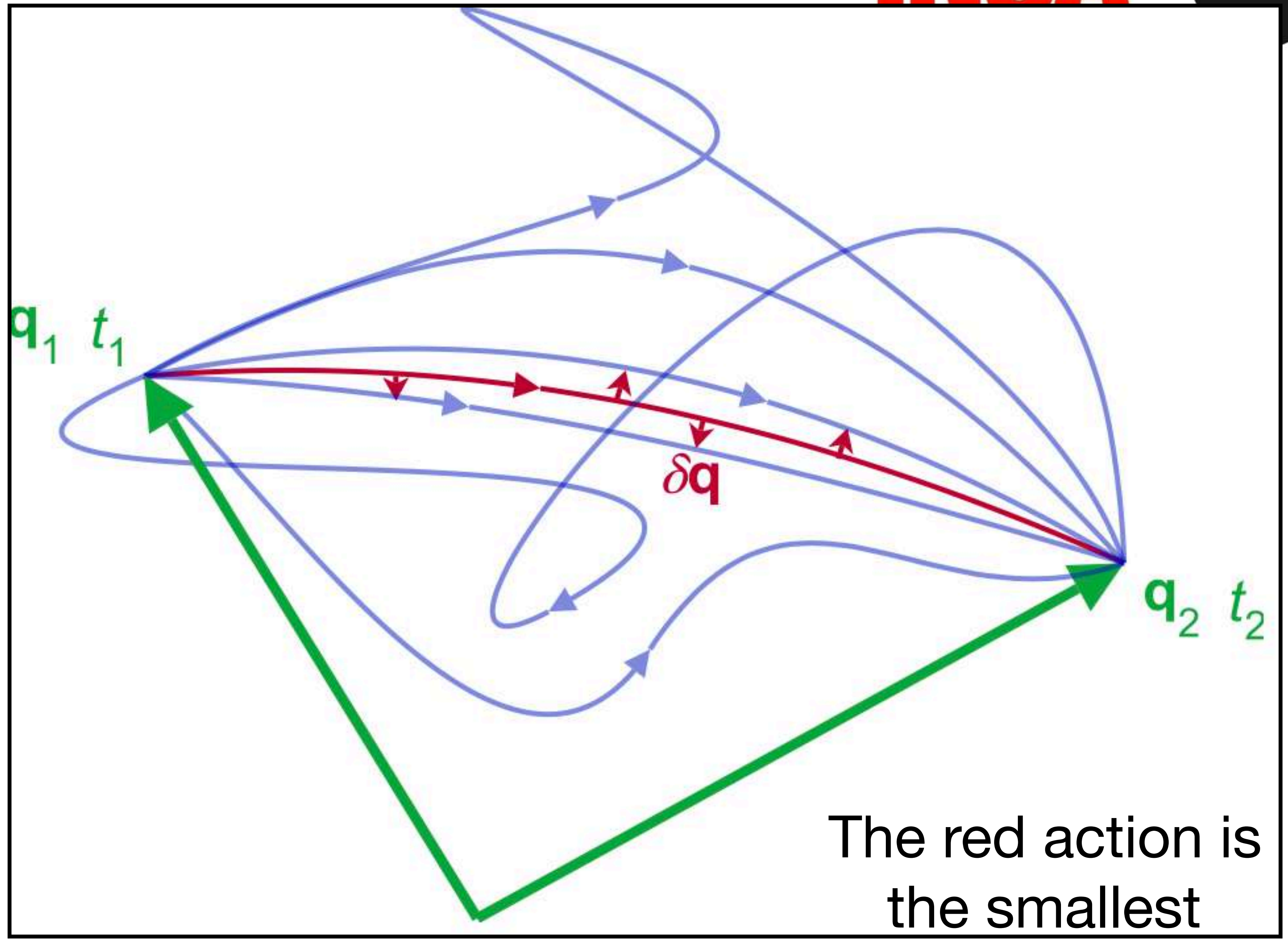

The red action is the smallest

- **William Rowan Hamilton (1805-m. 1865)**

ON A GENERAL METHOD OF EXPRESSING THE PATHS OF LIGHT, AND OF THE PLANETS, BY THE COEFFICIENTS OF A CHARACTERISTIC FUNCTION

By

William Rowan Hamilton

(Dublin University Review and Quarterly Magazine, 1 (1833), pp. 795–826.)

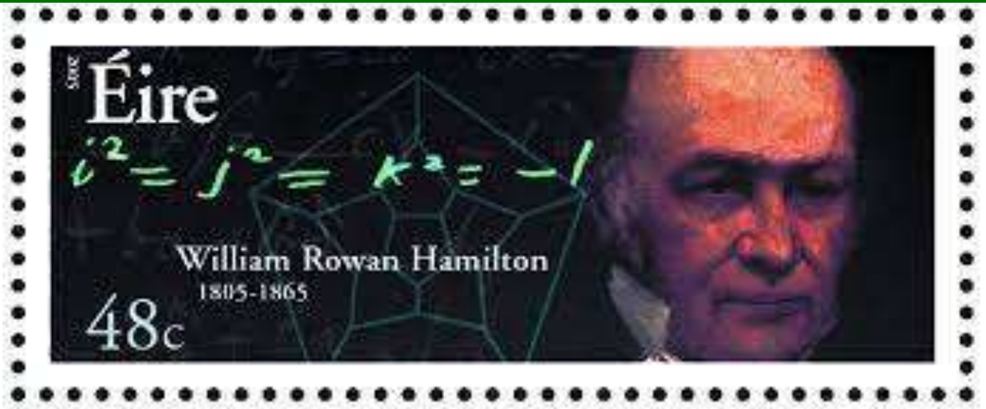

The action :

energy balance on a trajectory

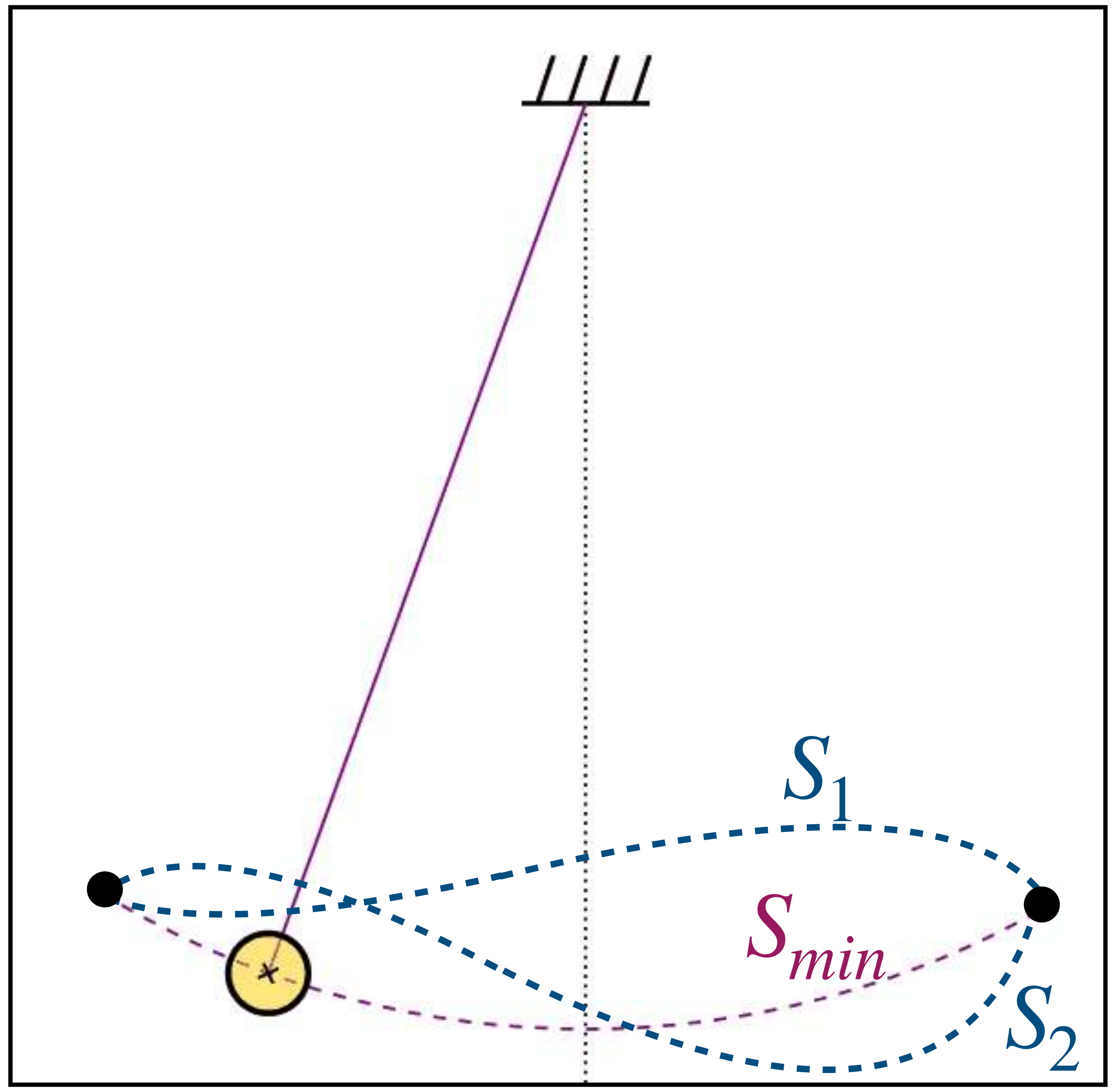

Newtonian, Lagrangian and Hamiltonian approaches to physics

➡ What is the best approach to solve this complex problem?

<u>The newton approach ?</u>
Possible but …
heavy and dirty calculus

$$\Sigma \overrightarrow{F} = m\overrightarrow{a}$$

<u>The variational approach ?</u>
100% equivalent but well
adapted mathematically

$$\mathscr{L} = K - V$$

$$\delta S = \delta \int_{t_0}^{t_1} \mathscr{L}(x, y, z, \dot{x}, \dot{y}, \dot{z}, t)dt = 0$$

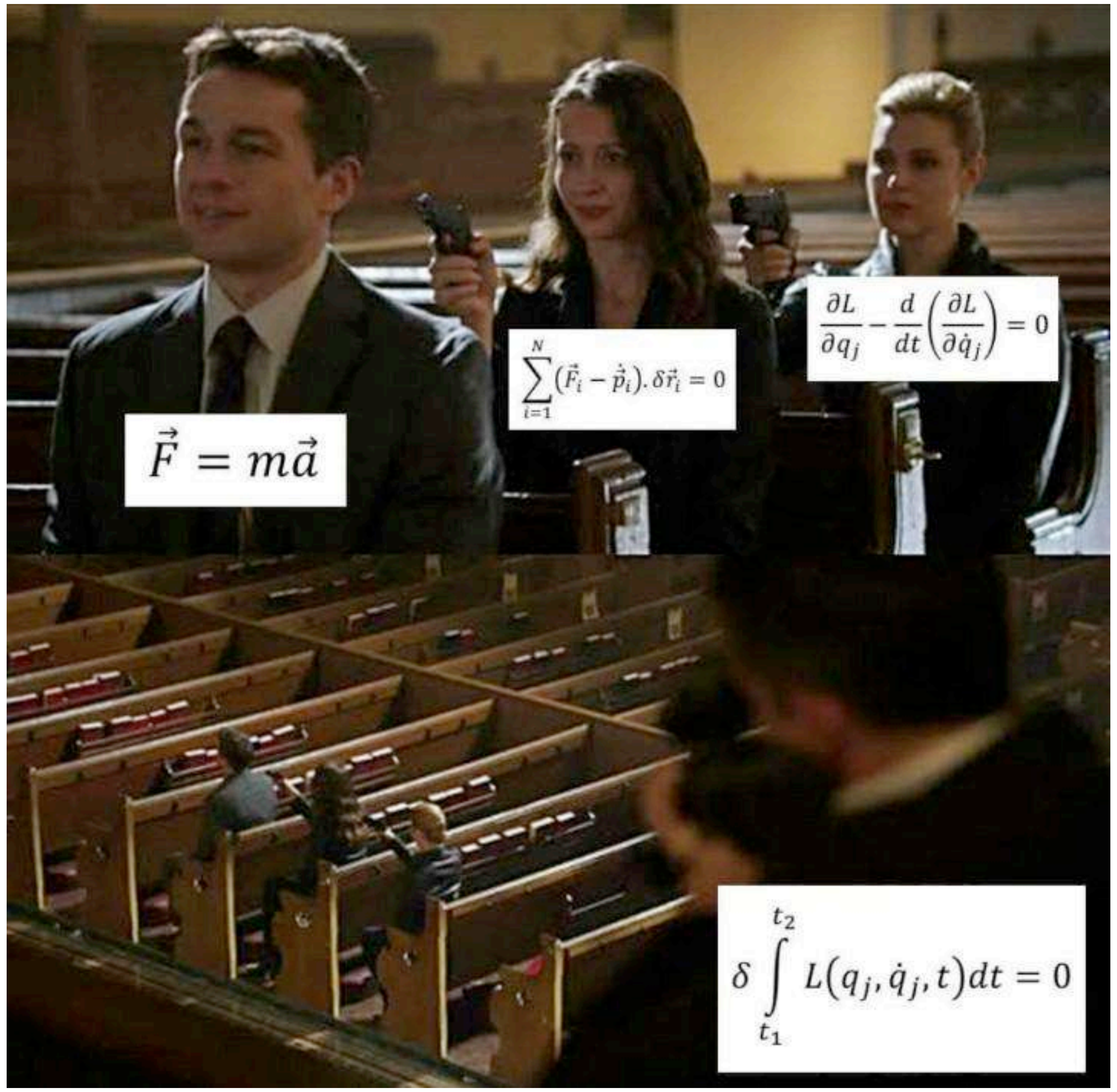

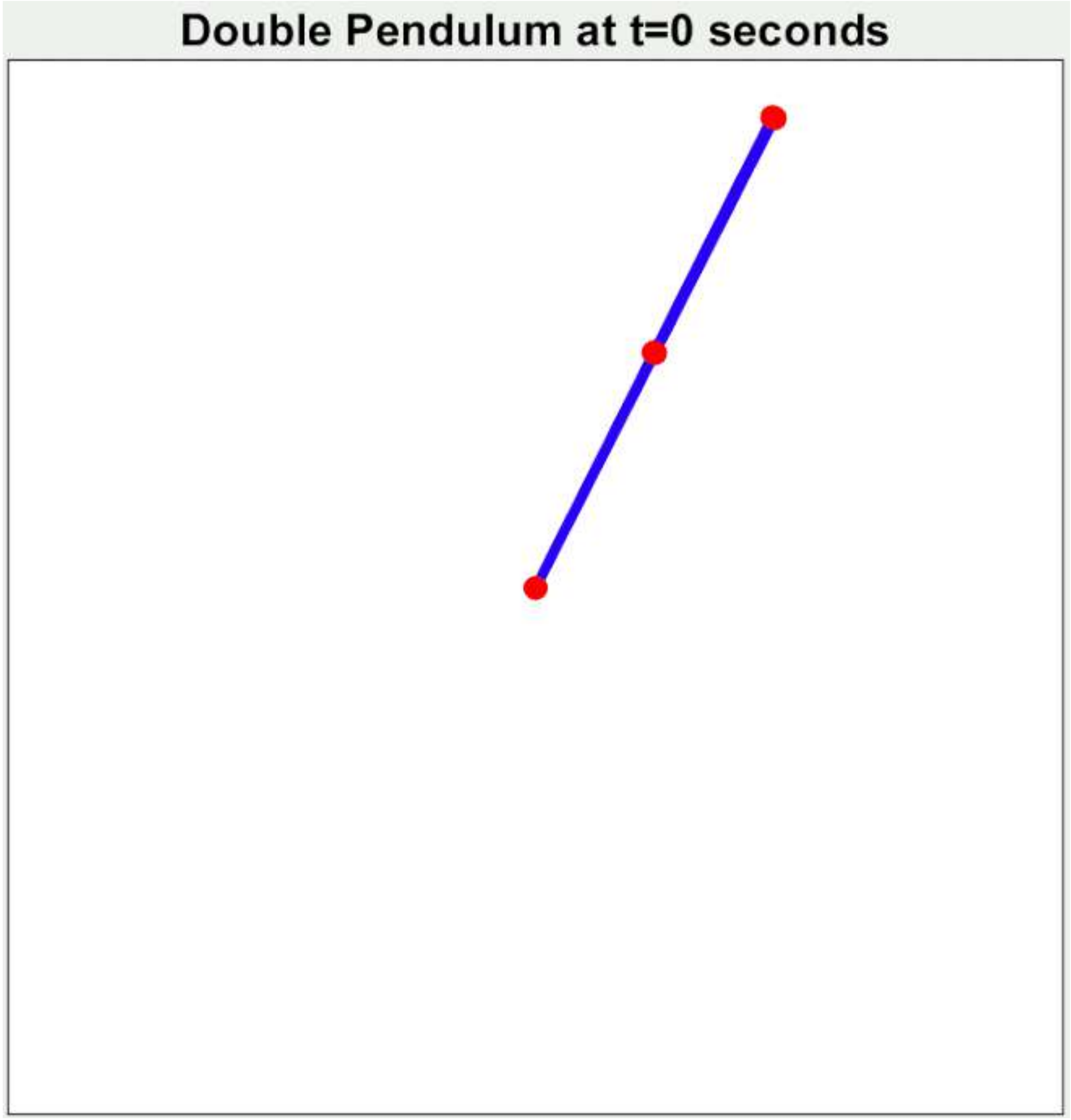

➡ Same as in optics with the time

➡Characteristic function in mechanics : **<u>the action S</u>**

Optical/mechanical equivalence: a simple example

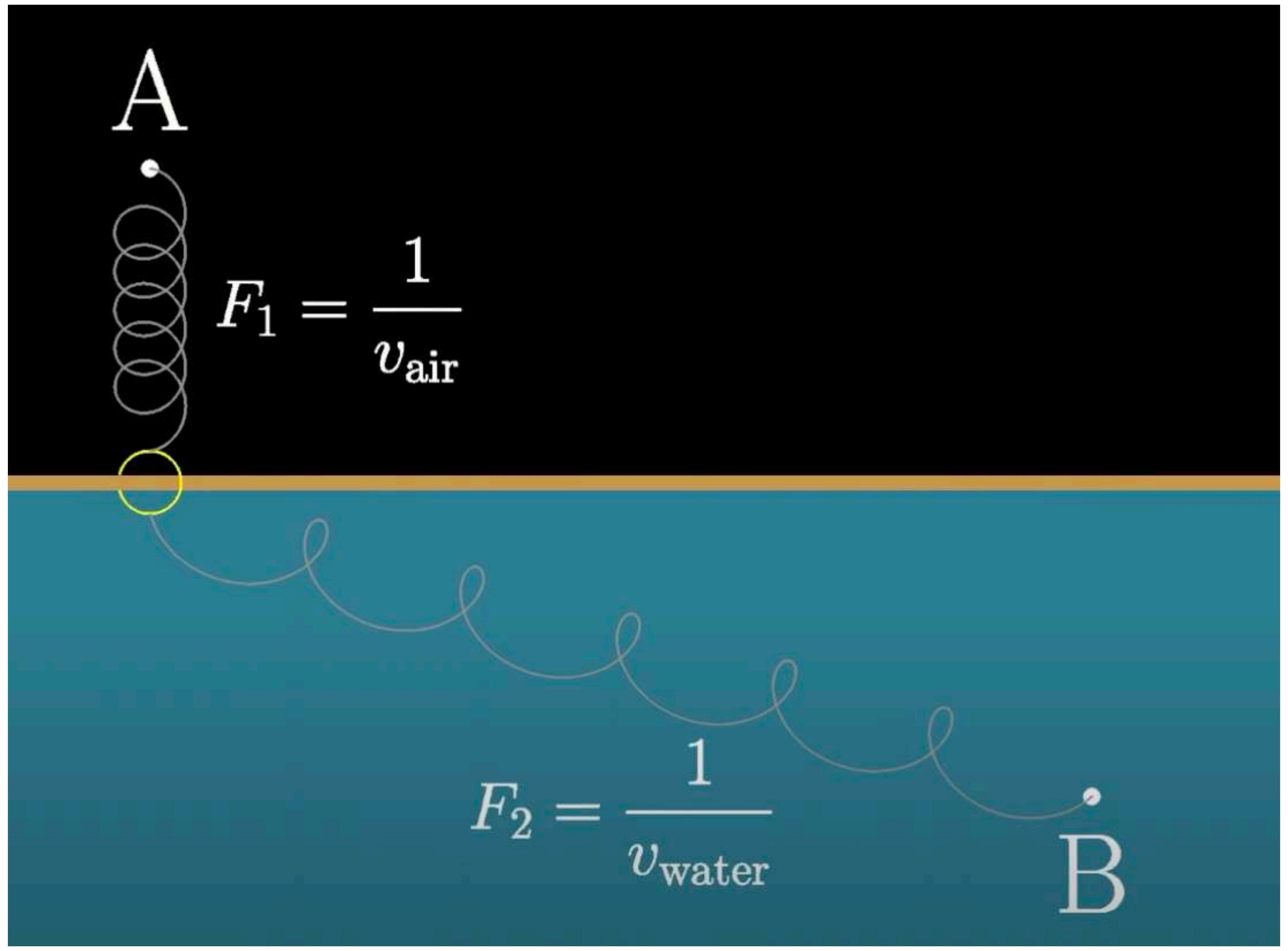

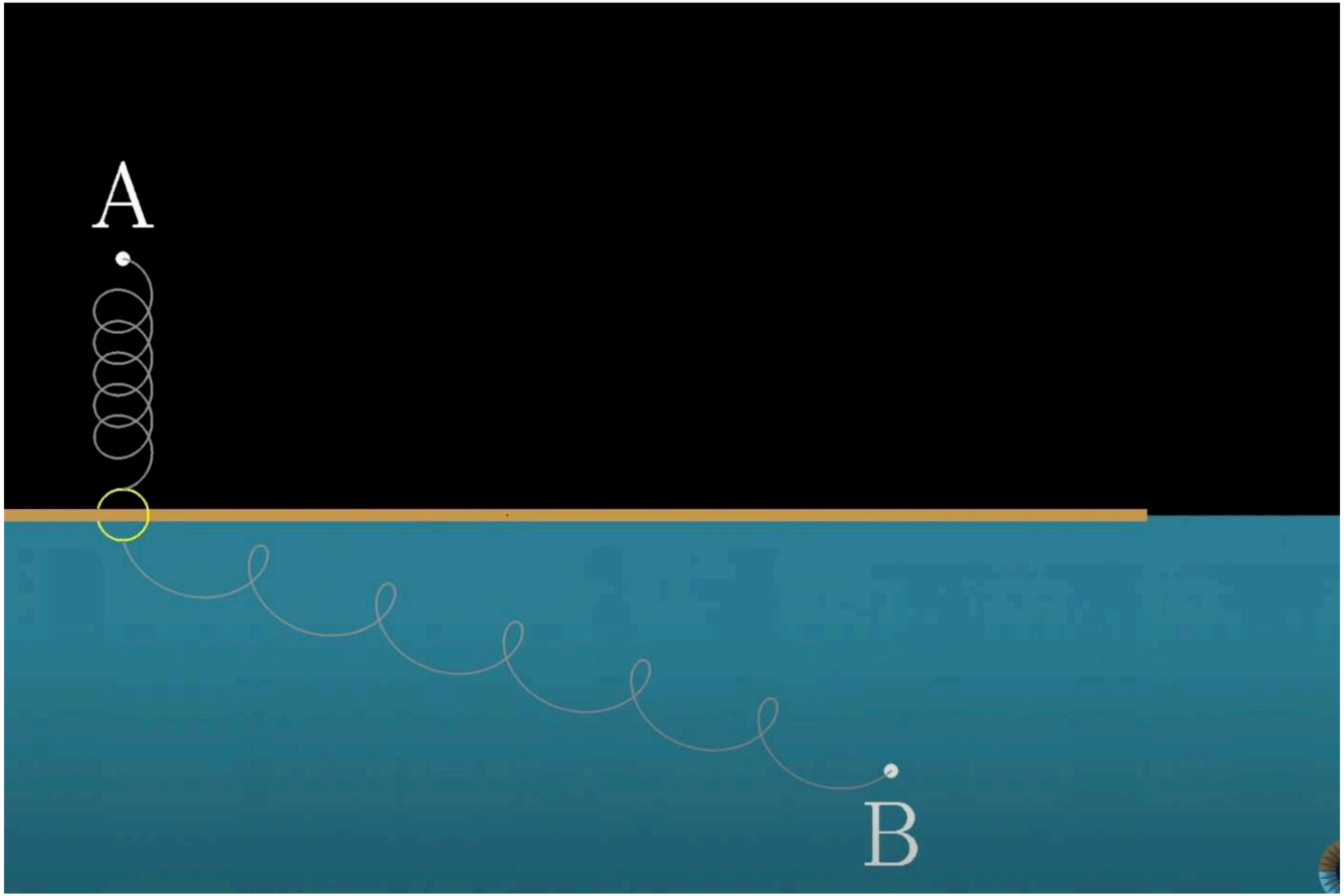

Discovery of electrons and the beginning of electron optics

- **Joseph John Thomson (1856- m. 1940)**
  « *Cathode rays (1897)* »

Discovery of electrons. Trajectories of these particles deflected by an electric or magnetic field.

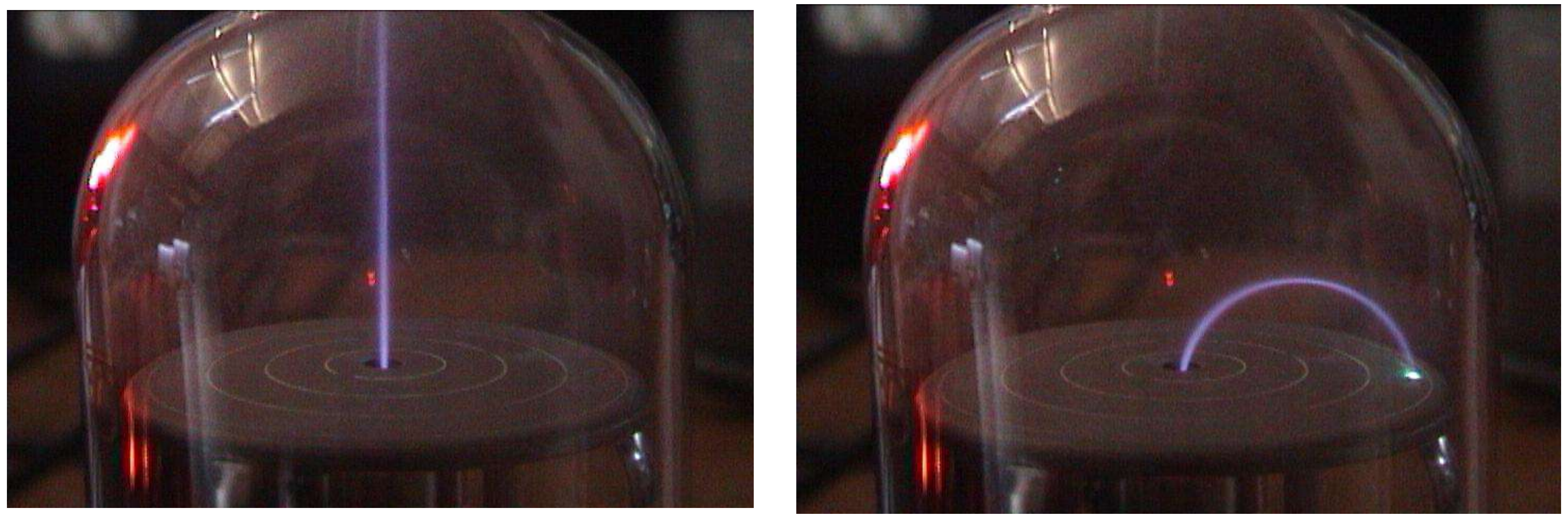

Analogy with the refraction of light

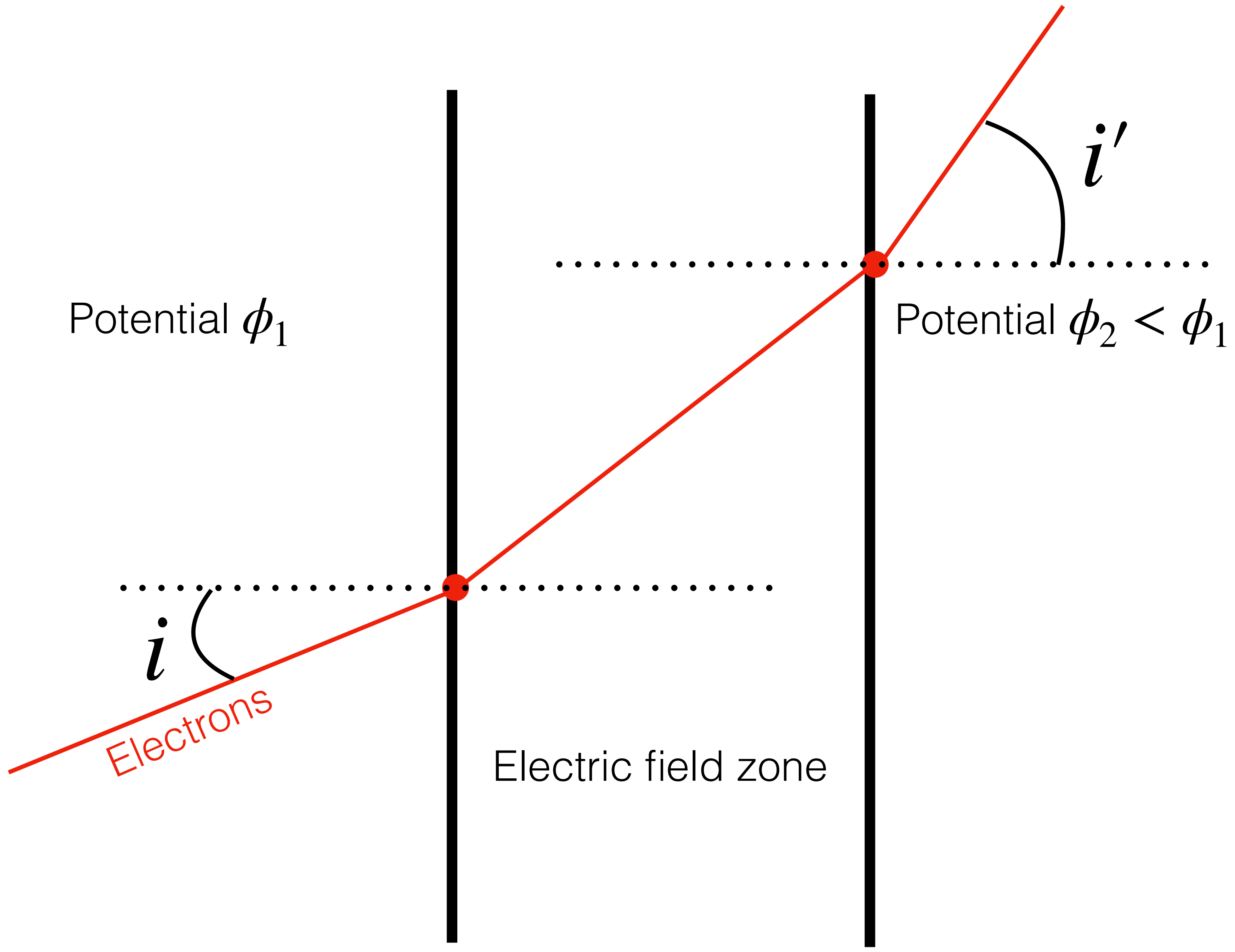

$$\frac{\sin(i)}{\sin(i')} = \frac{\sqrt{\Phi_2}}{\sqrt{\Phi_1}}$$

- **Louis de Broglie (1892-m. 1987)**
  « Recherches sur la théorie des quanta (1905) »

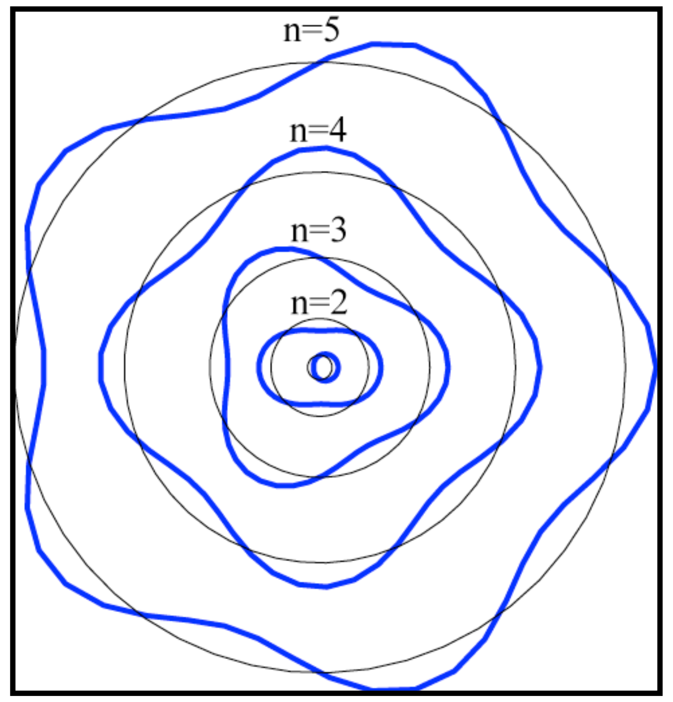

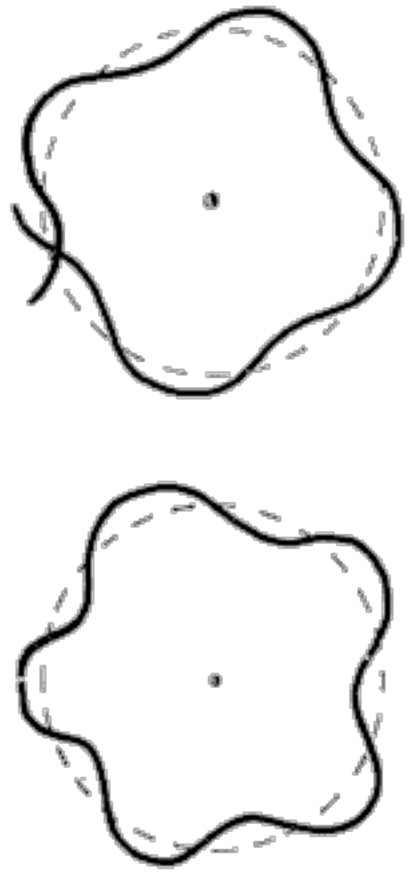

Abbe's formula

$$\Delta x \propto \frac{\lambda}{NA}$$

$$\Downarrow$$

De Broglie's wavelength of an electron

$$\lambda = \frac{h}{mv}$$

Acceleration (keV)	Wavelength (pm)
100	3.70
200	2.51
300	1.97
400	1.64
1000	0.87

Variational methods to study charged particles trajectories

Integral picture of classical mechanics : definition of **action** S

$$\delta S = \delta \int_{t_0}^{t_1} \mathscr{L}(x, y, z, \dot{x}, \dot{y}, \dot{z}, t)dt = 0$$

Lagrangian L

$$\mathscr{L} = K - V$$

Kinetic energy K

Potential energy V

After part integration we find a differential formulation of the least action principle :

Euler-Lagrange equations

$$\frac{\partial \mathscr{L}}{\partial \vec{r}} - \frac{d}{dt}\frac{\partial \mathscr{L}}{\partial \vec{v}} = 0$$

Strictly equivalent to the Newton's equations of dynamic

Lagrangian of a charged particle Q in an EM field $(\vec{A}, U)$

$$\mathscr{L} = m_r c^2 \left(1 - \sqrt{1 - (v^2/c^2)}\right) + Q\left(\vec{v}\,.\,\vec{A} - U\right)$$

Canonical impulsion

$$\vec{p} = \frac{\partial \mathscr{L}}{\partial \vec{v}} = m\vec{v} + Q\vec{A}$$

Hamiltonian H :

Legendre transformation of L

$$H(\vec{r}, \vec{p}, t) = \vec{p}\,.\,\vec{v} - \mathscr{L}(\vec{r}, \vec{v}, t)$$

➡ Considering a **static field** $\mathscr{L} = const$ ➡ $H = K + QU = E$ *Energy conservation principle*

Considering a **static field** the variational principle for a charged particle is written as follows:

$$\tilde{S} = S + E(t - t_0) = \int_{z_0}^{z} \tilde{\mathscr{L}} dz,$$

$$L = \frac{\tilde{S}}{q_0} = \int_{z_0}^{z} \mu dz \implies \mu = \frac{1}{q_0}\vec{p}\frac{d\vec{r}}{dz}$$

➡ ***$\tilde{S}/q_0$ is new the characteristic function L in CPO !!***

Least action principle in static field equivalent to Fermat's principle in conventional optic considering $\mu = \frac{1}{q_0}\vec{p}\frac{d\vec{r}}{dz}$

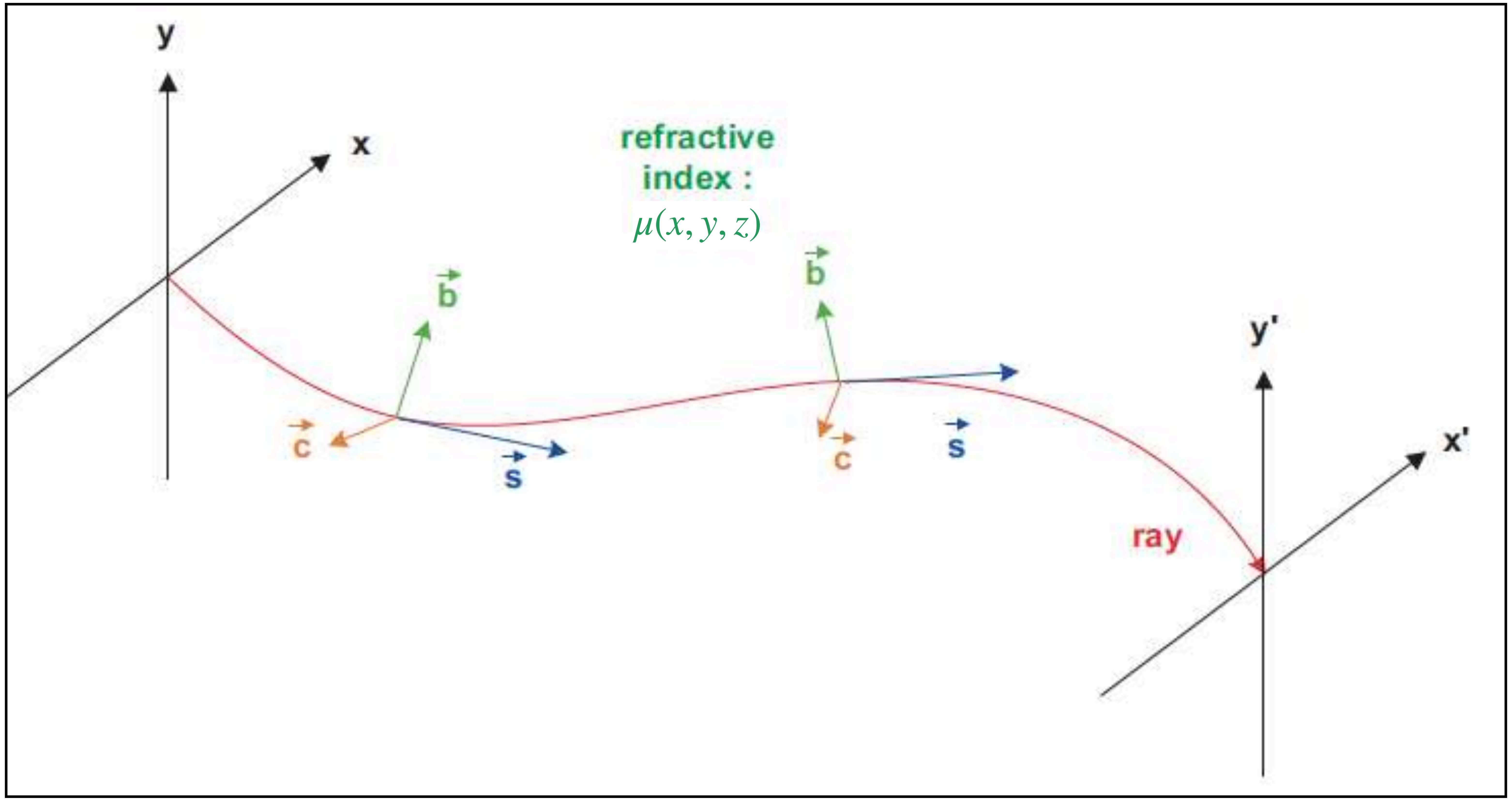

$$\delta L = \delta \int_{z_0}^{z} \left(n(x,y,z)\sqrt{1 + x'^2 + y'^2} \right) dz = 0$$

$$\delta L = \delta \int_{z_0}^{z} \frac{1}{q_0} \vec{p} \frac{d\vec{r}}{dz} dz = 0$$

$$\mu = \frac{1}{q_0} \left(m\vec{v} \cdot \frac{d\vec{r}}{dz} - e\vec{A} \cdot \frac{d\vec{r}}{dz} \right) = \mu_e + \mu_m$$

For electrons

3

Introduction to charged particle optics

Field and action expansion
Definition of the optical index for charged particles

Analysis of the optical index structure

$$\mu = \frac{1}{q_0}\left(m\vec{v}\cdot\frac{d\vec{r}}{dz} - e\vec{A}\cdot\frac{d\vec{r}}{dz}\right) = \mu_e + \mu_m$$

Electrostatic optical index

Scalar potential

$$\phi \implies \mu_e = \sqrt{\frac{\phi^*}{\Phi_0^*}(w'\overline{w}' + 1)}$$

$w = x + iy$

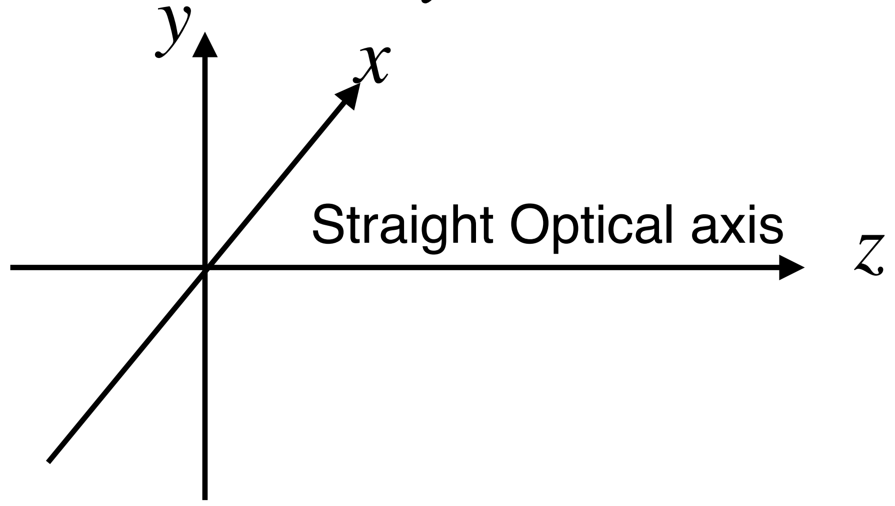

Magneto-static optical index

Vector potential

$$\vec{A} \implies \mu_m = -\frac{e}{q_0}(A_z + Re(\overline{A}w'))$$

$$\overline{A} = A_x + iA_y$$

We have to generate a localized zone of potential: the lens for charged particles

Three electrodes : ground/voltage/ground

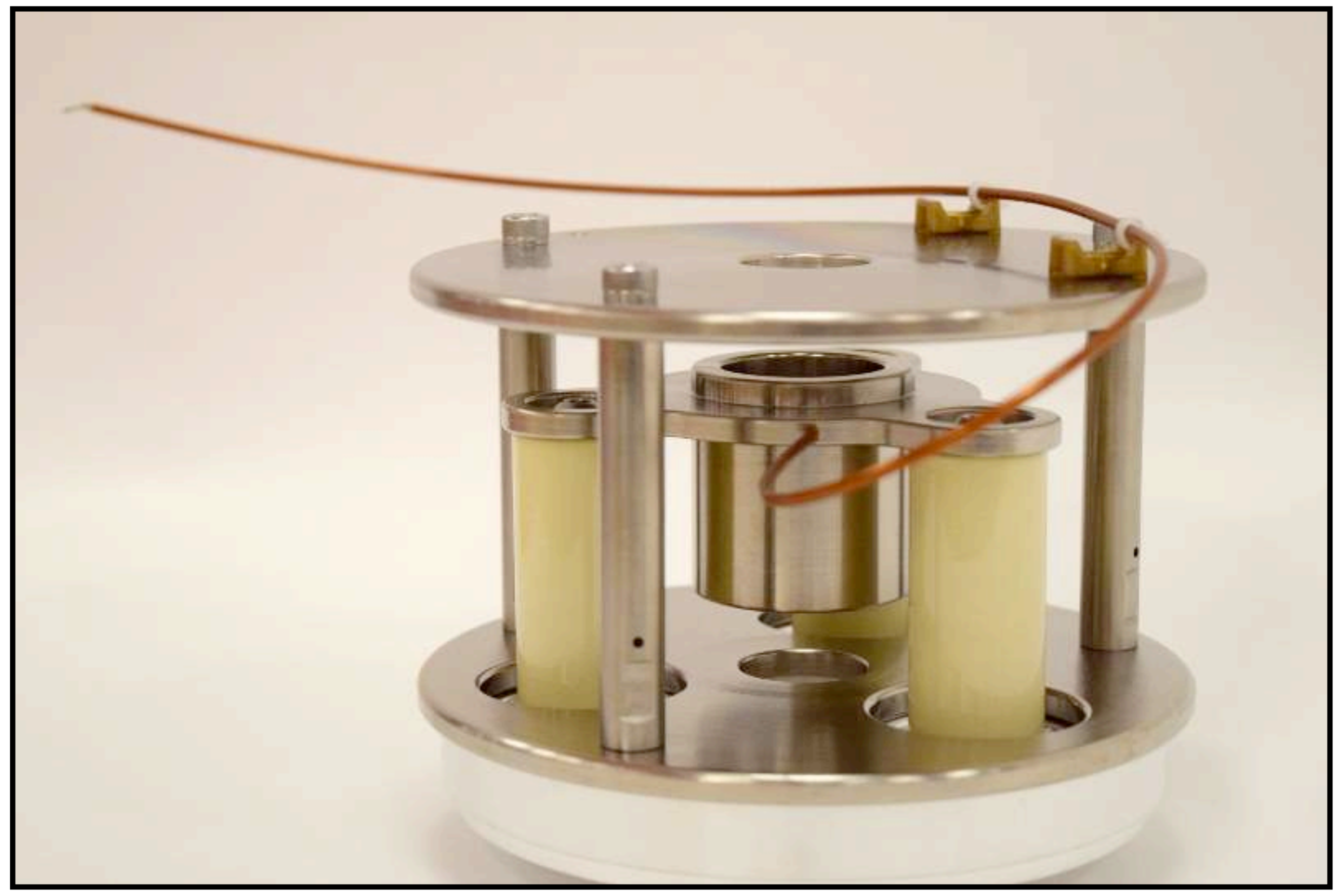

Map of the electrostatic potential $\phi(r,z)$

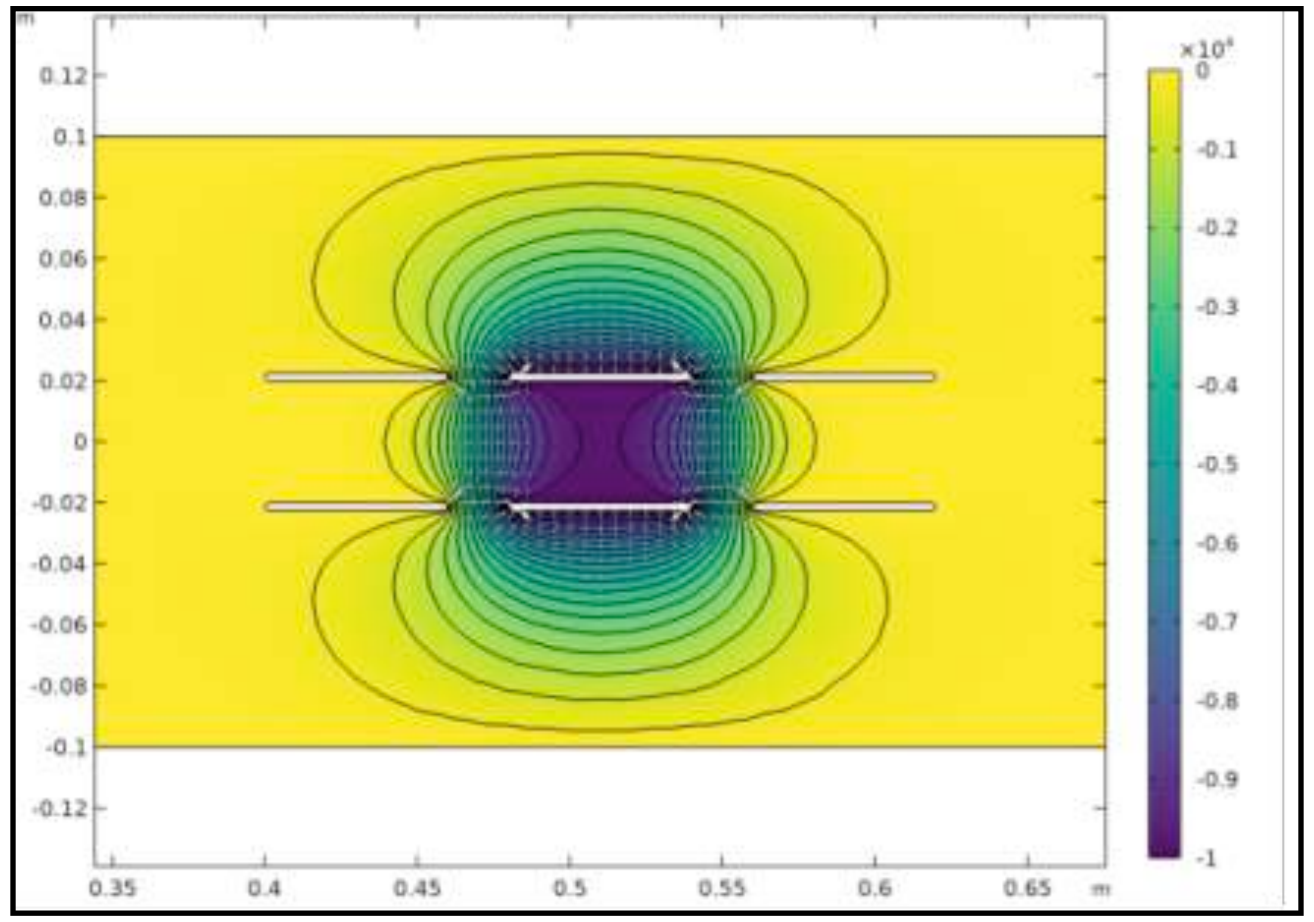

will act as a converging lens for the charged particles

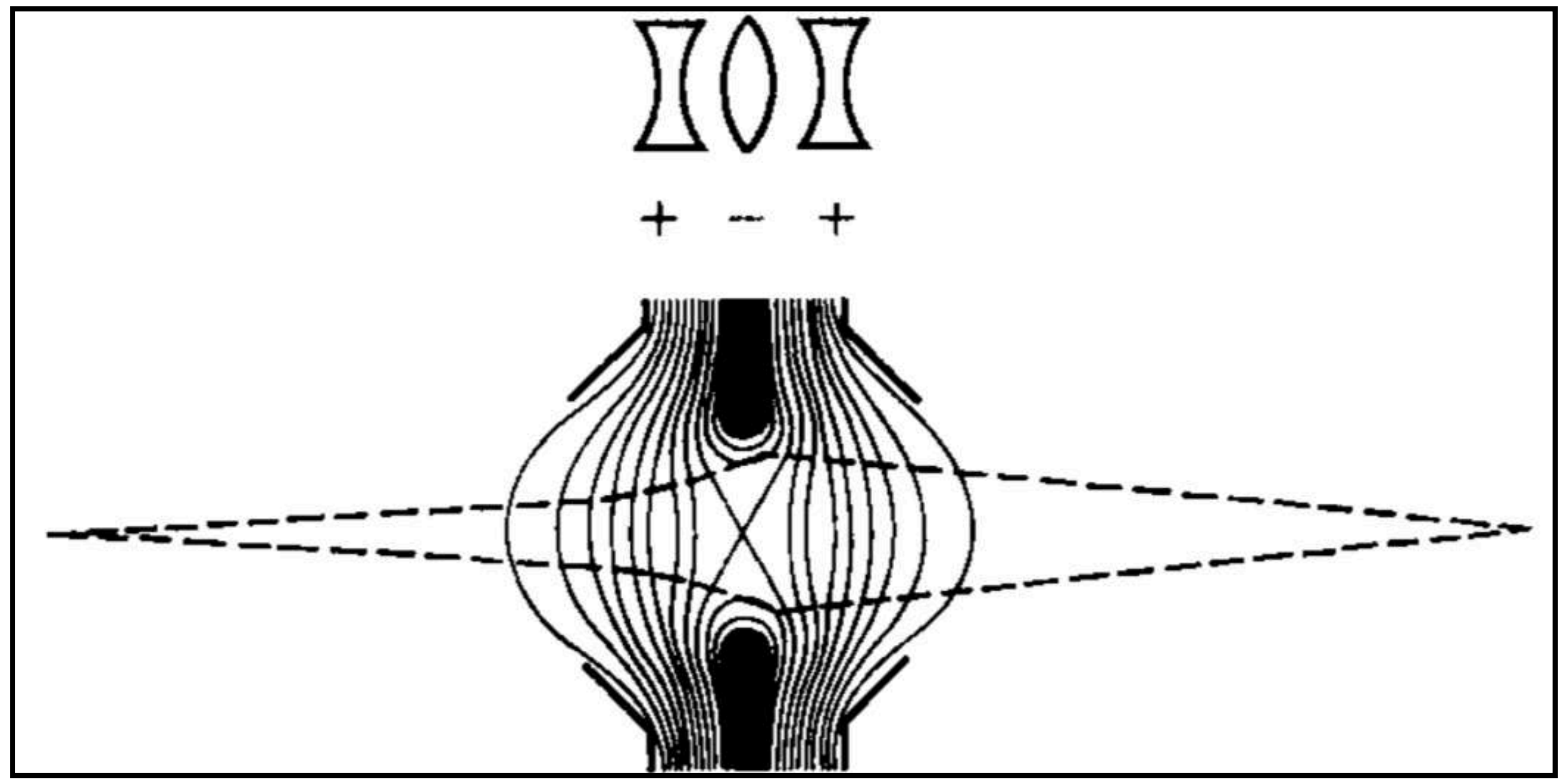

Back to LAP: development of charged particle optics

- **Walter Glaser (1906-m. 1960)**
  « Zur Bildfehlertheorie des Elektronenmikroskops » (1935).

First development of geometrical electron optics: based on the principle of least action

Zur Bildfehlertheorie des Elektronenmikroskops.

Von **Walter Glaser** in Prag.

Mit 2 Abbildungen. (Eingegangen am 16. August 1935.)

Nach einer vereinfachten Herleitung der Bildfehler werden die drei Zerdrehungsfehler ausführlich diskutiert und die Bezeichnungen: anisotropes Komma, anisotrope sphärische Aberration und anisotrope Verzeichnung dafür vorgeschlagen. Der Einfluß der Blendenstellung wird untersucht. Es wird das allgemeine rotationssymmetrische optische Mittel kurz behandelt und ein notwendiges und hinreichendes Kriterium für das identische Verschwinden der Zerdrehungsfehler angegeben.

Von früher[2]) her wissen wir, daß die Elektronenbewegung in einem elektromagnetischen Feld mit den Potentialen Φ und $\mathfrak{A}$ äquivalent ist dem optischen Strahlengang in einem anisotropen Medium mit dem Brechungsexponenten

$$\mu(\mathfrak{r}, \mathfrak{s}) = \sqrt{\Phi} + \eta(\mathfrak{A}\mathfrak{s}), \quad \eta = \sqrt{\frac{e}{2m}}. \tag{1}$$

Dabei wird das Potential Φ von einem Punkte aus gezählt, in dem die Elektronengeschwindigkeit Null ist. Die Elektronenstrahlen bestimmen sich somit aus dem Fermatschen Prinzip

$$\delta \int \mu(\mathfrak{r}, \mathfrak{s})\, d\sigma = 0. \tag{2}$$

The optical index for charged Particles

Fermat's principle

das gesuchte Seidelsche Eikonal. S_4 hat die Gestalt

$$S_4 = -\frac{A}{4} R^2 - \frac{B}{4} \varrho^2 - C \varkappa^2 - \frac{D}{2} R \varrho + E R \varkappa + F \varrho \varkappa + G_{00} R \sigma - 2 G_{01} \varkappa \sigma + G_{11} \varrho \sigma. \tag{56}$$

Wenn wir die Differenz $n_1 s_1 g_1'^2 h_1'^2 - n_0 s_0 g_0'^2 h_0'^2$ mit $\Delta n s g'^2 h'^2$ bezeichnen und analog mit anderen Differenzen verfahren, erhalten wir für die Koeffizienten des Eikonals (56) folgende Formeln:

$$\left.\begin{aligned}
A &= \tfrac{1}{2} \Delta n s g'^4 - \int_a^b [L g^4 + 2 M g^2 g'^2 + N g'^4]\, dz, \\
B &= \tfrac{1}{2} \Delta n s h'^4 - \int_a^b [L h^4 + 2 M h^2 h'^2 + N h'^4]\, dz, \\
C &= \tfrac{1}{2} \Delta n s g'^2 h'^2 - \int_a^b \left[L g^2 h^2 + 2 M g h g' h' + N g'^2 h'^2 - \frac{4}{n^2} K\right] dz, \\
D &= \tfrac{1}{2} \Delta n s g'^2 h'^2 - \int_a^b \left[L g^2 h^2 + M (g^2 h'^2 + g'^2 h^2) + N g'^2 h'^2 + \frac{8}{n^2} K\right] dz, \\
E &= \tfrac{1}{2} \Delta n s g'^3 h' - \int_a^b [L g^3 h + M (g^2 g' h' + g'^2 g h) + N g'^3 h]\, dz, \\
F &= \tfrac{1}{2} \Delta n s g' h'^3 - \int_a^b [L g h^3 + M (g h h'^2 + g' h' h^2) + N g' h'^3]\, dz,
\end{aligned}\right\} \tag{57a}$$

$$\left.\begin{aligned}
G_{00} &= \int_a^b \frac{1}{n} (P g^2 - Q g'^2)\, dz, \qquad G_{01} = \int_a^b \frac{1}{n} (P g h - Q g' h')\, dz, \\
G_{11} &= \int_a^b \frac{1}{n} (P h^2 - Q h'^2)\, dz.
\end{aligned}\right\} \tag{57b}$$

Reminder of the characteristic function L for a charged particle in a static field

$$L = \frac{\tilde{S}}{q_0} = \int_{z_0}^{z} \mu dz \implies \mu = \frac{1}{q_0} \vec{p} \frac{d\vec{r}}{dz}$$

$$L = \boxed{L^0} + \boxed{L^2} + \boxed{L^4} + \ldots.$$

Decomposition of the characteristic function n into several parts: paraxial + aberrations : **same work as <u>Schwarzschild</u> for conventional optics**

Field decomposition for straight optic axis system

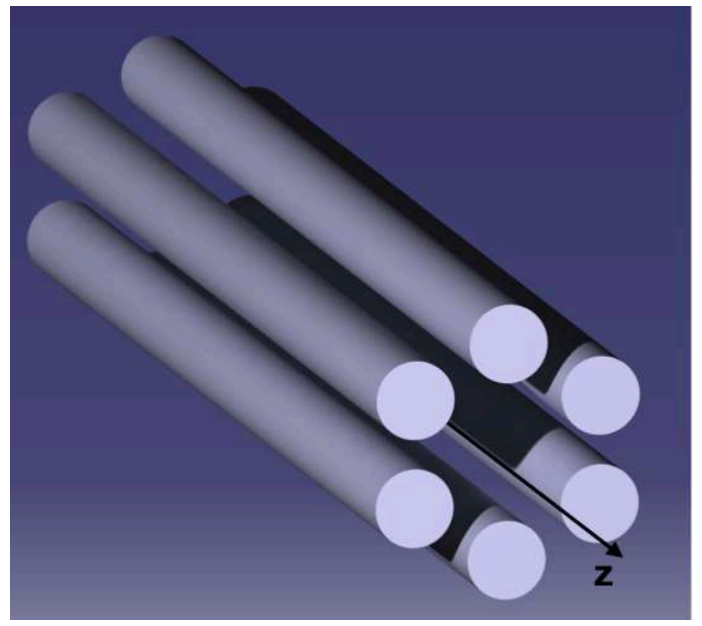

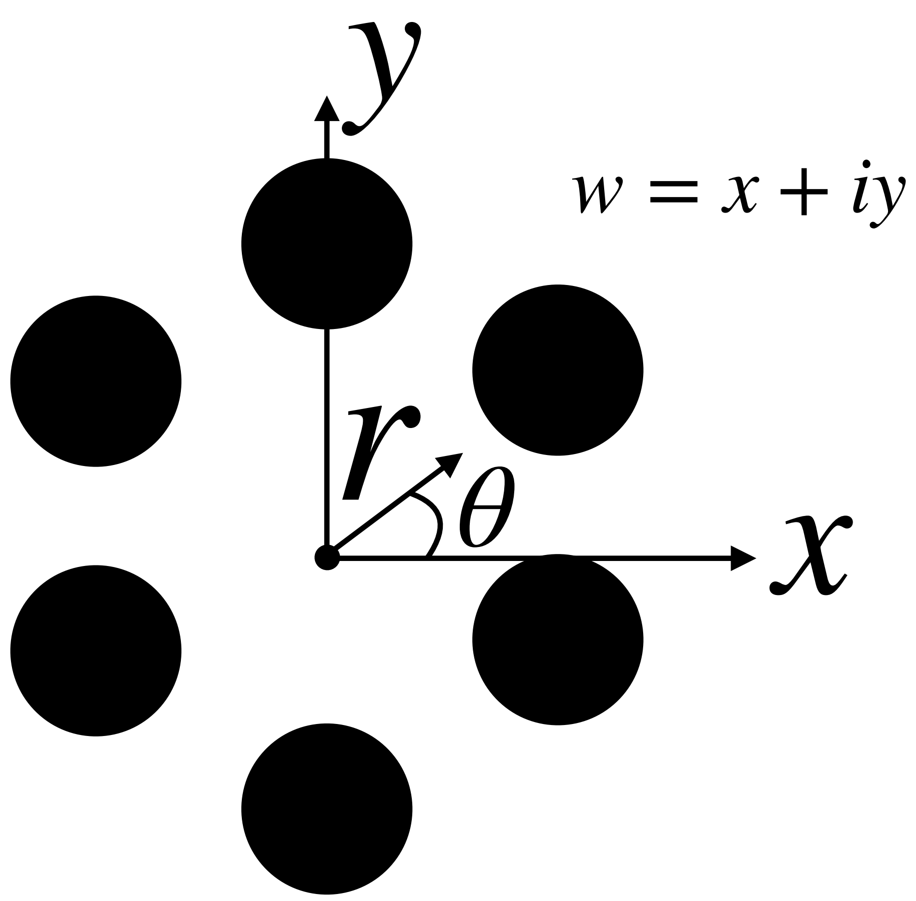

$w = x + iy = re^{i\theta}$

(I) Azimuthal Fourier decomposition : only in straight optics axis

$$\phi(r,\theta,z) = \sum_{\nu=0}^{\infty} \phi_\nu(r,\theta,z)$$

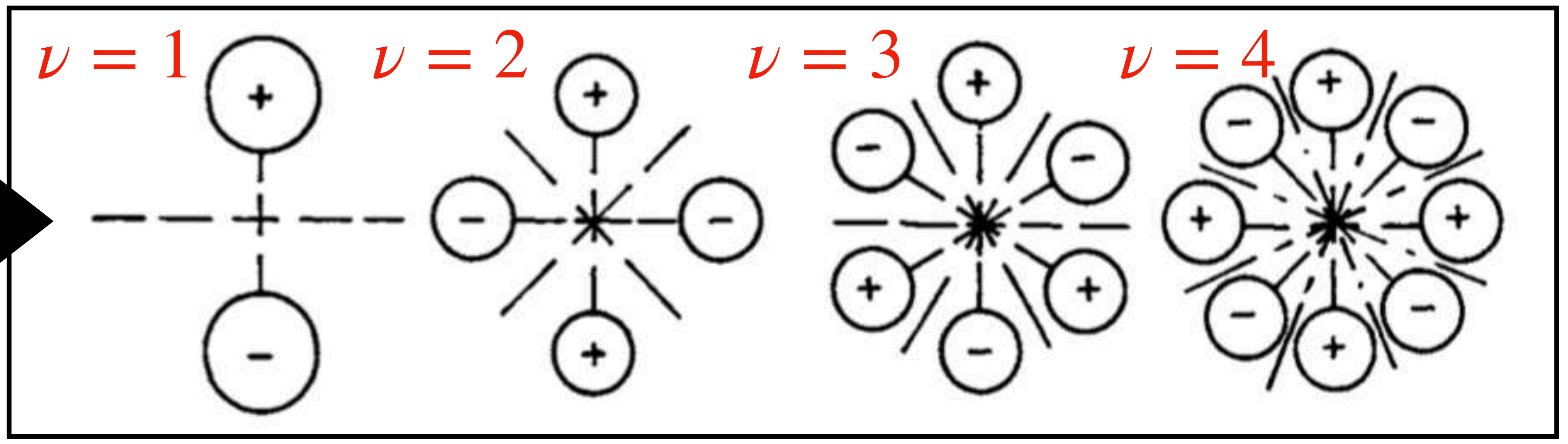

(II) Taylor expansion of each Fourier component $\phi_\nu(r,\theta,z)$ and knowing that Laplace equations should be fulfilled for each Fourier component $\Delta\phi_\nu = 0$

➡Example of the rotationally symmetric component $\phi_0(r,z)$

◉ Notation

$$\Phi' = \frac{\partial \Phi}{\partial z}$$

$$\phi_0(r,z) = \Phi_0(z) - \Phi_0''(z) \times \frac{r^2}{4} + \Phi_0^{[4]}(z) \times \frac{r^4}{64} - \Phi_0^{[6]}(z) \times \frac{r^6}{2304} + - \ldots$$

Only axial potential $\Phi_0(z)$ and it's derivatives relative to z are needed !!

$$\phi(r,\theta,z) = \underbrace{\sum_{\nu=0}^{\infty}}_{\textbf{Fourier}} \underbrace{\sum_{\lambda=0}^{\infty}}_{\textbf{Taylor}} \frac{(-1)^\lambda \times \nu! \times r^{2\lambda+\nu}}{4^\lambda \times \lambda! \times (\nu+\lambda)!} \times [\Phi_{\nu;r}^{[2\lambda]}(z) \times cos(\nu \times \theta) + \Phi_{\nu;i}^{[2\lambda]}(z) \times sin(\nu \times \theta)]$$

In complex coordinate system $w = x + iy$

$$\phi = \sum_{\nu=0}^{\infty} \sum_{\lambda=0}^{\infty} (-1)^\lambda \frac{\nu!}{\lambda!(\lambda+\nu)!} \left(\frac{w\overline{w}}{4}\right)^\lambda Re(\Phi_\nu^{[2\lambda]}(z)\overline{w}^\nu)$$

A sum of polynomial functions.

Rotationally symmetric lens

Electrostatic

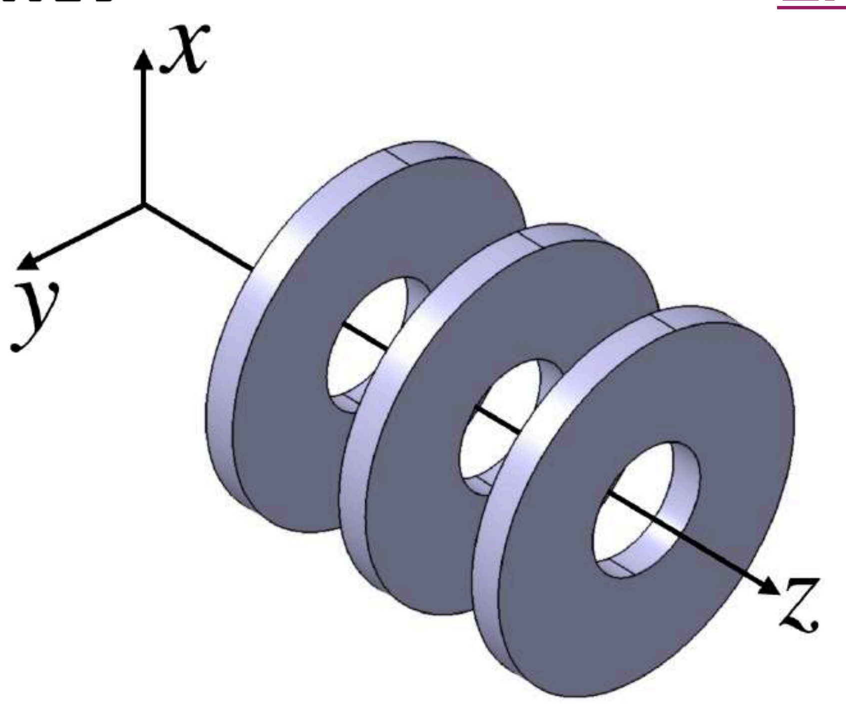

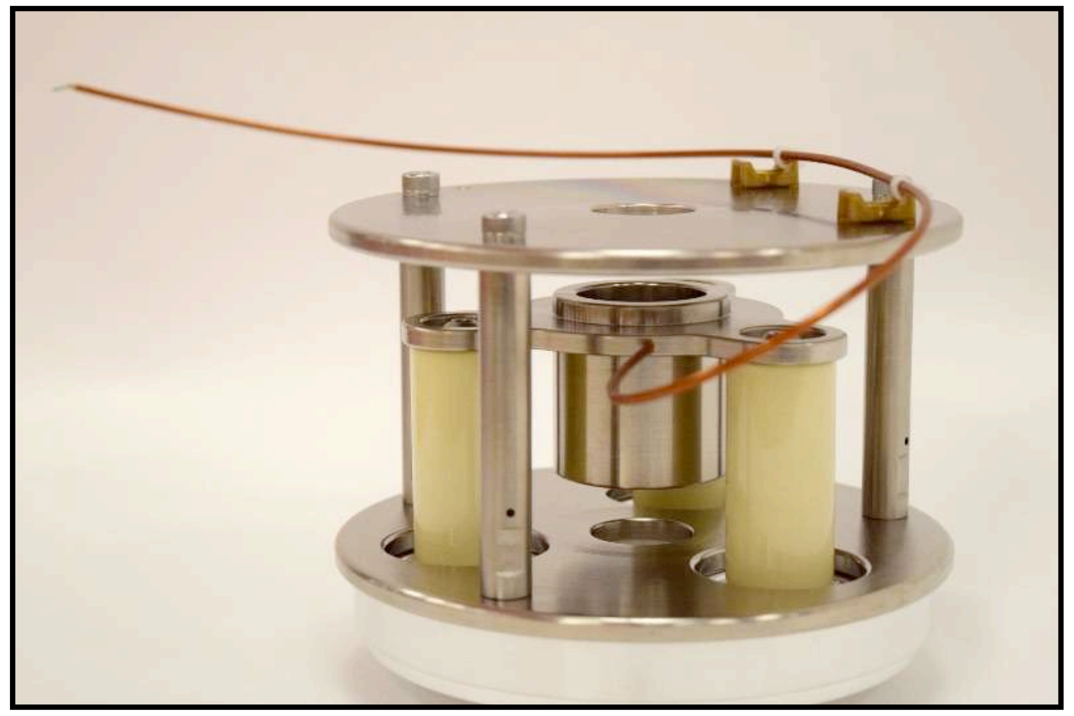

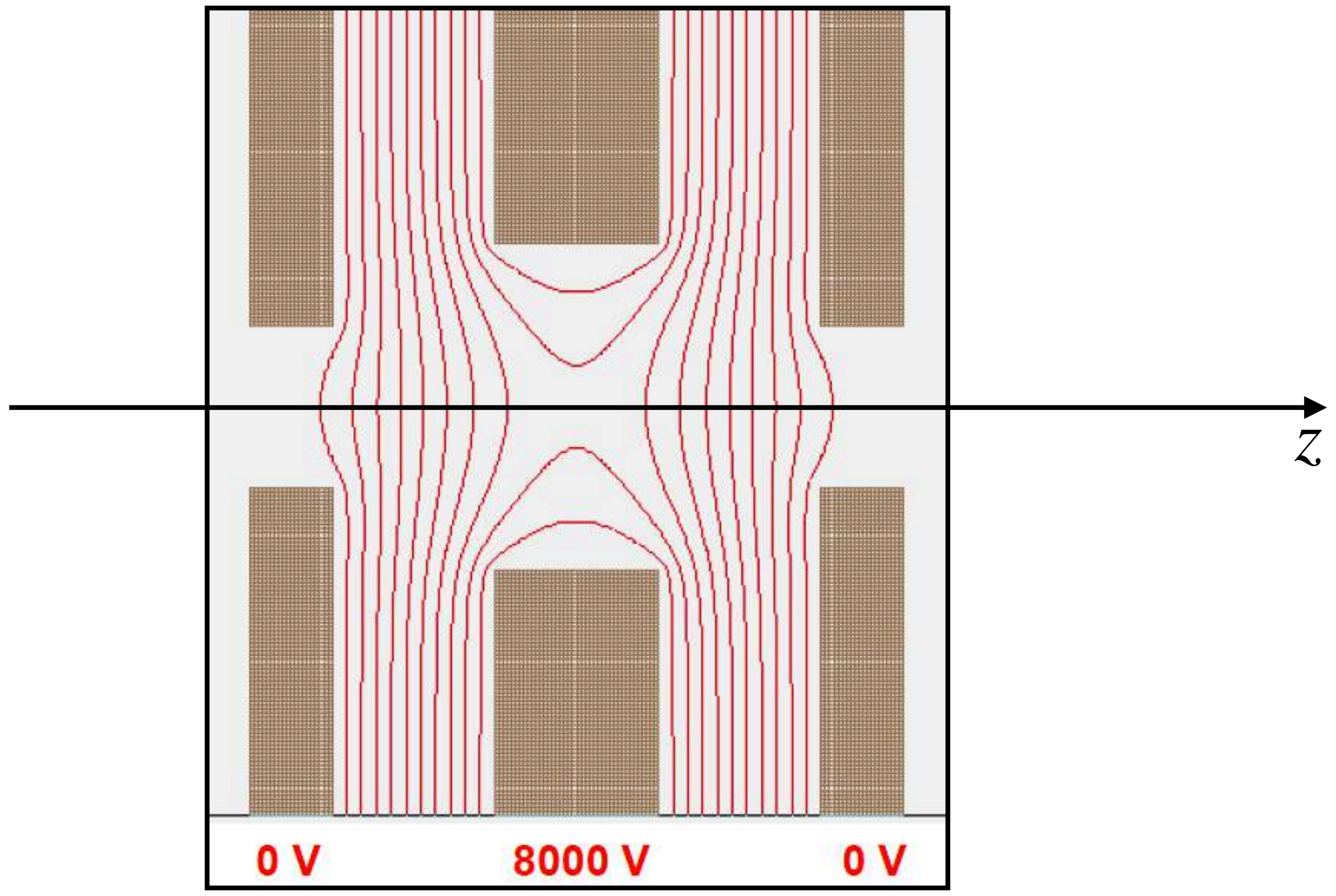

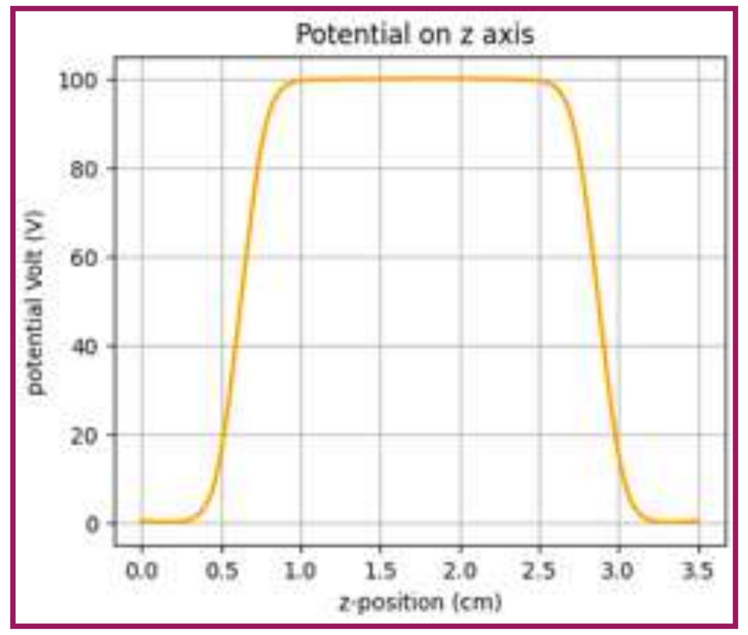

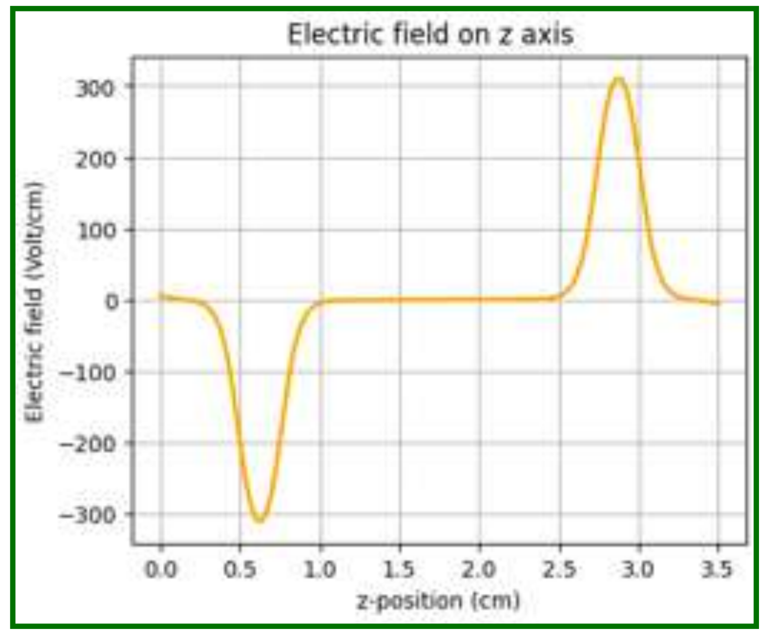

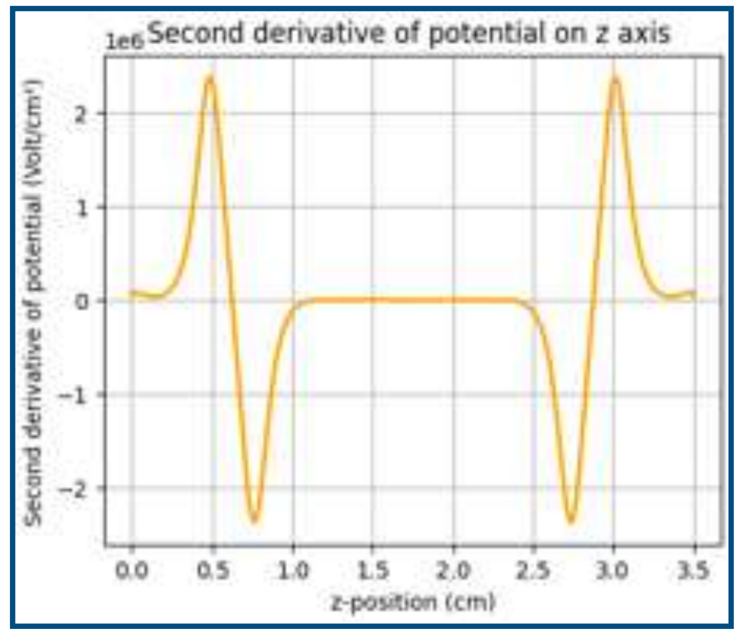

$$\phi_0(r,z) = \boxed{\Phi_0(z)} - \boxed{\Phi_0''(z)} \times \frac{r^2}{4} + \Phi_0^{[4]}(z) \times \frac{r^4}{64} - \Phi_0^{[6]}(z) \times \frac{r^6}{2304} + - \ldots$$

Magnetostatic

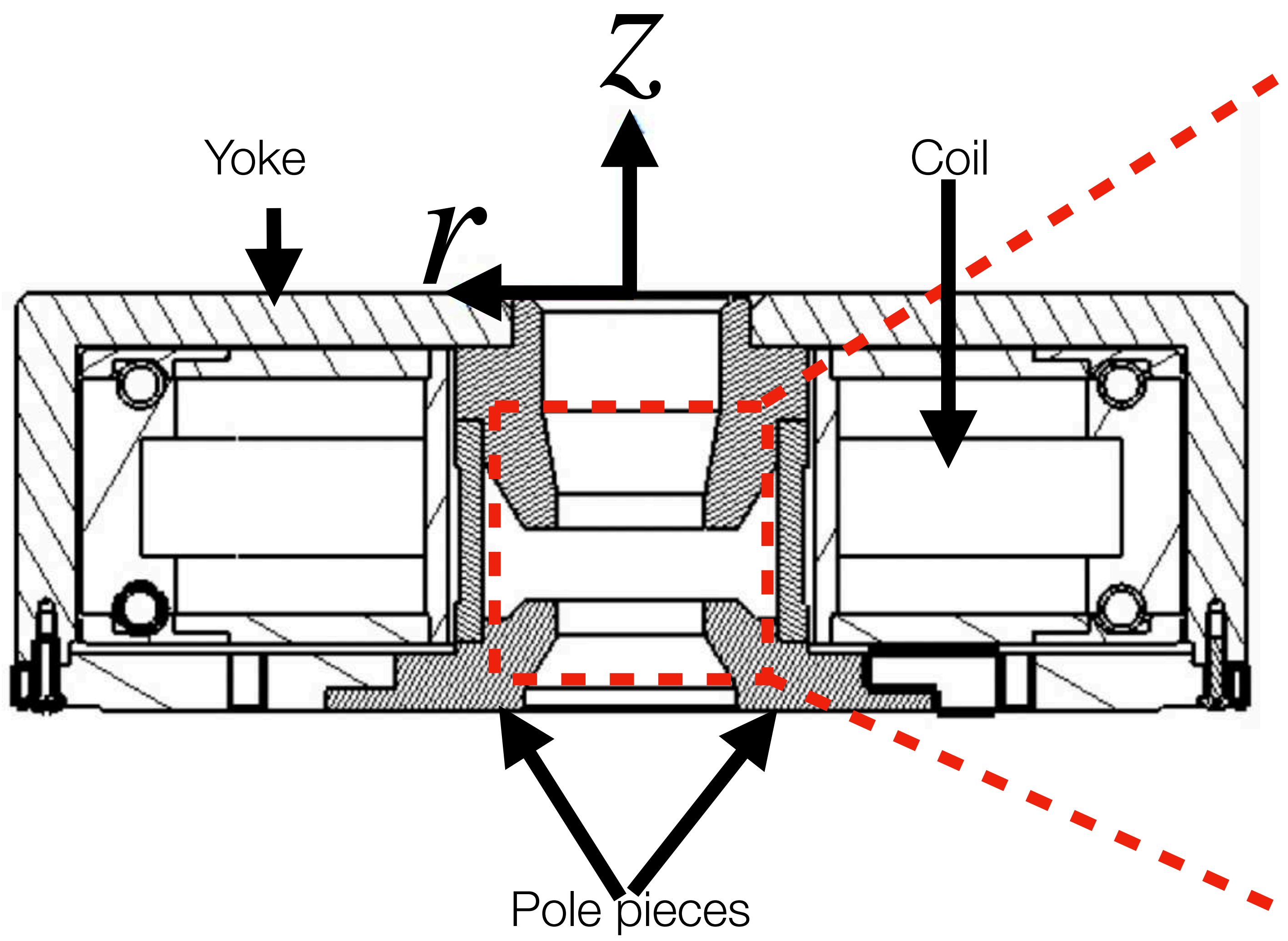

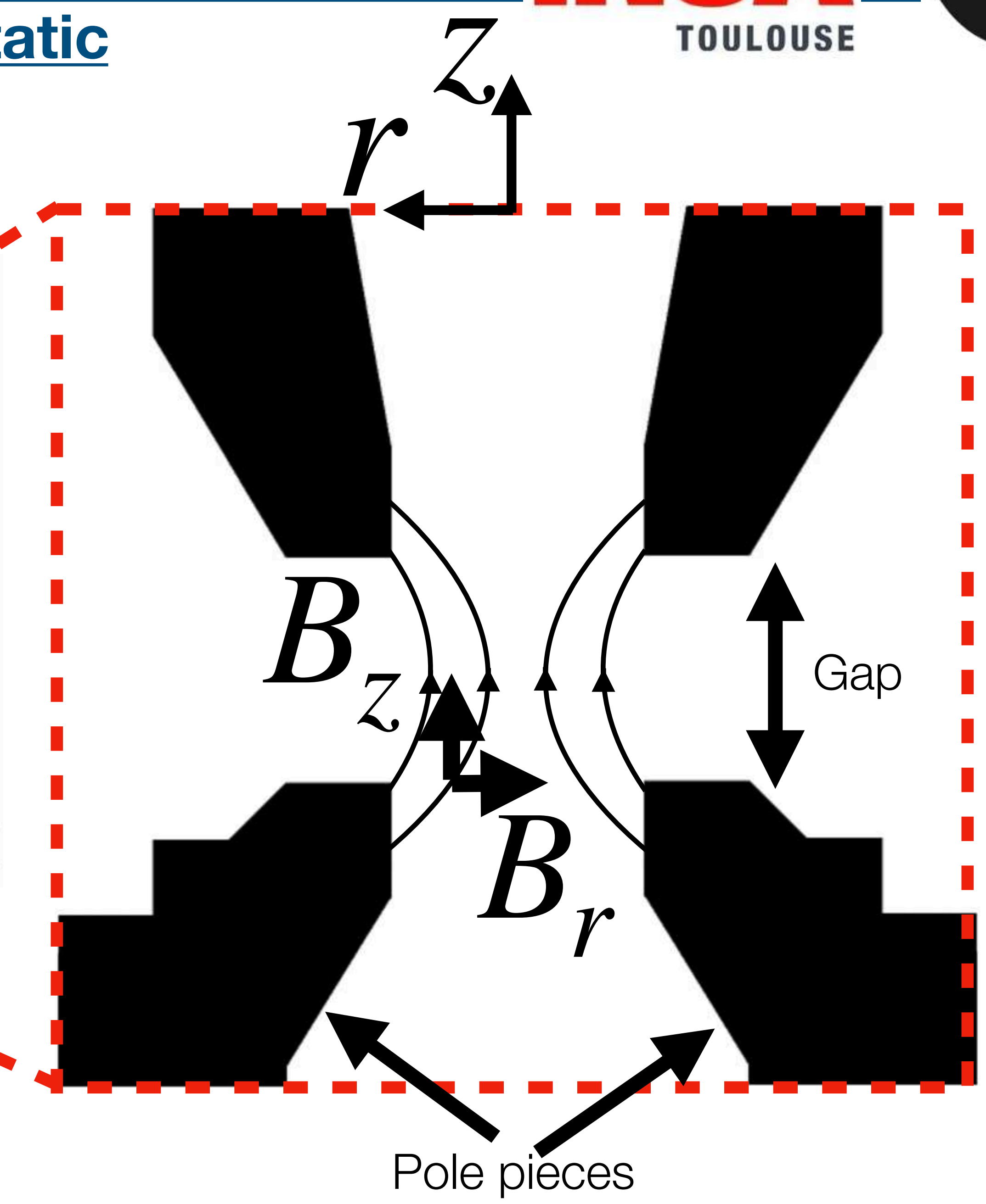

$$\vec{B} = \vec{\nabla} \wedge \vec{A} = -\vec{\nabla}.\psi(\vec{r}) \Rightarrow \psi_\nu = \sum_{\lambda=0}^{\infty} (-)^\lambda \frac{\nu!}{\lambda!(\lambda+\nu)!} \left(\frac{w\overline{w}}{4}\right)^\lambda Re(\Psi_\nu^{[2\lambda]}(z)\overline{w}^\nu)$$

$$\psi_0(r,z) = \Psi_0(z) - \Psi_0''(z) \times \frac{r^2}{4} + \Psi_0^{[4]}(z) \times \frac{r^4}{64} - \Psi_0^{[6]}(z) \times \frac{r^6}{2304} + - \ldots$$

$\Psi_0'(z) = B_z(0,z)$

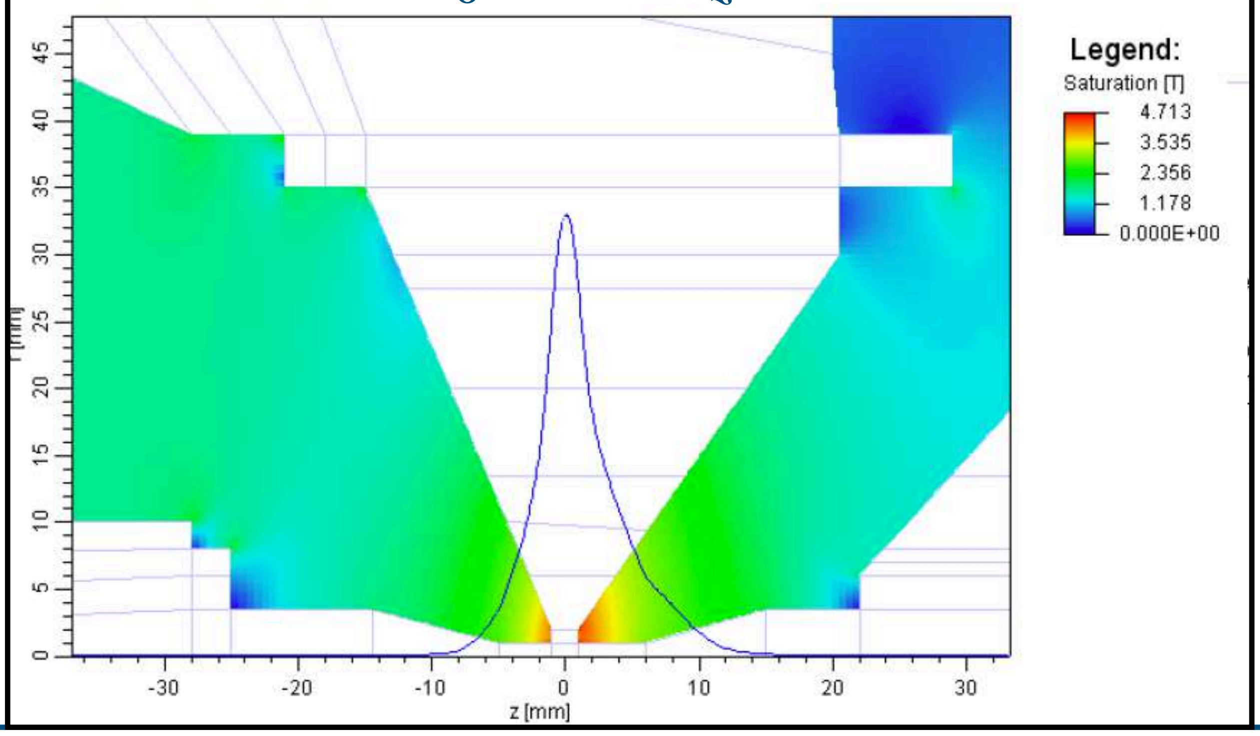

Main applications of rotational symmetric field

Electrostatic

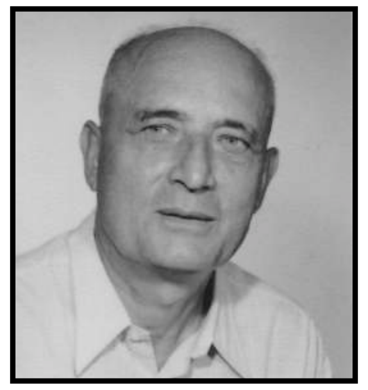

- **Pierre Grivet (1911-m. 1992)**
  « Electrostatic Electron Microscope (1941) »

Electrostatic lenses in a TEM

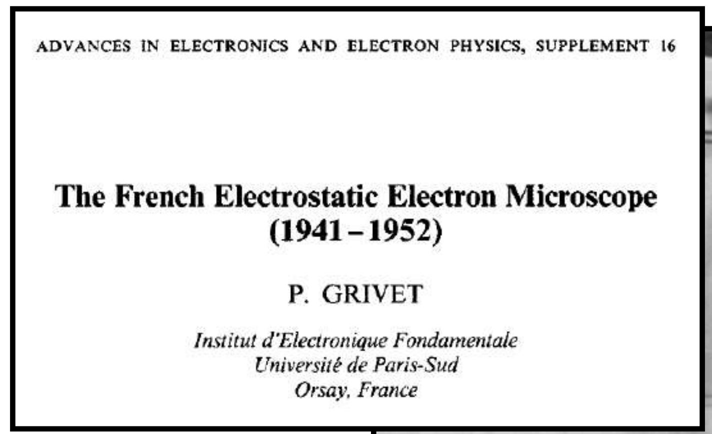
ADVANCES IN ELECTRONICS AND ELECTRON PHYSICS, SUPPLEMENT 16

The French Electrostatic Electron Microscope (1941–1952)

P. GRIVET

Institut d'Electronique Fondamentale
Université de Paris-Sud
Orsay, France

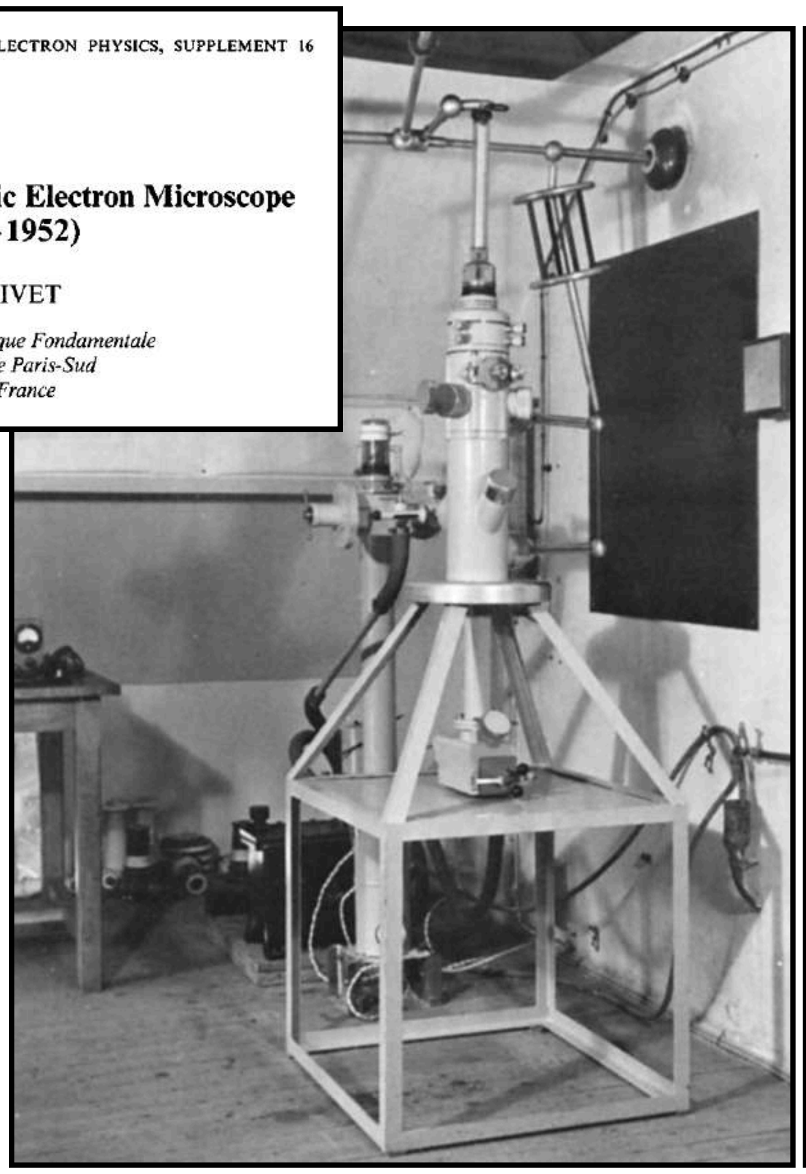

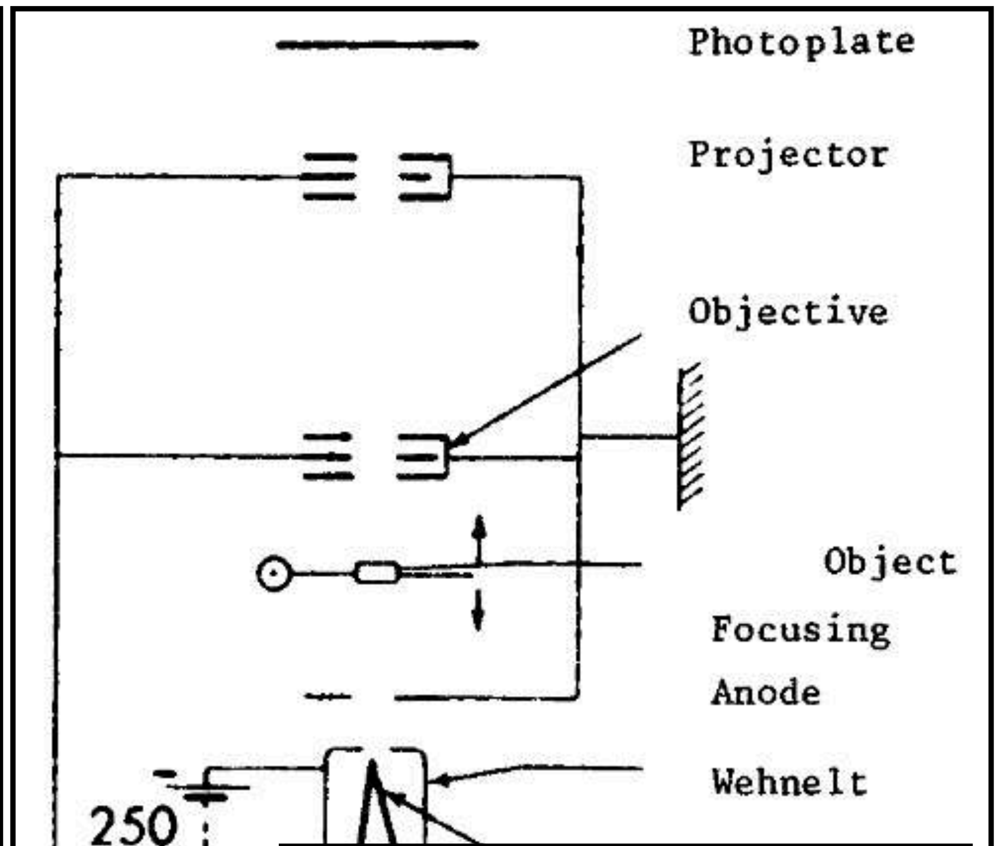

Behind the development of the FIB (focused ion beam)

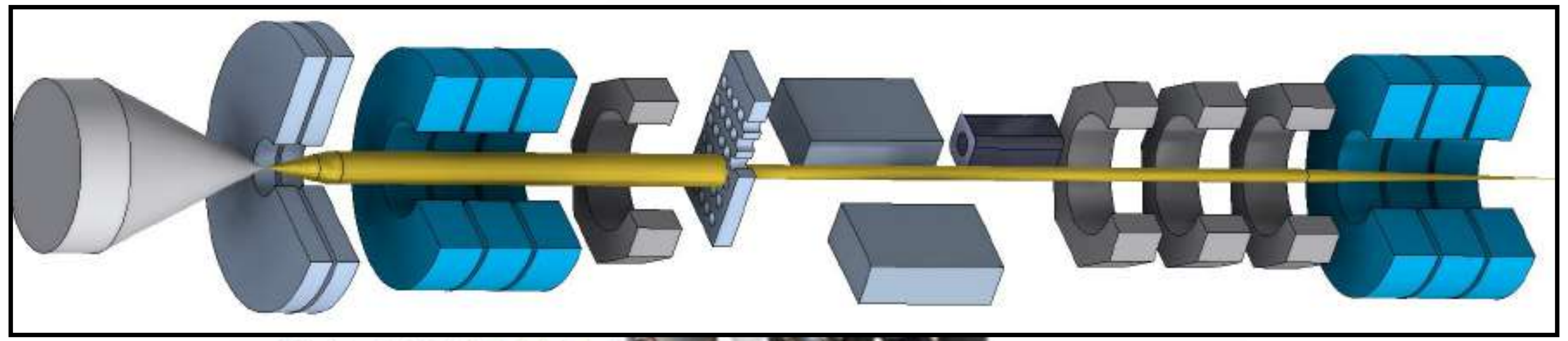

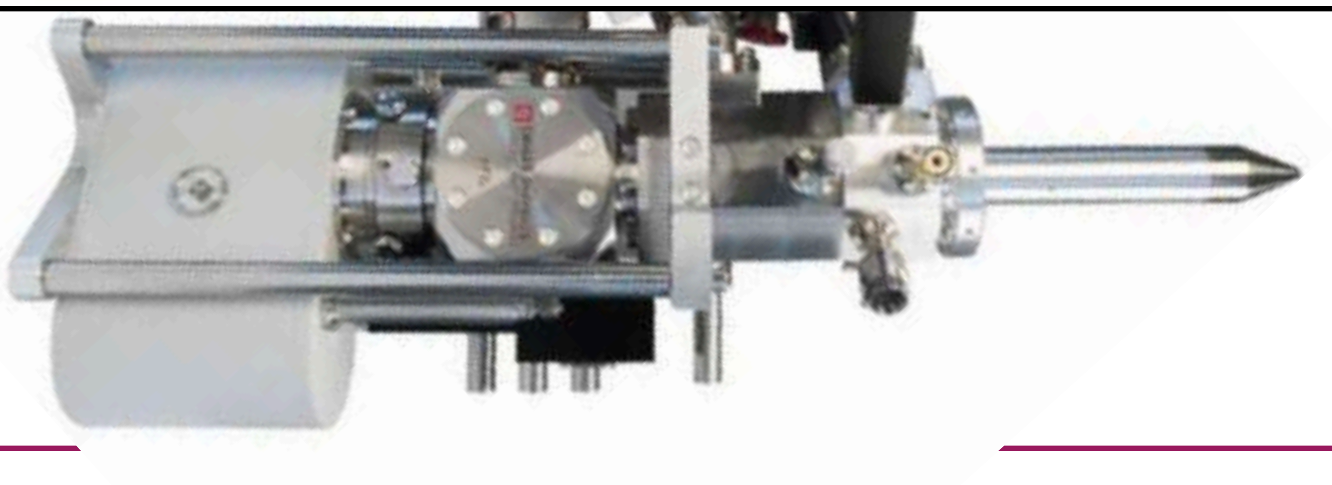

Magnetostatic

- **Ernst August Friedrich Ruska (1906-m. 1988)**
  « Das Elektronenmikroskop (1932) »

Development of the transmission electron microscope

(Mitteilung aus dem Hochspannungslaboratorium der Technischen Hochschule Berlin.)

Das Elektronenmikroskop.

Von **M. Knoll** und **E. Ruska** in Berlin.

Mit 11 Abbildungen. (Eingegangen am 16. Juni 1932.)

Die wichtigsten elektronenoptischen Abbildungssysteme und ihre Eignung für die vergrößerte Abbildung elektronenemittierender Objekte werden diskutiert. Die allgemeinen Bedingungen für fehlerfreie Bilder, Definition und Grenze des Auflösungsvermögens werden angegeben. Ein magnetisches Elektronenmikroskop mit kalter Kathode für schnelle Elektronen und die Ausführung magnetischer Linsen werden beschrieben und mehrere Mikrophotogramme wiedergegeben. Die Untersuchungsmethoden des Elektronenmikroskops und geeignete Abbildungssysteme für ein Ionenmikroskop werden besprochen.

Mikrophotogramme.

Fig. 8a zeigt ein über eine runde Blende gespanntes Molybdändrahtnetz, das durch ein mittels der Kondensorlinse konzentriertes Strahlbündel einer Metallentladungsröhre von hinten „beleuchtet" wurde. Zum Vergleich wurde in einem gewöhnlichen Projektionsmikroskop (Zeiss) dieselbe Netzblende in gleicher Vergrößerung aufgenommen (Fig. 8b). Man sieht, daß

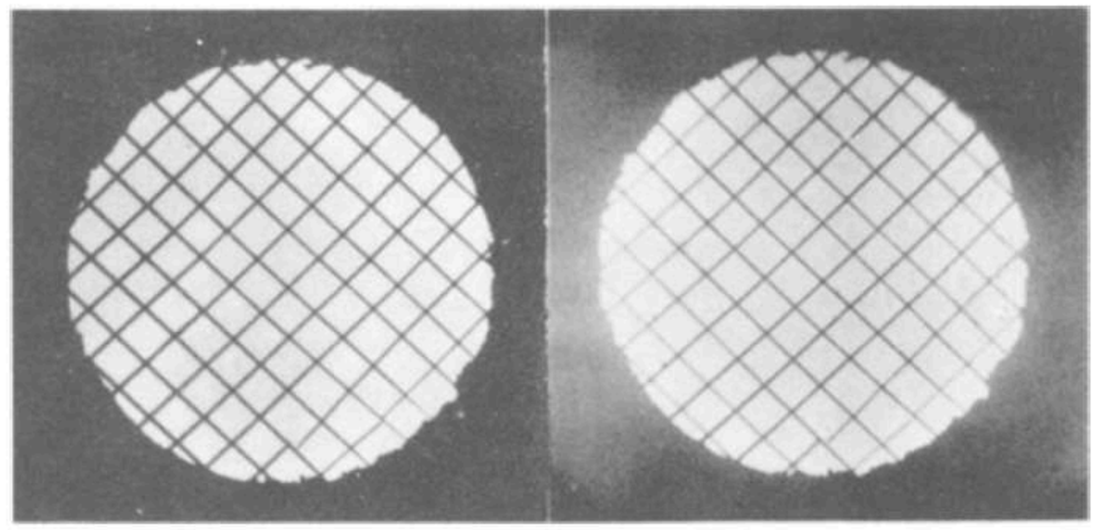

Fig. 8a. Fig. 8b.

Fig. 8. Vergleich zwischen elektronen- und lichtoptischer Abbildung. Molybdändrahtnetz, Drahtabstand 0,3 mm, 12 fach in einer Stufe auf vergoldetem Glasleuchtschirm vergrößert; Beschleunigungsspannung 70 kV. a) durch Elektronenmikroskop. b) durch normales Mikroskop.

Zur Erzeugung der Elektronenbilder auf dem am Boden des Metallrohres befindlichen Leuchtschirm dienen eisengekapselte Sammelspulen, die „Objektivspule" (mit einem möglichst kleinen Innendurchmesser), und die größere „Projektionsspule", welche das durch die Objektivspule in Höhe des Okularmikrometers erzeugte Zwischenbild weiter vergrößert. Eine Vergrößerung in zwei Stufen ergibt bei einer bestimmten geforderten Gesamtvergrößerung bei gleicher kleinster Spulenbrennweite eine bedeutend kürzere Länge des Mikroskops; für geringe Vergrößerungen kommt man mit der Objektivspule allein aus. Die oberhalb der Objektivspule sichtbare „Kondensorspule" dient in Analogie zur Anordnung beim normalen Mikroskop zur Strahlsammlung der „Beleuchtungsquelle" auf das Objekt.

Als Leuchtschirm zur Sichtbarmachung der Elektronenbilder dient (wegen der großen Strukturfeinheit) bei schnelleren Elektronen (> 25 kV) eine Glasplatte, die durch Kathodenzerstäubung mit einer Metallschicht von etwa 100 mμ versehen ist[3]). Diese mit der Anode verbundene Schicht verhindert die Aufladung des Schirms und erhöht durch Reflexion an dem Metallspiegel die Lichtstärke der Fluoreszenzbilder. Der Glasschirm ist möglichst dünn (< 0,1 mm) zu wählen, damit er bei intensiver Bestrahlung unter der Er-

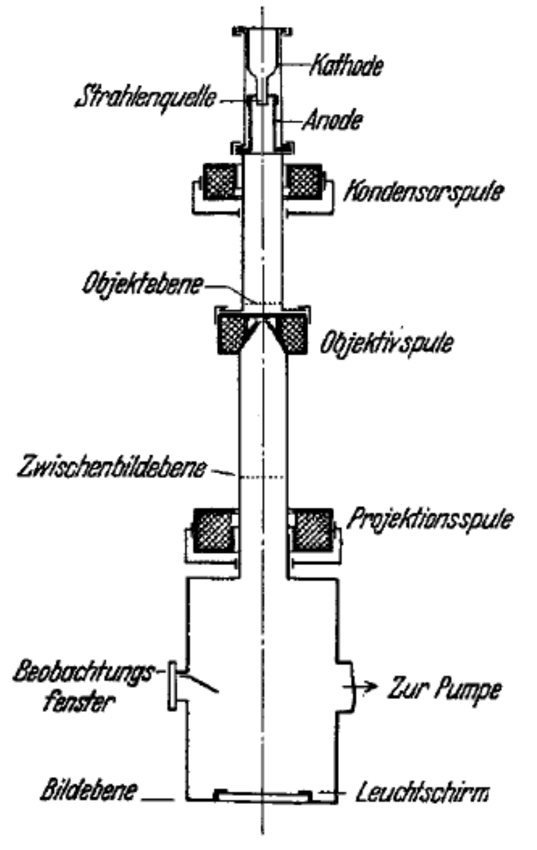

Fig. 5. Magnetisches Elektronenmikroskop mit kalter Kathode.

Optical index expansion

➡ We have to start from the optical indices:

Electrostatic case

$$\mu_e = \sqrt{\frac{\phi^*}{\Phi_0^*}(w'\overline{w}' + 1)}$$

$$\phi = \sum_{\nu=0}^{\infty}\sum_{\lambda=0}^{\infty}\dots$$

Index expansion into a sum polynomial functions of power n of the variables $w, \overline{w}, w'$ et $\overline{w}'$

$$\mu_{(e)} = \sum_{n=0}^{\infty}\mu_{(e)}^{(n)}$$

Magnetostatic case

$$\mu_m = -\frac{e}{q_0}(A_z + Re(\overline{A}w'))$$

$$\psi = \sum_{\nu=0}^{\infty}\sum_{\lambda=0}^{\infty}\dots$$

Index expansion into a sum polynomial functions of power n of the variables $w, \overline{w}, w'$ et $\overline{w}'$

$$\mu_{(m)} = \sum_{n=0}^{\infty}\mu_{(m)}^{(n)}$$

$$\mu^{(n)} = \mu_e^{(n)} + \mu_m^{(n)}$$

Keep polynomial functions of power $n \leq 2$ ➡ **Paraxial optics** with $L = L^0 + L^2$

Contribution of polynomial functions of power $n > 2$ ➡ **Aberrations** $L^4 + \dots$

4

Paraxial charged particle optics

Second order optical index
Paraxial equations
Electrostatic vs magnetostatic standard optics

Magnetostatic case

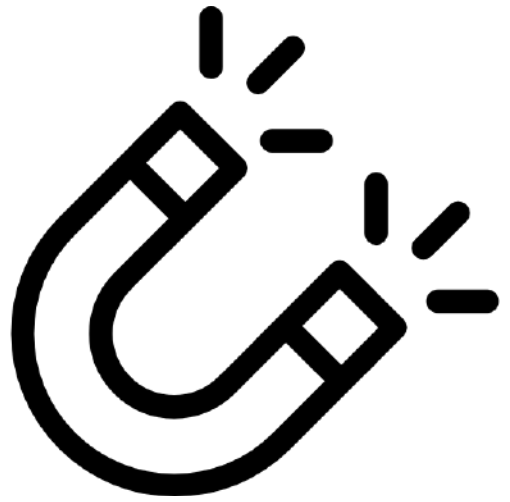

$$\boxed{\mu_m^{(0)} = 0}$$

$$\boxed{\mu_m^{(1)} = -\frac{e}{q_0} Im(\Psi_1 \overline{w})}$$

$$\boxed{\mu_m^{(2)} = \frac{e}{q_0} Im\left(\frac{w\overline{w}}{4}\Psi_0''(z) + \frac{1}{2}\Psi_0'(z)\overline{w}w' - \Psi_2(z)\overline{w}^2\right)}$$

Electrostatic case

$$\boxed{\mu_e^{(0)} = \sqrt{\frac{\Phi_0^*(z)}{\Phi_0^*(z_0)}}}$$

$$\boxed{\mu_e^{(1)} = \frac{\gamma_0}{2\sqrt{\Phi_0^*(z_0)\Phi_0^*(z)}} Re\left(\Phi_1(z)\overline{w}\right)}$$

$$\boxed{\mu_e^{(2)} = \frac{1}{2}\sqrt{\frac{\Phi_0^*(z)}{\Phi_0^*(z_0)}} Re\left[w'\overline{w'} - \frac{w\overline{w}}{\Phi_0^*(z)}\left(\frac{\gamma_0\Phi_0''(z)}{4} + \frac{\Phi_1(z)\overline{\Phi}_1(z)}{8\Phi_0^*(z)}\right) + \frac{\overline{w}^2}{\Phi_0^*(z)}\left(\gamma_0\Phi_2(z) - \frac{\Phi_1^2(z)}{8\Phi_0^*(z)}\right)\right]}$$

Effect on paraxial :

Rotationally symmetric field $\nu = 0$

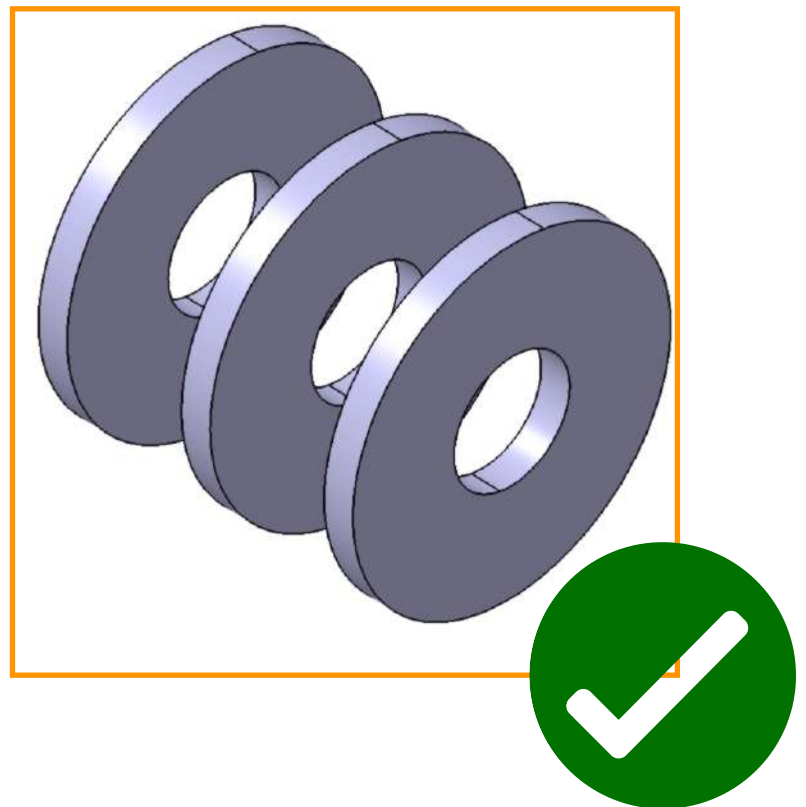

Dipolar field $\nu = 1$

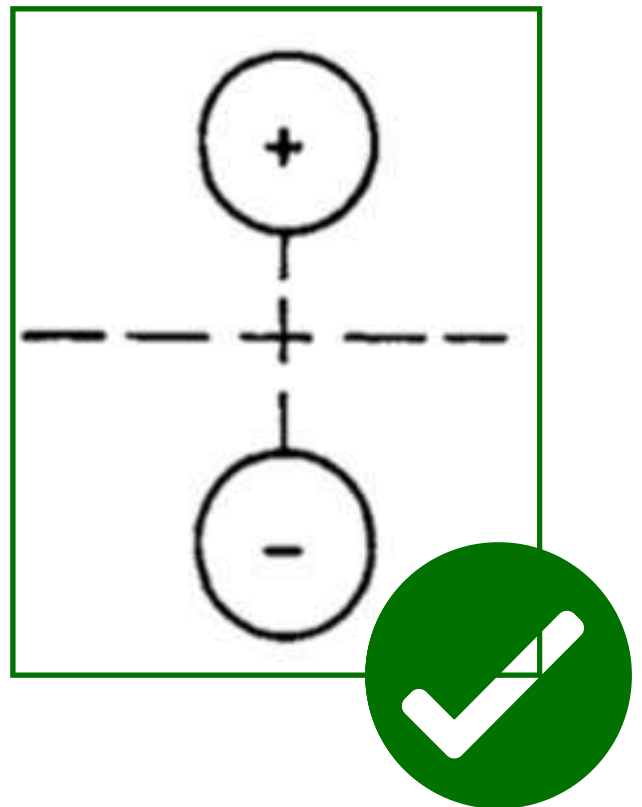

Quadrupolar field $\nu = 2$

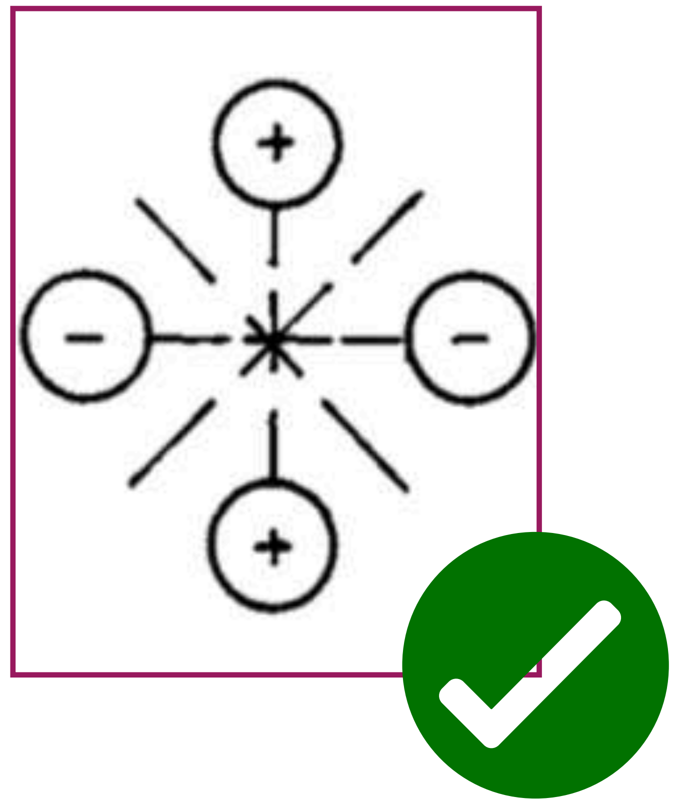

No paraxial action :

Hexapolar $\nu = 3$, octopolar $\nu = 4$, …

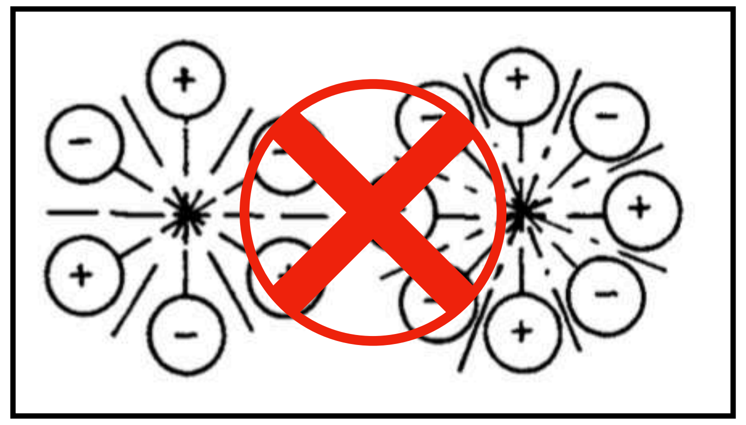

Paraxial straight axis optics : $n \leq 2$

1. To determine the trajectories we simply have to resolve the least action principle applied to the characteristic function $\delta L = 0$

2. Lagrange showed that this is equivalent to resolve the set of Euler-Lagrange differential equations : $\frac{d}{dz}\frac{\partial \mu}{\partial \overline{w}'} - \frac{\partial \mu}{\partial \overline{w}} = 0$

In paraxial, these equations become : $\frac{d}{dz}\frac{\partial(\mu^{(0)} + \mu^{(1)} + \mu^{(2)})}{\partial \overline{w}'} - \frac{\partial(\mu^{(0)} + \mu^{(1)} + \mu^{(2)})}{\partial \overline{w}} = 0$

After inserting all the previous polynomial functions extracted from the field expansion we found « naturally » the paraxial equation of any charged particle optics system with straight optical axis :

$$\boxed{w'' + \frac{\gamma_0}{2\Phi_0^*}(\Phi_0' + iv_0\Psi_0')w' + \frac{\gamma_0}{4\Phi_0^*}\left(\Phi_0'' + iv_0\Psi_0'' + \frac{\Phi_1\overline{\Phi}_1}{2\gamma_0\Phi_0^*}\right)w - \frac{\gamma_0}{\Phi_0^*}\left(\Phi_2 + iv_0\Psi_2 - \frac{\Phi_1^2}{8\gamma_0\Phi_0^*}\right)\overline{w} = \frac{\gamma_0}{2\Phi_0^*}(\Phi_1 + iv_0\Psi_1)}$$

We find again the contribution of Fourier components : Rotationally symmetric field $\nu = 0$ Dipolar field $\nu = 1$ Quadrupolar field $\nu = 2$

The **Wien condition** state that if an electrostatic dipolar field is applied in the system, a magneto static dipolar field must be present to have a straight optic axis ($w = 0$). The relation between the two magnitudes should fulfill

$$\boxed{\Phi_1 + iv_0\Psi_1 = 0}$$

- Notation

$w = x + iy$

$v_0 = \frac{1}{\gamma_0}\sqrt{\frac{2e\Phi_0^*(z)}{m_e}}$

Dipolar field and Wien Filter as mass separator

- Dipolar field tilt the optical axis relatively : use to align the beam (known as deflectors)

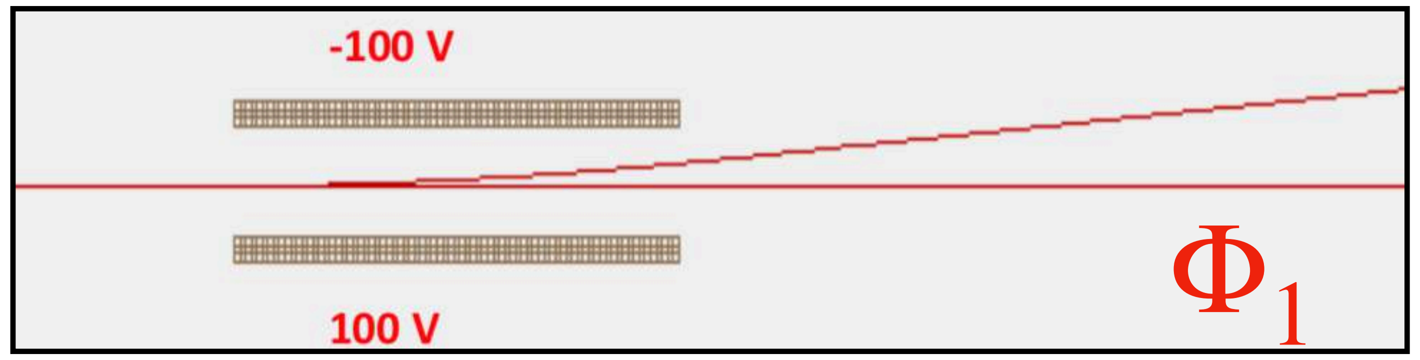

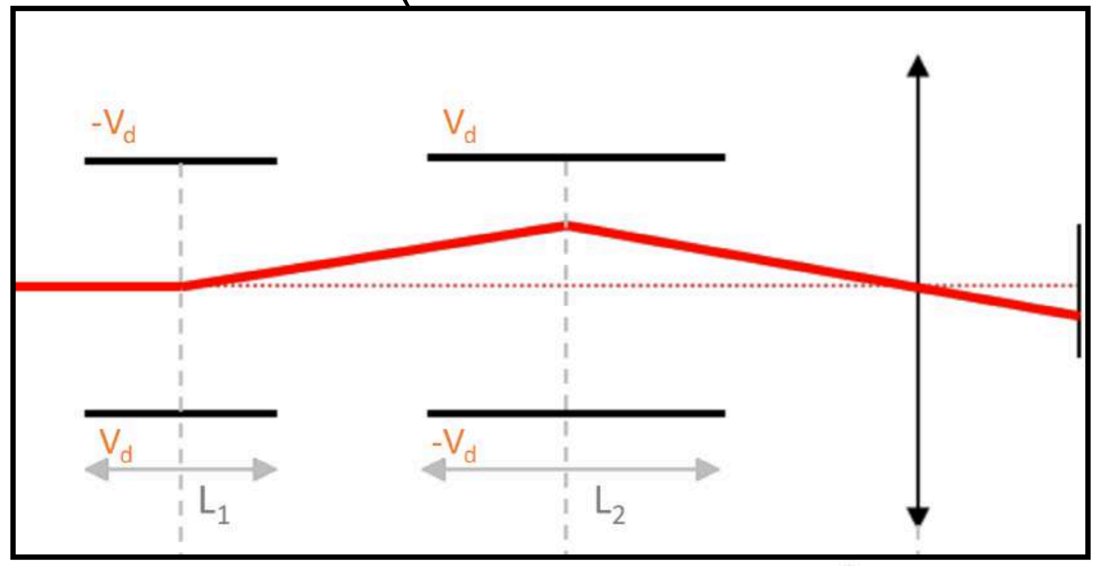

- Application of Wien condition : the Wien filter

$$\boxed{\Phi_1 + i v_0 \Psi_1 = 0}$$

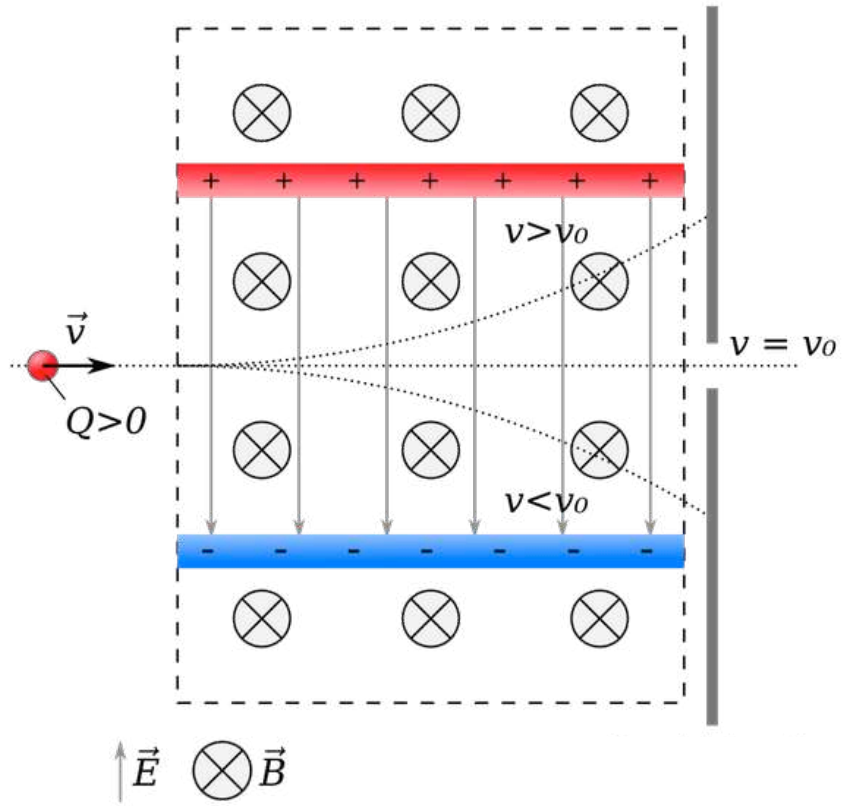

- An example of a Wien filter by students : fabrication and calculation

Their realization

Resolution of paraxial equation

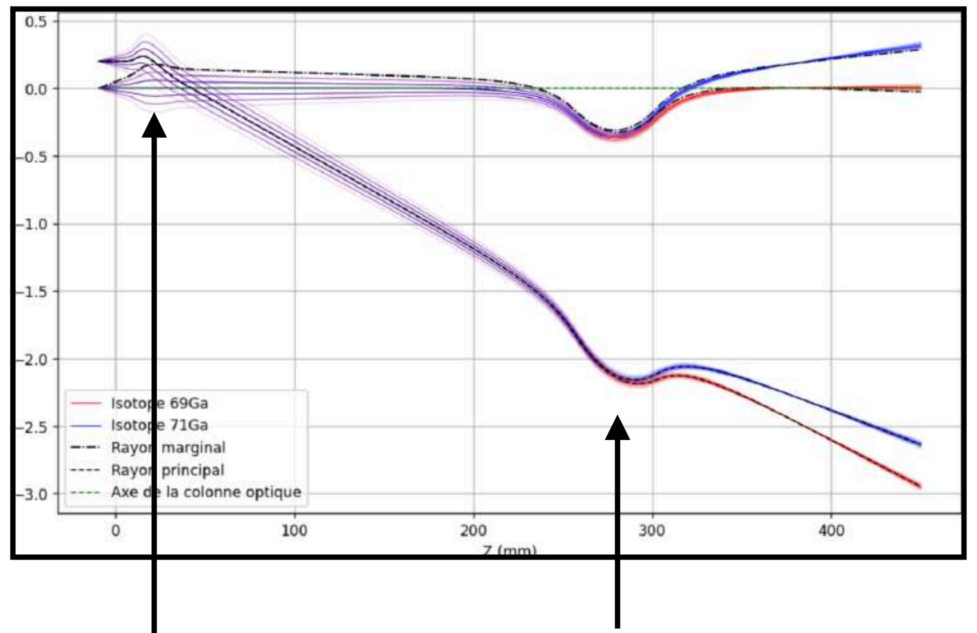

Einzel lens Φ_0 Wien filter Φ_1, Ψ_1

Results in a Ga FIB (separation of isotopes)

$\Phi_1, \Psi_1 = 0$

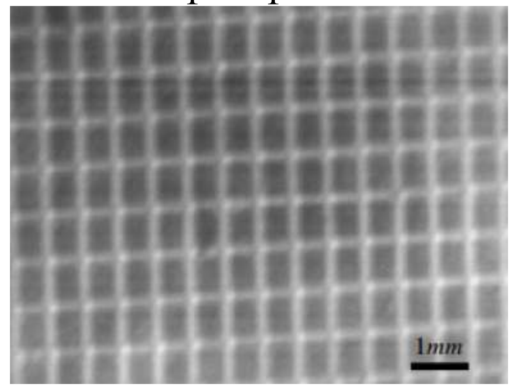

$\Phi_1, \Psi_1 \neq 0$

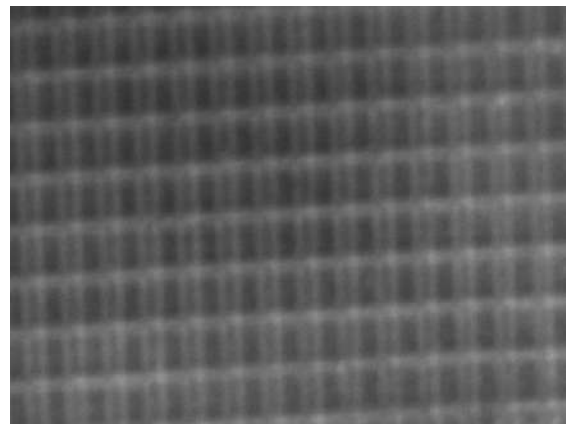

Mass selection of the primary ions in FIB

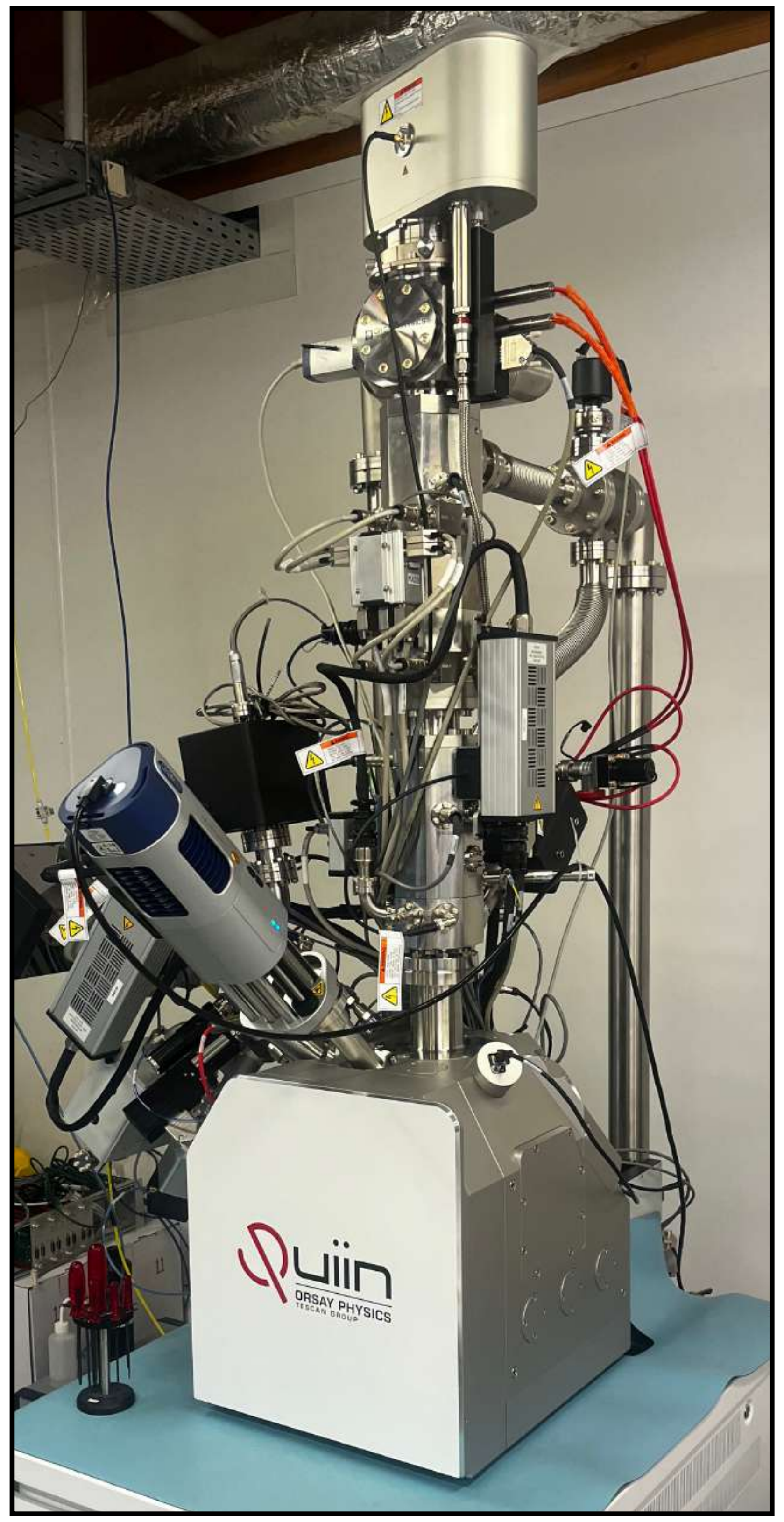

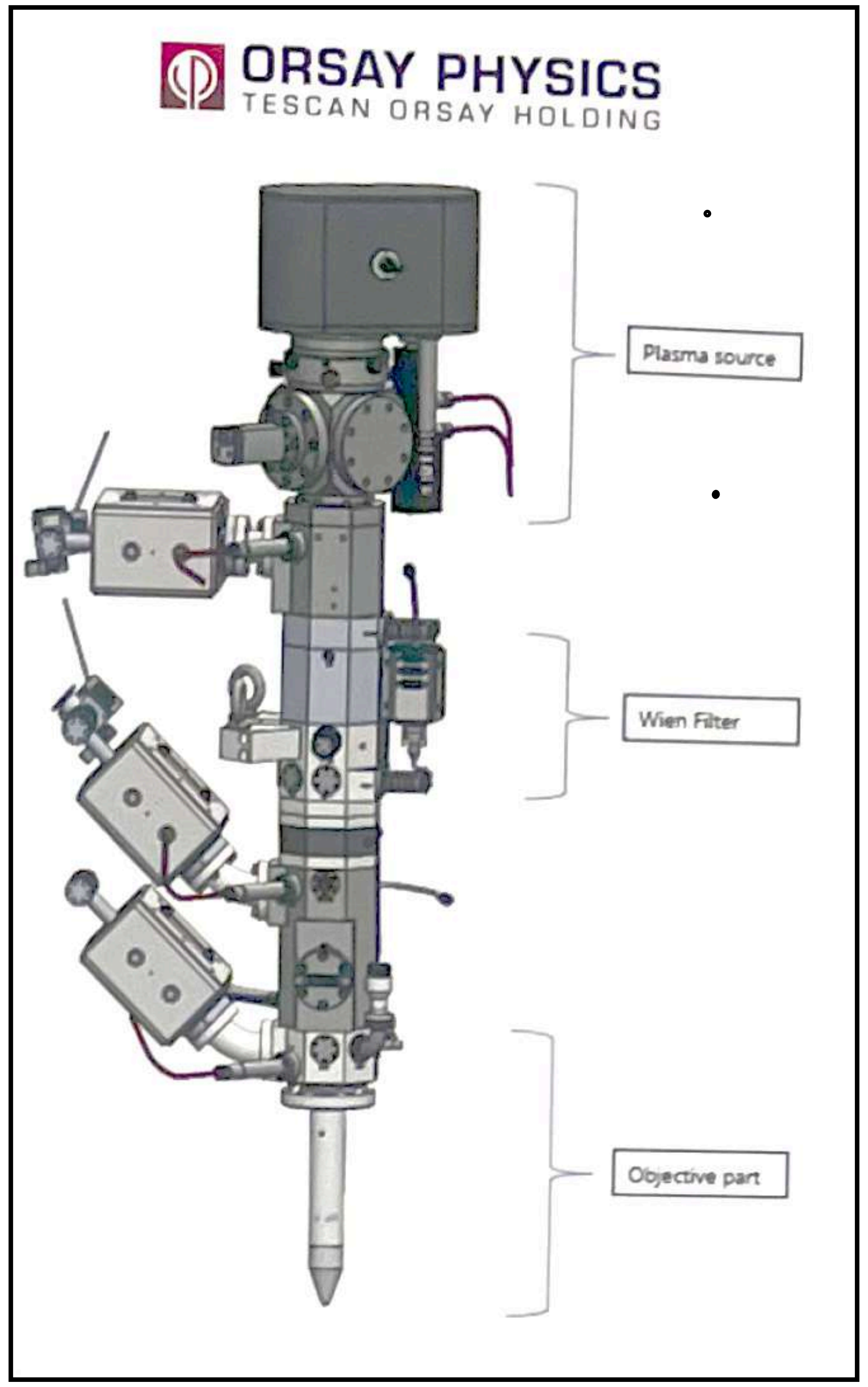

Other application of EXB Wien filter in EM : monochromators (Thermofisher and Jeol)

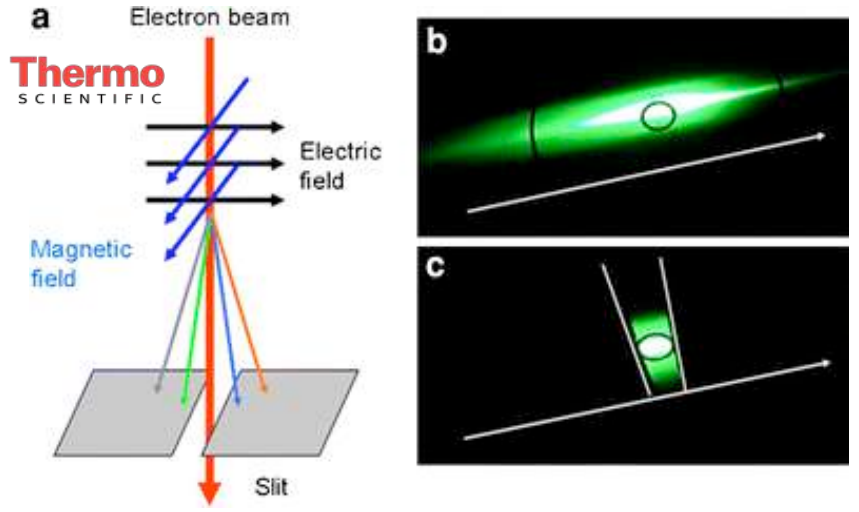

Other applications of dipolar fields in curved axis optics : the sectors

Beware : Equations are slightly different as the field expansion cannot be performed using $w = x + iy$ variables.
You need to define new variables relative to the curved optic axis but the general idea remains the same.

See Rose's book to have the detail of the new field expansion, paraxial equations and aberrations

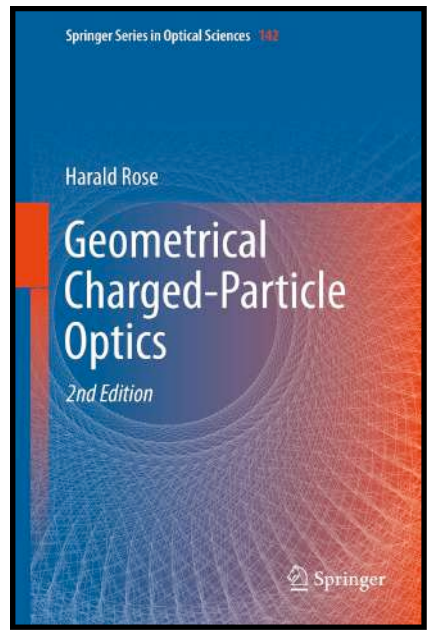

Electrostatic sector

General overview

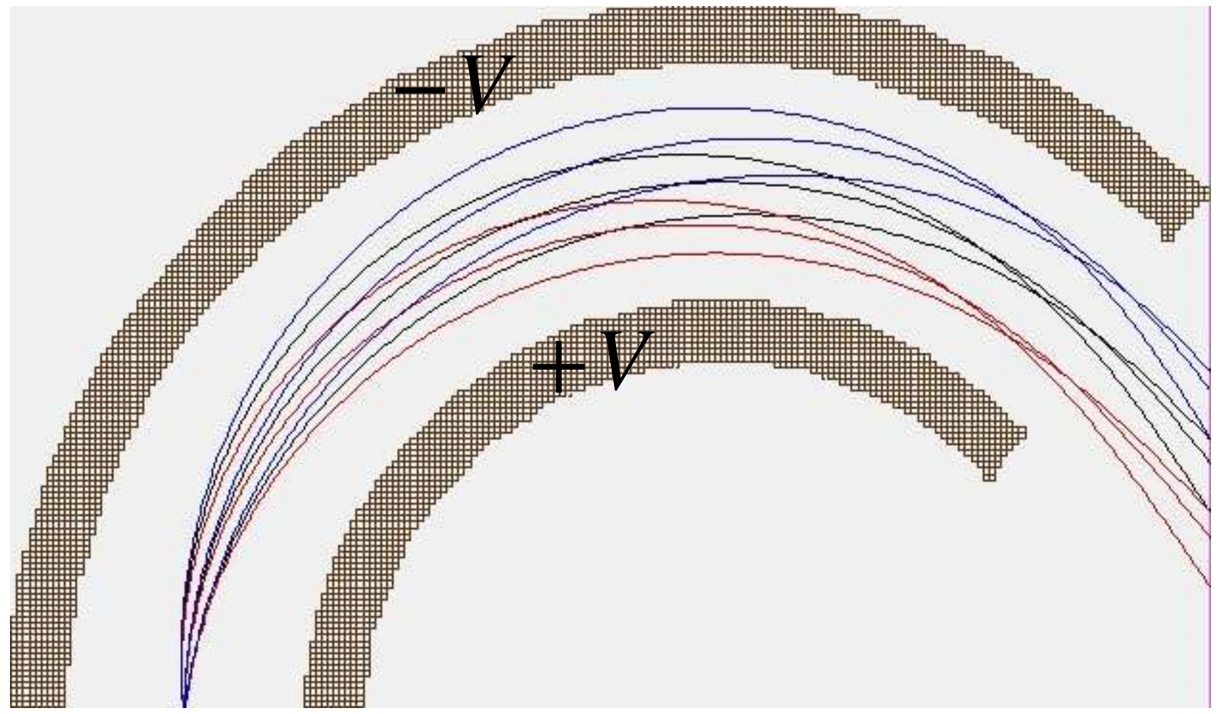

Application : analyser

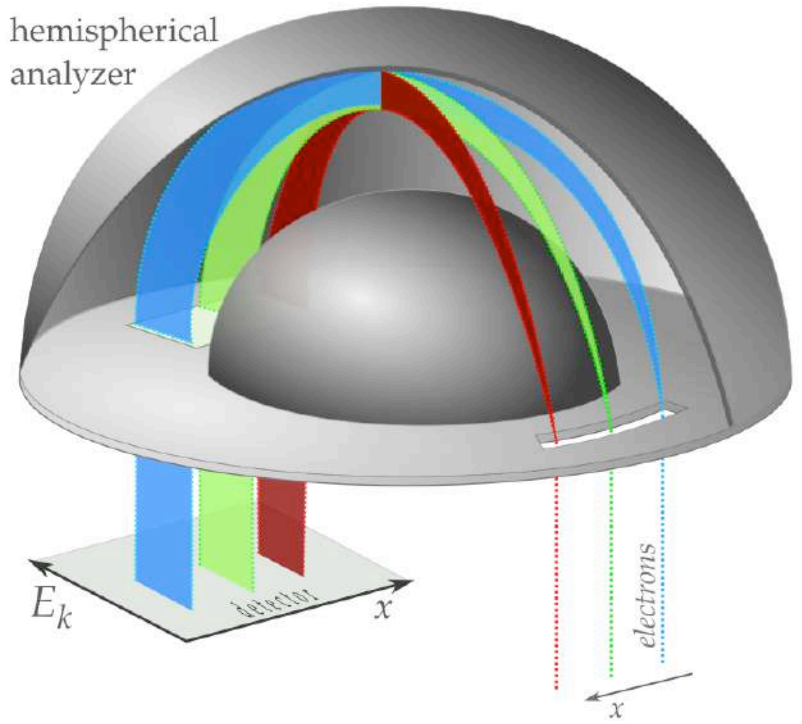

- Focalisation and dispersion along one direction
- Nothing along the perpendicular direction

Application in EM : monochromator

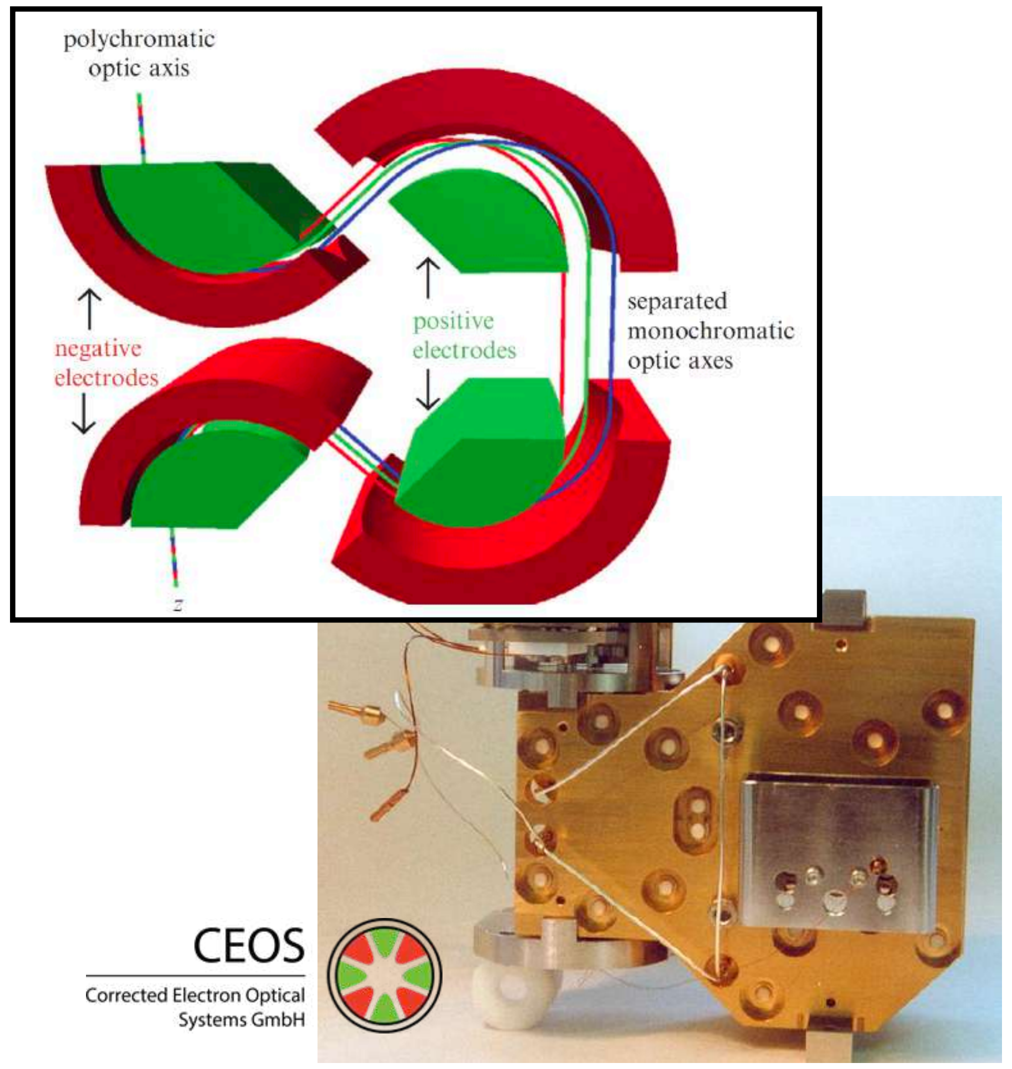

XPS instruments

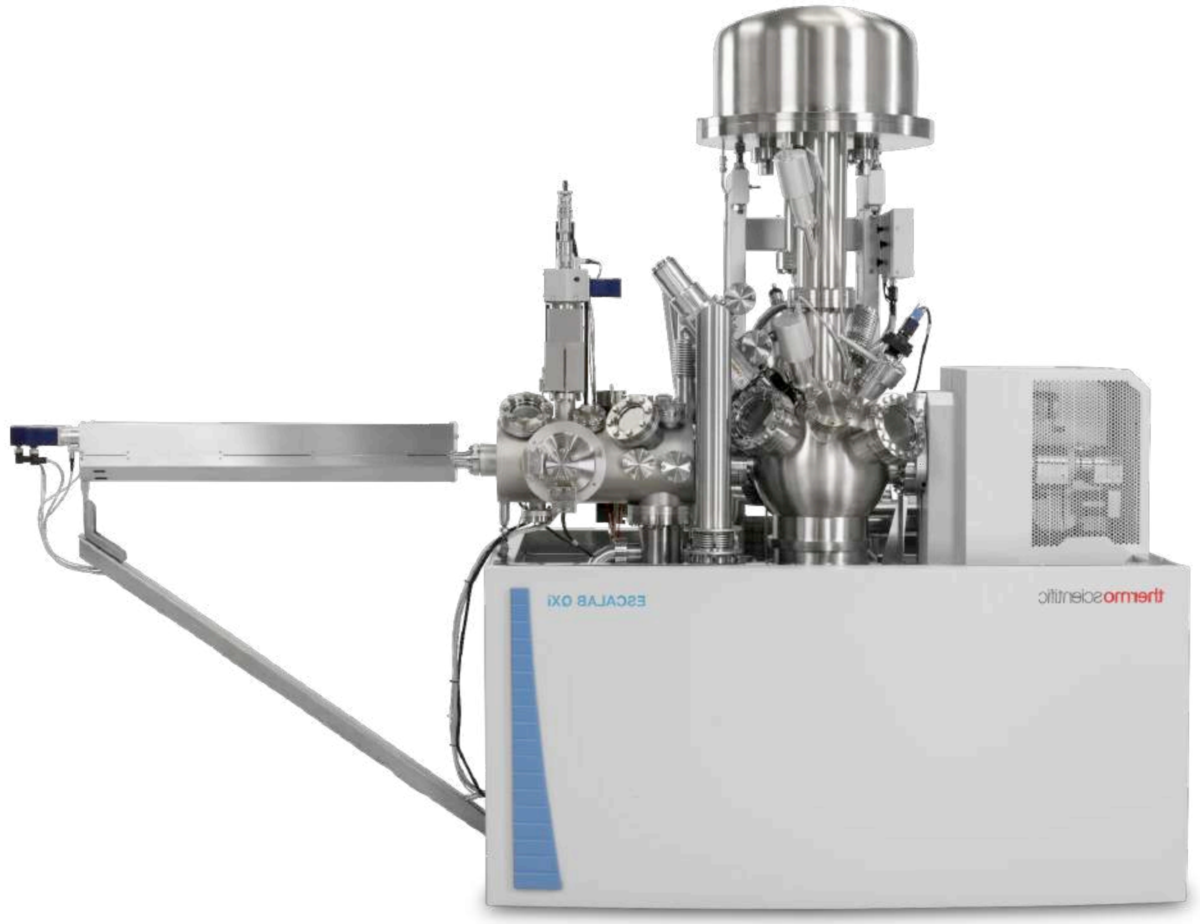

Magnetostatic sector

General overview

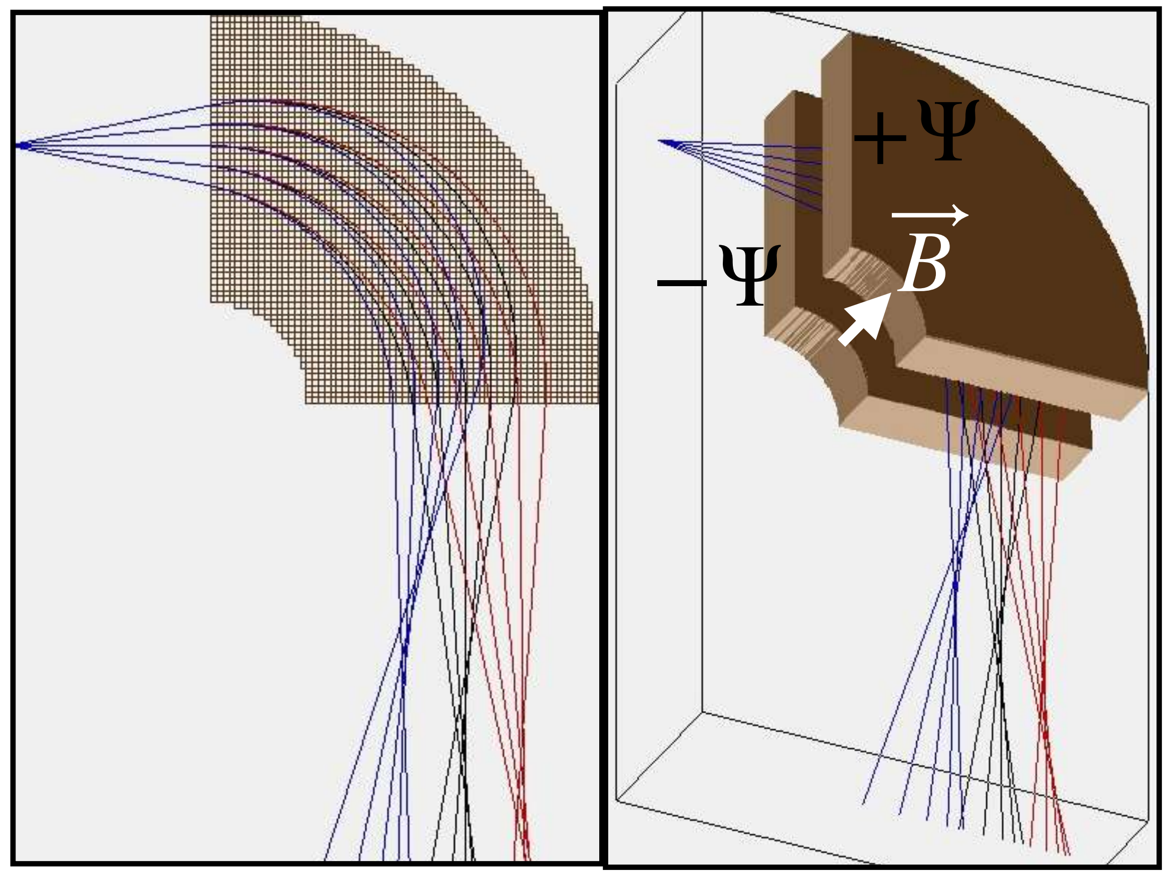

Application: mass analyser
(for example SIMS)

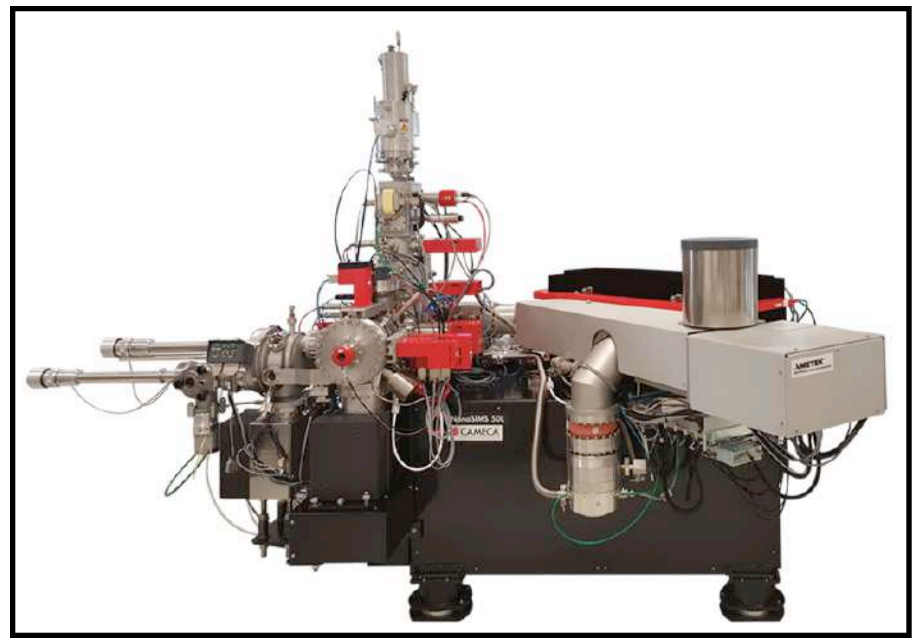

- Focalisation and dispersion along one direction
- Nothing along the perpendicular direction

Application in EM : monochromator and Spectrometer (Gatan, Nion, CEOS, …)

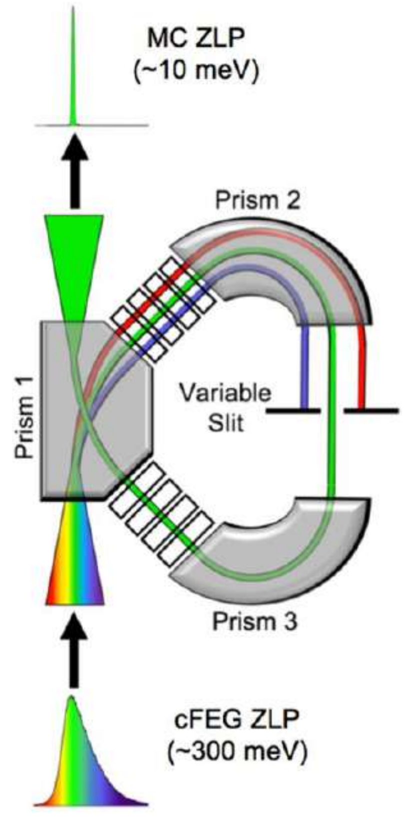

Let's start from the general paraxial equations …

$$w'' + \frac{\gamma_0}{2\Phi_0^*}(\Phi_0' + iv_0\Psi_0')w' + \frac{\gamma_0}{4\Phi_0^*}\left(\Phi_0'' + iv_0\Psi_0'' + \frac{\Phi_1\overline{\Phi}_1}{2\gamma_0\Phi_0^*}\right)w - \frac{\gamma_0}{\Phi_0^*}\left(\Phi_2 + iv_0\Psi_2 - \frac{\Phi_1^2}{8\gamma_0\Phi_0^*}\right)\overline{w} = \frac{\gamma_0}{2\Phi_0^*}(\Phi_1 + iv_0\Psi_1)$$

We assume $\Phi_1 = \Psi_1 = \Phi_2 = \Psi_2 = 0$. The paraxial equation is simplified with only $\nu = 0$ components contribution

$$w'' + \frac{\gamma_0}{2\Phi_0^*}(\Phi_0' + iv_0\Psi_0')w' + \frac{\gamma_0}{4\Phi_0^*}\left(\Phi_0'' + iv_0\Psi_0''\right)w = 0$$

We rewrite the complex coordinate system : $w(z) = u(z)e^{i\chi}$ defining the amplitude of the trajectory $u(z)$ and the phase χ known as Larmor rotatio

Second-order differential equation (with varying factors)

$$u'' + \frac{\gamma_0\Phi_0'}{2\Phi_0^*}u' + \frac{\gamma_0}{4\Phi_0^*}\left(\Phi_0'' + \frac{e}{2m_e}\Psi_0'^2\right)u = 0 \qquad \Longrightarrow \chi = -\sqrt{\frac{e}{8m_e}}\int_{z_0}^{z}\frac{\Psi_0'}{\sqrt{\Phi_0^*}}dz$$

There are 2 independent solutions :

Initial conditions :

$u_\alpha \backslash u_\alpha(z_0) = 0, u_\alpha'(z_0) = 1$ Marginal ray/Axial ray

$u_\pi \backslash u_\pi(z_0) = 1, u_\pi'(z_0) = 0$ Principal ray/Chief Ray/Field Ray

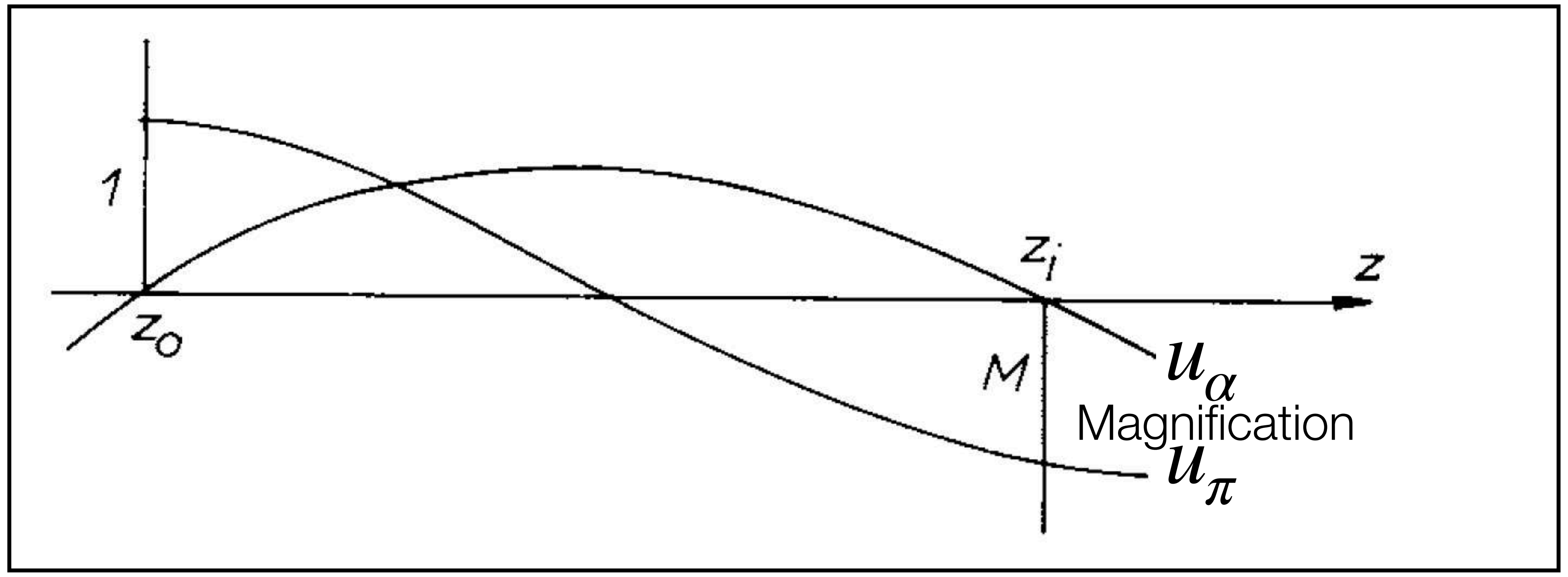

The solution for any ray is written as a simple linear combination of the two fundamental solutions : $u = c_1u_\alpha + c_2u_\pi$.

If $u_0 = u(z_0)$ and $u_0' = u'(z_0)$ then we have : $\boxed{u(z) = u_0'u_\alpha(z) + u_0u_\pi(z)}$

Paraxial properties of electrostatic lenses : the Einzel lens

Let's first consider a pure electrostatic system with rotational symmetry.

$$w'' + \frac{\gamma_0}{2\Phi_0^*}(\Phi_0' + iv_0\Psi_0')w' + \frac{\gamma_0}{4\Phi_0^*}\left(\Phi_0'' + iv_0\Psi_0''\right) w = 0$$

➡ We have $\Psi_0 = 0$, and we can extract two equations as $w(z) = x(z) + iy(z)$

➡ $$\boxed{x'' + \frac{1}{2}\frac{\Phi_0'}{\Phi_O^*}x' + \frac{1}{4}\frac{\Phi_0''}{\Phi_O^*}x = 0} \qquad \boxed{y'' + \frac{1}{2}\frac{\Phi_0'}{\Phi_O^*}y' + \frac{1}{4}\frac{\Phi_0''}{\Phi_O^*}y = 0}$$

1. Define geometry and voltages
2. Calculate potential distribution

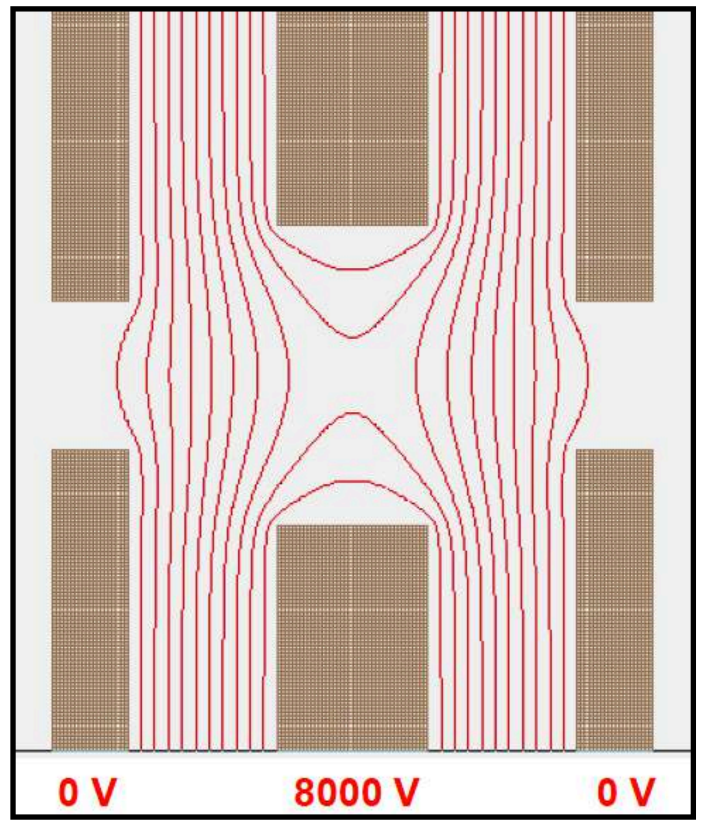

3. Extract axial potential $\Phi_0(z)$
4. Compute $\Phi_0'(z)$, $\Phi_0''(z)$

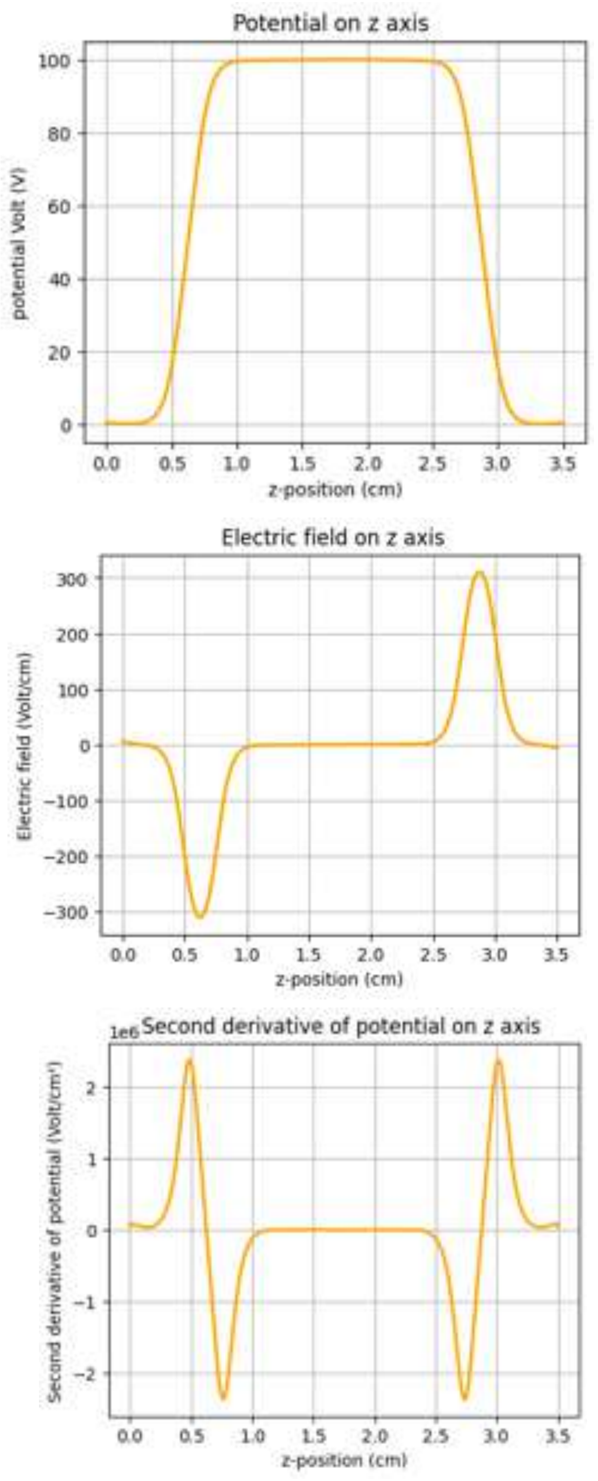

5. Resolve paraxial equation using R-K algorithm

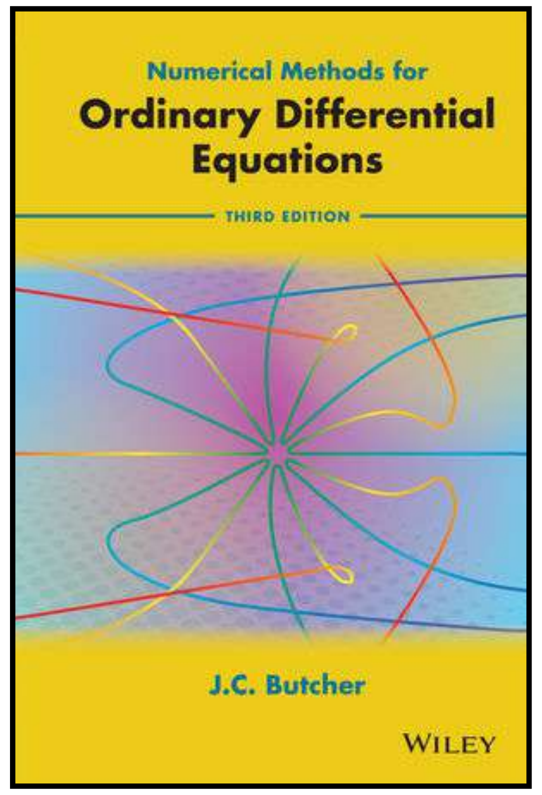

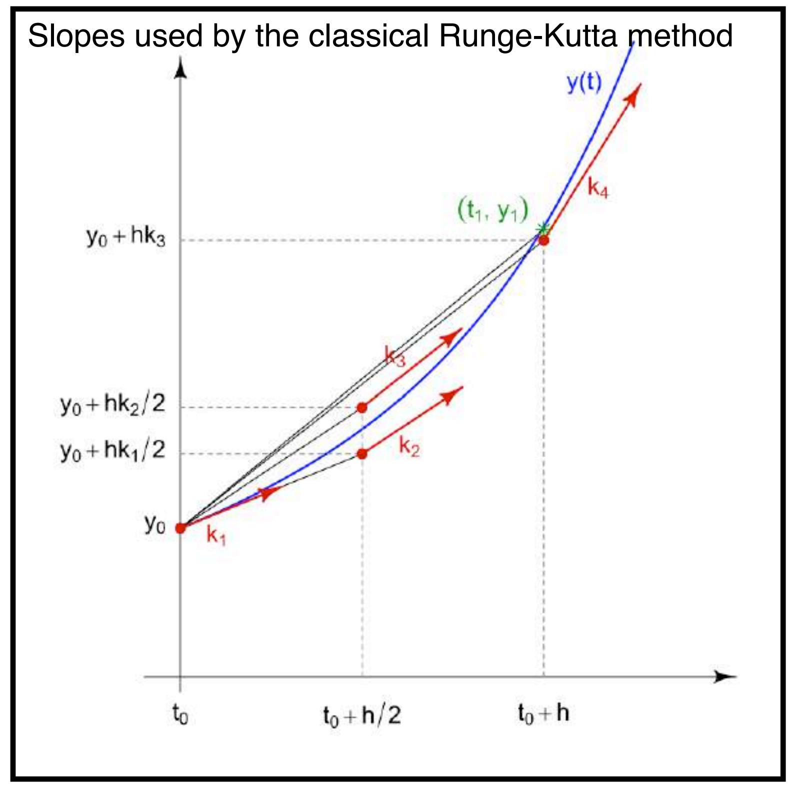

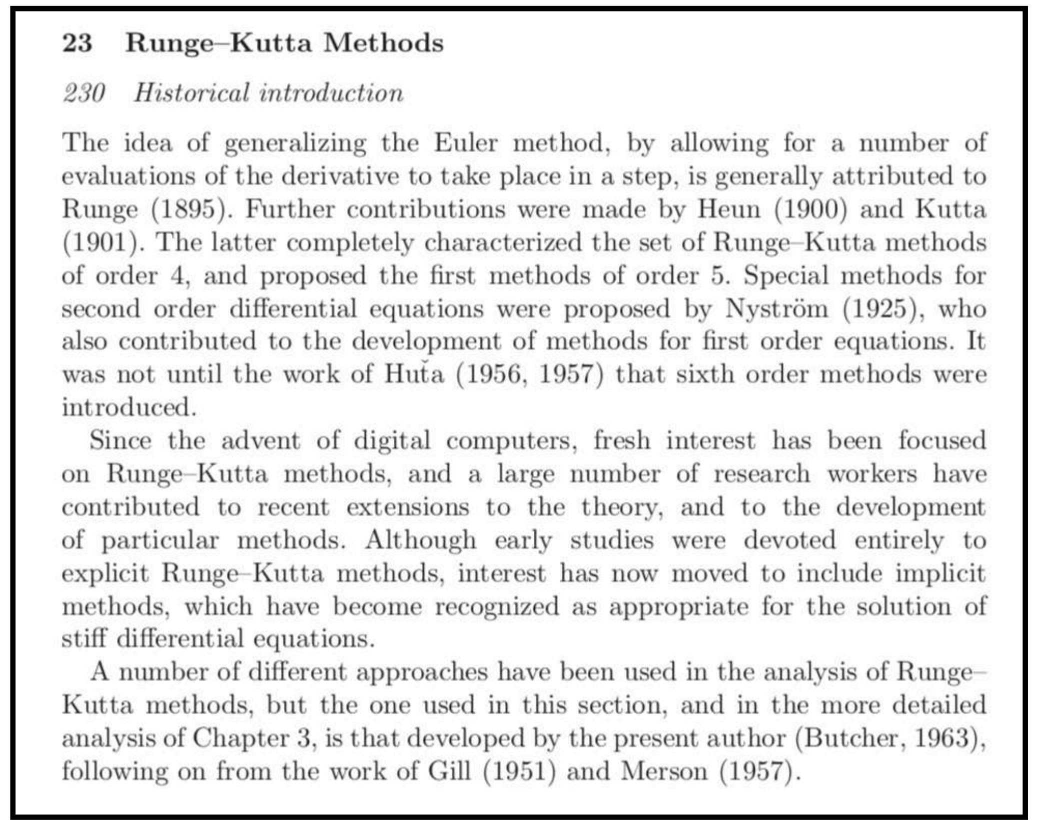

23 Runge–Kutta Methods

230 Historical introduction

The idea of generalizing the Euler method, by allowing for a number of evaluations of the derivative to take place in a step, is generally attributed to Runge (1895). Further contributions were made by Heun (1900) and Kutta (1901). The latter completely characterized the set of Runge–Kutta methods of order 4, and proposed the first methods of order 5. Special methods for second order differential equations were proposed by Nyström (1925), who also contributed to the development of methods for first order equations. It was not until the work of Huťa (1956, 1957) that sixth order methods were introduced.

Since the advent of digital computers, fresh interest has been focused on Runge–Kutta methods, and a large number of research workers have contributed to recent extensions to the theory, and to the development of particular methods. Although early studies were devoted entirely to explicit Runge–Kutta methods, interest has now moved to include implicit methods, which have become recognized as appropriate for the solution of stiff differential equations.

A number of different approaches have been used in the analysis of Runge–Kutta methods, but the one used in this section, and in the more detailed analysis of Chapter 3, is that developed by the present author (Butcher, 1963), following on from the work of Gill (1951) and Merson (1957).

6. Draw the 2 fundamental rays from which any ray can be obtained

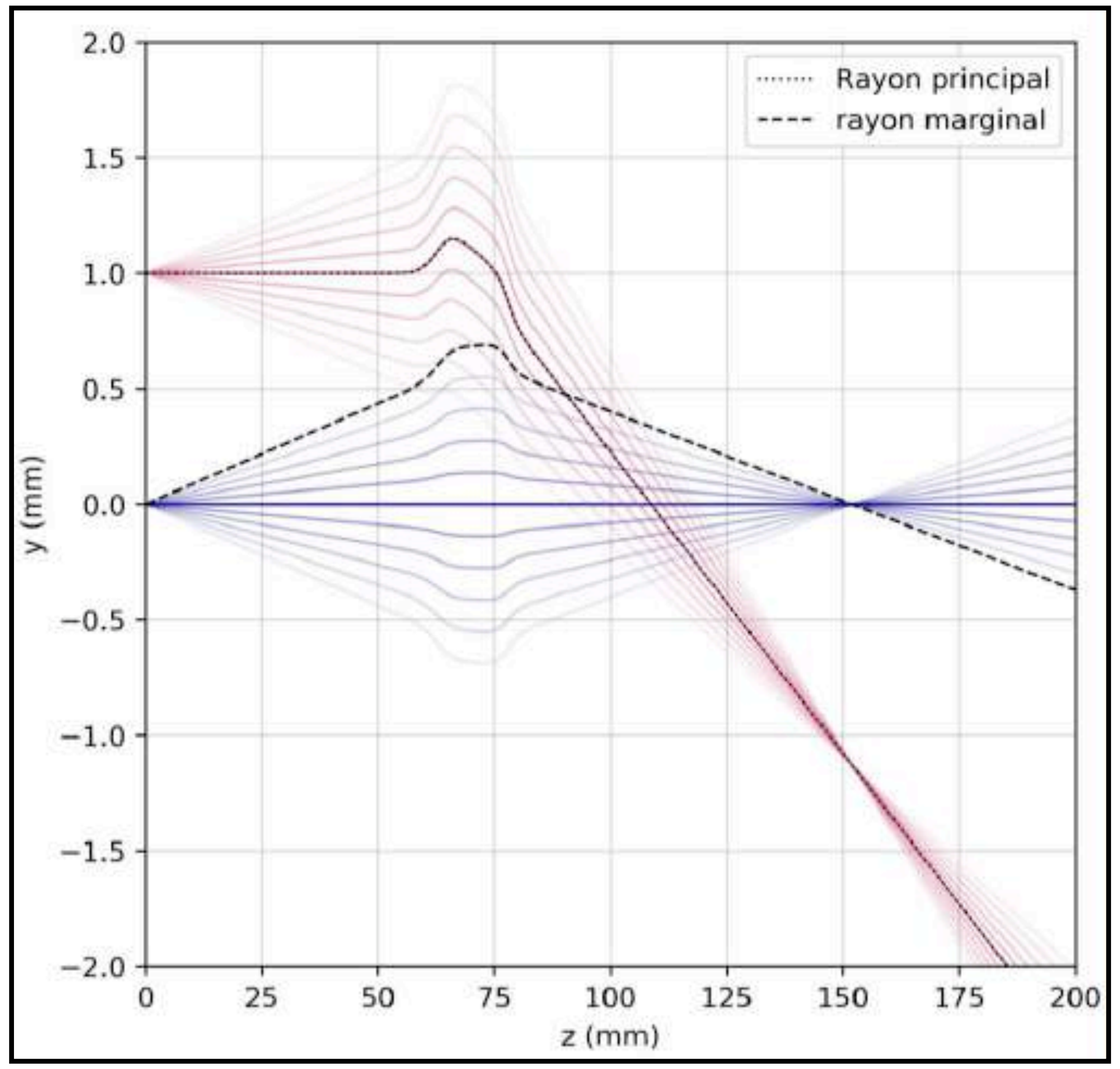

Focal distance (if $\Phi_0(z_0) = \Phi_0(z_i)$)

$$\frac{1}{f} \approx \frac{3}{16}\int_{z_0}^{z_i} \frac{\Phi_0'^2(z)}{\Phi_0(z)^2}dz > 0$$

➡ *No diverging lens*

Simulation of an electrostatic column

General overview of the FIB column

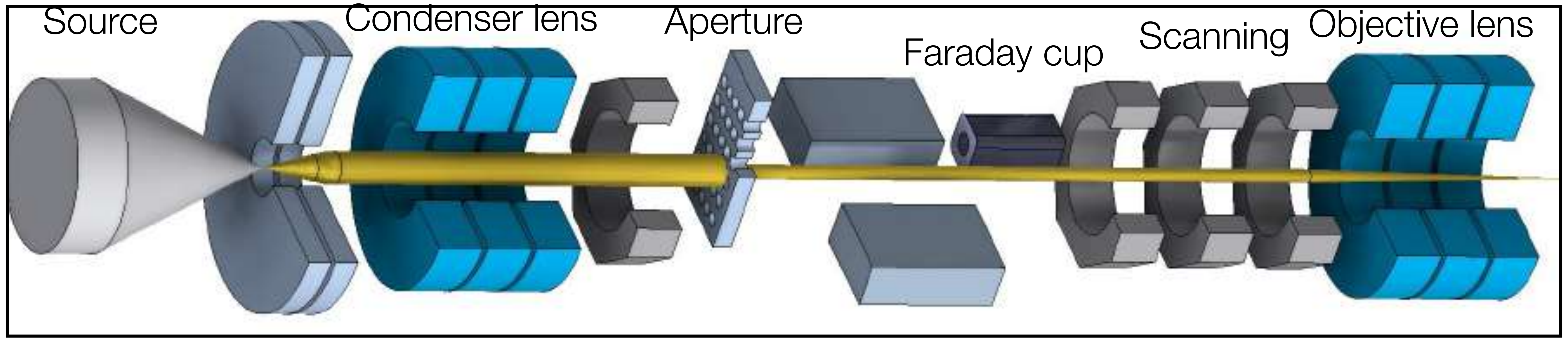

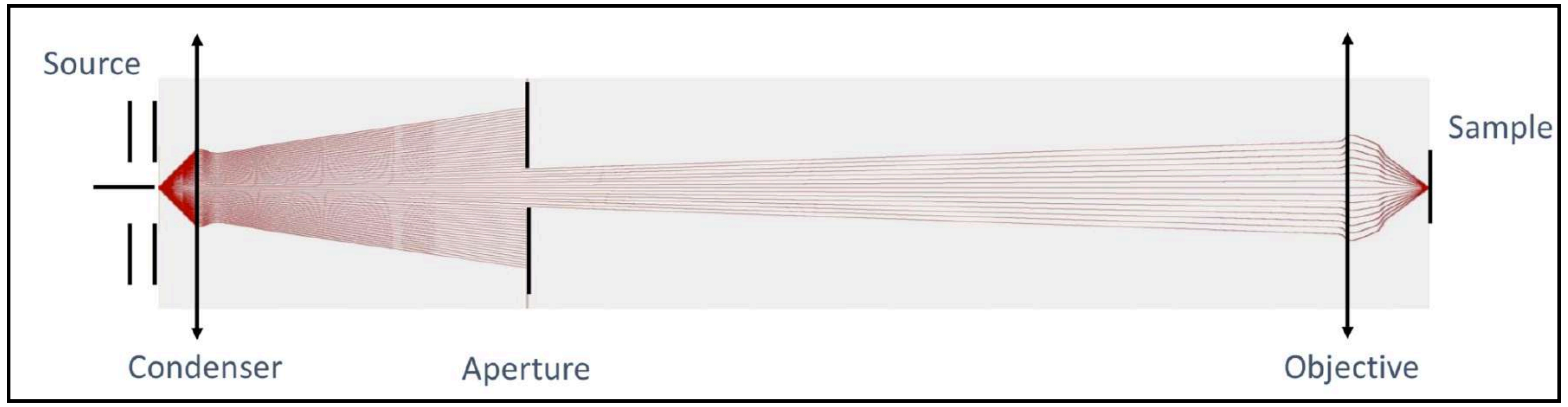

Two main optical modes simulated :

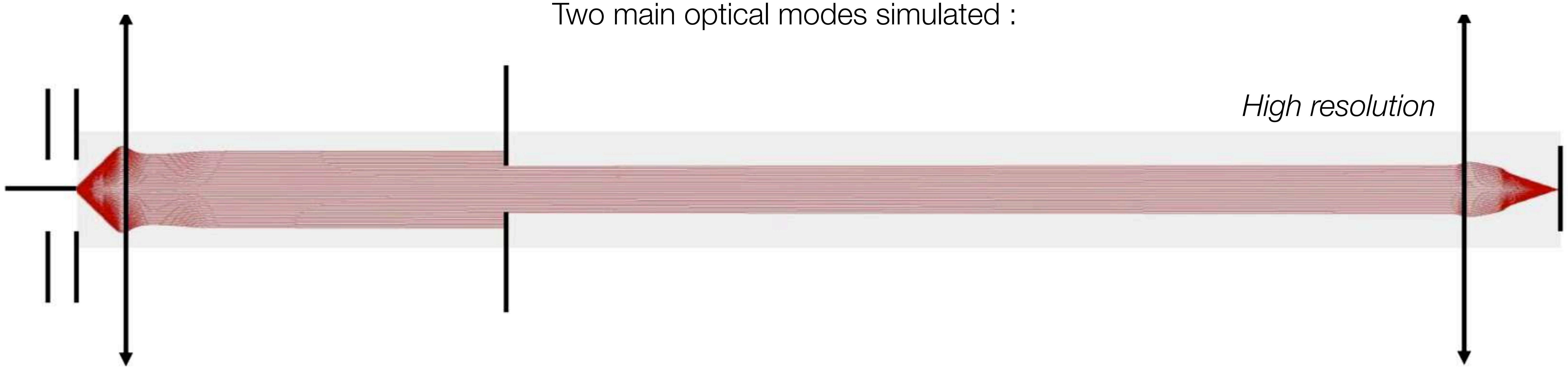

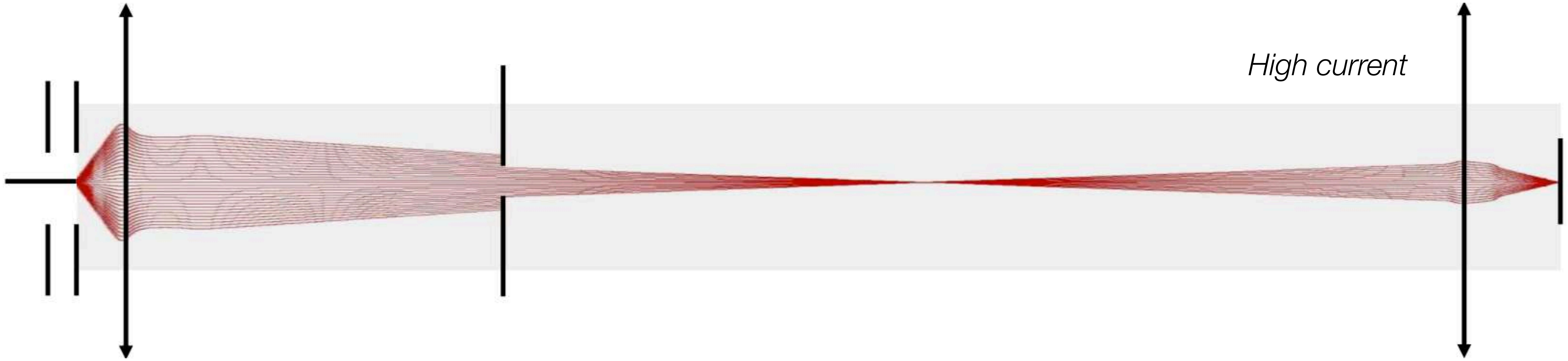

Experimental spots

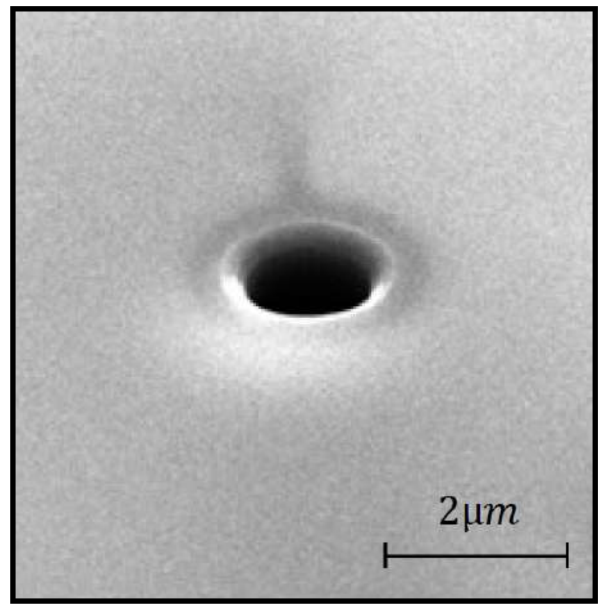

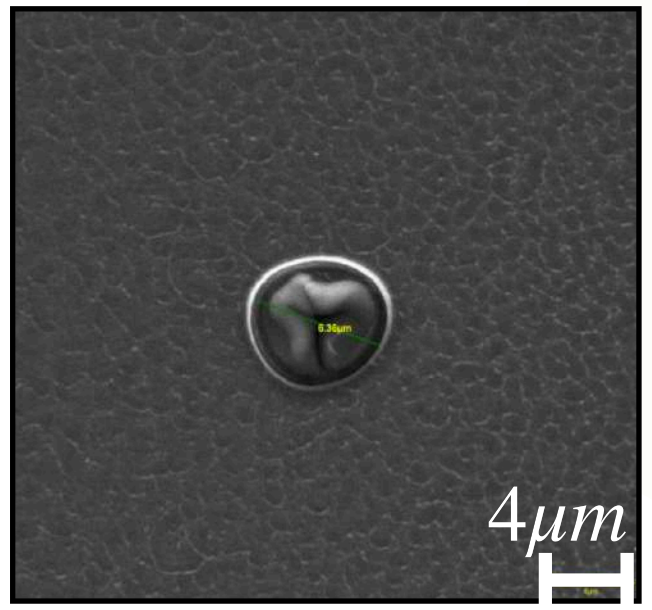

ORSAY PHYSICS
TESCAN GROUP

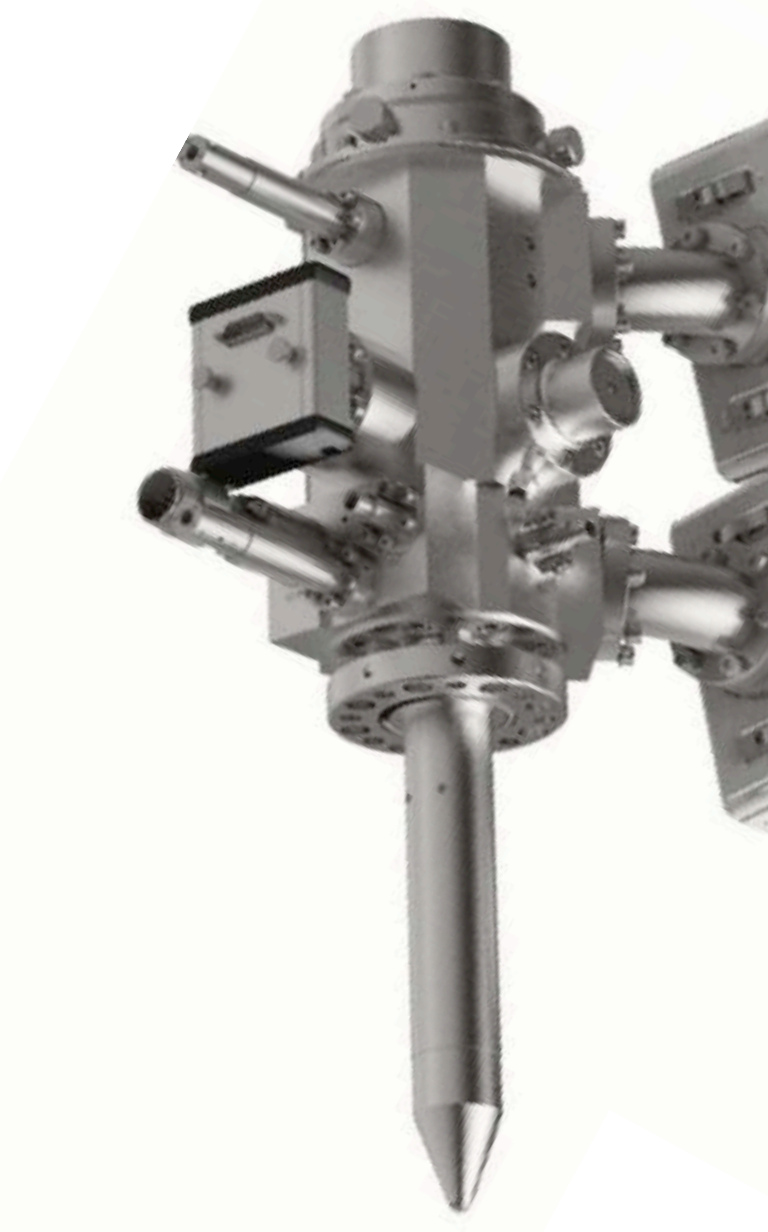

Paraxial properties of magnetostatic lenses : the electromagnetic lens

➡ Paraxial equation for magnetic system with rotational symmetry $(\Psi_0 \neq 0, \Phi_0 = 0)$

$$w(z) = x(z) + iy(z) = u(z)e^{i\chi}$$

$$u'' + \frac{\gamma_0}{4\Phi_0^*}\left(\frac{e}{2m_e}\Psi_0'^2\right)u = 0$$

➡

Simplified paraxial equation

$$u'' + k^2(z)u = 0$$

Larmor rotation

$$\chi = -\sqrt{\frac{e}{8m_e}}\int_{z_0}^{z}\frac{\Psi_0'(z)}{\sqrt{\Phi_0^*}}dz = -\frac{1}{2}\frac{Q}{\sqrt{2K_0 m}}\int_{z_0}^{z}B(z)dz$$

Focal distance

$$\frac{1}{f} = \frac{Q^2}{8K_0 m}\int_{z_0}^{z_i}B^2(z)dz > 0$$

➡ *No diverging lens*

1.Define geometry and voltages
2.Calculate potential distribution
3.Extract axial field $\Psi_0'(z) = B(z)$

4. Resolve paraxial equation using R-K algorithm
5. Plot trajectories in (x, y, z) space.
- Due to Larmor rotation not easy to visualise

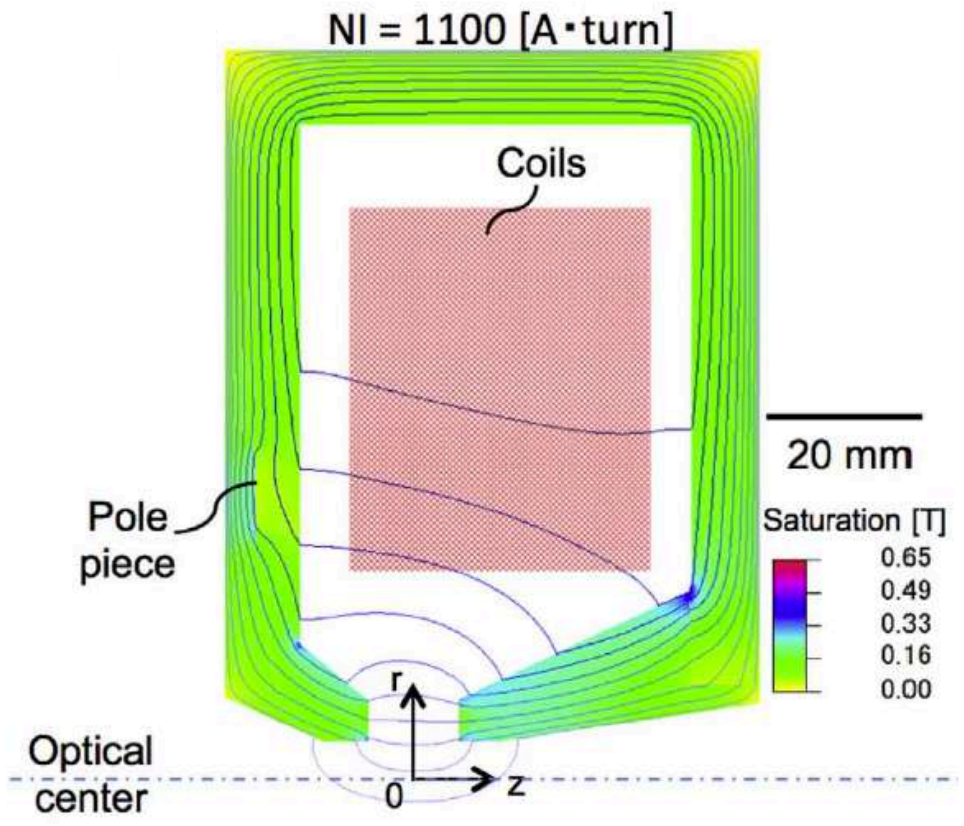

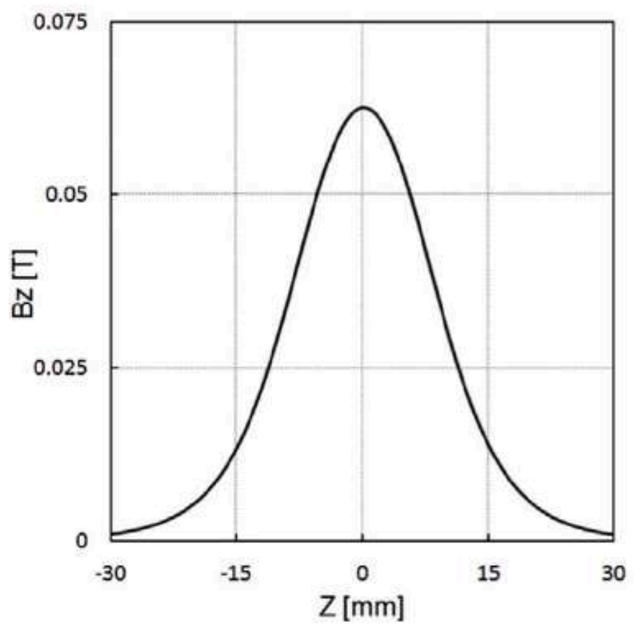

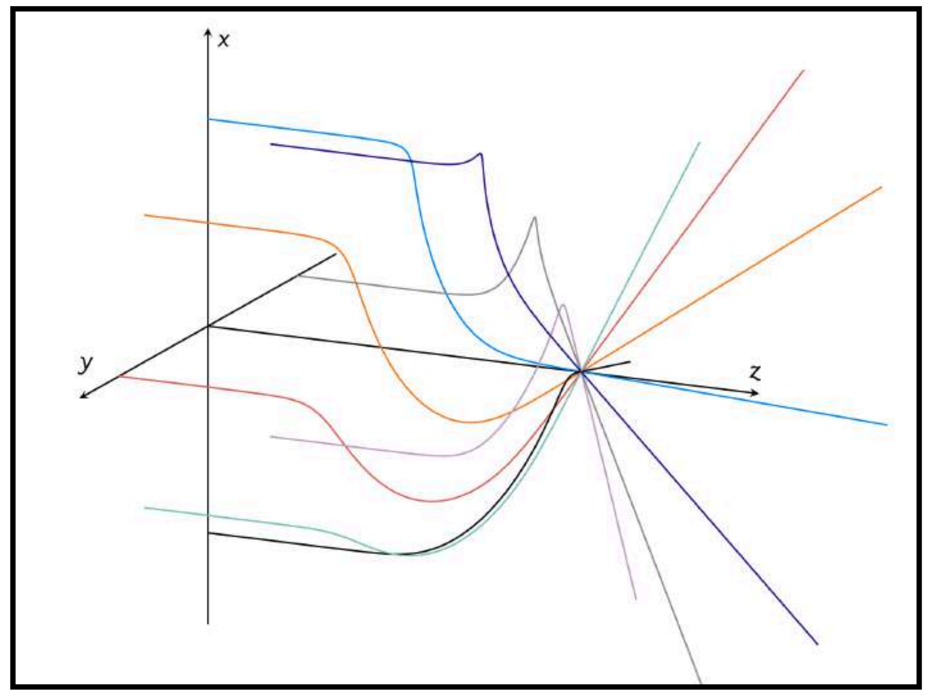

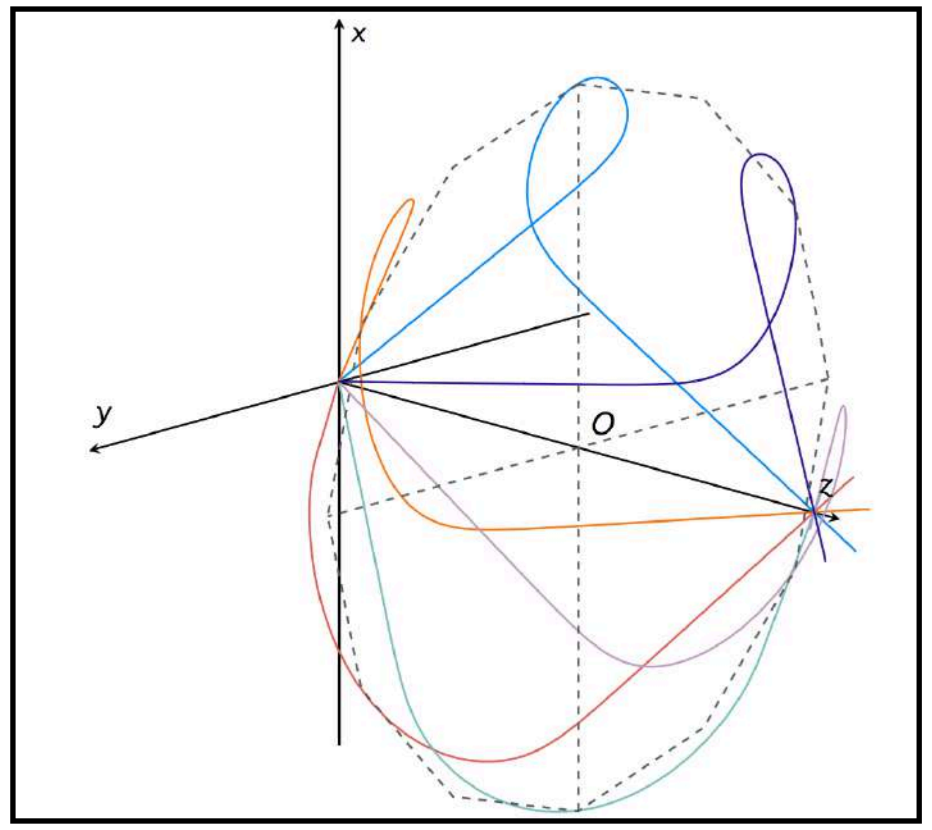

5. Plot of the two paraxial solutions (1 lens in that case) in (u, z)

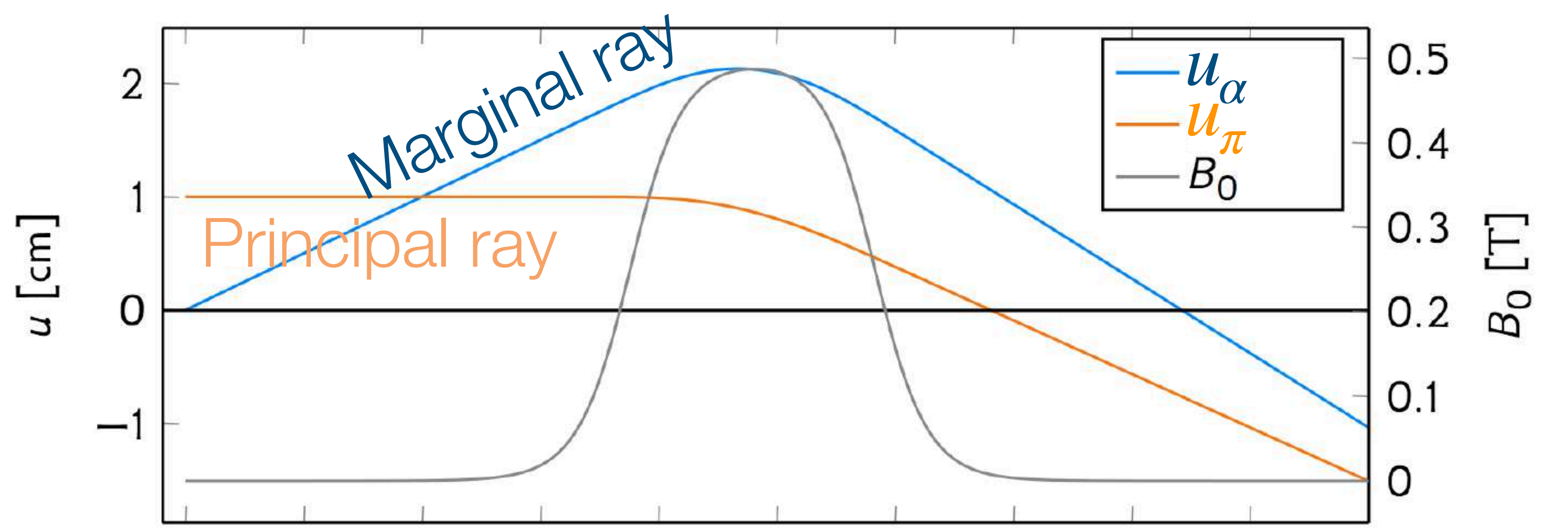

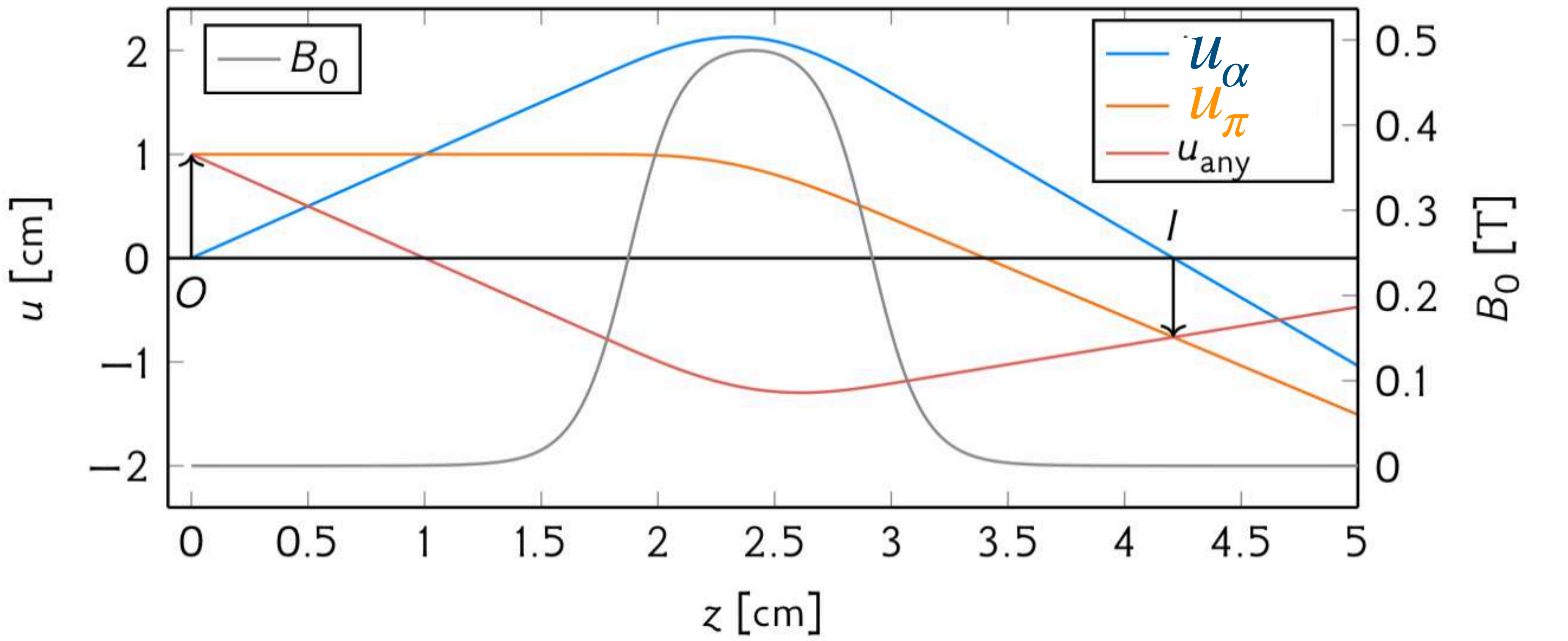

Simulation of a complete magnetostatic TEM column

Marginal ray of a double lens system in (u, z)

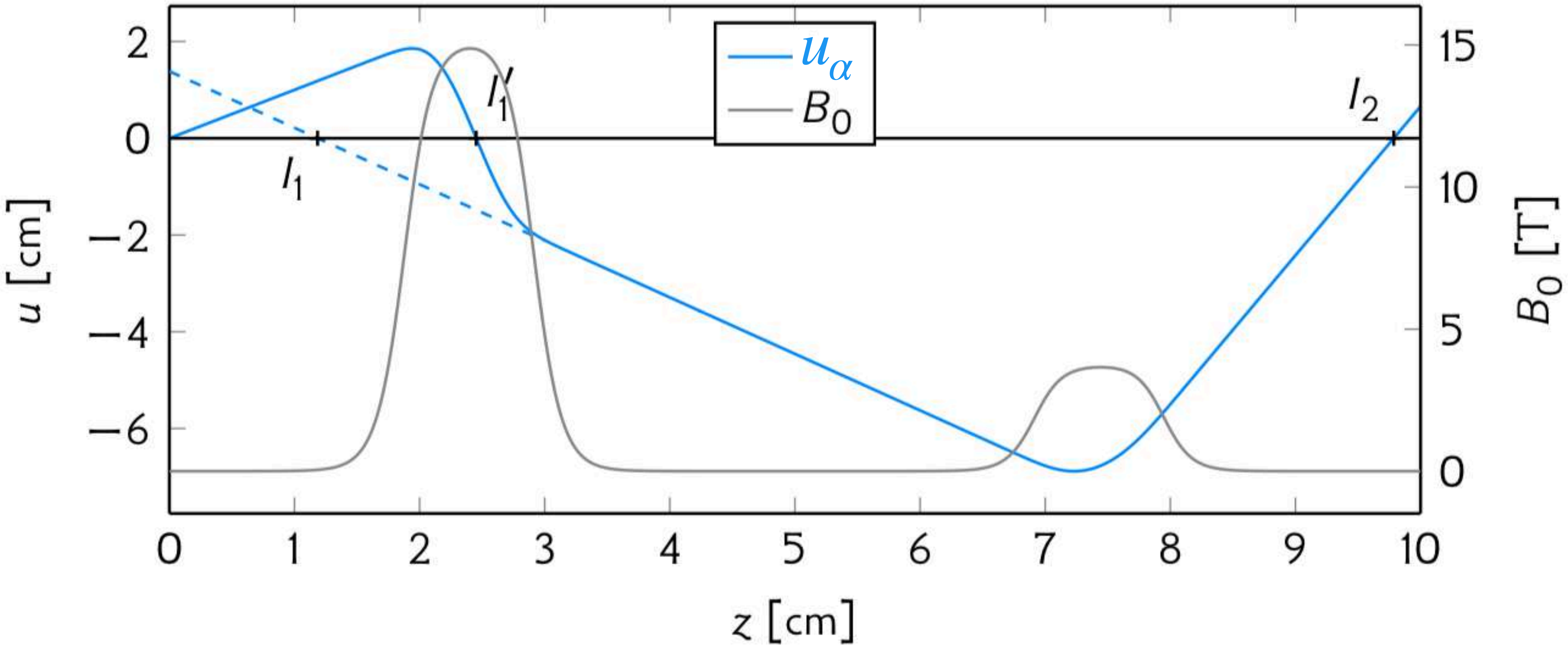

The I2TEM instrument in Toulouse :

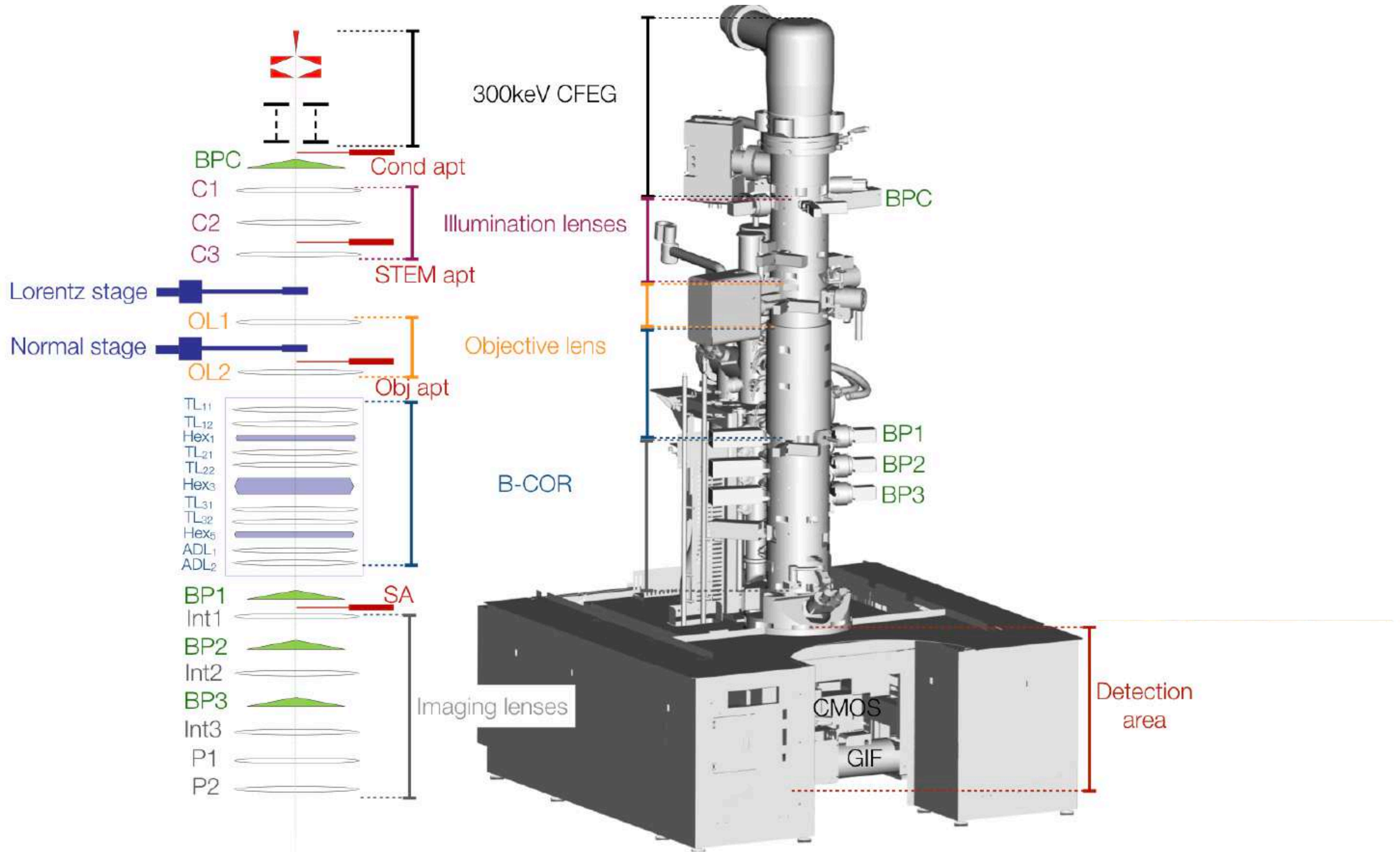

Paraxial and real tracing simulations :

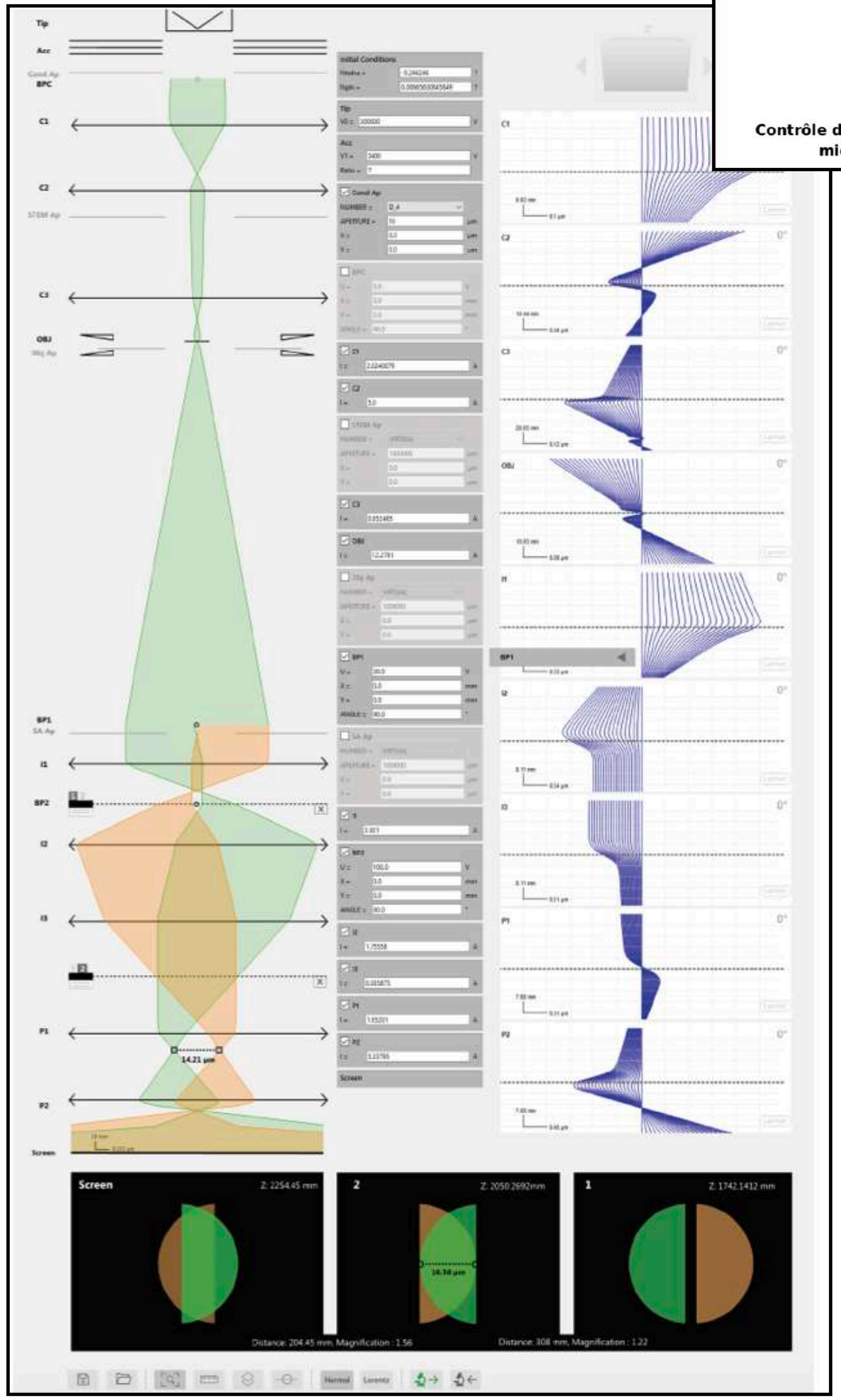

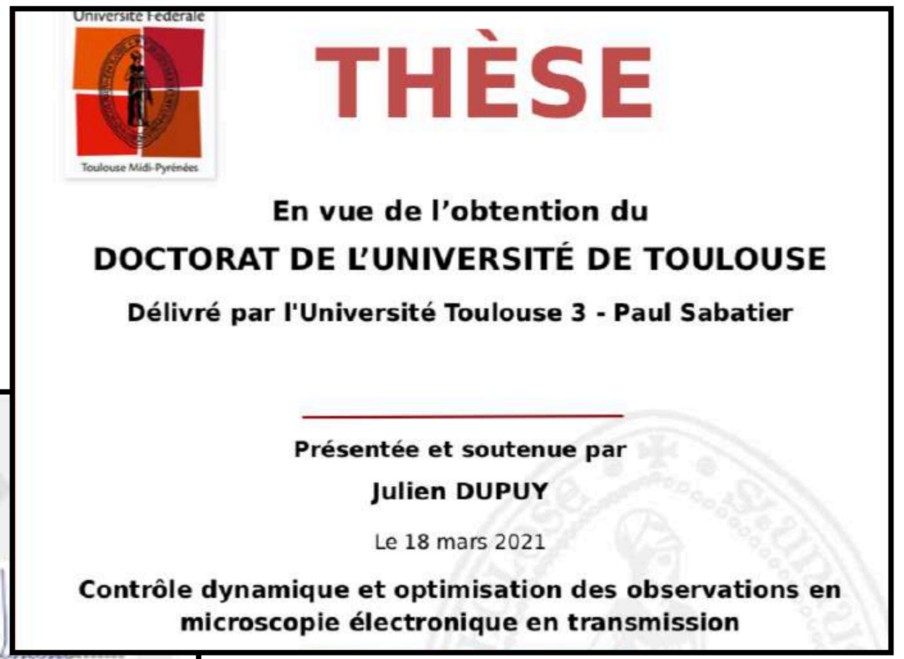

Paraxial properties of electrostatic lenses : overview of immersion system

A. Immersion lens

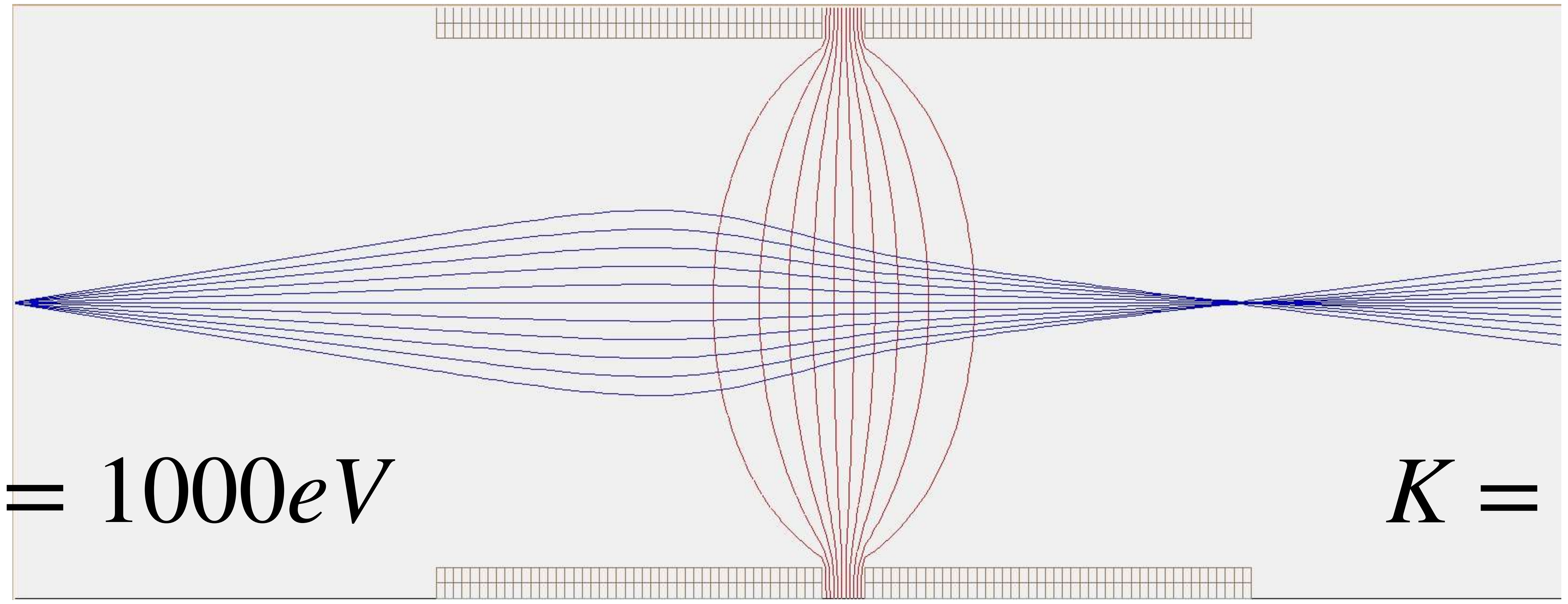

Energy change between object and image area

$$\mu_e^{(0)} = \sqrt{\frac{\Phi_0^*(z)}{\Phi_0^*(z_0)}} \neq 1$$

$$\frac{1}{f} \approx \frac{3}{16}\left(\frac{\Phi_0(z_0)}{\Phi_0(z_i)}\right)^{\left(\frac{1}{4}\right)} \int_{z_0}^{z_i} \frac{\Phi_0'^2(z)}{\Phi_0(z)^2} dz$$

B. Einzel (unipotential) lens

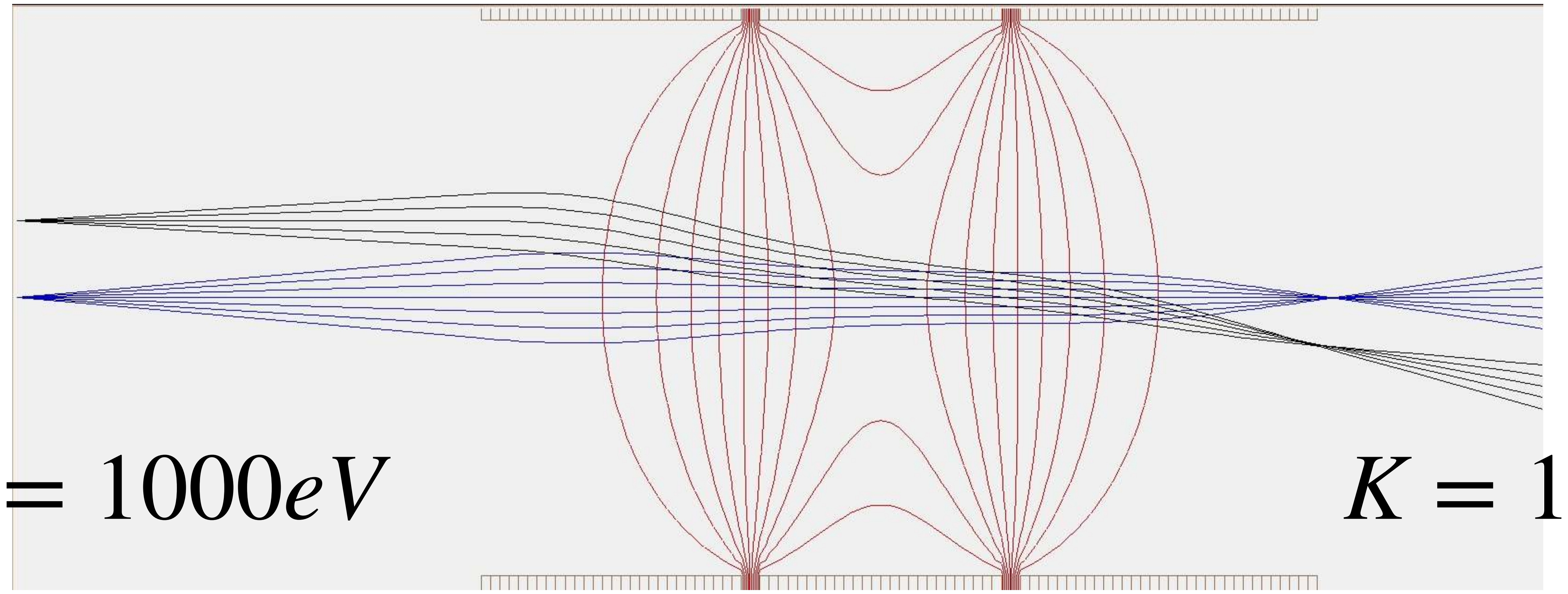

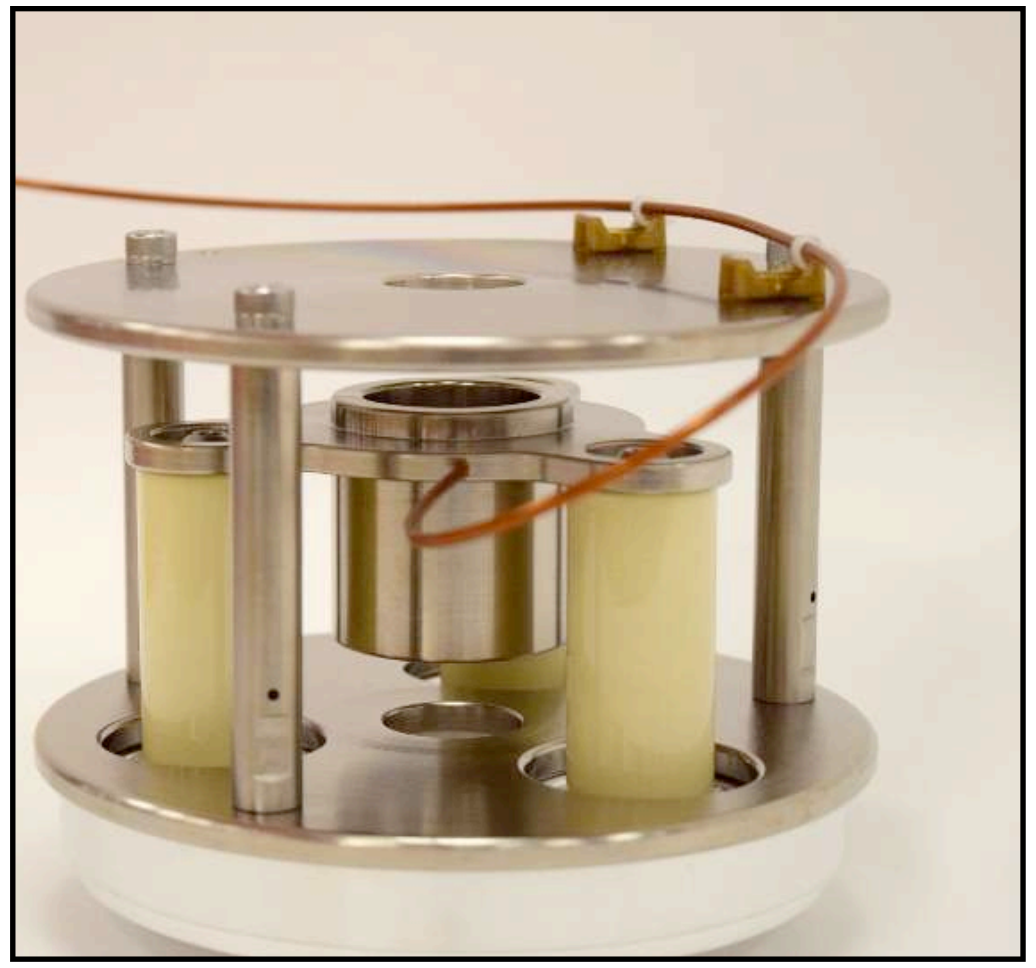

Energy not change between object and image area

$$\mu_e^{(0)} = \sqrt{\frac{\Phi_0^*(z)}{\Phi_0^*(z_0)}} = 1$$

$$\frac{1}{f} \approx \frac{3}{16} \int_{z_0}^{z_i} \frac{\Phi_0'^2(z)}{\Phi_0(z)^2} dz > 0$$

The electron source : overview of this particular immersion system

Thermionic electron source (very intense, low brightness)

Metallic filament

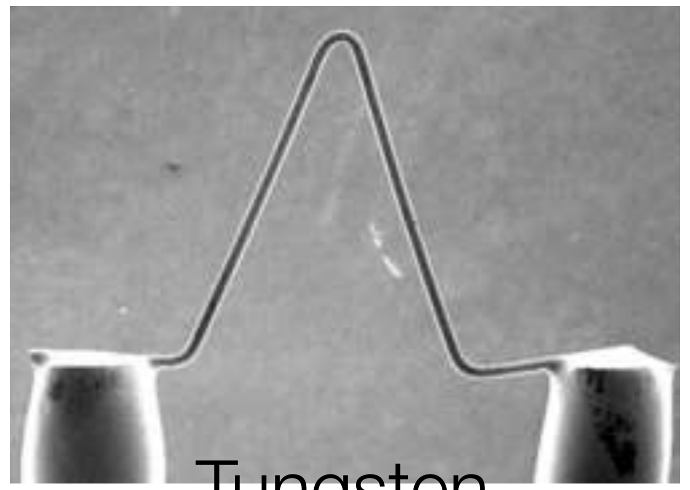

Tungsten
ϕ= 4.5eV
2800K

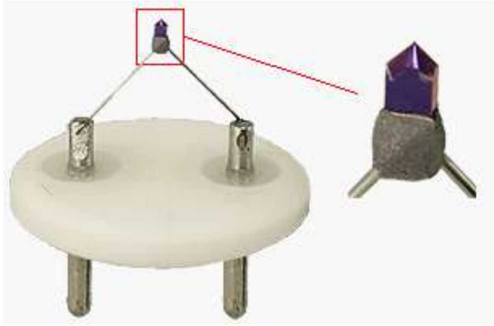

LaB6
ϕ= 2.5eV
2000K

Potential calculation

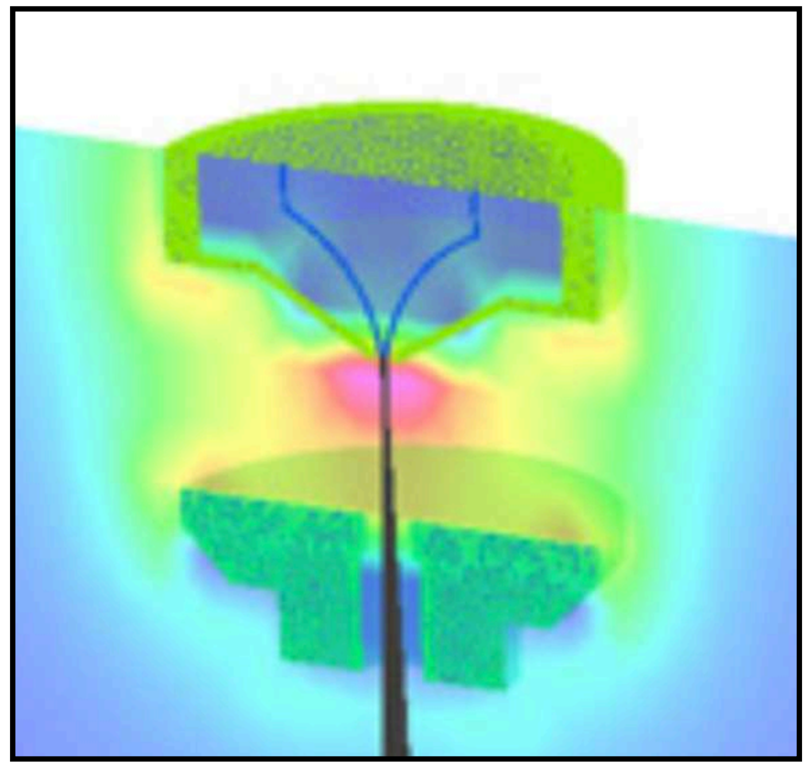

Electron optical configuration

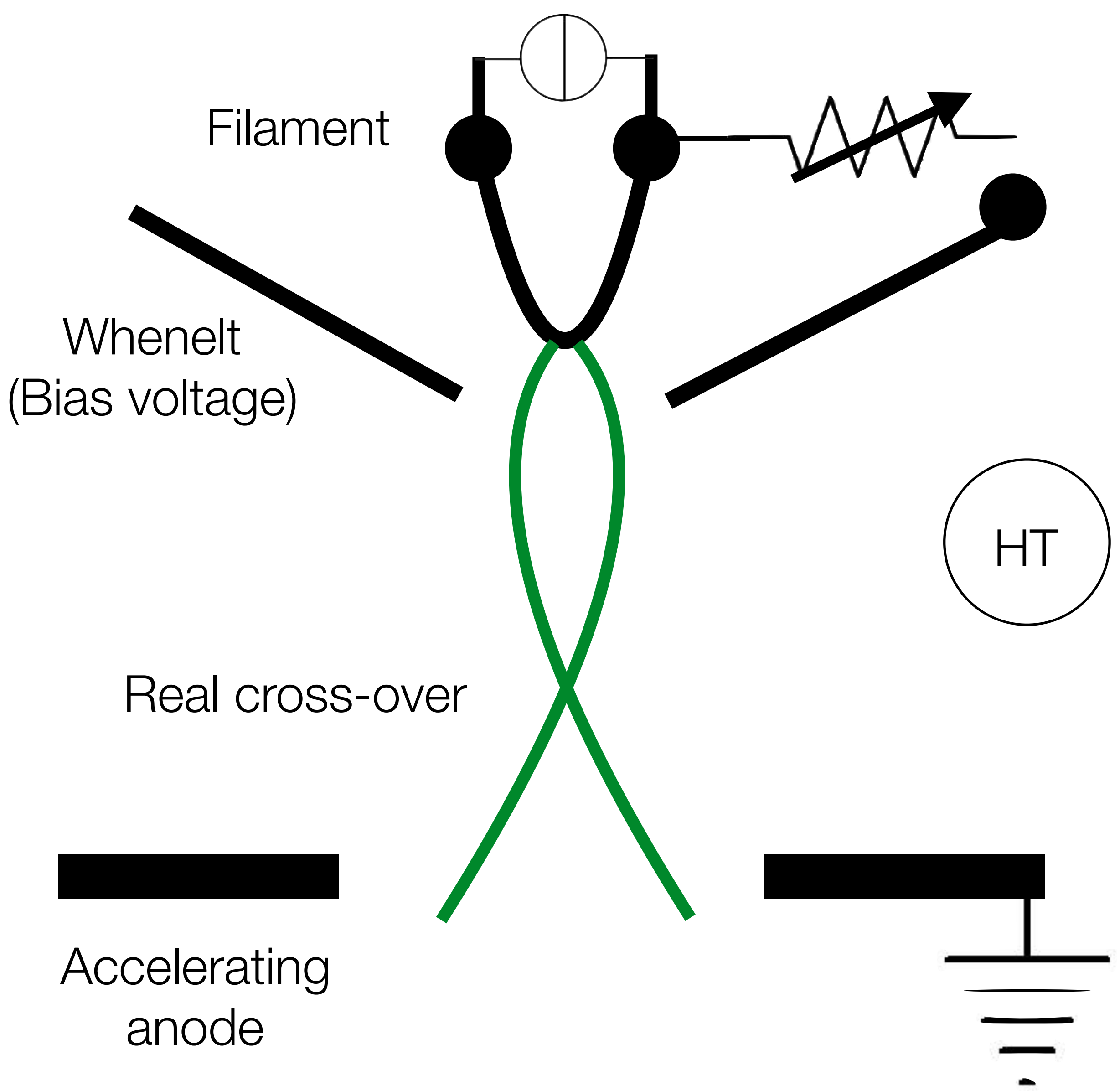

Real tracing method
and not paraxial

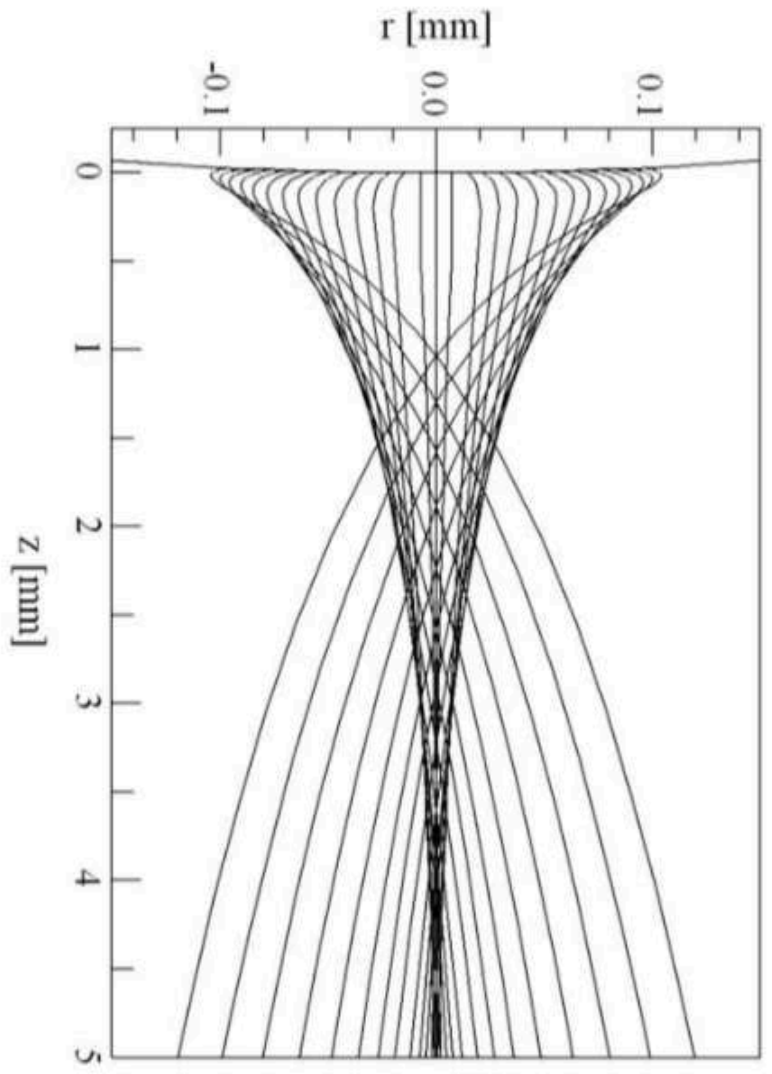

Cold Field Emission source (CFE) (small intensity, high brightness)

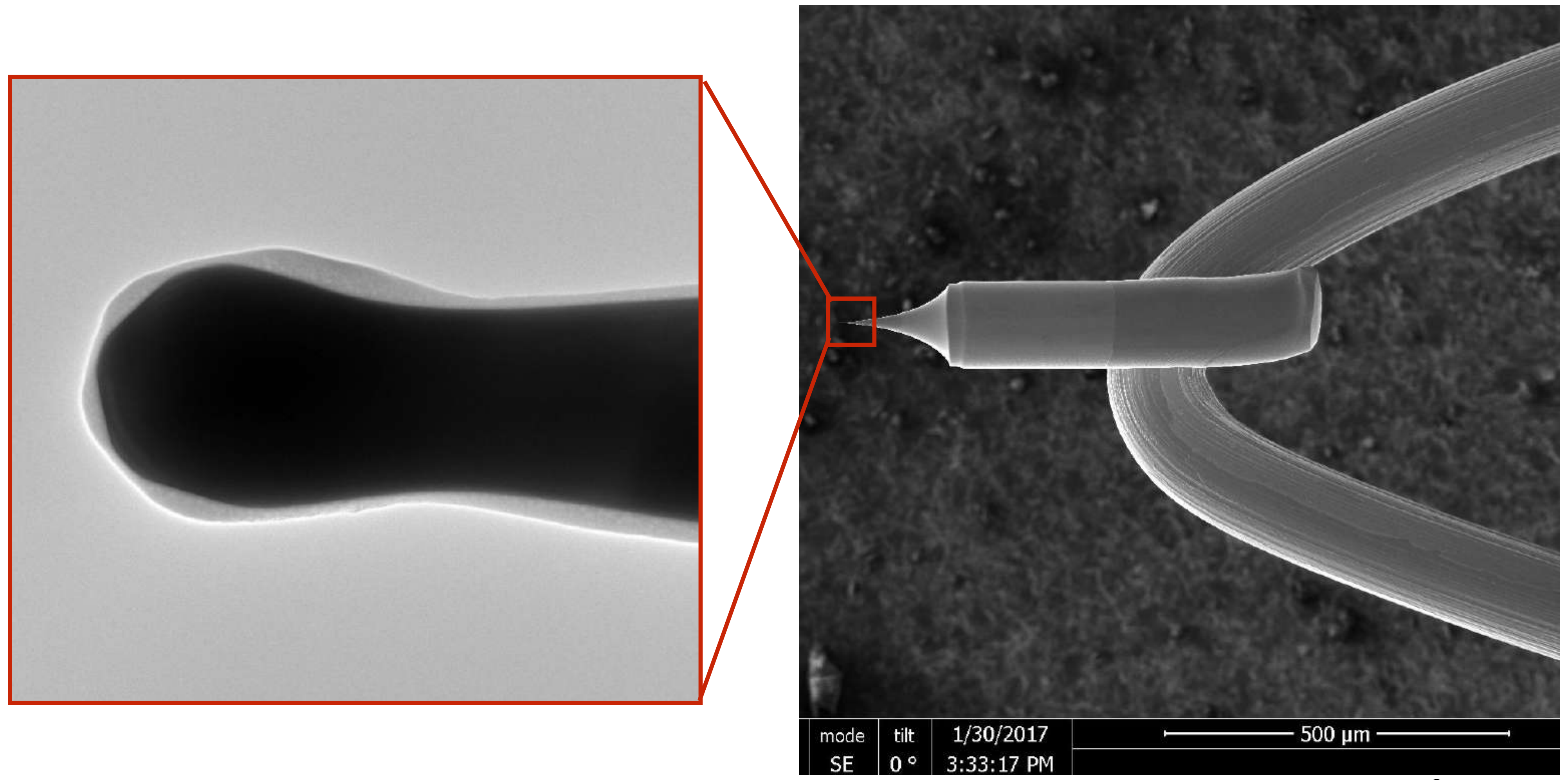

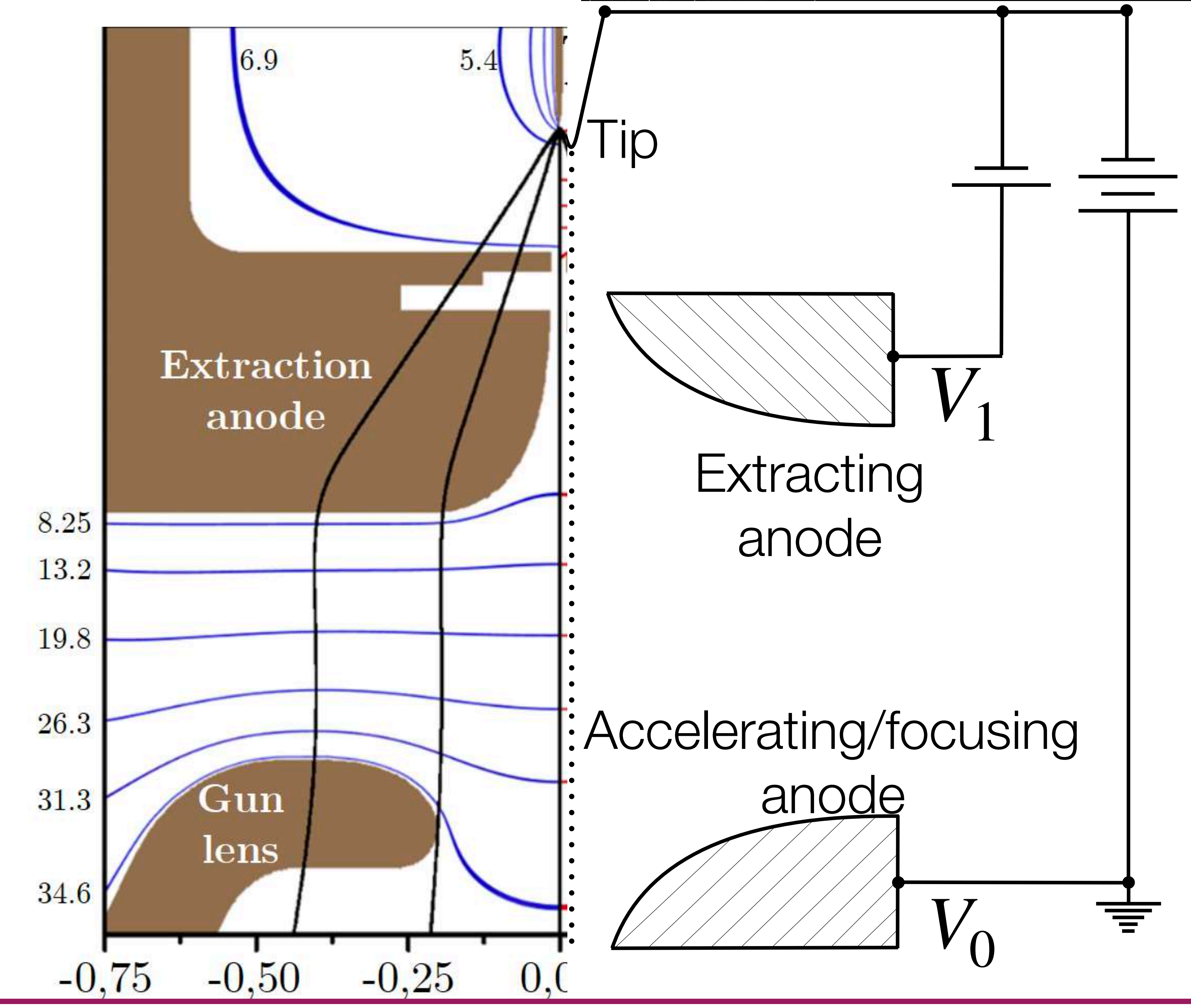

The Schottky field emission (SFE) electron source

General overview

Tip + suppressor

The SFE assembly

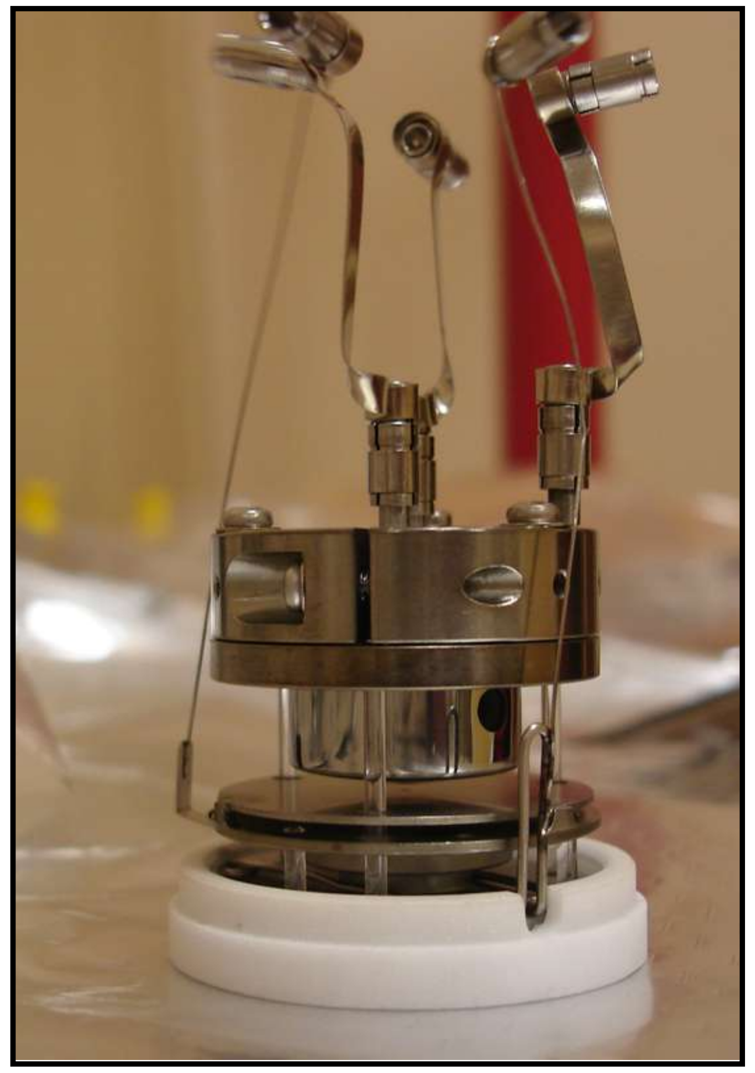

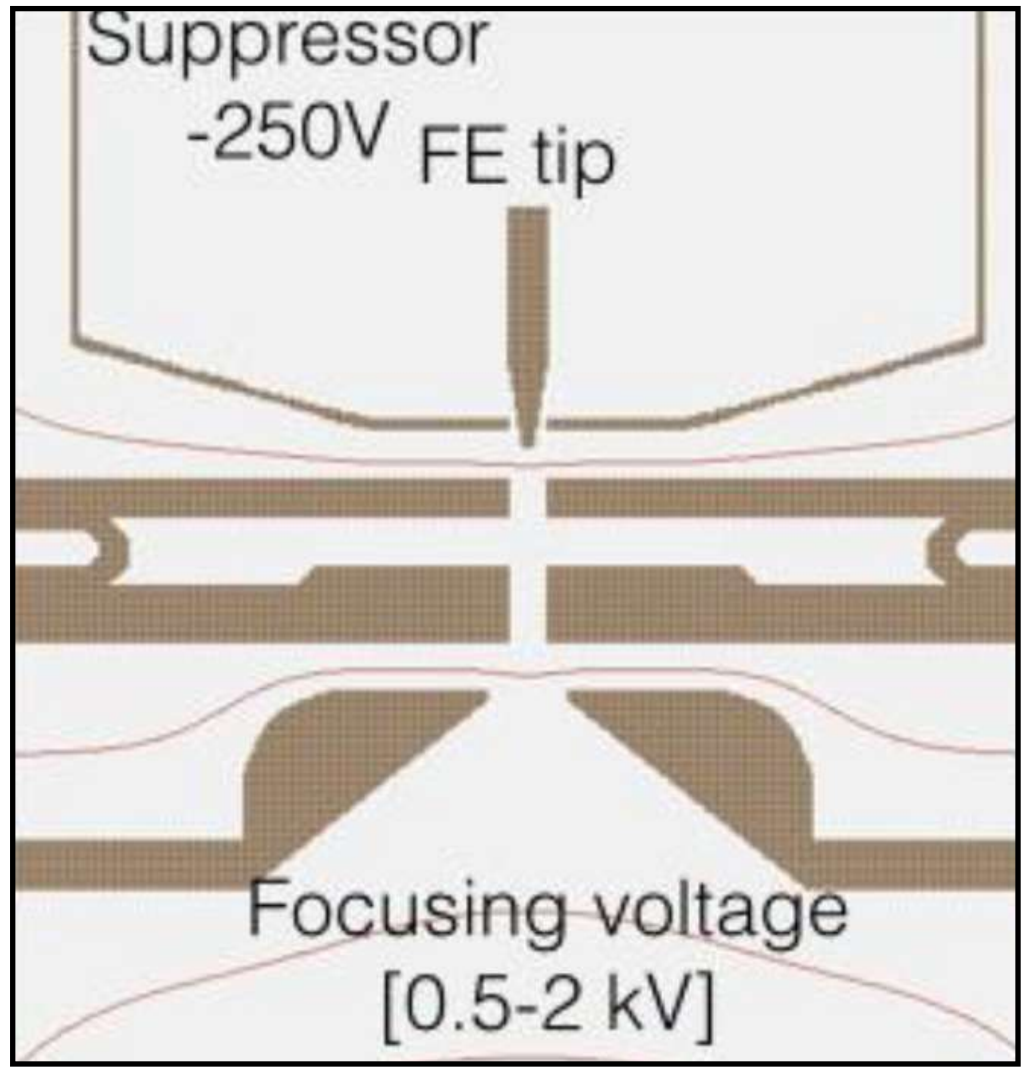

Optical simulation

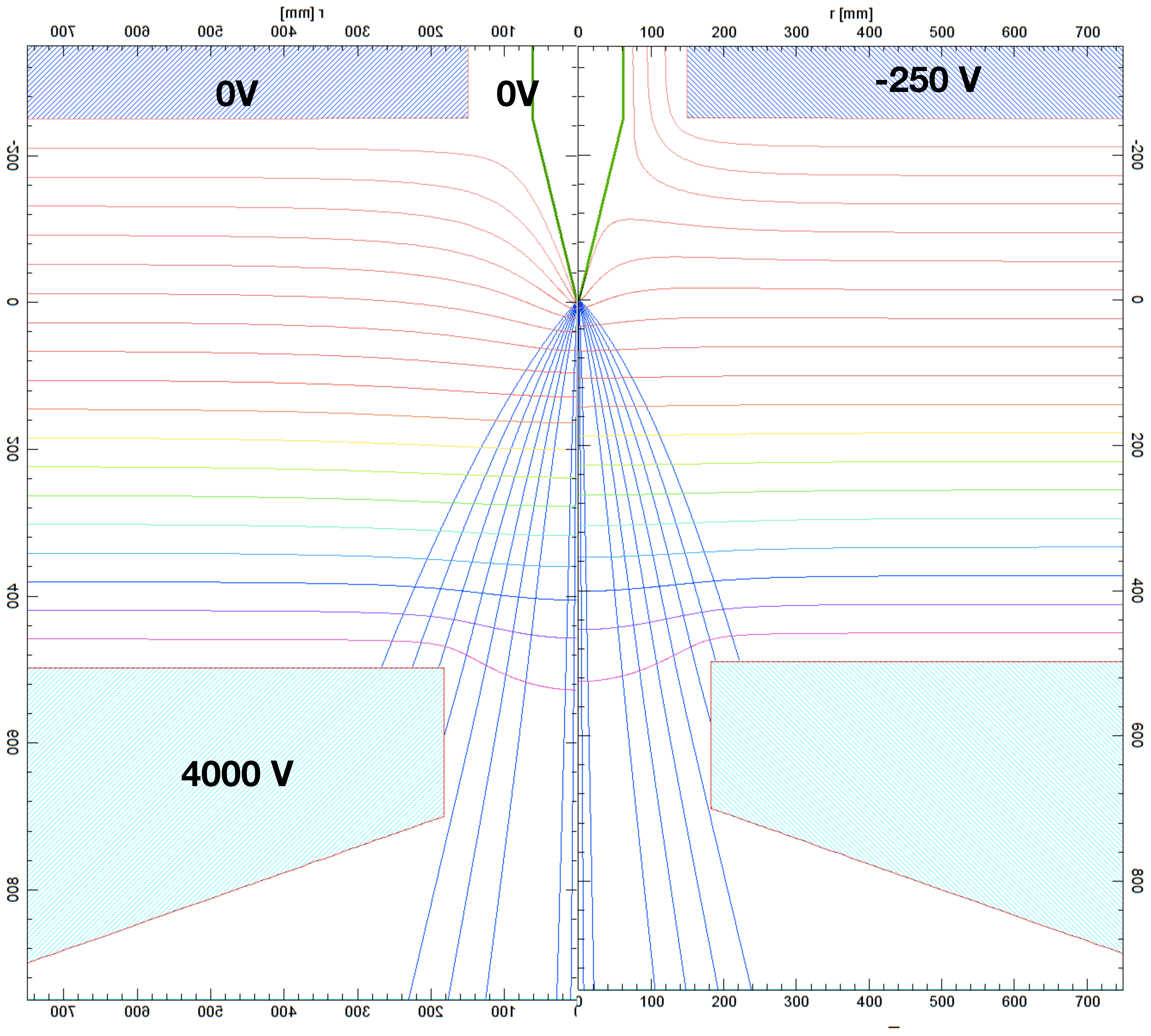

Quadrupole lens : paraxial properties

Let's start from the general paraxial equations …

$$\boxed{w'' + \frac{\gamma_0}{2\Phi_0^*}(\Phi_0' + iv_0\Psi_0')w' + \frac{\gamma_0}{4\Phi_0^*}\left(\Phi_0'' + iv_0\Psi_0'' + \frac{\Phi_1\overline{\Phi}_1}{2\gamma_0\Phi_0^*}\right)w - \frac{\gamma_0}{\Phi_0^*}\left(\Phi_2 + iv_0\Psi_2 - \frac{\Phi_1^2}{8\gamma_0\Phi_0^*}\right)\overline{w} = \frac{\gamma_0}{2\Phi_0^*}(\Phi_1 + iv_0\Psi_1)}$$

$w(z) = x(z) + iy(z)$

We assume $\Phi_1 = \Psi_1 = \Phi_0 = \Psi_0 = 0$. The paraxial equation is simplified with only the contribution of the $\nu = 2$ component

$$\boxed{\begin{aligned} x'' + k^2 x &= 0 \\ y'' - k^2 y &= 0 \end{aligned}}$$

A. Electrostatic quadrupole

$$k = k_E = \sqrt{(e\Phi_2)/(Kr_0^2)}$$

B. Magnetostatic quadrupole

$$k = k_M = \sqrt{(2e\Psi_2)/(pr_0^2)}$$

$k(z) =$ **const**

Periodic solutions along x :

$$\boxed{\begin{aligned} x(z) &= x_0 cos(kz) + \frac{a_0}{k} sin(kz) \\ a(z) &= -x_0 k sin(kz) + a_0 cos(kz) \end{aligned}}$$

Diverging solutions along y :

$$\boxed{\begin{aligned} y(z) &= y_0 cosh(kz) + \frac{a_0}{k} sinh(kz) \\ b(z) &= y_0 k sinh(kz) + b_0 cosh(kz) \end{aligned}}$$

◉ Notation

$a = tan\alpha = dx/dz = p_x/p_z$

$b = tan\beta = dy/dz = p_y/p_z$

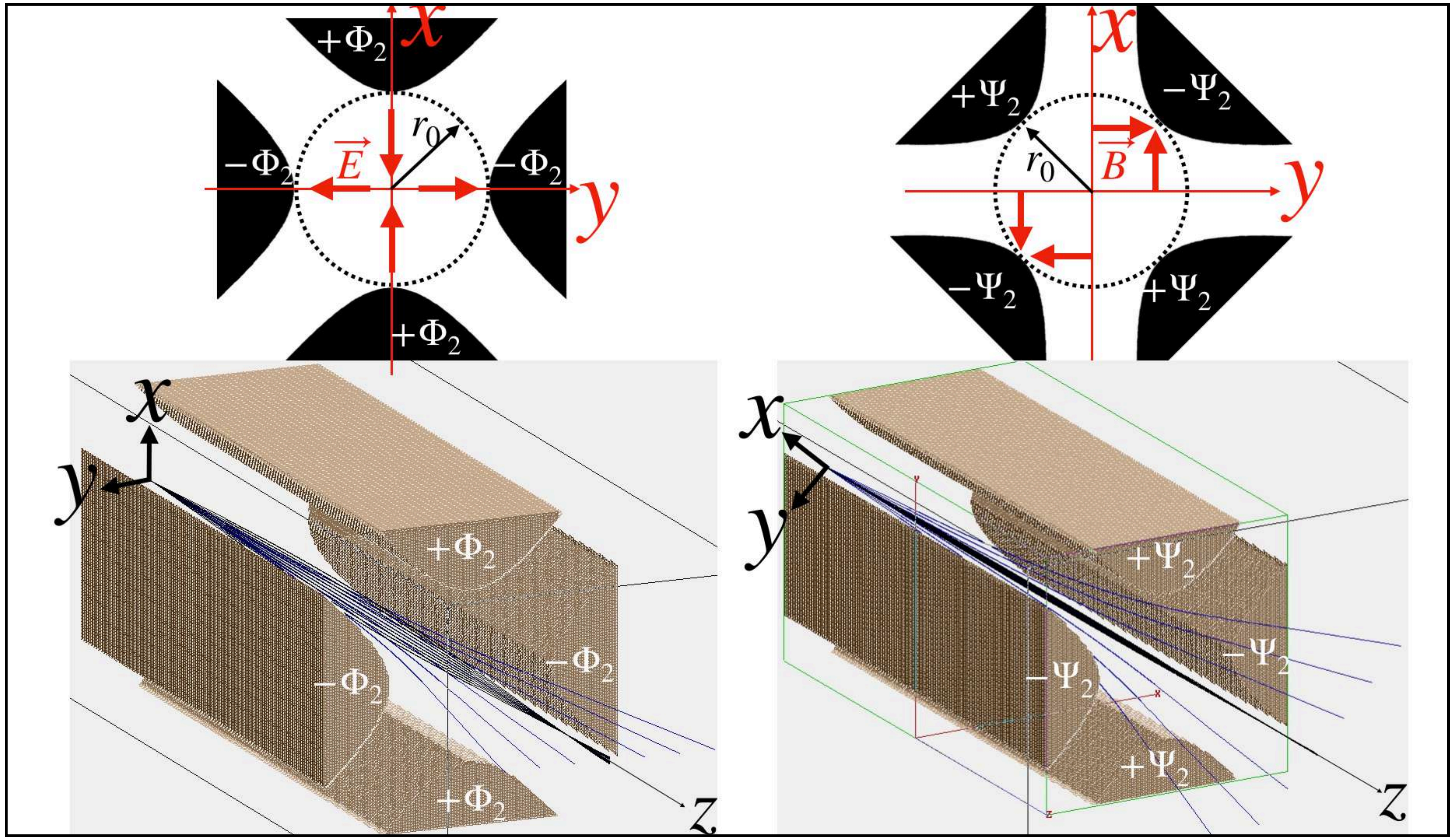

Correction of deviation from rotation symmetry : the stigmator

A. Electrostatic quadrupole

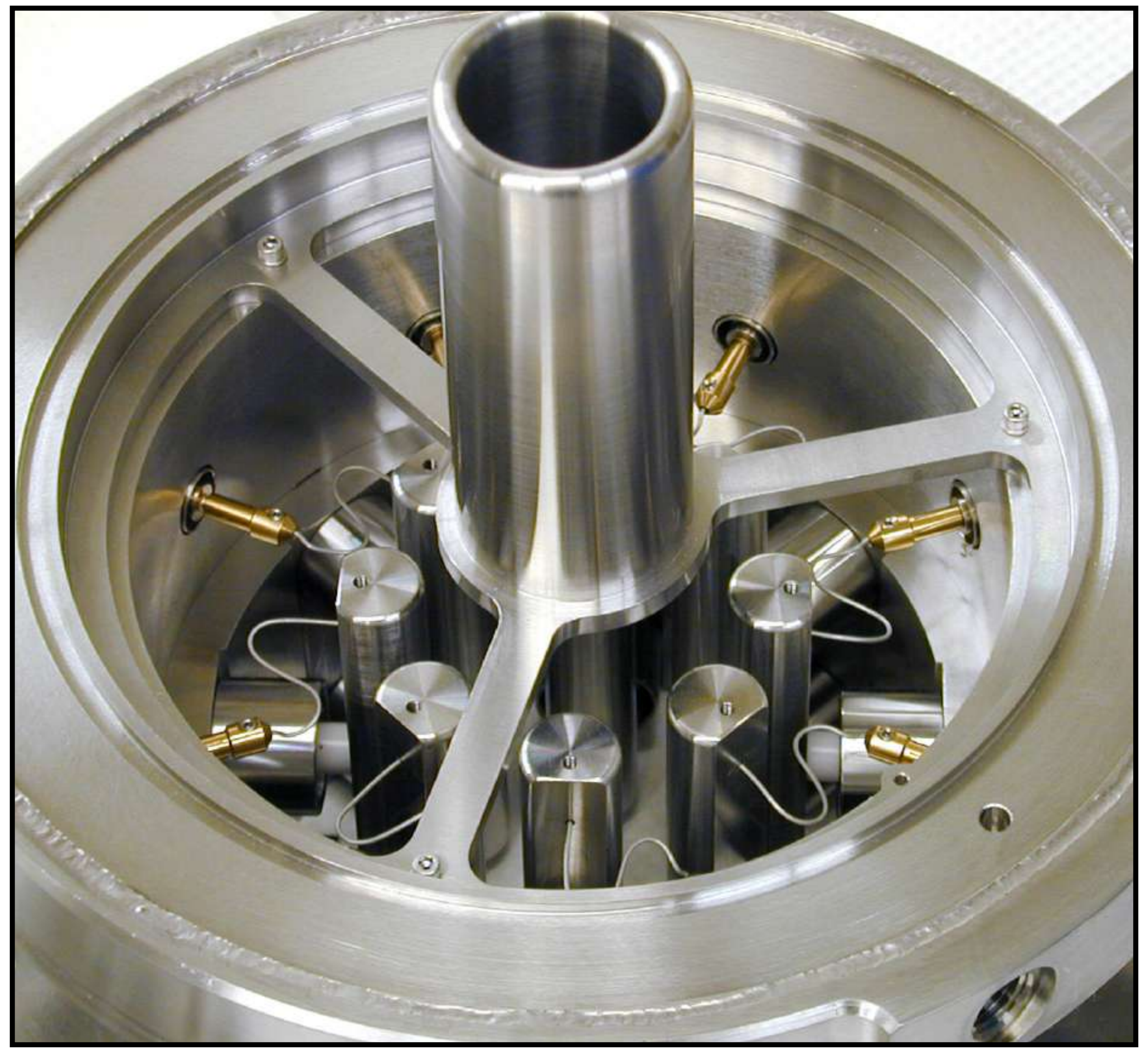

B. Magnetostatic quadrupole

Paraxial action of quadrupoles are used to compensate small paraxial focusing error along perpendicular directions observed in rotational system (electrostatic or magnetic)

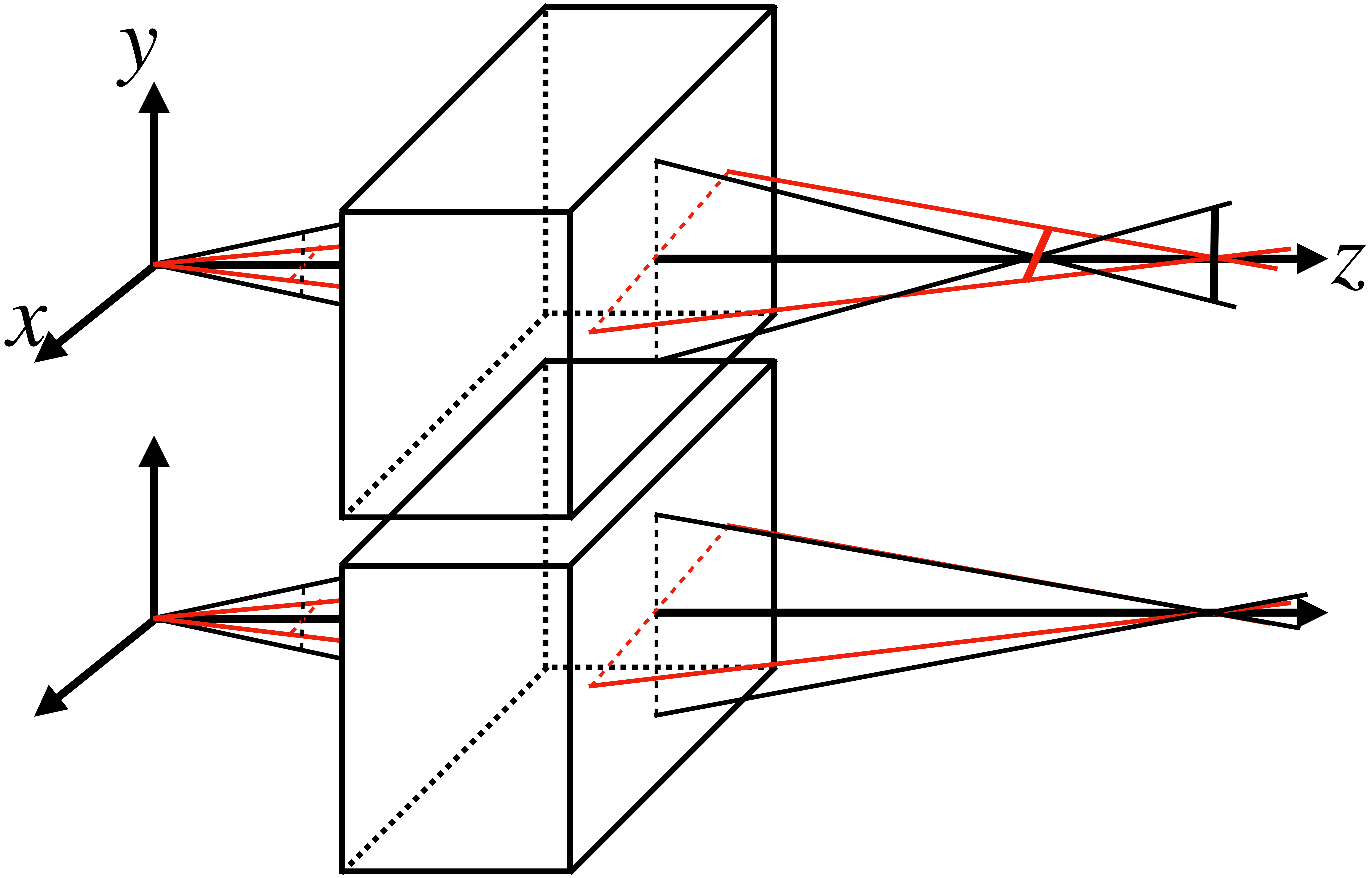

Often called « Axial astigmatism » (not an aberration coming from $L^{(4)} + \ldots$ terms of the eikonal)

Stigmatic imaging with quadrupoles multiplets

- Quadrupoles doublet : anamorphic focusing

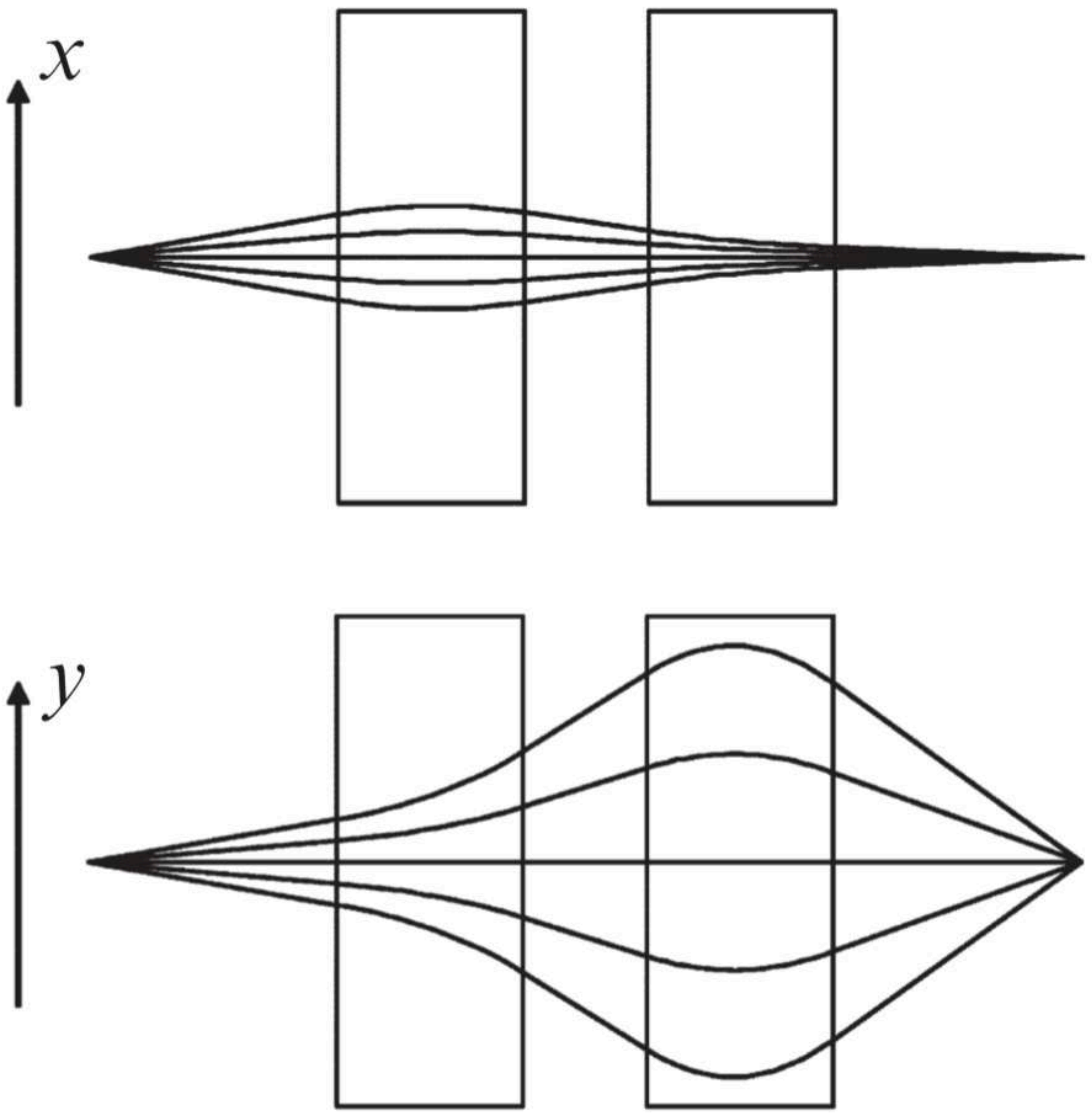

- Quadrupoles quadruplet (Russian quadruplet) : non-anamorphic focusing (like round lens)

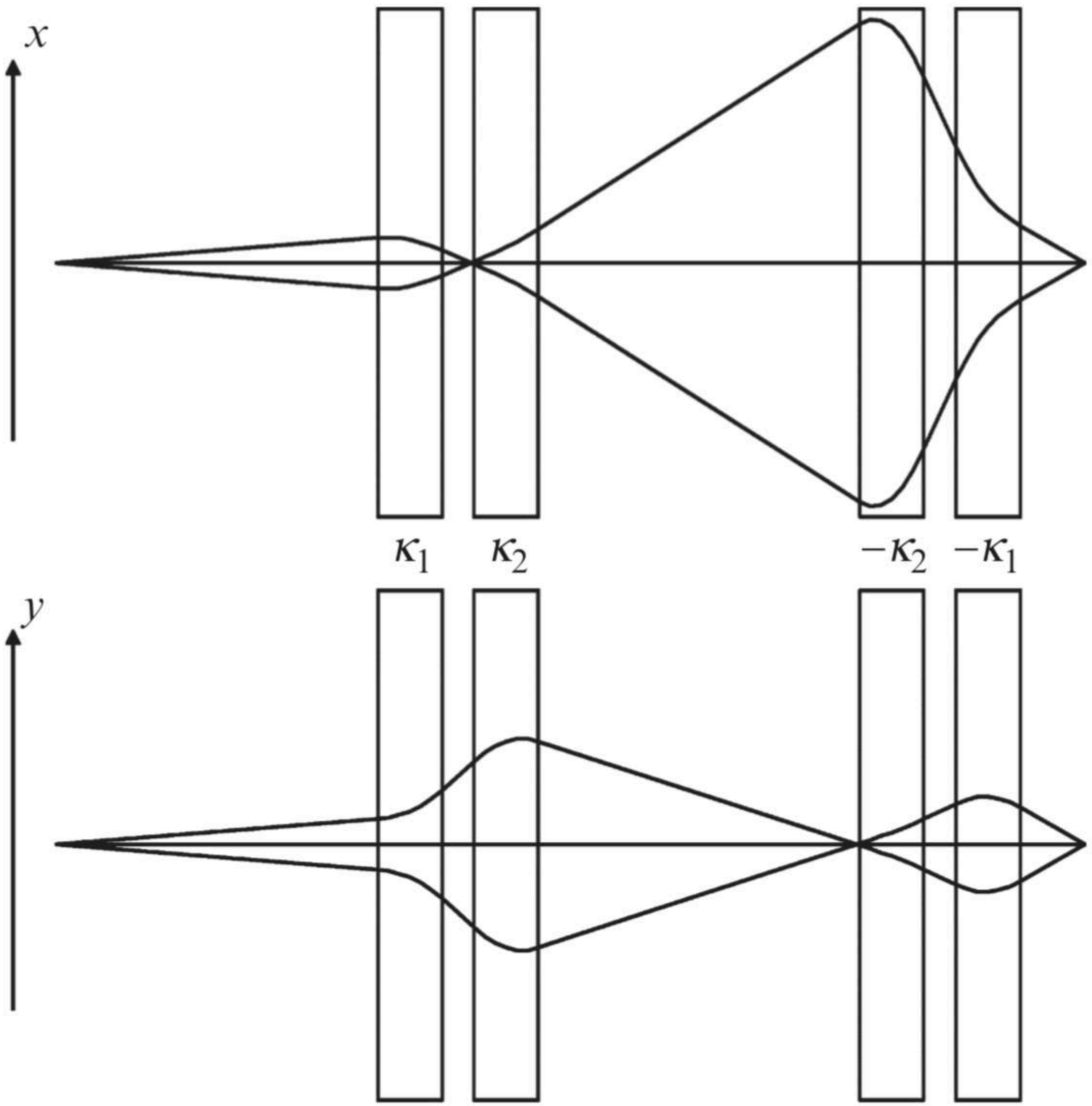

Electron Energy Loss Spectrometer : EELS

Post-column spectrometer

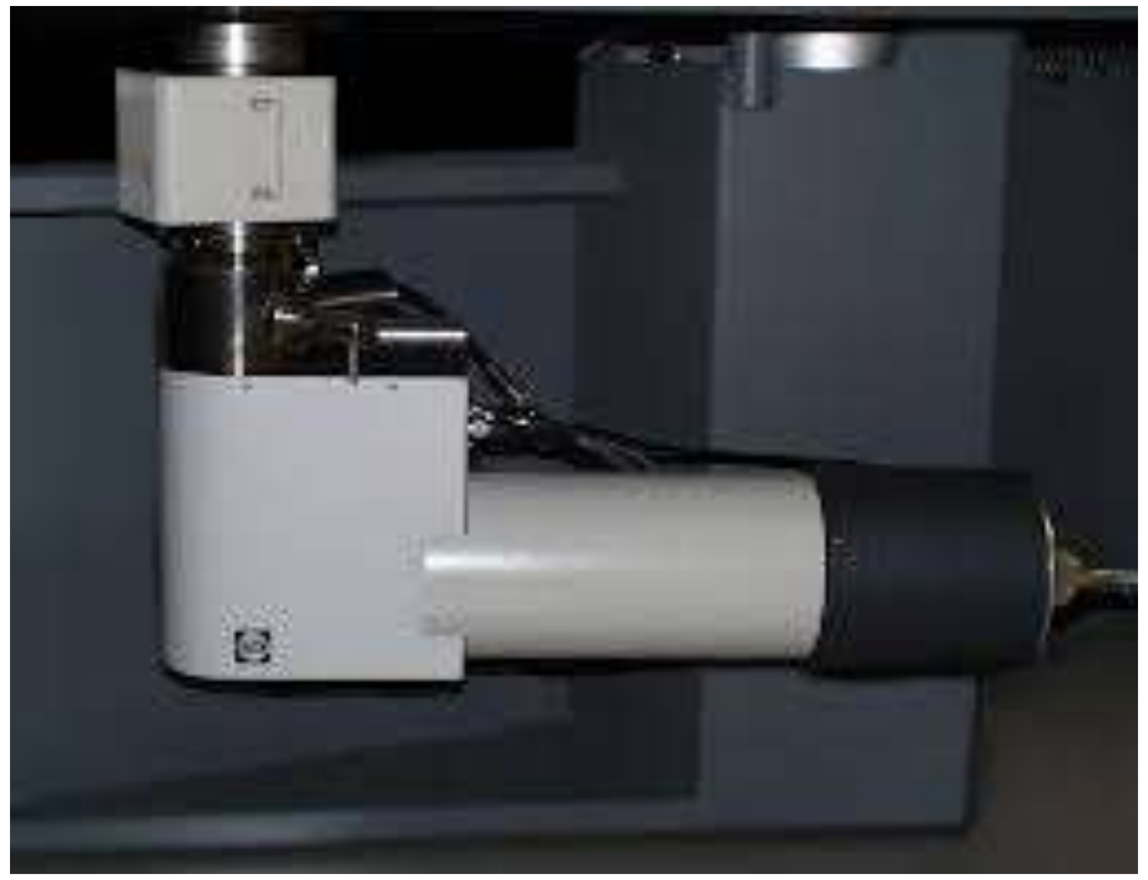

- Along the dispersion direction of the sector

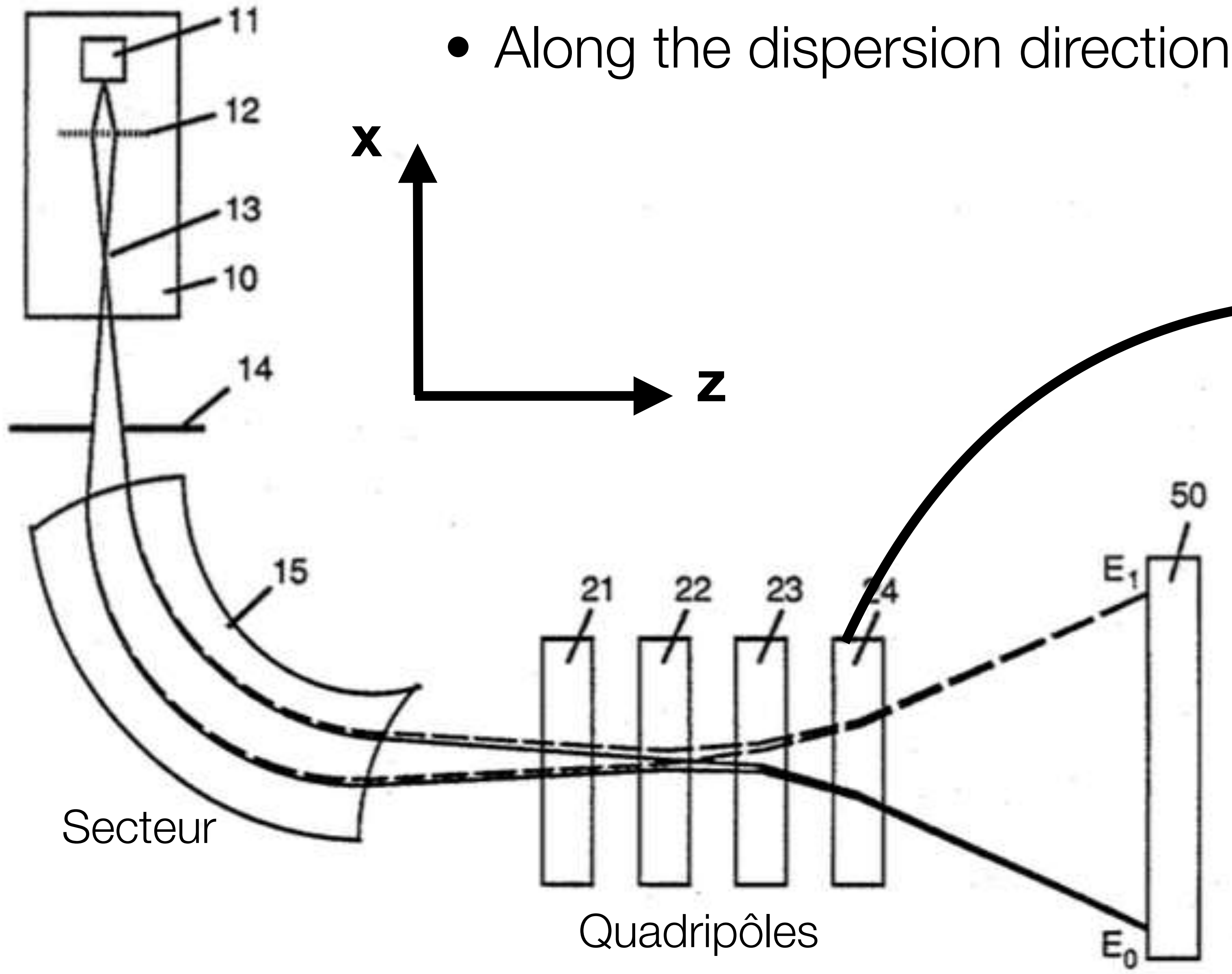

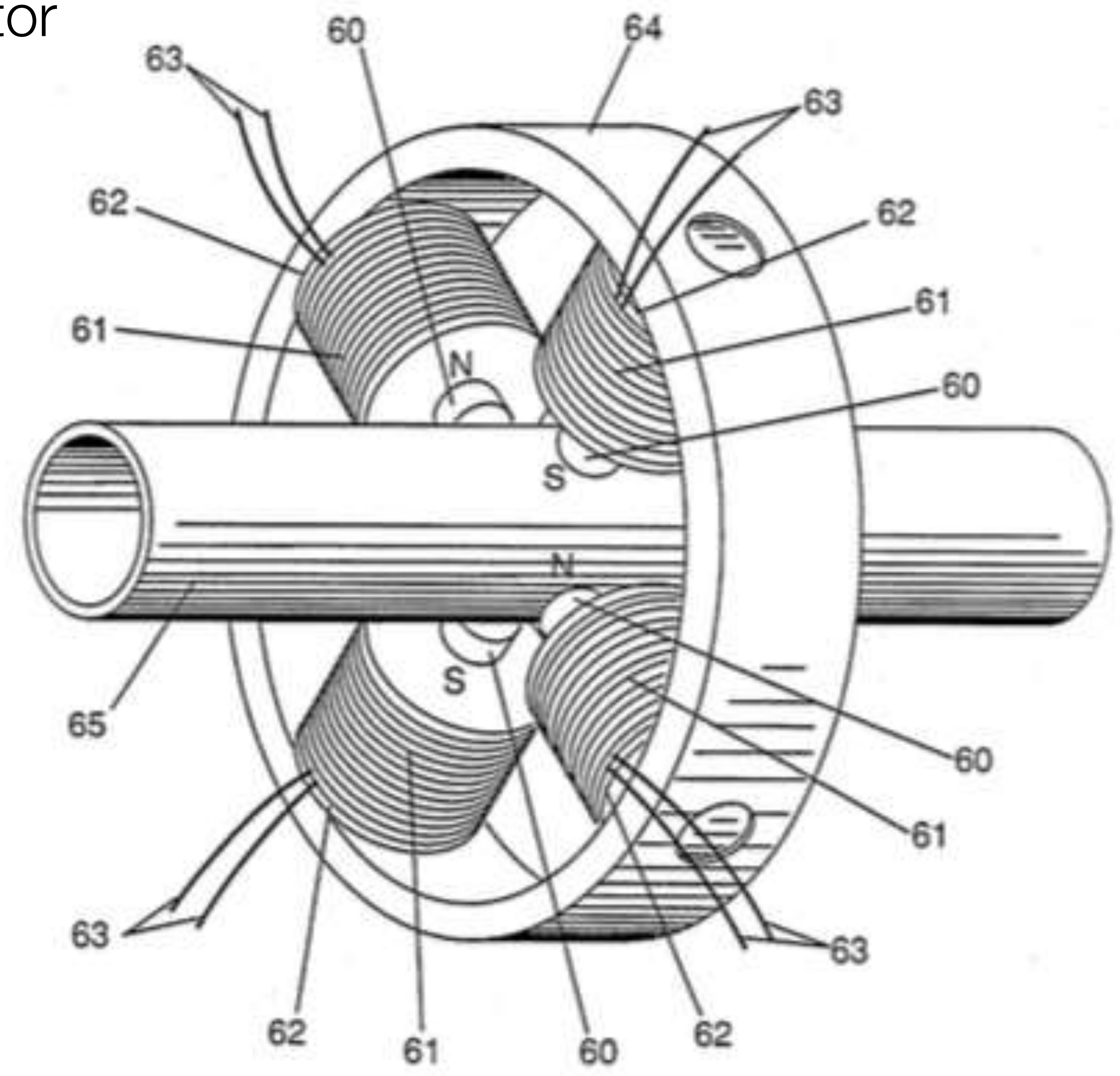

- Along the direction perpendicular to the sector dispersion direction

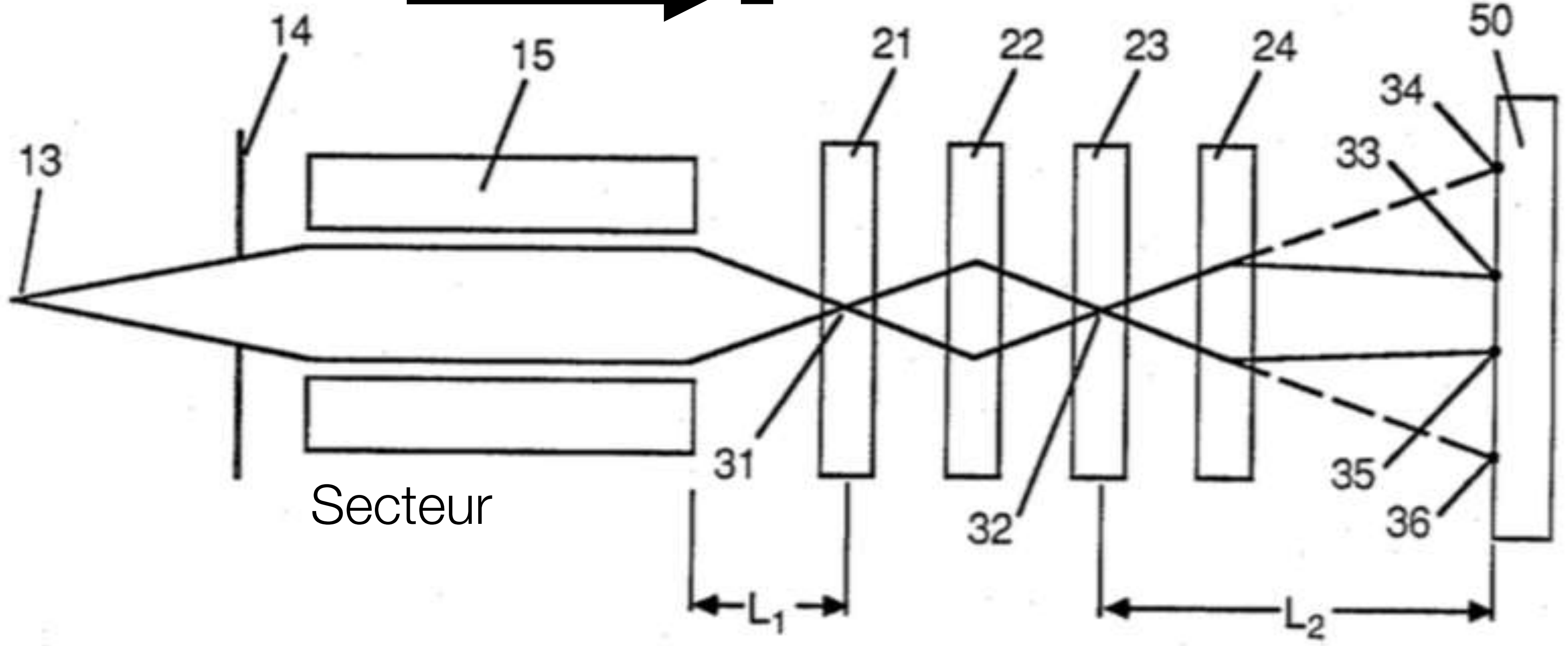

United States Patent [19] Krivanek

[11] Patent Number: 4,743,756
[45] Date of Patent: May 10, 1988

[54] PARALLEL-DETECTION ELECTRON ENERGY-LOSS SPECTROMETER
[75] Inventor: Ondrej L. Krivanek, Oakland, Calif.
[73] Assignee: Gatan Inc., Pleasanton, Calif.
[21] Appl. No.: 83,629
[22] Filed: Aug. 10, 1987

allel recorded electron energy loss spectra with low signal to background, Rev. Sci./wk. 56(2), 231–239.
Johnson, Csillay, Monson & Stern, A photodiode, parallel detection system for energy loss spectrometry, 39th Annual EMSA meeting Proc.
Design of a Parallel detection system for EELS, Egerton, 39th Annual EMSA meeting Proc.

Electron Energy Loss Spectrometer : EELS

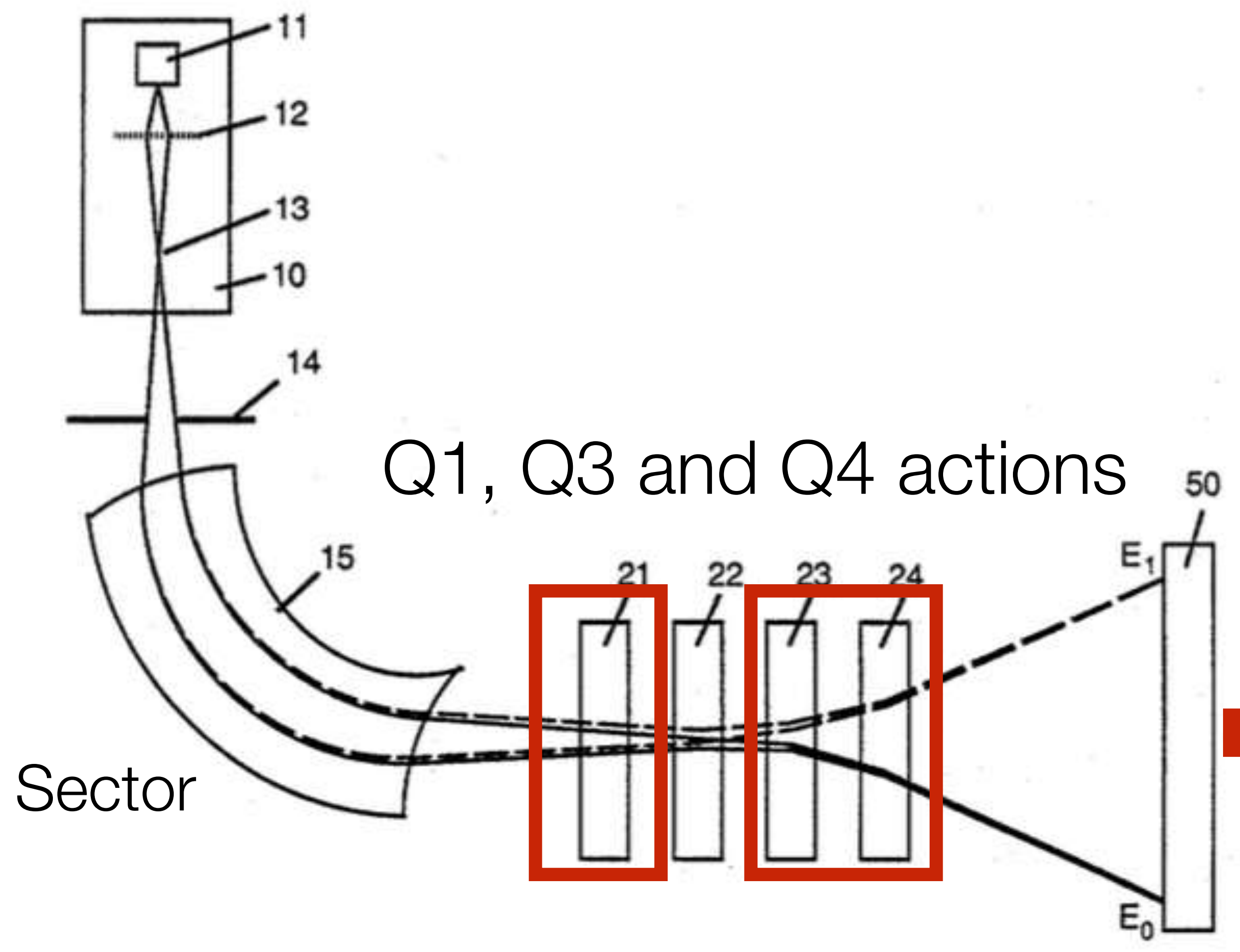

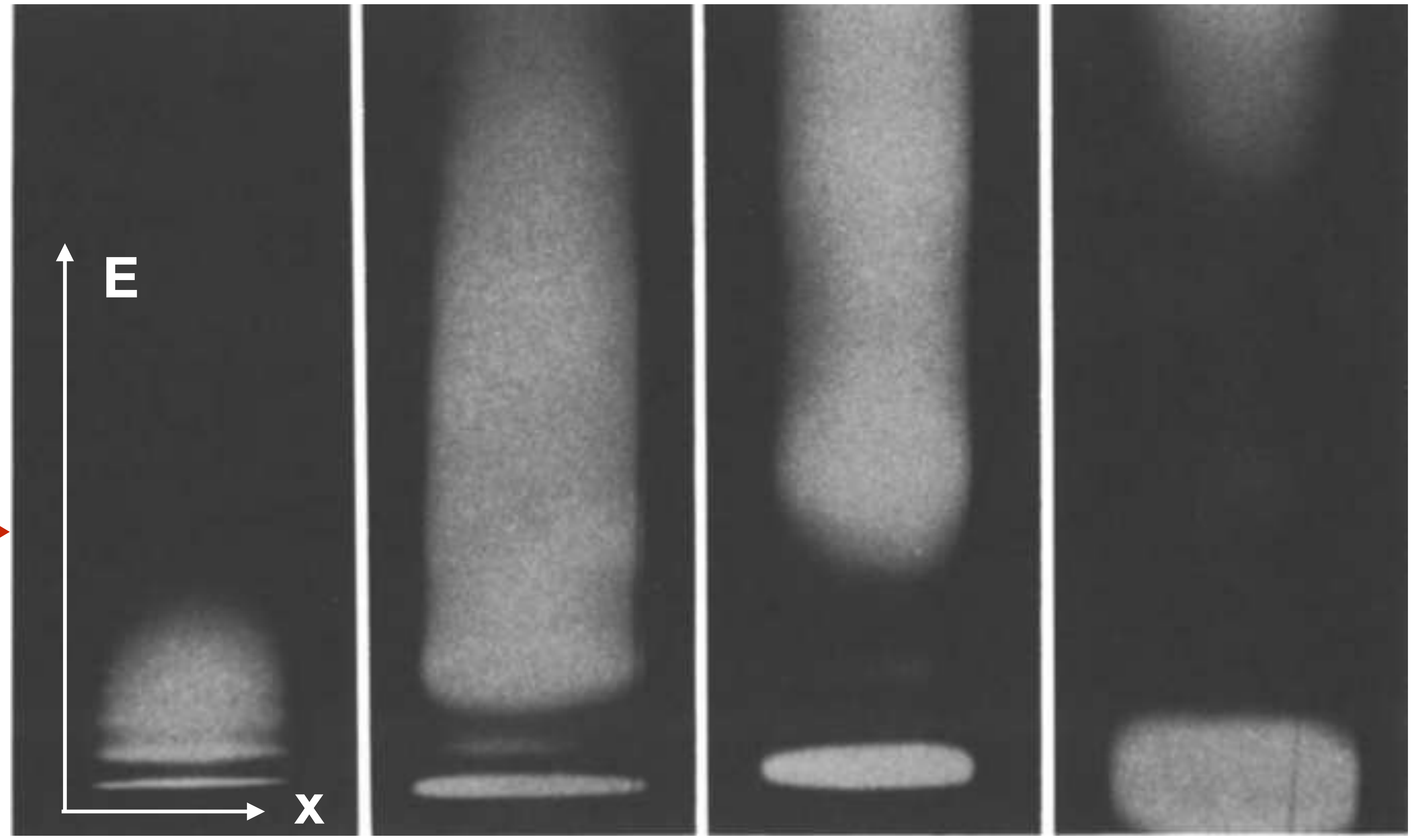

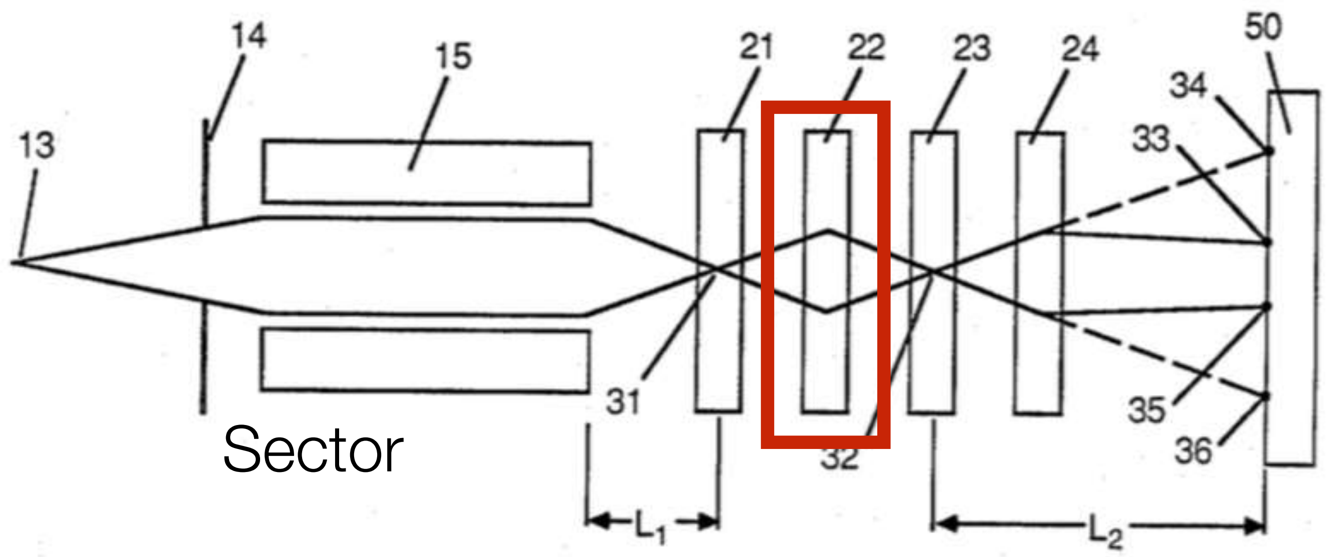

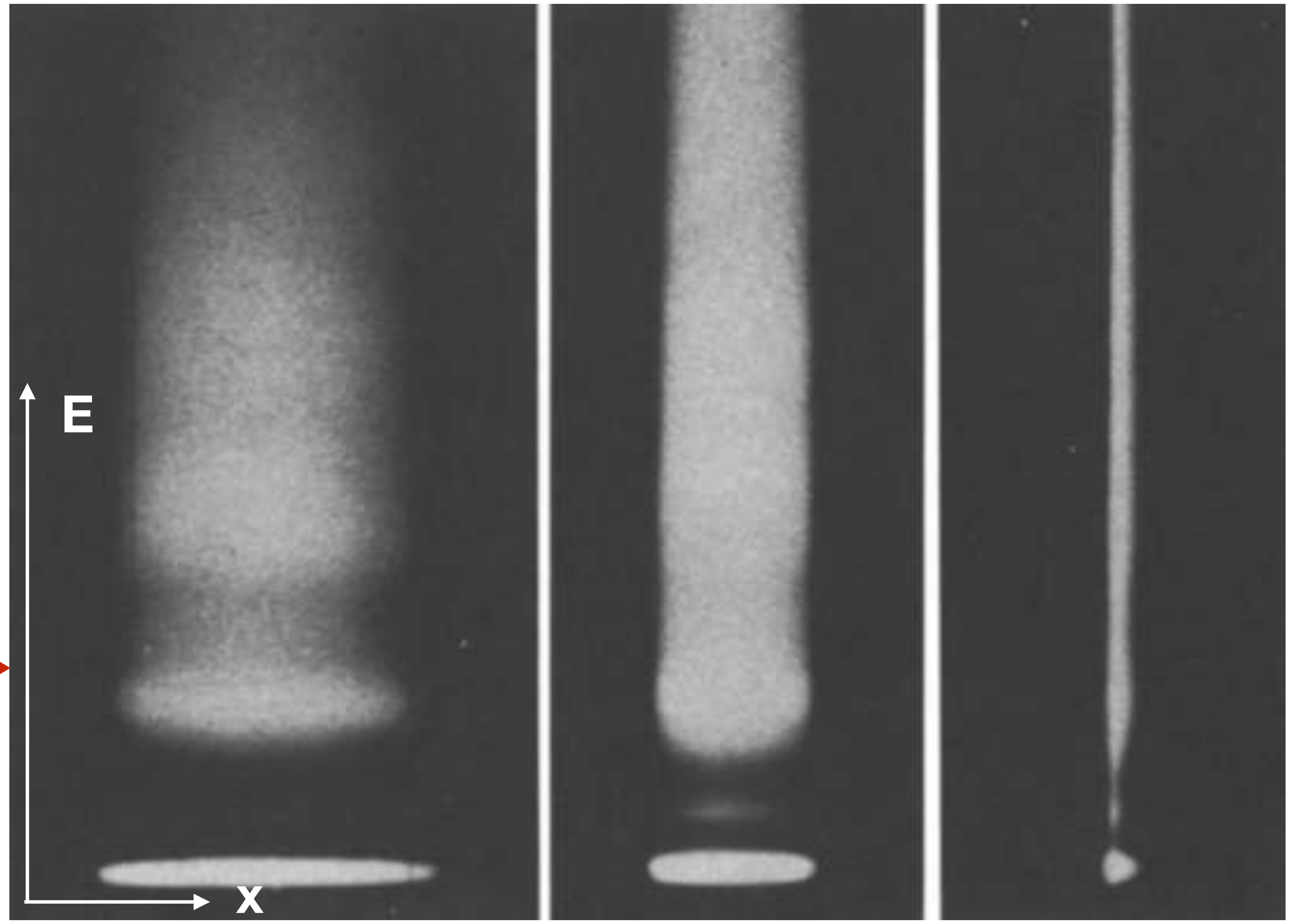

Paraxial properties : to remember

Electrostatic

- Round and quadrupole can focus
- Action depends only on the beam ratio charge/energy
- Time of flight can be used to separate mass (TOF SIMS)
- Energy can change between object/image
- Electrodes quality important

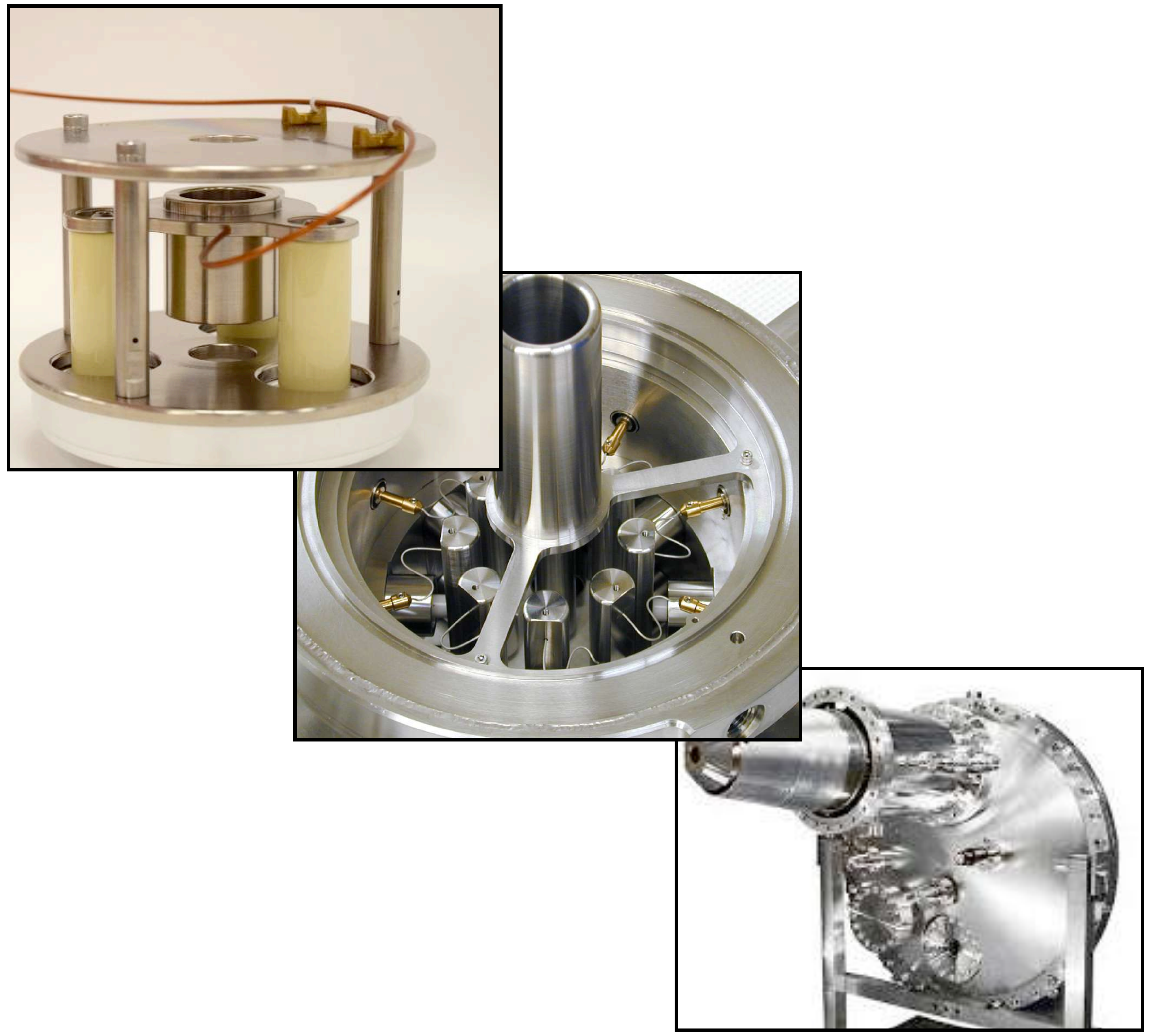

Magnetostatic

- Round and quadrupole can focus
- Action depends on beam impulsion/charge (mass dependent)
- Can be used to separate mass, not adapted to focus heavy ions
- Magnetic material properties important (hysteresis, saturation,…)

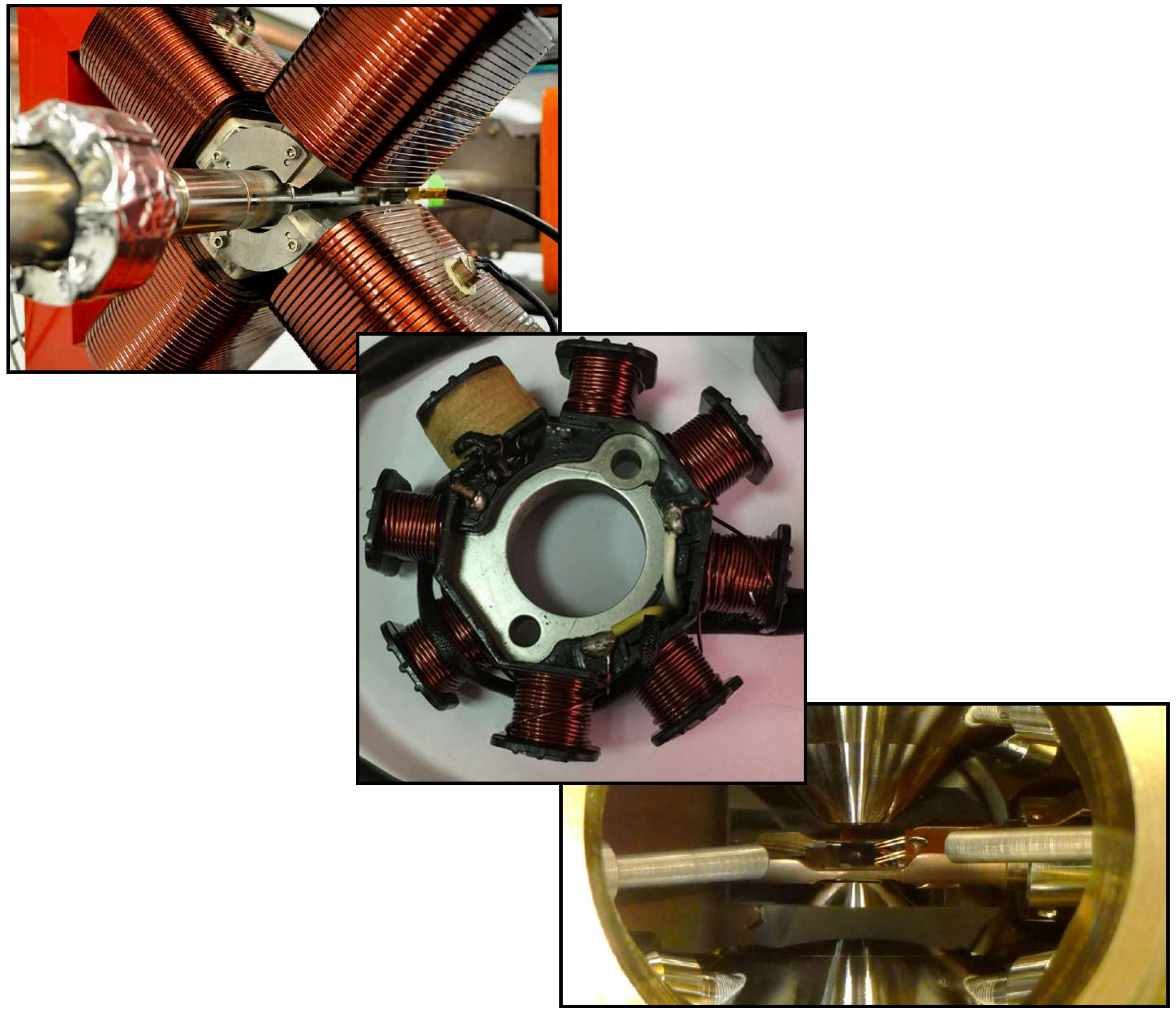

- Mix : Wien condition

$$\Phi_1 + i v_0 \Psi_1 = 0$$

Used to filter velocity v_0

What about the aberrations ?

Effect of fourth order terms L^4 of the expansion : Scherzer's theorem

After Glaser's work on aberrations expansion arrive …

- **Otto Scherzer (1909-m. 1982)**
  « Uber einige Fehler von Elektronenlinsen» (1936).

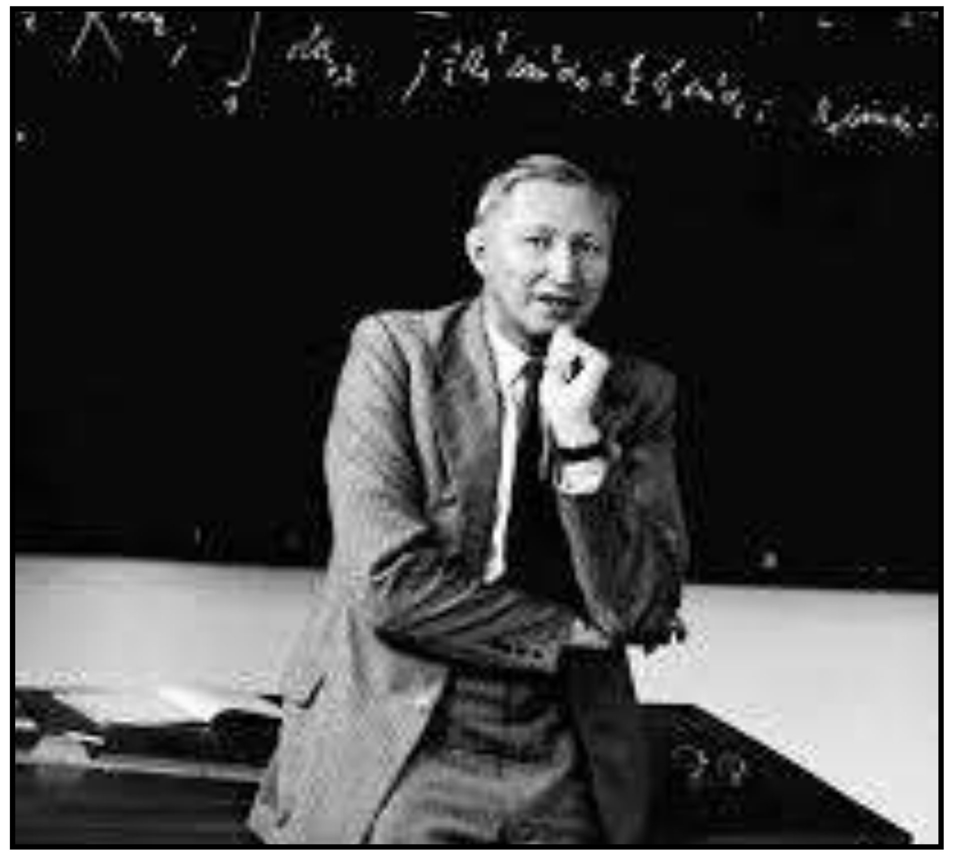

Über einige Fehler von Elektronenlinsen.

Von **O. Scherzer** in Darmstadt.

Mit 3 Abbildungen. (Eingegangen am 4. Juni 1936.)

Unmöglichkeit des Achromaten. Die Bildfehler dritter Ordnung. Unvermeidbarkeit der sphärischen Aberration.

$$C_s = \frac{1}{16}\int_{z_o}^{z_i}\left\{b^4h^4 + 2\left(hb' + h'b\right)^2 h^2 + 2b^2h^2h'^2\right\}dz$$

$$C_c = \frac{1}{4}\int_{z_o}^{z^i} b^2h^2\,dz$$

4. Unvermeidbarkeit der sphärischen Aberration.

He shows that if we have a system define by static rotationally fields :

$$\Psi_0 \neq 0, \Phi_0 \neq 0$$

Aberration terms of the eikonal expansion are unavoidable

$$L = L^0 + L^2 + \underbrace{\boxed{L^4}}_{>0} + \ldots.$$

This is known as *Scherzer's theorem*

Cancel fourth order terms L^4 of the expansion : Scherzer's propositions

- **Otto Scherzer (1909-m. 1982)**
  « Sphärische und chromatische Korrektur von Elektronen-Linsen » (1947).

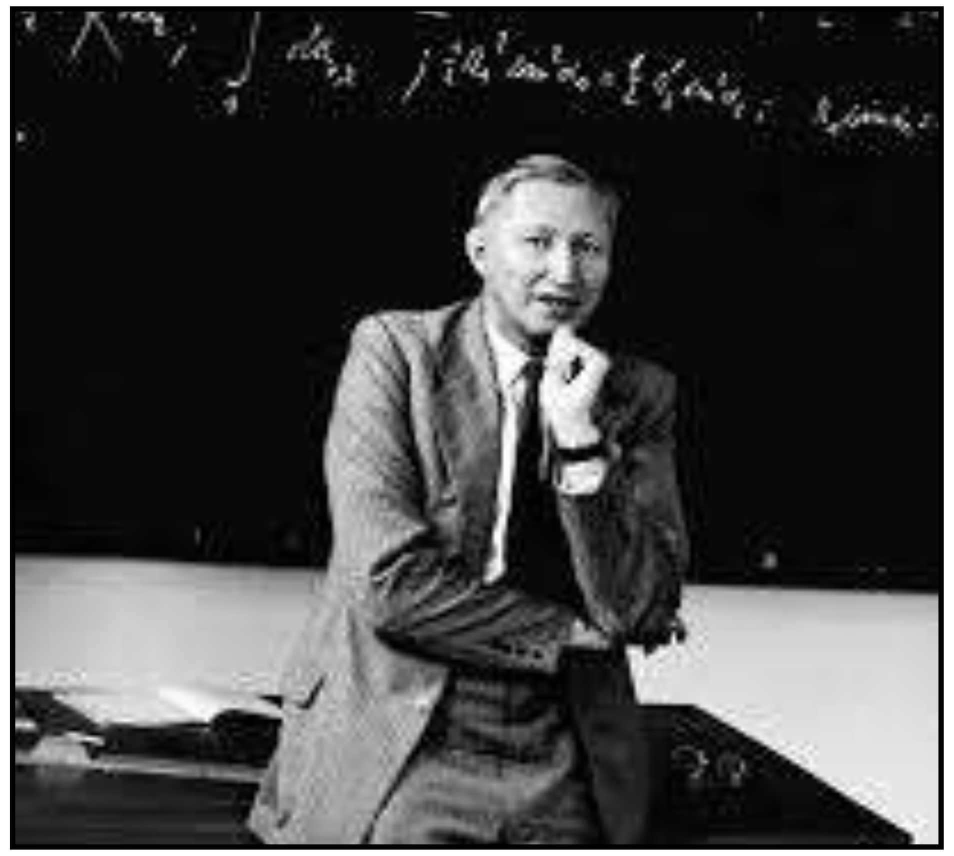

Scherzer shows that octopole field $\nu = 4$ can be used to invert the sign of spherical aberration

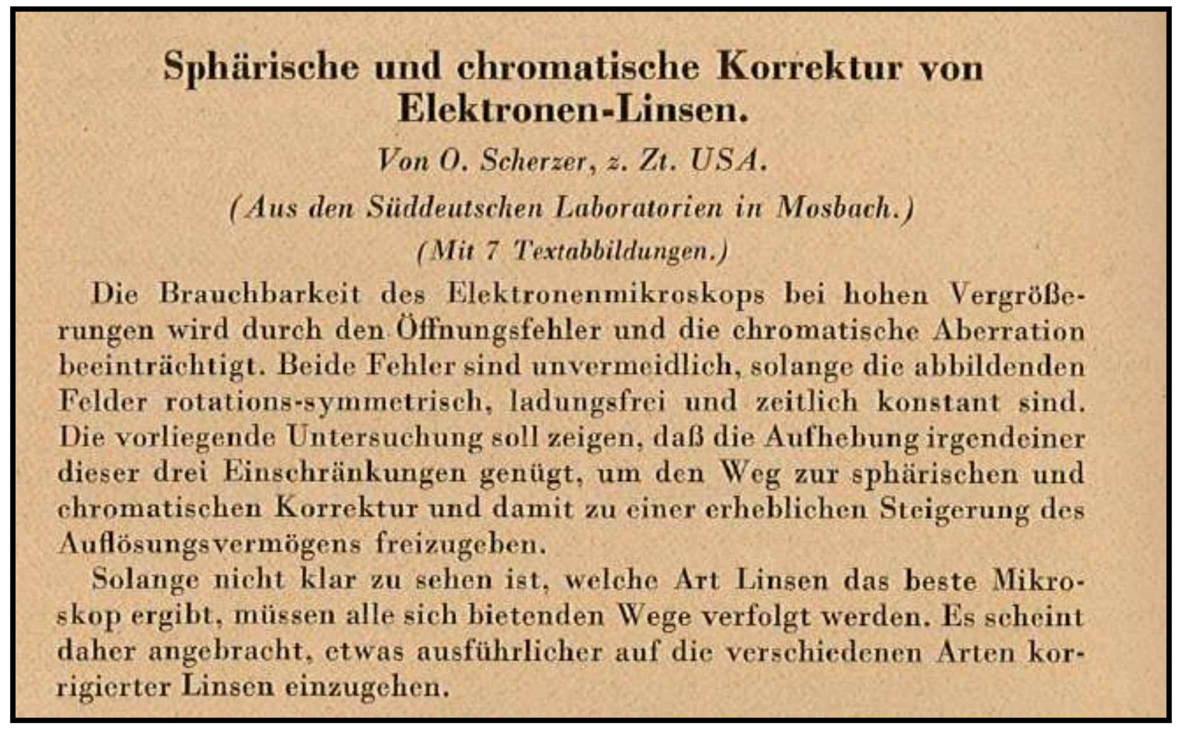

Sphärische und chromatische Korrektur von Elektronen-Linsen.

Von O. Scherzer, z. Zt. USA.

(Aus den Süddeutschen Laboratorien in Mosbach.)

(Mit 7 Textabbildungen.)

Die Brauchbarkeit des Elektronenmikroskops bei hohen Vergrößerungen wird durch den Öffnungsfehler und die chromatische Aberration beeinträchtigt. Beide Fehler sind unvermeidlich, solange die abbildenden Felder rotations-symmetrisch, ladungsfrei und zeitlich konstant sind. Die vorliegende Untersuchung soll zeigen, daß die Aufhebung irgendeiner dieser drei Einschränkungen genügt, um den Weg zur sphärischen und chromatischen Korrektur und damit zu einer erheblichen Steigerung des Auflösungsvermögens freizugeben.

Solange nicht klar zu sehen ist, welche Art Linsen das beste Mikroskop ergibt, müssen alle sich bietenden Wege verfolgt werden. Es scheint daher angebracht, etwas ausführlicher auf die verschiedenen Arten korrigierter Linsen einzugehen.

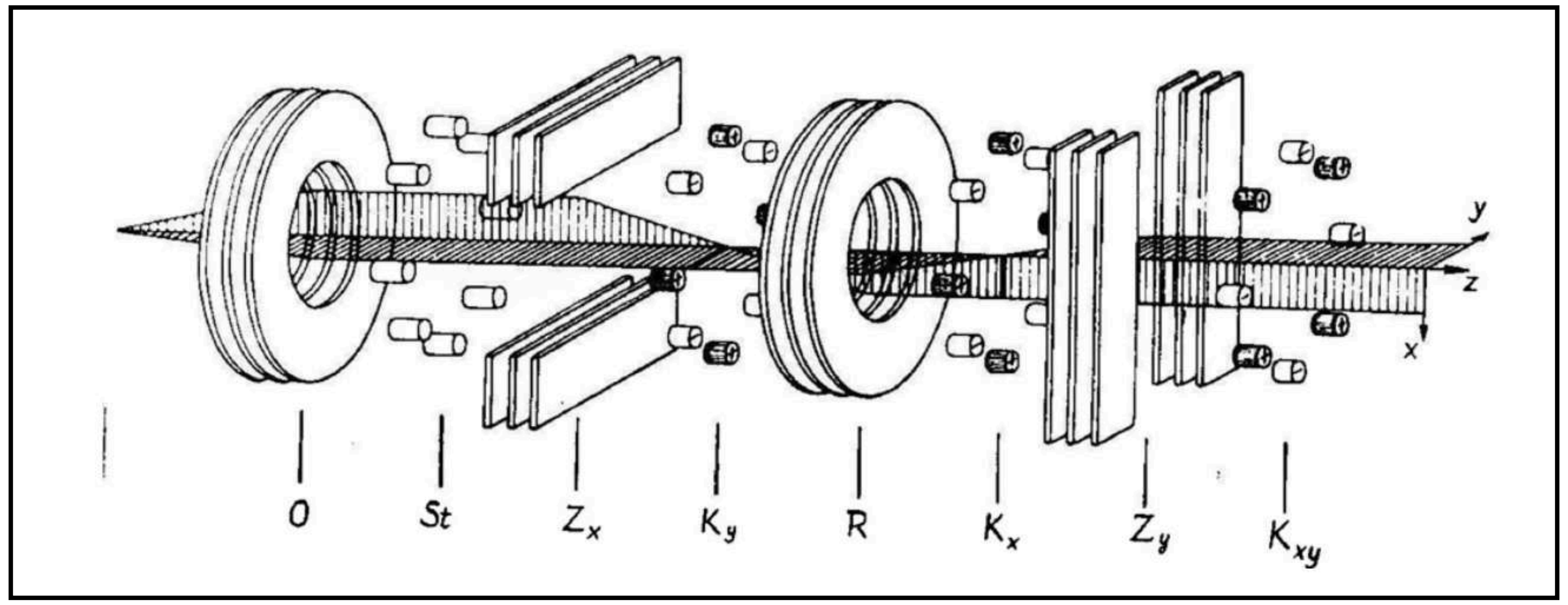

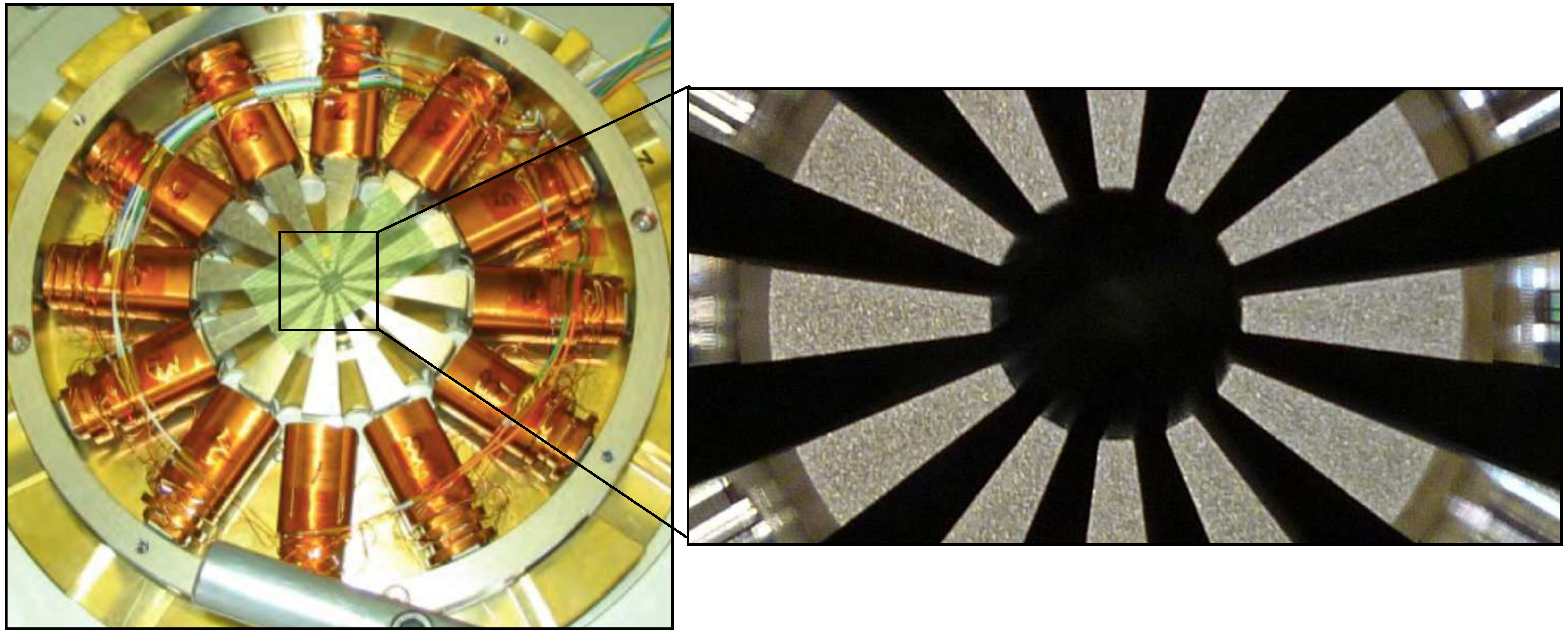

Hexapole
Ψ_3, Φ_3

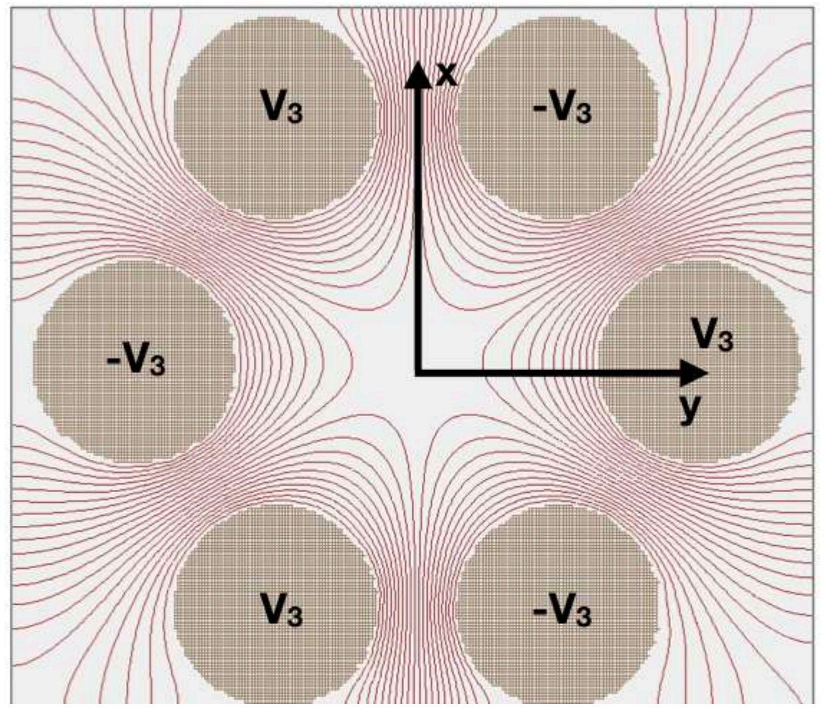

Octopole
Ψ_4, Φ_4

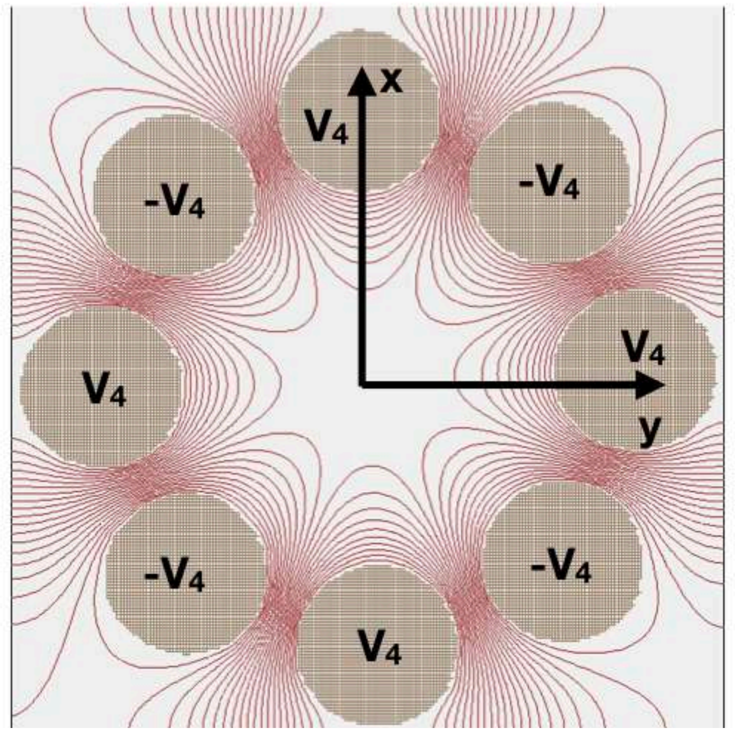

Cancel fourth order terms L^4 of the expansion : Rose's proposition

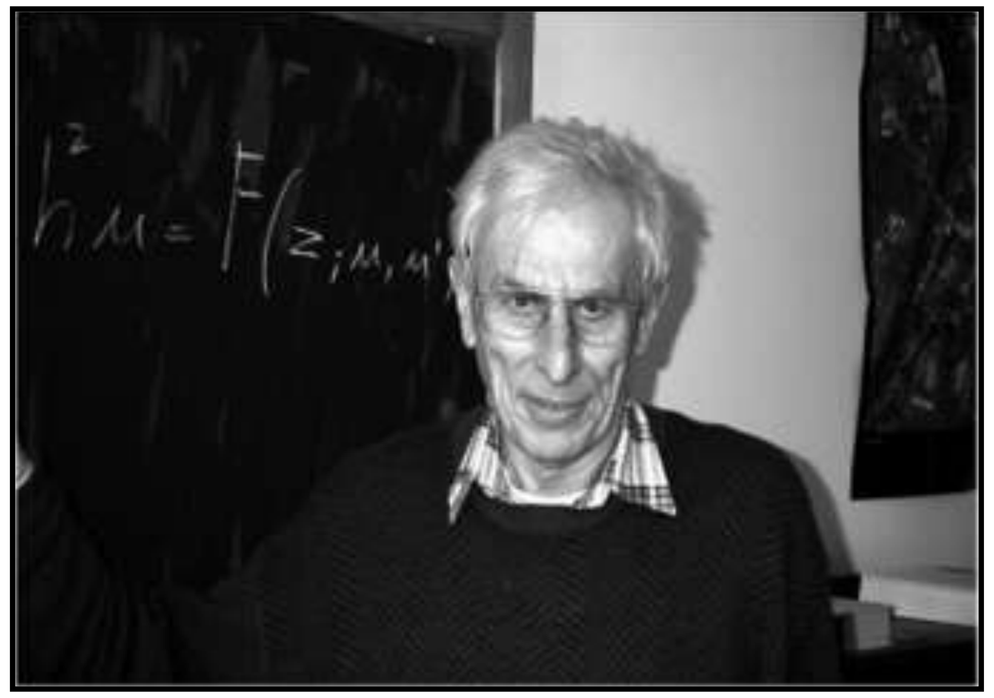

- **Harald Rose (1935-)**

  « Outline of a spherically corrected semiaplanatic medium-voltage transmission electron microscope» (1990).

Design of the first TEM and STEM spherical aberration corrected optics (semiaplanatic)

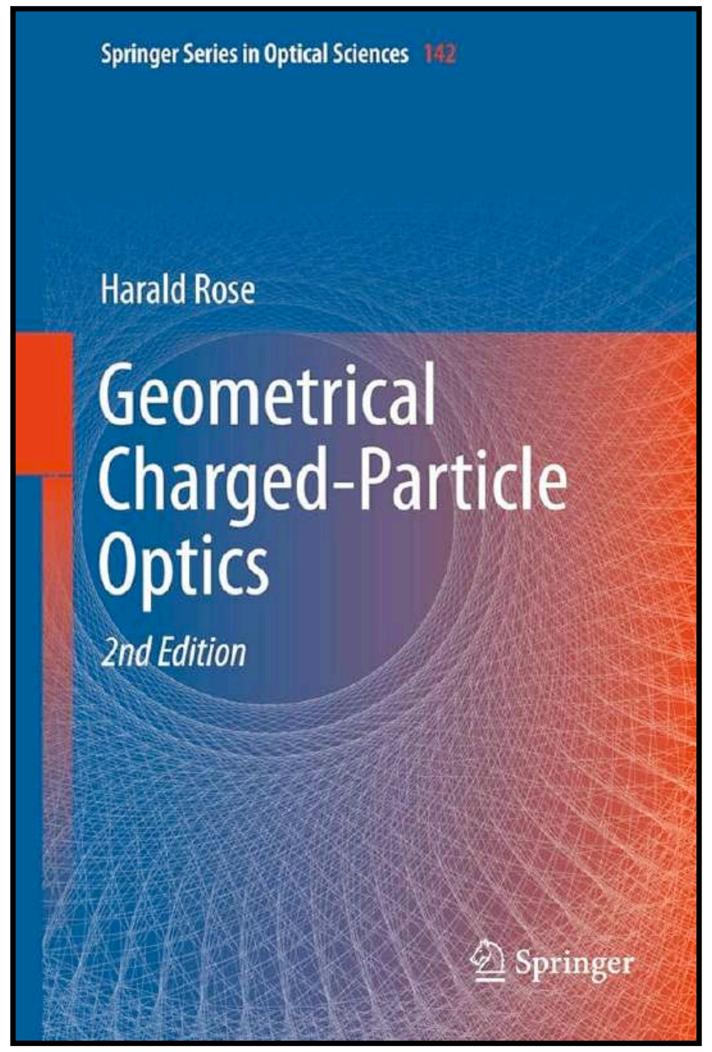

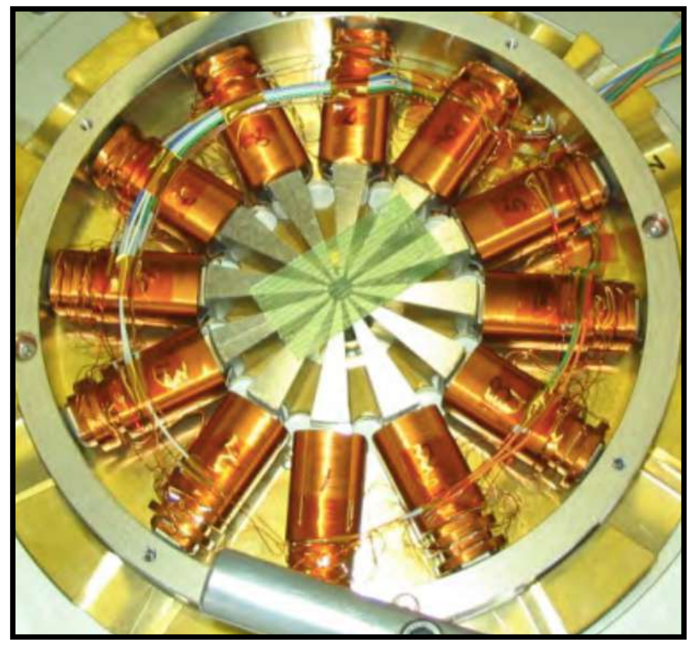

Students of Pr. Rose have the created the **CEOS GmbH company**

CEOS
Corrected Electron Optical Systems GmbH

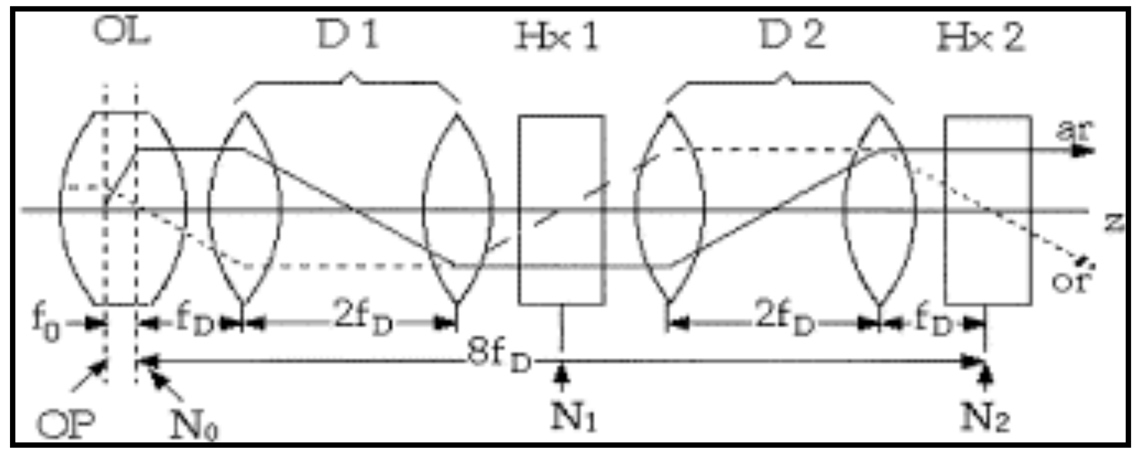

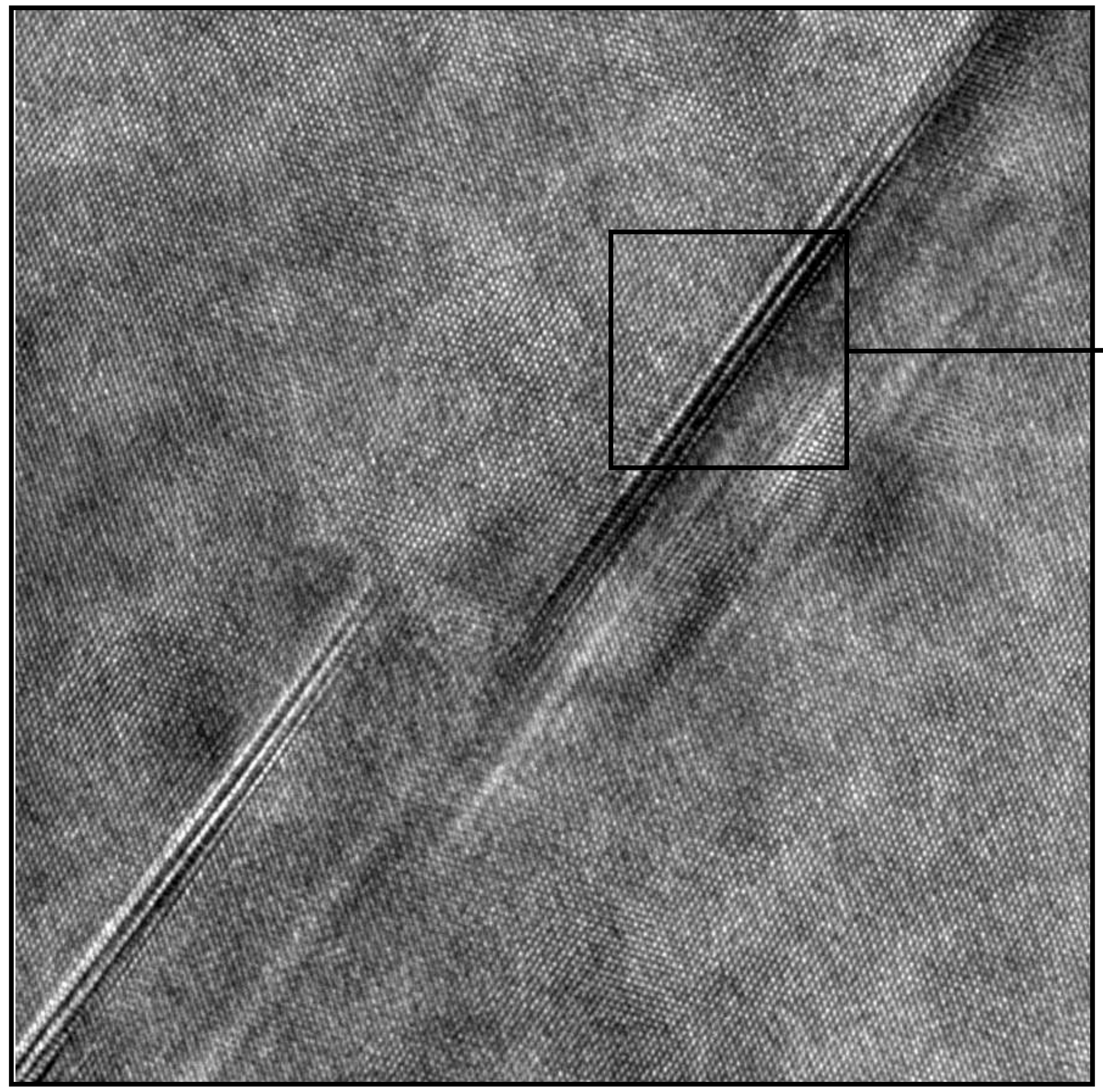

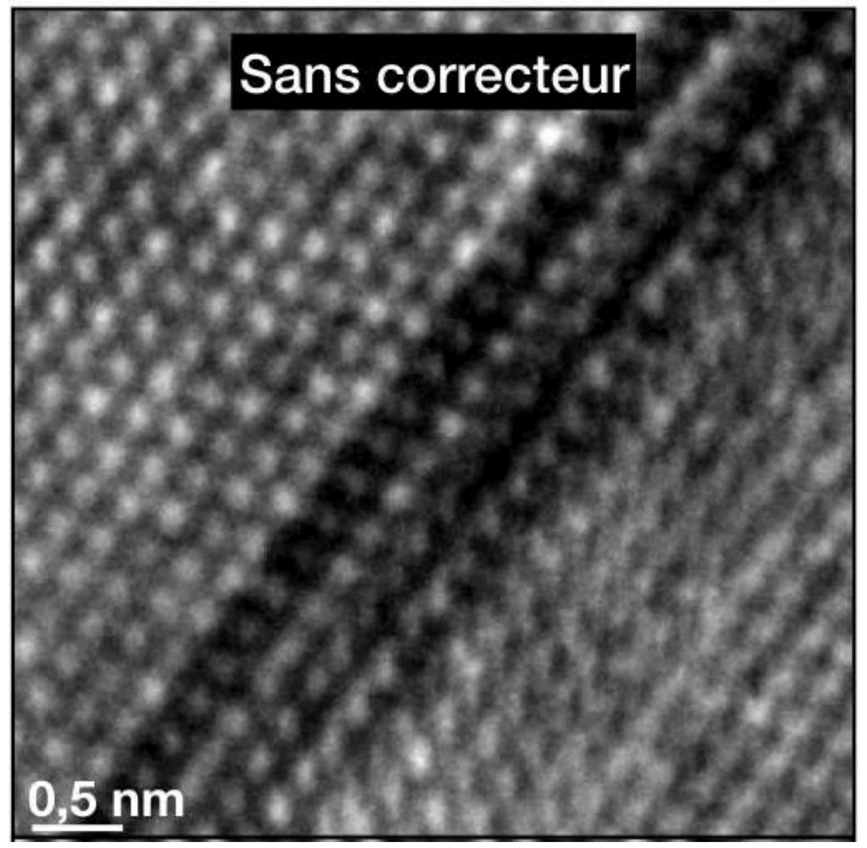

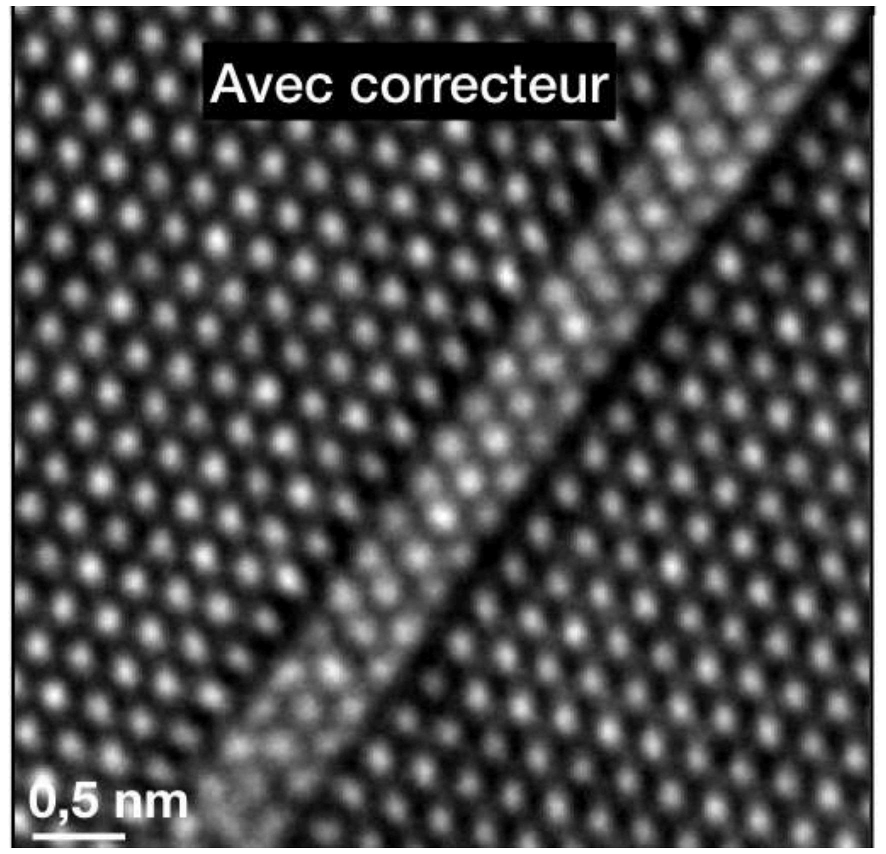

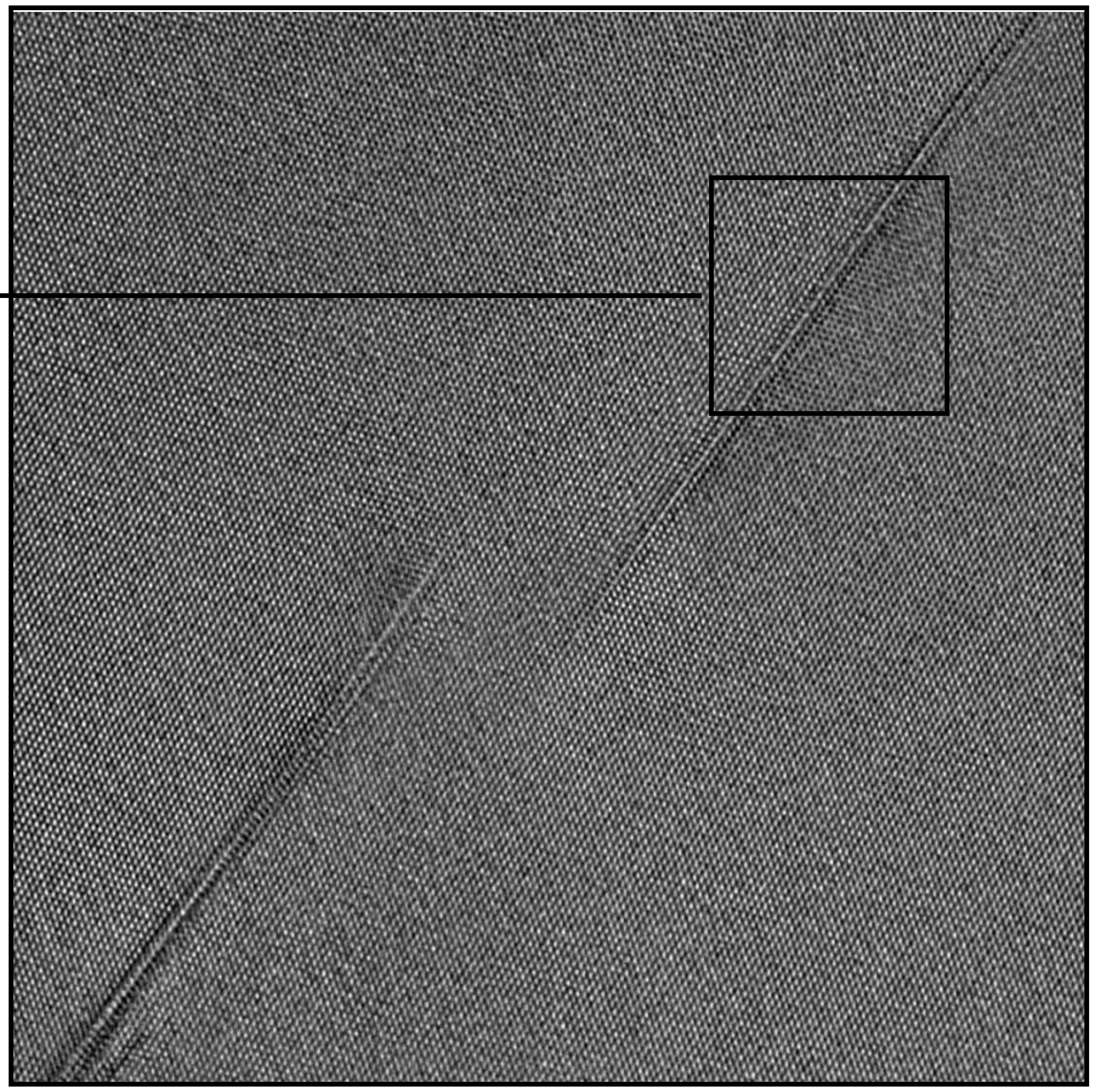

Currently: instrument optically limited by L^6 and not yet the diffraction limit

5

Aberrations in Charged particles optics

High order optical index
Wavefront aberrations
Scherzer theorem
Correction of spherical aberration

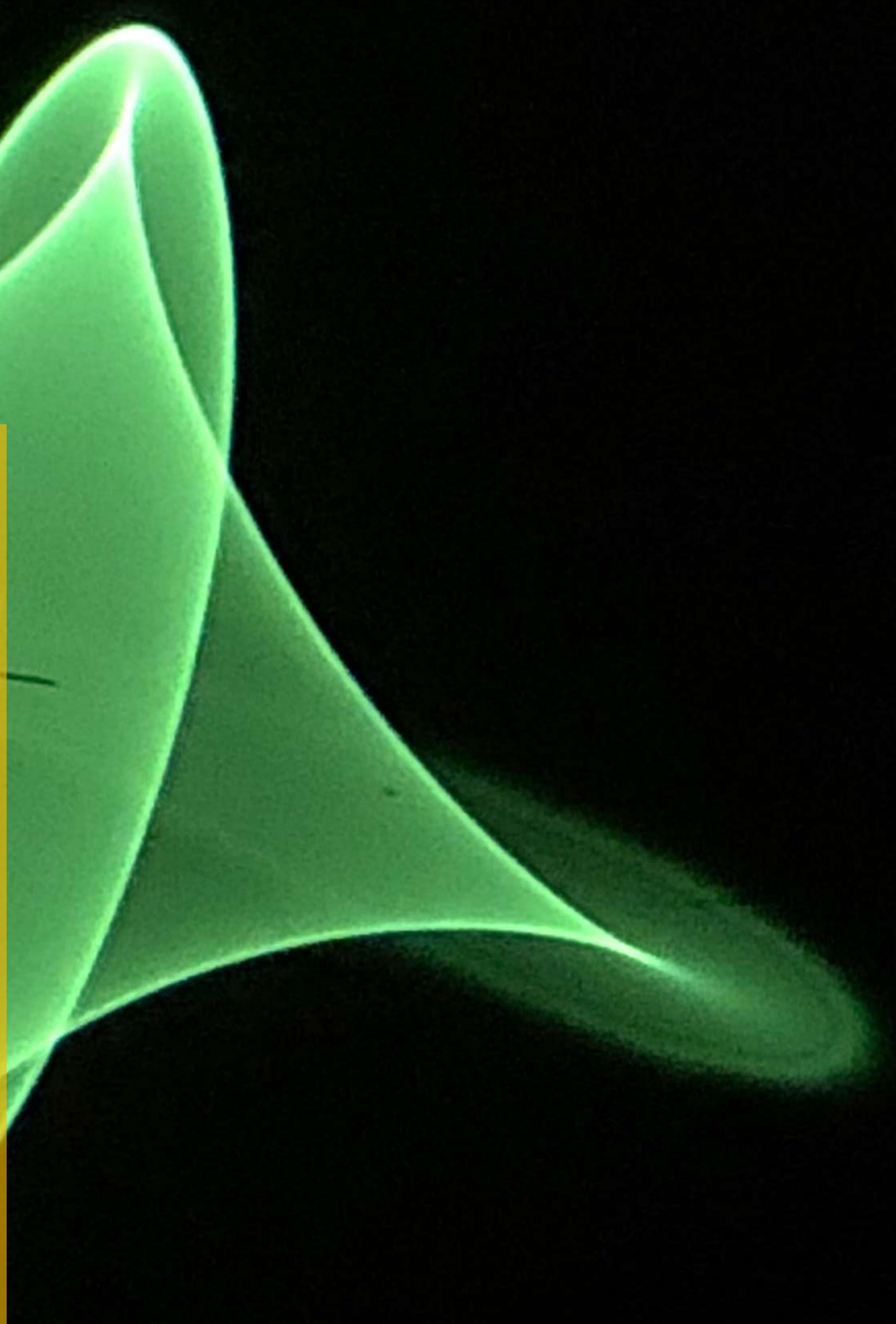

Aberrations ($n > 2$) : $n = 4$ Seidel or primary geometric aberrations

➡ Below, the indices obtained have been expressed for the round contributions Ψ_0, Φ_0 and quadripolar Ψ_2 only …

4th order magneto static index

$$\mu_m^{(4)} = -\frac{e}{q_0} Re \Big\{ \overline{w}_0'^3 w_0' \Big[\frac{i}{12}\Psi_2'' u_\alpha^4 + \frac{i}{6}\Psi_2' u_\alpha^3 (u_\alpha' + i\chi' u_\alpha)\Big] e^{-2i\chi}$$

$$+\overline{w}_0^3 w_0 \Big[\frac{i}{12}\Psi_2'' u_\pi^4 + \frac{i}{6}\Psi_2' u_\pi^3 (u_\pi' + i\chi' u_\pi)\Big] e^{-2i\chi}$$

$$+w_0' \overline{w}_0^3 \Big[\frac{i}{12}\Psi_2'' u_\alpha u_\pi^3 + \frac{i}{6}\Psi_2' u_\pi^3 (u_\alpha' + i\chi' u_\alpha)\Big] e^{-2i\chi}$$

$$+w_0 \overline{w}_0'^3 \Big[\frac{i}{12}\Psi_2'' u_\alpha^3 u_\pi + \frac{i}{6}\Psi_2' u_\alpha^3 (u_\pi' + i\chi' u_\pi)\Big] e^{-2i\chi}$$

$$+w_0' \overline{w}_0'^2 \overline{w}_0 \Big[\frac{i}{4}\Psi_2'' u_\alpha^3 u_\pi + \frac{i}{2}\Psi_2' u_\alpha^2 u_\pi (u_\alpha' + i\chi' u_\alpha)\Big] e^{-2i\chi}$$

$$+w_0 \overline{w}_0' \overline{w}_0^2 \Big[\frac{i}{4}\Psi_2'' u_\alpha u_\pi^3 + \frac{i}{2}\Psi_2' u_\alpha u_\pi^2 (u_\pi' + i\chi' u_\pi)\Big] e^{-2i\chi}$$

$$+w_0' \overline{w}_0' \overline{w}_0^2 \Big[\frac{i}{4}\Psi_0'' u_\alpha^2 u_\pi^2 + \frac{i}{2}\Psi_2' u_\alpha u_\pi^2 (u_\alpha' + i\chi' u_\alpha)\Big] e^{-2i\chi}$$

$$+w_0 \overline{w}_0'^2 \overline{w}_0 \Big[\frac{i}{4}\Psi_2'' u_\alpha^2 u_\pi^2 + \frac{i}{2}\Psi_2' u_\alpha^2 u_\pi (u_\pi' + i\chi' u_\pi)\Big] e^{-2i\chi}$$

$$+\overline{w}_0'^2 w_0'^2 \Big[-\frac{i}{16}\Psi_0''' u_\alpha (u_\alpha^2 u_\alpha' + i\chi' u_\alpha^3)\Big] + \overline{w}_0^2 w_0^2 \Big[-\frac{i}{16}\Psi_0''' u_\pi (u_\pi^2 u_\pi' + i\chi' u_\pi^3)\Big]$$

$$+\overline{w}_0^2 w_0'^2 \Big[-\frac{i}{16}\Psi_0''' u_\alpha (u_\alpha' u_\pi^2 + i\chi' u_\alpha u_\pi^2)\Big] + \overline{w}_0'^2 w_0^2 \Big[-\frac{i}{16}\Psi_0''' u_\pi (u_\alpha^2 u_\pi' + i\chi' u_\alpha^2 u_\pi)\Big]$$

$$+w_0 w_0' \overline{w}_0'^2 \Big[-\frac{i}{16}\Psi_0''' \Big(u_\alpha (u_\alpha^2 u_\pi' + i\chi' u_\alpha^2 u_\pi) + u_\pi (u_\alpha^2 u_\alpha' + i\chi' u_\alpha^3)\Big)\Big]$$

$$+w_0 \overline{w}_0^2 w_0' \Big[-\frac{i}{16}\Psi_0''' \Big(u_\pi (u_\alpha' u_\pi^2 + i\chi' u_\alpha u_\pi^2) + u_\alpha (u_\pi^2 u_\pi' + i\chi' u_\pi^3)\Big)\Big]$$

$$+w_0'^2 \overline{w}_0' \overline{w}_0 \Big[-\frac{i}{8}\Psi_0''' u_\alpha (u_\alpha u_\alpha' u_\pi + i\chi' u_\alpha^2 u_\pi)\Big] + w_0^2 \overline{w}_0 \overline{w}_0' \Big[-\frac{i}{8}\Psi_0''' u_\pi (u_\alpha u_\pi u_\pi' + i\chi' u_\alpha u_\pi^2)\Big]$$

$$w_0 \overline{w}_0 w_0' \overline{w}_0' \Big[-\frac{i}{8}\Psi_0''' \Big(u_\alpha (u_\alpha u_\pi u_\pi' + i\chi' u_\alpha u_\pi^2) + u_\pi (u_\alpha u_\alpha' u_\pi + i\chi' u_\alpha^2 u_\pi)\Big)\Big]$$

4th order electrostatic index

$$\mu_e^{(4)} = \frac{1}{8}\sqrt{\frac{\Phi_0^*}{\Phi_0^*(z_0)}} Re \Big\{ w_0'^2 \overline{w}_0'^2 \Big[-(u_\alpha'^2 + \chi'^2 u_\alpha^2)^2 - \frac{\gamma_0}{2\Phi_0^*}\Phi_0'' u_\alpha^2 (u_\alpha'^2 + \chi'^2 u_\alpha)$$

$$+\frac{1}{16\Phi_0^*}\Big(\gamma_0 \Phi_0'''' - \frac{\Phi_0''^2}{\Phi_0^*}\Big) u_\alpha^4\Big]$$

$$+w_0'^2 \overline{w}_0' \overline{w}_0 \Big[-2 (u_\alpha'^2 + \chi'^2 u_\alpha^2)(u_\alpha' u_\pi' + \chi'^2 u_\alpha u_\pi - i\chi'(u_\alpha' u_\pi - u_\alpha u_\pi')) - \frac{\gamma_0}{2\Phi_0^*}\Phi_0'' \Big(u_\alpha^2 (u_\alpha' u_\pi'$$

$$+\chi'^2 u_\alpha u_\pi - i\chi'(u_\alpha' u_\pi - u_\alpha u_\pi')) + u_\alpha u_\pi (u_\alpha'^2 + \chi'^2 u_\alpha^2)\Big) + \frac{1}{8\Phi_0^*}\Big(\gamma_0 \Phi_0'''' - \frac{\Phi_0''^2}{\Phi_0^*}\Big) u_\alpha^3 u_\pi\Big]$$

$$+w_0'^2 \overline{w}_0^2 \Big[-(u_\alpha' u_\pi' + \chi'^2 u_\alpha u_\pi - i\chi'(u_\alpha' u_\pi - u_\alpha u_\pi'))^2 - \frac{\gamma_0}{2\Phi_0^*}\Phi_0'' u_\alpha u_\pi (u_\alpha' u_\pi' + \chi'^2 u_\alpha u_\pi$$

$$-i\chi'(u_\alpha' u_\pi - u_\alpha u_\pi')) - \frac{1}{16\Phi_0^*}\Big(\gamma_0 \Phi_0'''' - \frac{\Phi_0''^2}{\Phi_0^*}\Big) u_\alpha^2 u_\pi^2\Big]$$

$$+\overline{w}_0' w_0' \overline{w}_0 w_0 \Big[-2 (u_\alpha'^2 + \chi'^2 u_\alpha^2)(u_\pi'^2 + \chi'^2 u_\pi^2) - 2 (u_\alpha' u_\pi' + \chi'^2 u_\alpha u_\pi + i\chi'(u_\alpha' u_\pi - u_\alpha u_\pi'))(u_\alpha' u_\pi'$$

$$+\chi'^2 u_\alpha u_\pi - i\chi'(u_\alpha' u_\pi - u_\alpha u_\pi')) - \frac{\gamma_0}{2\Phi_0^*}\Phi_0'' \Big(u_\alpha^2 (u_\pi'^2 + \chi'^2 u_\pi^2) + u_\pi^2 (u_\alpha'^2 + \chi'^2 u_\alpha^2)$$

$$+u_\alpha u_\pi (u_\alpha' u_\pi' + \chi'^2 u_\alpha u_\pi)\Big) + \frac{1}{4\Phi_0^*}\Big(\gamma_0 \Phi_0'''' - \frac{\Phi_0''^2}{\Phi_0^*}\Big) u_\alpha^2 u_\pi^2\Big]$$

$$+w_0' w_0 \overline{w}_0^2 \Big[-2 (u_\pi'^2 + \chi'^2 u_\pi^2)(u_\alpha' u_\pi' + \chi'^2 u_\alpha u_\pi - i\chi'(u_\alpha' u_\pi - u_\alpha u_\pi')) - \frac{\gamma_0}{2\Phi_0^*}\Phi_0'' \Big(u_\pi^2 (u_\alpha' u_\pi'$$

$$+\chi'^2 u_\alpha u_\pi - i\chi'(u_\alpha' u_\pi - u_\alpha u_\pi')) + u_\alpha u_\pi (u_\pi'^2 + \chi'^2 u_\pi^2)\Big) + \frac{1}{8\Phi_0^*}\Big(\gamma_0 \Phi_0'''' - \frac{\Phi_0''^2}{\Phi_0^*}\Big) u_\alpha u_\pi^3\Big]$$

$$+w_0^2 \overline{w}_0^2 \Big[-(u_\pi'^2 + \chi'^2 u_\pi^2)^2 - \frac{\gamma_0}{2\Phi_0^*}\Phi_0'' u_\pi^2 (u_\pi'^2 + \chi'^2 u_\pi^2) + \frac{1}{16\Phi_0^*}\Big(\gamma_0 \Phi_0'''' - \frac{\Phi_0''^2}{\Phi_0^*}\Big) u_\pi^4\Big]\Big\}$$

- Rotationnaly symetric field Ψ_0, Φ_0 induce :
  - Aperture aberration (spherical)
  - Fields aberrations :
    - Coma,
    - Petzval curvature,
    - Field astigmatism
    - Distorsion

- Quadrupolar component Ψ_2 induces :
  - Aperture aberrations (star and rosette)
  - Fields aberrations (many comas terms, …)

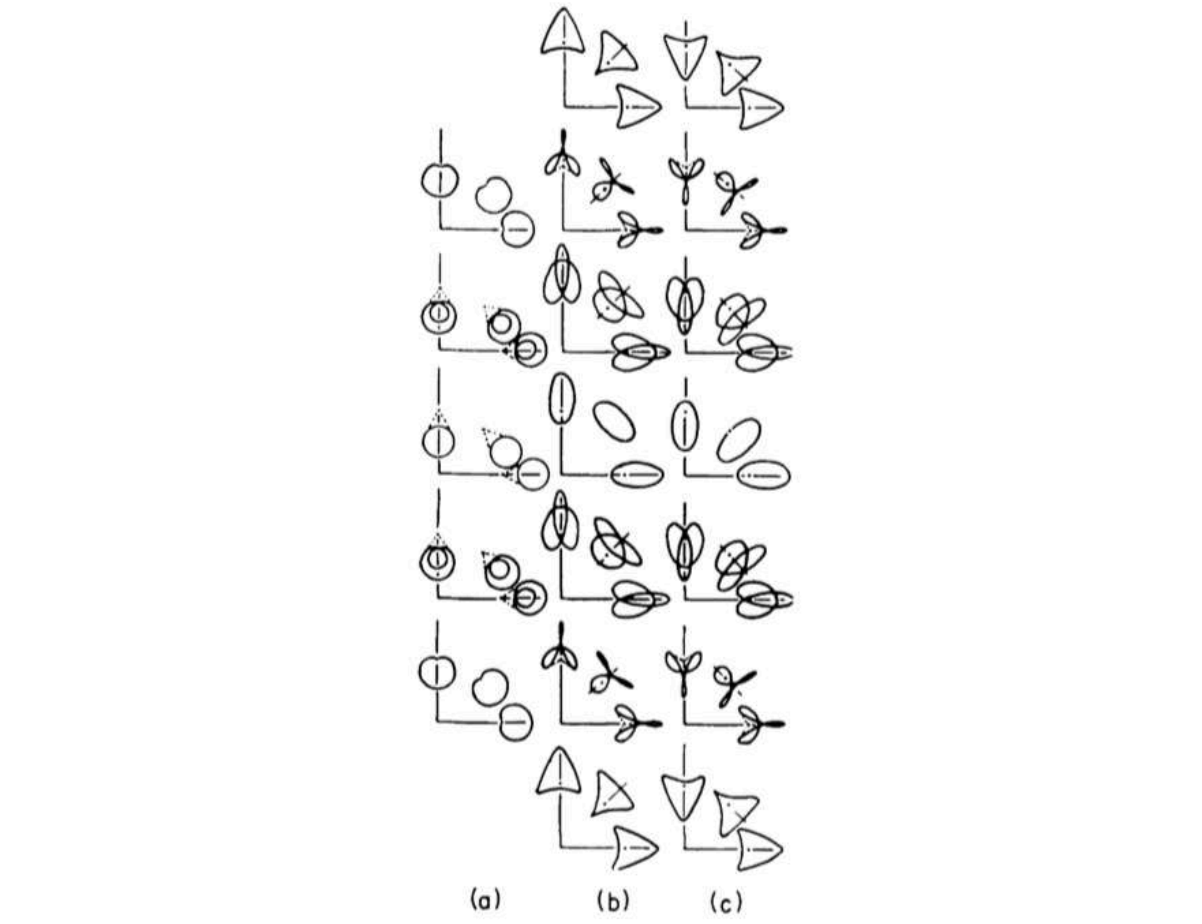

FIG. 7. Third-order comas. (a) Conjugate coma; (b) elliptical coma; (c) conjugate elliptical coma. The fourth row down shows the aberration figures in the Gaussian image plane, and the other rows, the same figures as they appear in other current planes. (From Burfoot, 1956.)

- After Scherzer, we can show that Ψ_3, Φ_3 and Ψ_4, Φ_4 can be used to cancel out the aperture aberration caused by Ψ_0, Φ_0 (see Pr. Rose's book for details)

Wavefront aberrations: the most common aperture terms

➡ Object point (no field) in the optical axis (such as a SEM, TEM, STEM or FIB source). We then assume $\overline{w}_0 = 0, w_0 = 0$

$$W = \frac{\tilde{S}}{q_0} = \int_{z_0}^{z} \mu dz \implies Re\left[A_0\overline{w}'_0 + \frac{1}{2}C_{df}|w'_0|^2 + \frac{1}{2}A_1\overline{w}'^2_0 + \overline{B}_2|w'_0|^2\overline{w}'_0 + \frac{1}{3}A_2\overline{w}'^3_0 + \frac{1}{4}C_s|w'_0|^4 + \overline{S}_3|w'_0|^2\overline{w}'^2_0\right]$$

➡ We obtain a sum of polynomials functions of different orders depending on the variables of the entrance pupil $(\overline{w}'_0, w'_0)$. Each function is weighted by an aberration coefficient :

Equations intégrales des coefficients

$$A_0 = \frac{ie}{q_0}\int_{z_0}^{z} u_\alpha \Psi_1 e^{-i\chi} dz$$

• **Beam tilt**

$$C_{df} = \int_{z_0}^{z}\left[\sqrt{\frac{\Phi_0^*}{\Phi_0^*(z_0)}}\left(u'^2_\alpha + \chi'^2 u_\alpha^2 - \frac{\gamma_0}{4\Phi_0^*}\Phi''_0 u_\alpha^2\right) + \frac{e\chi'}{q_0}\Psi'_0 u_\alpha^2\right] dz$$

• **Defocus**

$$A_1 = \frac{2ie}{q_0}\int_{z_0}^{z} \Psi_2 u_\alpha^2 e^{-2i\chi} dz$$

• **Axial astigmatism (ordre 1)**

$$\overline{B}_2 = -\frac{ie}{4q_0}\int_{z_0}^{z} dz \left[\frac{1}{2}\Psi''_1 u_\alpha^3 + \Psi_1\left(u_\alpha^2 u'_\alpha + i\chi' u_\alpha^3\right)\right] e^{-i\chi}$$

• **Axial Coma**

$$A_2 = \frac{3ie}{q_0}\int_{z_0}^{z} \Psi_3 u_\alpha^3 e^{-3i\chi} dz$$

• **Axial astigmatism(ordre 2)**

$$C_s = \frac{1}{2}\int_{z_0}^{z} dz \left[\sqrt{\frac{\Phi_0^*}{\Phi_0^*(z_0)}}\left(-\left(u'^2_\alpha + \chi'^2 u_\alpha^2\right)^2 - \frac{\gamma_0}{2\Phi_0^*}\Phi''_0 u_\alpha^2\left(u'^2_\alpha + \chi'^2 u_\alpha^2\right) + \frac{1}{16}\left(\gamma_0 \Phi''''_0 - \frac{\Phi''^2_0}{\Phi_0^*}\right)u_\alpha^4\right) - \frac{e}{2q_0}\Psi'''_0 \chi' u_\alpha^4\right]$$

• **Spherical aberration**

$$\overline{S}_3 = -\frac{ie}{q_0}\int_{z_0}^{z} dz \left[\frac{\Psi''_2}{6}u_\alpha^4 + \frac{\Psi'_2}{3}\left(u'_\alpha + i\chi' u_\alpha\right) u_\alpha^3\right] e^{-2i\chi}$$

• **Star**

Polynomial sum gives the final wavefront

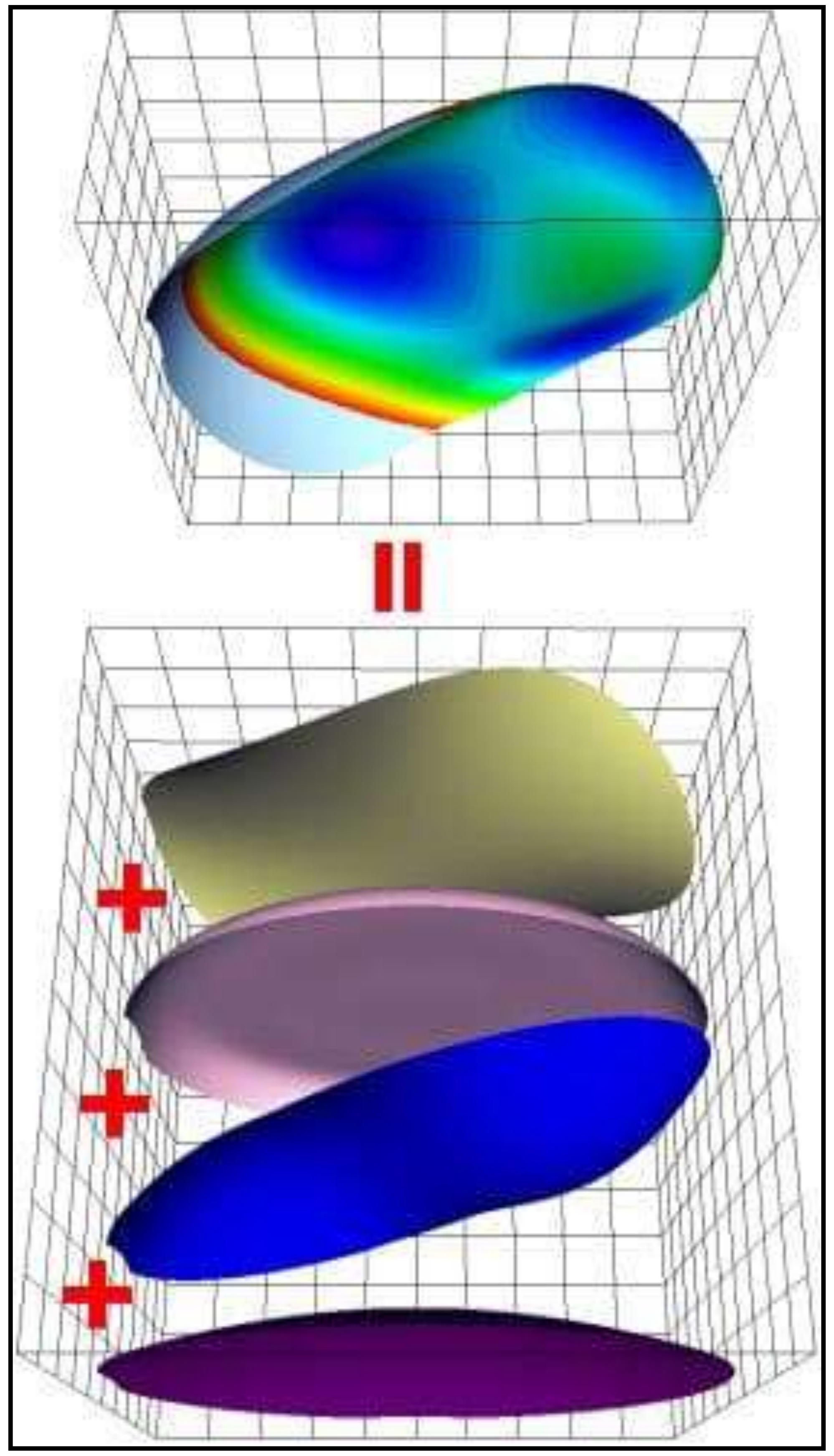

6

Overview of the general method to study a CPO element

How does it work in practice? evaluation of the terms in the field

➡ The first step is to calculate and map the potential (electrostatic or magnetostatic or both) in the volume of your optical element in 3D.

➡ To do this, we need to solve the Laplace equation (differential equation) starting from the boundary conditions:
Dirichlet (fixed potential on the surface of the electrodes) or Neumann (field $\vec{E} \cdot \vec{n}$ fixed on the surface of the electrodes, $\vec{n}$ being the normal to the surface)

There are 3 main strategies for solving these differential equations:

$$\Delta\phi(\vec{r}) = 0 \qquad \Delta\psi(\vec{r}) = 0$$

Cut the volume into squares.
Calculate derivatives by difference
Finite difference method (FDM)

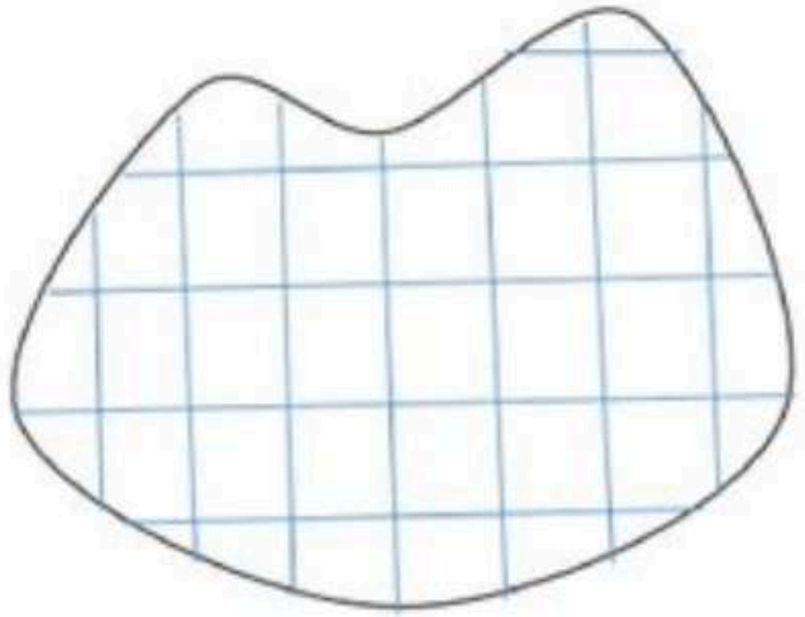

FDM: 27 internal nodes

Cut the volume into elements.
Minimise the EM energy density
in each of the volumes.
Finite Element Method (FEM)

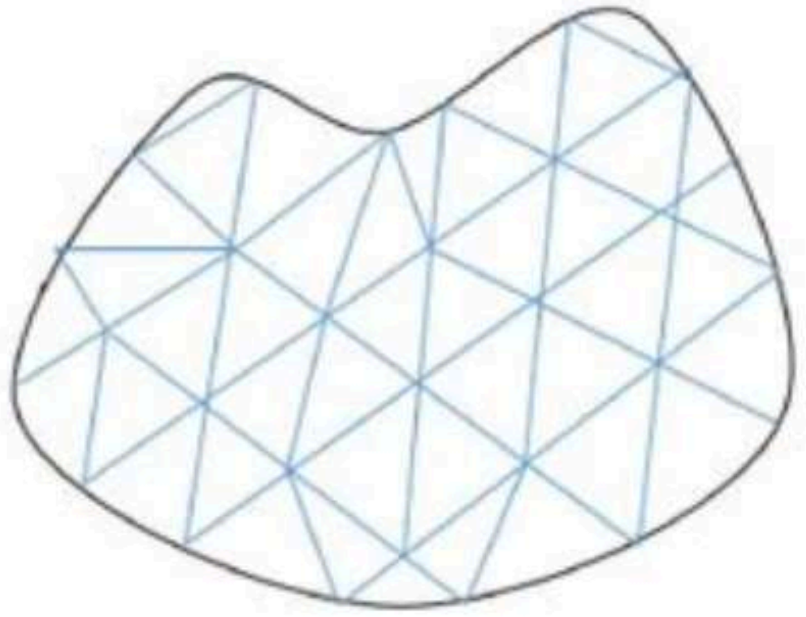

FEM: 42 elements

Cut the boundaries into elements.
Use the potentials/fields of the elements
to find the potential in the volume
using Green's functions
Boundary element method (BEM)

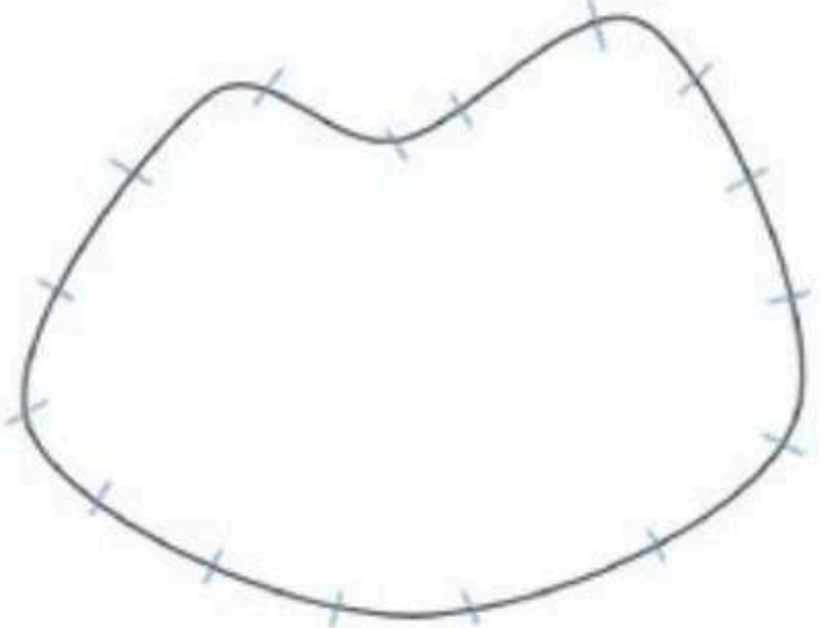

BEM: 16 elements

➡ Let's take the example of calculating the field of a magnetic quadrupole using FEM (COMSOL multiphysics software).

Definition of geometry and boundary conditions

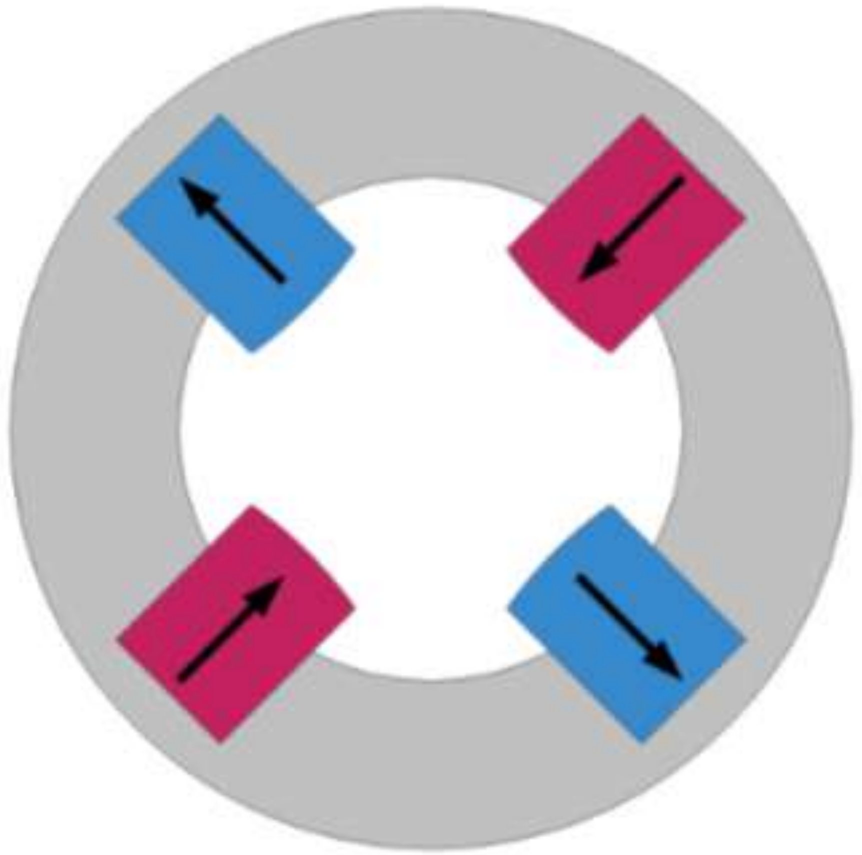

Meshing of different volumes

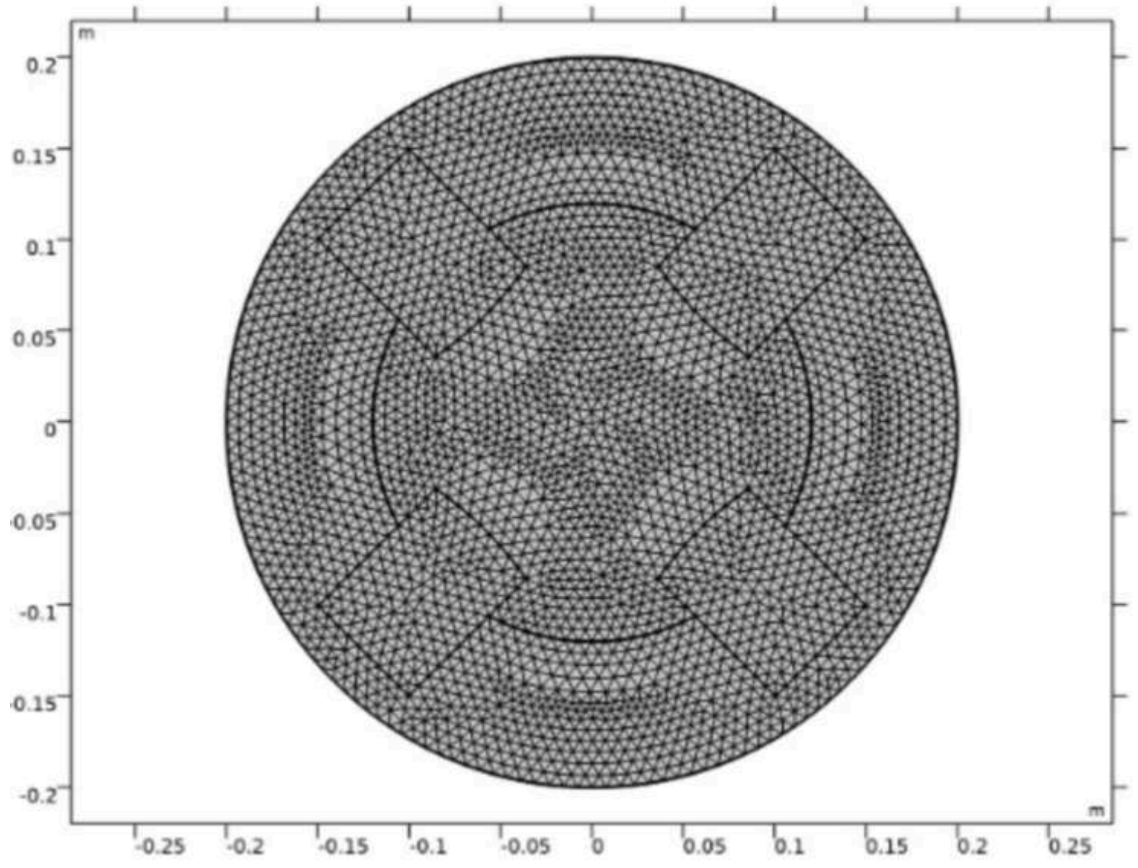

Calculation and mapping of $\vec{B}$

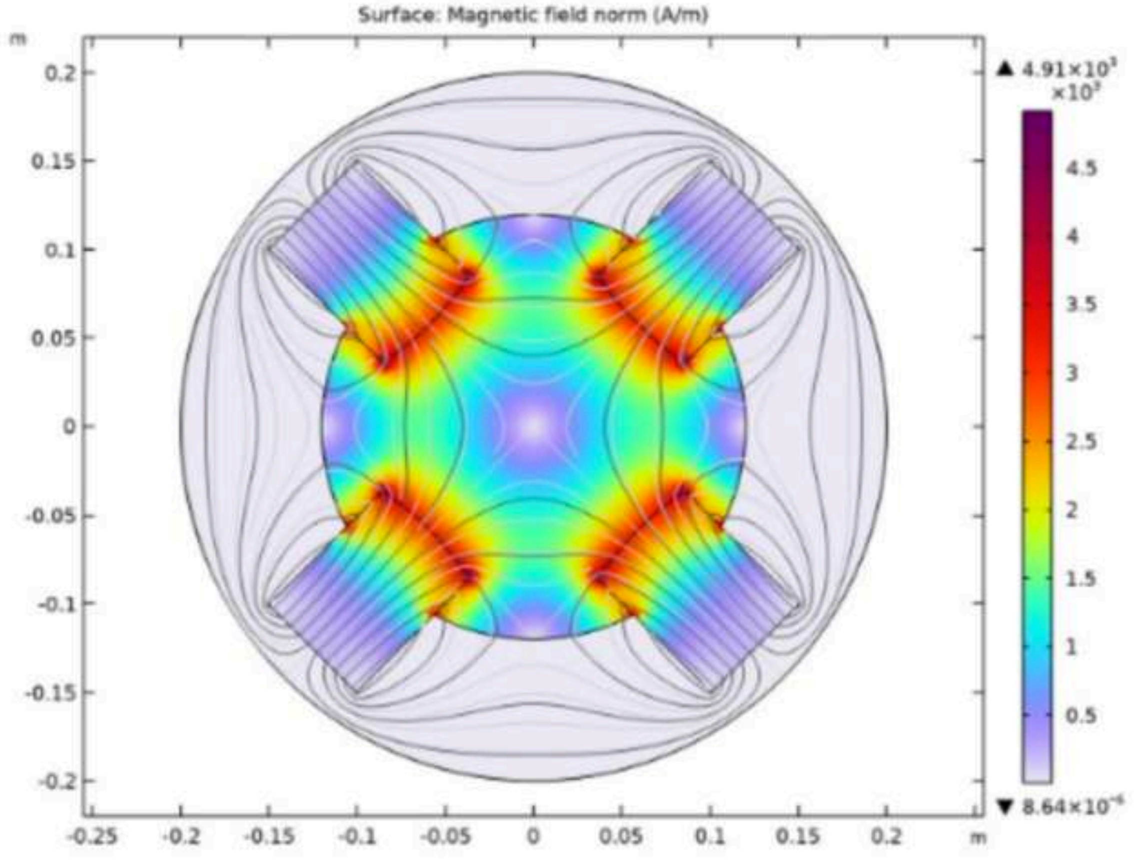

How does it work in practice? evaluation of the terms in the field

➡ Once the potential ϕ, ψ has been determined in 3D, we can extract the various multipolar components Φ_ν, Ψ_ν using ϕ, ψ derivatives :

$$\boxed{\Phi_\nu = \frac{2-\delta_{o\nu}}{\nu!}\left(\frac{\partial^\nu \phi}{\partial \bar{w}^\nu}\right)_{w=0} \in \mathbb{C}}$$

➡ We can then solve the paraxial equation : $w'' + \frac{\gamma_0}{2\Phi_0^*}(\Phi_0' + i v_0 \Psi_0')w' + \frac{\gamma_0}{4\Phi_0^*}\left(\Phi_0'' + i v_0 \Psi_0'' + \frac{\Phi_1 \overline{\Phi}_1}{2\gamma_0 \Phi_0^*}\right) w - \frac{\gamma_0}{\Phi_0^*}\left(\Phi_2 + i v_0 \Psi_2 - \frac{\Phi_1^2}{8\gamma_0 \Phi_0^*}\right)\overline{w} = \frac{\gamma_0}{2\phi_0^*}(\Phi_1 + i v_0 \Psi_1)$

➡ To achieve this, numerical integration methods of the Runge-Kutta 4 type are generally used.

➡ We then plot the two paraxial solutions (marginal, principal)

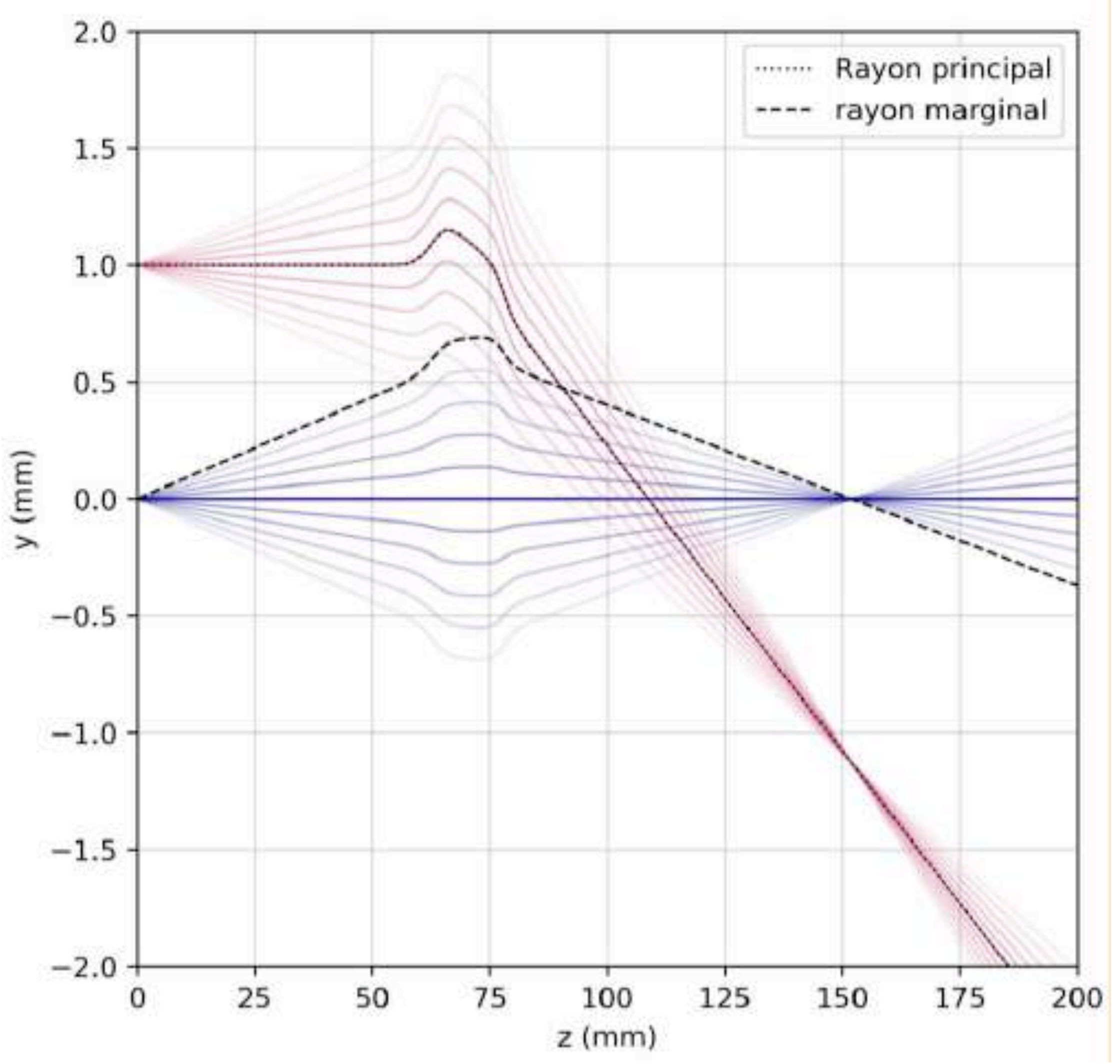

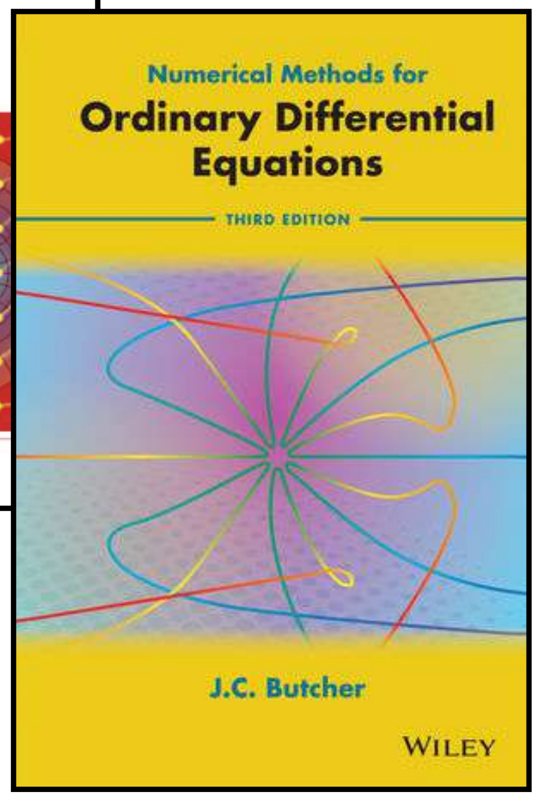

p 93 ➡

23 Runge–Kutta Methods

230 Historical introduction

The idea of generalizing the Euler method, by allowing for a number of evaluations of the derivative to take place in a step, is generally attributed to Runge (1895). Further contributions were made by Heun (1900) and Kutta (1901). The latter completely characterized the set of Runge–Kutta methods of order 4, and proposed the first methods of order 5. Special methods for second order differential equations were proposed by Nyström (1925), who also contributed to the development of methods for first order equations. It was not until the work of Huťa (1956, 1957) that sixth order methods were introduced.

Since the advent of digital computers, fresh interest has been focused on Runge–Kutta methods, and a large number of research workers have contributed to recent extensions to the theory, and to the development of particular methods. Although early studies were devoted entirely to explicit Runge–Kutta methods, interest has now moved to include implicit methods, which have become recognized as appropriate for the solution of stiff differential equations.

A number of different approaches have been used in the analysis of Runge–Kutta methods, but the one used in this section, and in the more detailed analysis of Chapter 3, is that developed by the present author (Butcher, 1963), following on from the work of Gill (1951) and Merson (1957).

➡ Calculation of Φ_ν, Ψ_ν derivatives along the z axis and then integrating the integral equations to determine aberrations (integration using numerical methods such as Simpson's method). ➡ $C_s = \frac{1}{2}\int_{z_0}^{z} dz \left[\sqrt{\frac{\Phi_0^*}{\Phi_0^*(z_0)}}\left(-\left(u_\alpha'^2 + \chi'^2 u_\alpha^2\right)^2 - \frac{\gamma_0}{2\Phi_0^*}\Phi_0'' u_\alpha^2\left(u_\alpha'^2 + \chi'^2 u_\alpha^2\right) + \frac{1}{16}\left(\gamma_0 \Phi_0'''' - \frac{\Phi_0''^2}{\Phi_0^*}\right)u_\alpha^4\right) - \frac{e}{2q_0}\Psi_0'''\chi' u_\alpha^4\right]$

How does it work in practice? evaluation of the terms in the field

1. Calculation of the EM field and determination of the on-axis field (FEM for EOD) :

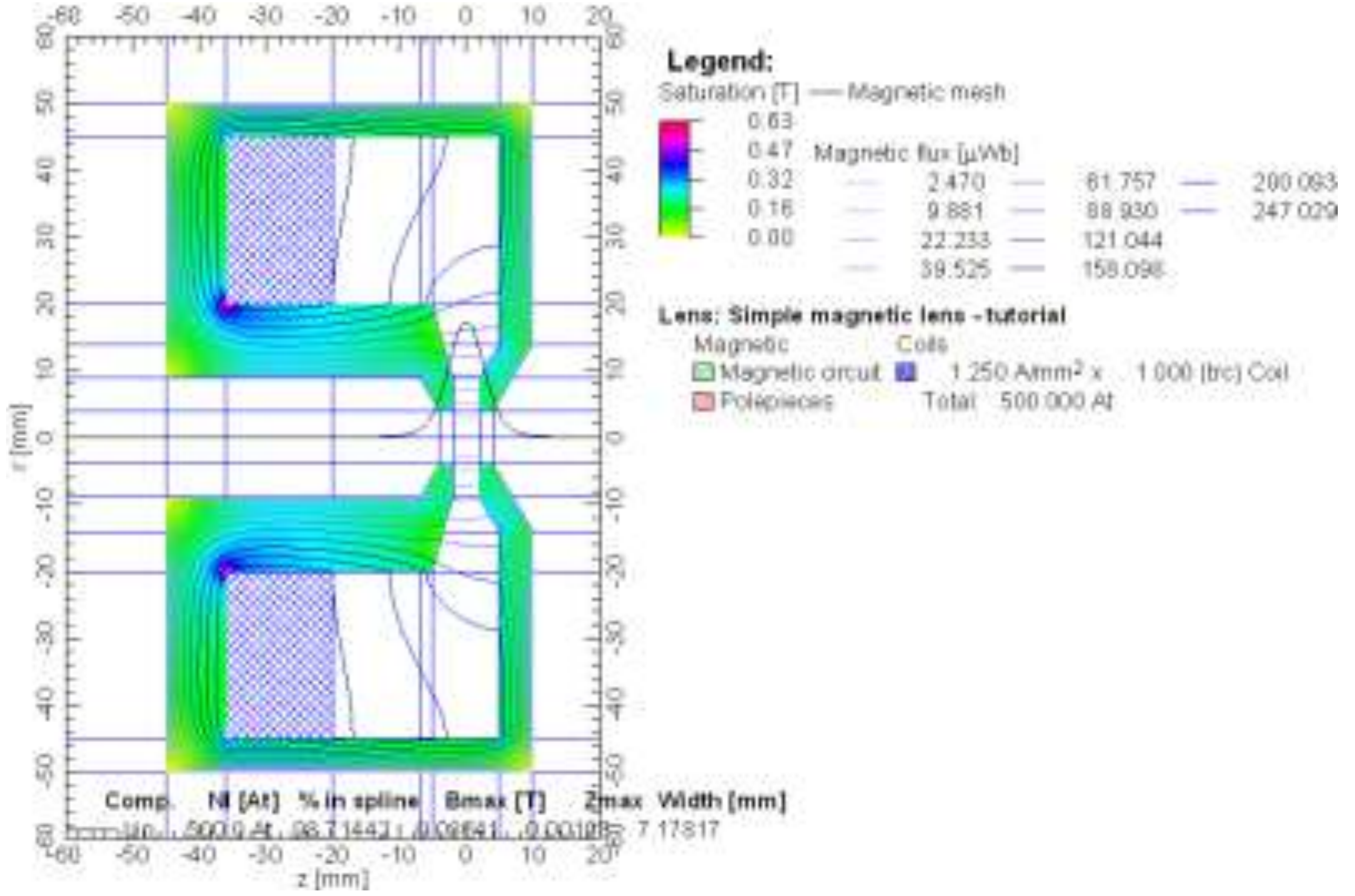

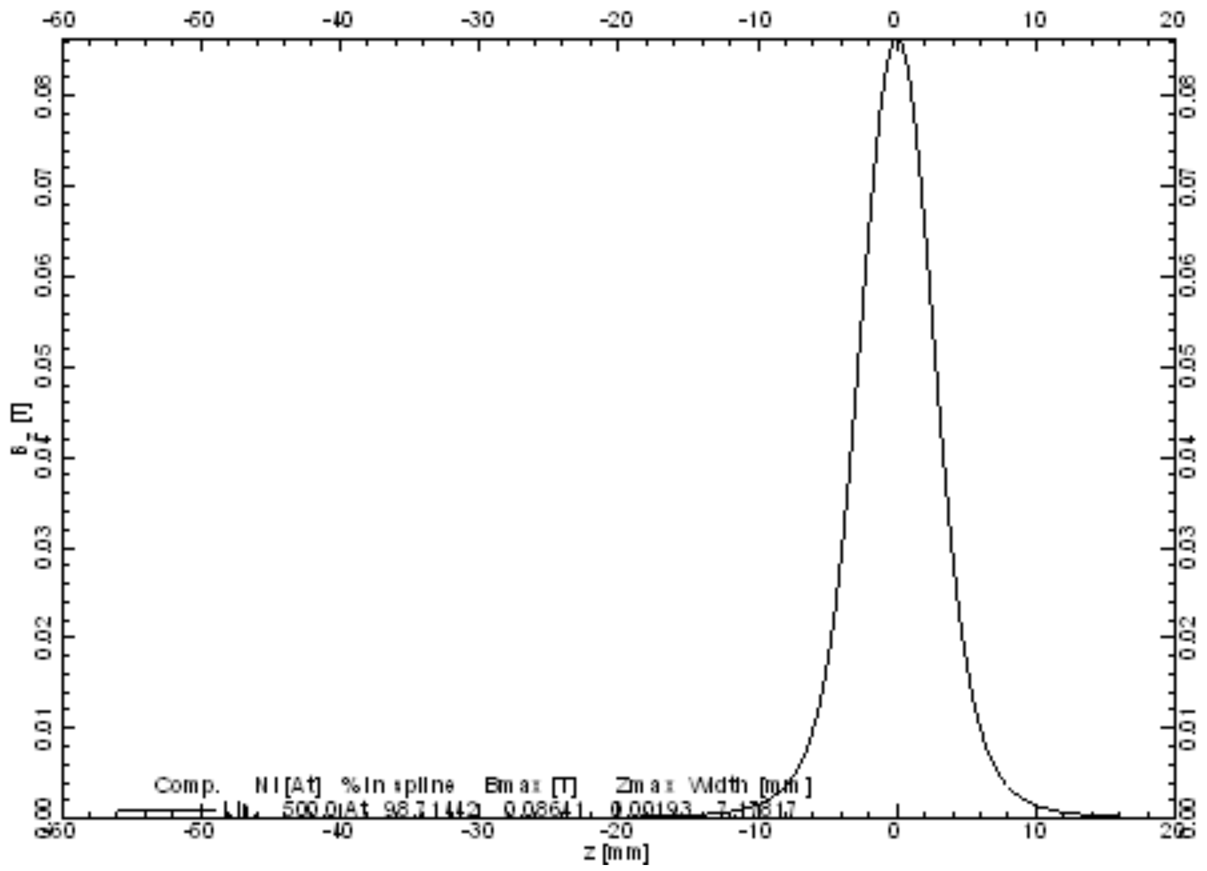

2. Paraxial solutions: marginal + principal (Runge-Kutta)

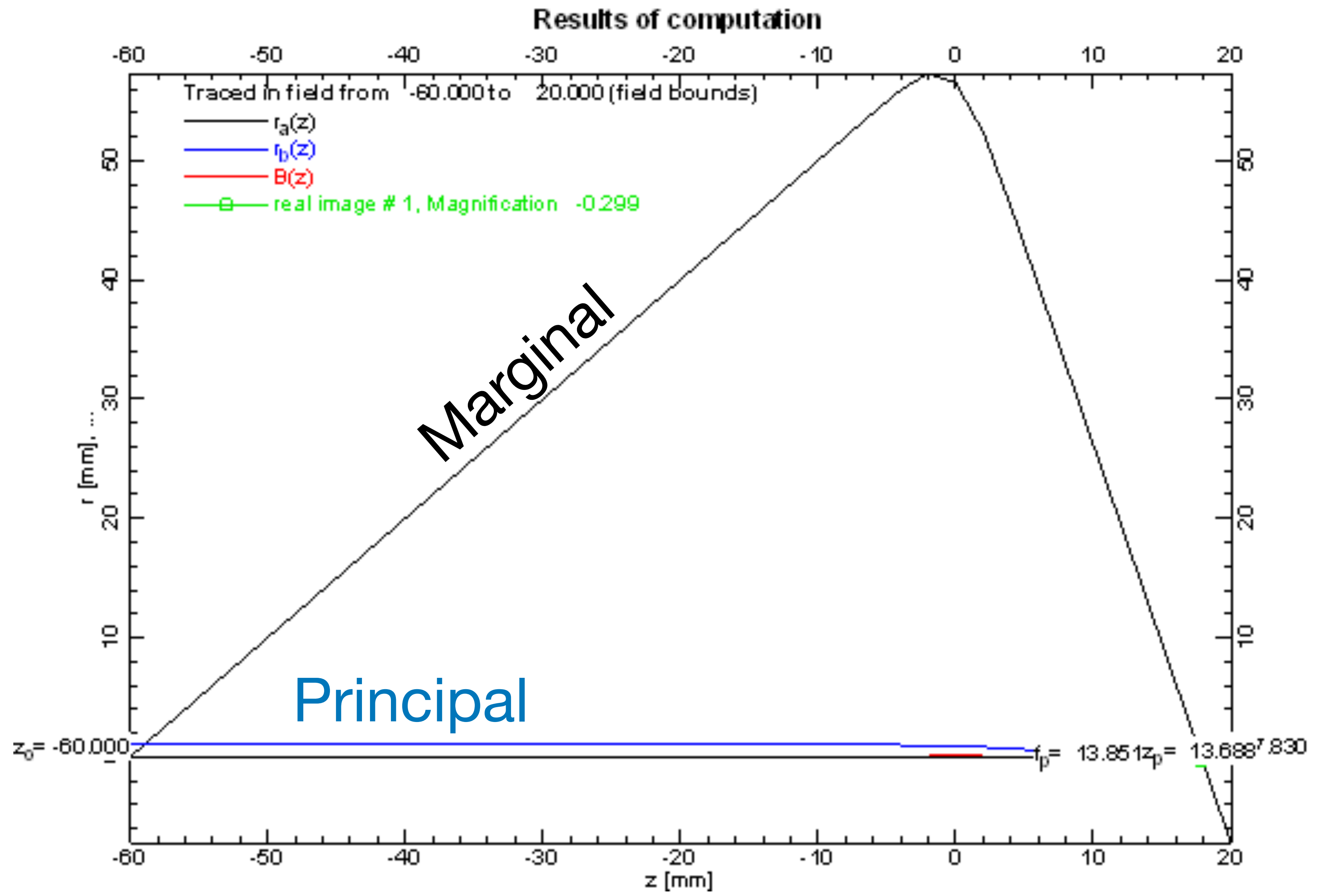

3. Paraxial properties + aberrations

```
Computation with asymptotic object
V*              =   1.00000000E+00 V
U               =   1.00000000E+00 eV
image #         =    1 (asymptotic)
z object        =   -5.0000000     mm
z image         =     60.0000      mm
rotation        =    0.0000000     rad
                     0.0000000     deg
dir. magnif.    =    -6.216739
ang. magnif.    =   -0.1608560
V* object       =   1.00000000E+00 V
V* image        =   1.00000000E+00 V
1-M*Ma*sqrt(p(zi)/p(zo))       =  -5.29420952E-12
fproj           =    9.0820777     mm
zproj           =    3.5390932     mm
```

```
Aberration coefficients related to object
 axial spherical aber.:   9.0529E+01                mm
 iso,aniso coma length:   8.9721E+00,  0.0000E+00
 field curvature:         1.1784E+00                1/mm
 iso,aniso astigmatism:   2.5496E-01,  0.0000E+00 1/mm
 iso,aniso distortion:    4.6112E-02,  0.0000E+00 1/mm^2
 axial chromatic:         1.2484E+02                mm
 iso,aniso chromatic:     6.6222E+00,  0.0000E+00

Aberration coefficients for aperture
Aperture position at z=      0.0000000E+00 mm
  |ra| =   1.1462E+01, |rb| =   1.0872E+00

 axial spherical aber.:   9.0529E+01                mm
 iso,aniso coma length:  -8.2012E+00,  0.0000E+00
 field curvature:         1.1053E+00                1/mm
 iso,aniso astigmatism:   2.1840E-01,  0.0000E+00 1/mm
 iso,aniso distortion:   -1.4315E-02,  0.0000E+00 1/mm^2
 axial chromatic:         1.2484E+02                mm
 iso,aniso chromatic:    -5.2188E+00,  0.0000E+00
```

7

Introduction to main aberration corrector solutions

Quadrupole-octopole solution
Hexapole solution

How can we correct aberrations ? The Scherzer move

- **Otto Scherzer (1909-m. 1982)**
  « Sphärische und chromatische Korrektur von Elektronen-Linsen » (1947).

Sphärische und chromatische Korrektur von Elektronen-Linsen.

Von O. Scherzer, z. Zt. USA.

(Aus den Süddeutschen Laboratorien in Mosbach.)

(Mit 7 Textabbildungen.)

Die Brauchbarkeit des Elektronenmikroskops bei hohen Vergrößerungen wird durch den Öffnungsfehler und die chromatische Aberration beeinträchtigt. Beide Fehler sind unvermeidlich, solange die abbildenden Felder rotations-symmetrisch, ladungsfrei und zeitlich konstant sind. Die vorliegende Untersuchung soll zeigen, daß die Aufhebung irgendeiner dieser drei Einschränkungen genügt, um den Weg zur sphärischen und chromatischen Korrektur und damit zu einer erheblichen Steigerung des Auflösungsvermögens freizugeben.

Solange nicht klar zu sehen ist, welche Art Linsen das beste Mikroskop ergibt, müssen alle sich bietenden Wege verfolgt werden. Es scheint daher angebracht, etwas ausführlicher auf die verschiedenen Arten korrigierter Linsen einzugehen.

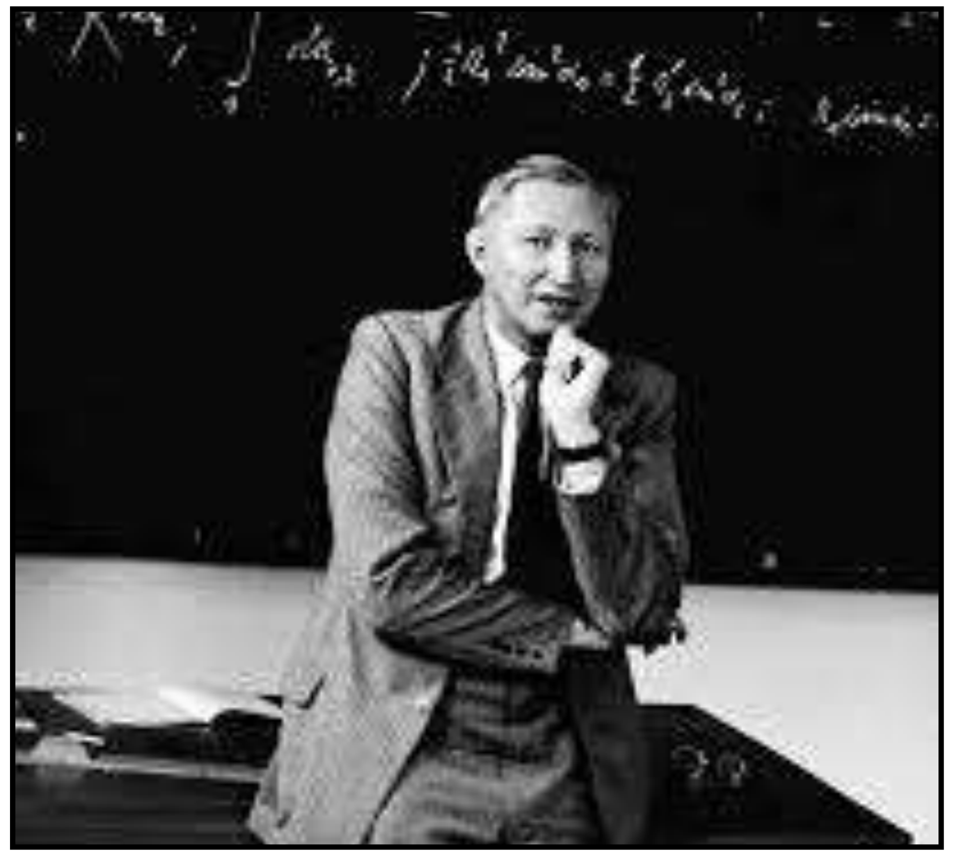

Wir erhalten so für die durch das Korrekturfeld hervorgerufenen Verschiebungen in der Bildebene in Analogie zu (2,4):

$$\left.\begin{aligned} x_{bk} &= \frac{-V}{\sqrt{\Phi_a}}\int_{z_a}^{z_b}\frac{\varepsilon_x x_a}{\sqrt{\Phi}}\,dz = \frac{2V}{\sqrt{\Phi_a}}\int_{z_a}^{z_b}\frac{\Phi_4}{\sqrt{\Phi}}\left(3\alpha\beta^2 x_a^2 y_a^2 - \alpha^3 x_a^4\right)dz;\\ y_{bk} &= \frac{-V}{\sqrt{\Phi_a}}\int_{z_a}^{z_b}\frac{\varepsilon_y y_a}{\sqrt{\Phi}}\,dz = \frac{2V}{\sqrt{\Phi_a}}\int_{z_a}^{z_b}\frac{\Phi_4}{\sqrt{\Phi}}\left(3\alpha^2\beta x_a^2 y_a^2 - \beta^3 y_a^4\right)dz. \end{aligned}\right\}\quad (3,4)$$

Die Korrekturforderung $x_{bu} + x_{bk} = 0$; $y_{bu} + y_{bk} = 0$ ist nun verhältnismäßig einfach zu erfüllen. Ein negatives Φ_4 an einer Stelle, wo $x_a\, y_a \neq 0$ ist, bringt nach (3,2) und (3,4) den Koeffizienten von $\alpha\beta^2$ und, wegen

➡

Sphärische und chromatische Korrektur von Elektronenlinsen 121

positives Φ_4 in der Umgebung der Nullstelle von y_α beseitigt den (durch den vorherigen Schritt noch vergrößerten) Koeffizienten von α^3, ein positives Φ_4 in der Umgebung der Nullstelle von x_α tut dasselbe mit dem Koeffizienten von β^3. Damit ist der Öffnungsfehler dritter Ordnung beseitigt.

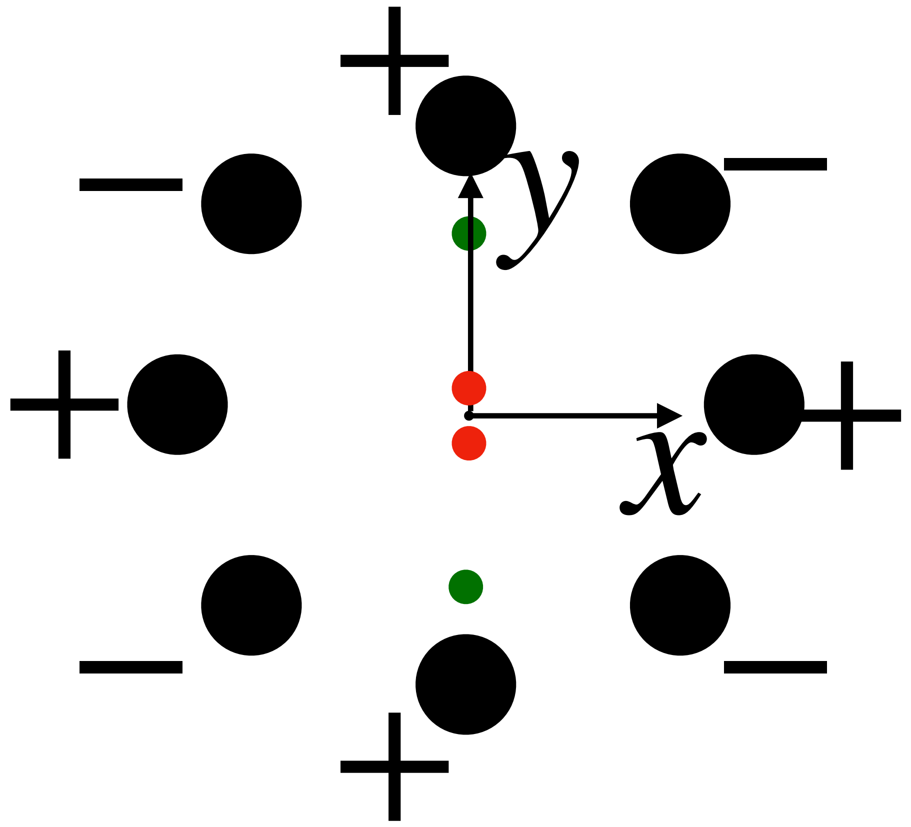

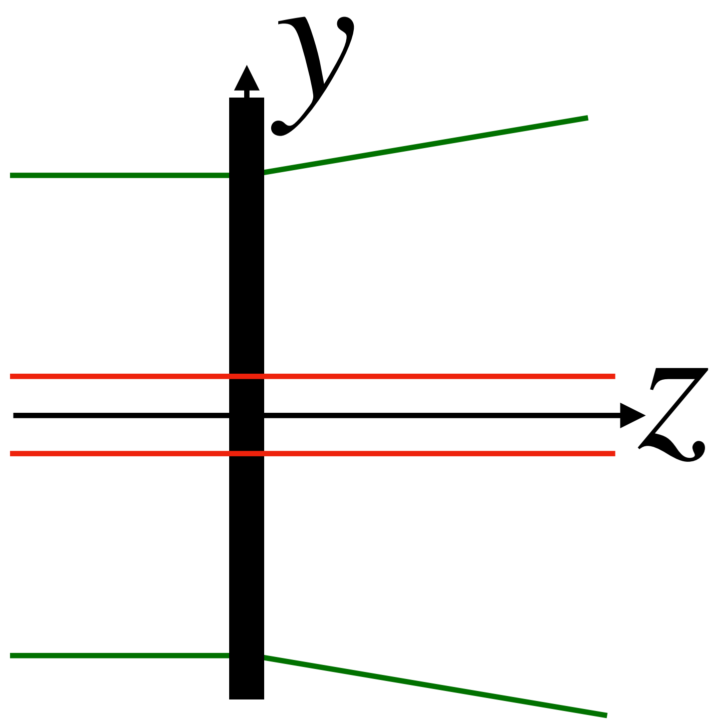

Combinaison of Φ_2, Ψ_2 (for paraxial) and Φ_4, Ψ_4 for spherical aberration correction

The quadrupoles/octopoles solution

Quadrupole-Octopole association

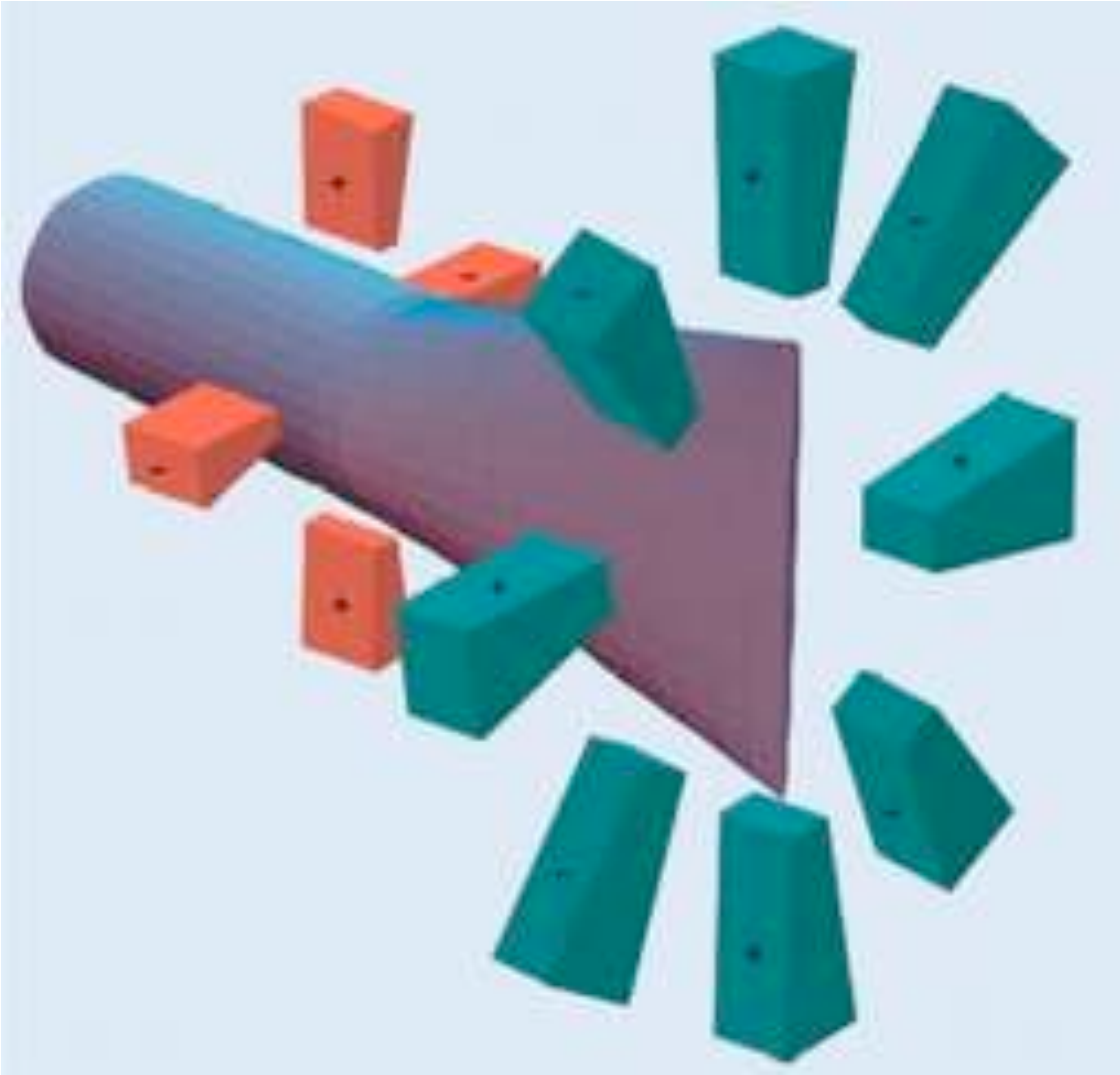

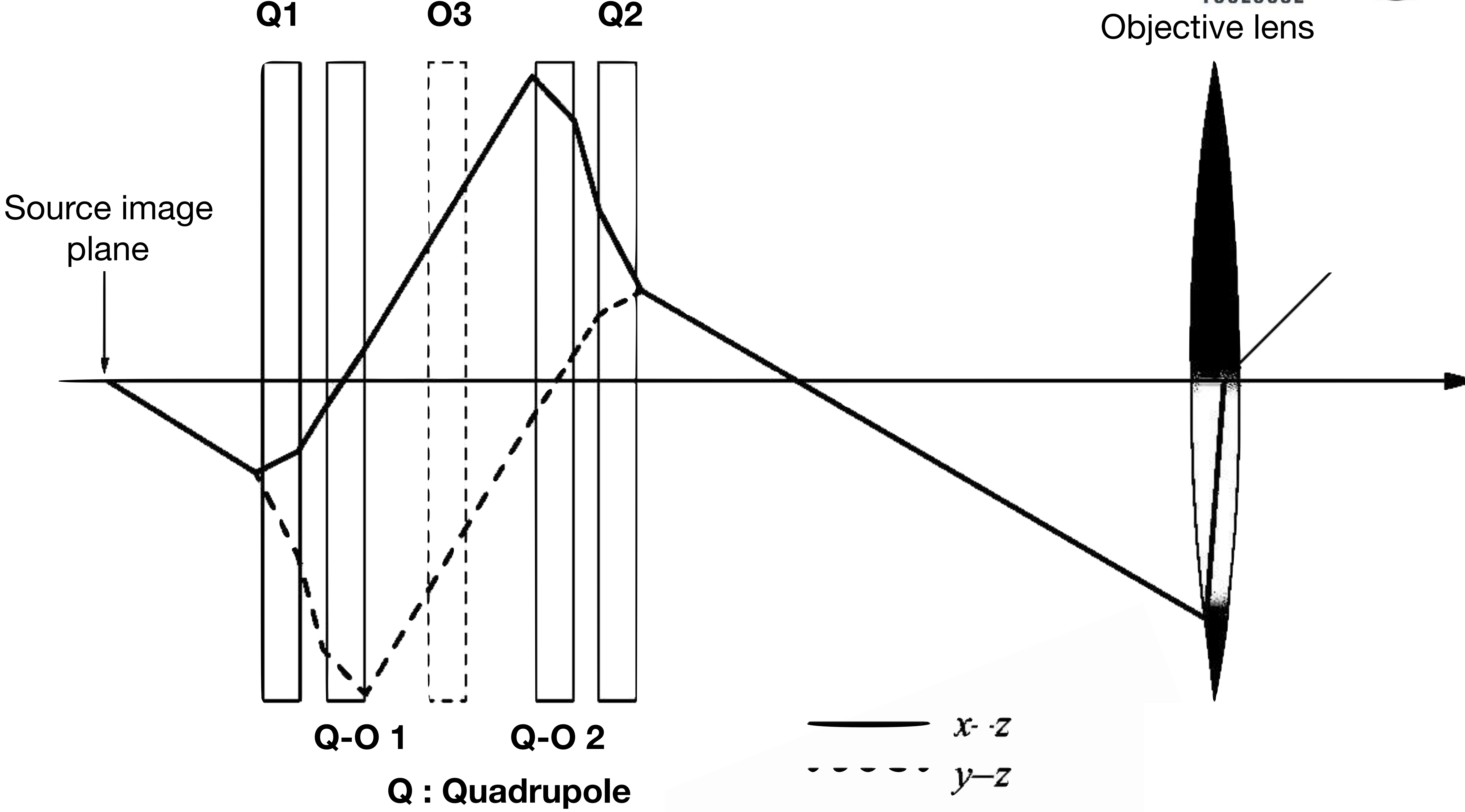

Q : Quadrupole

O : Octopole

Q-O : Superimposed quadrupole-Octopole fields

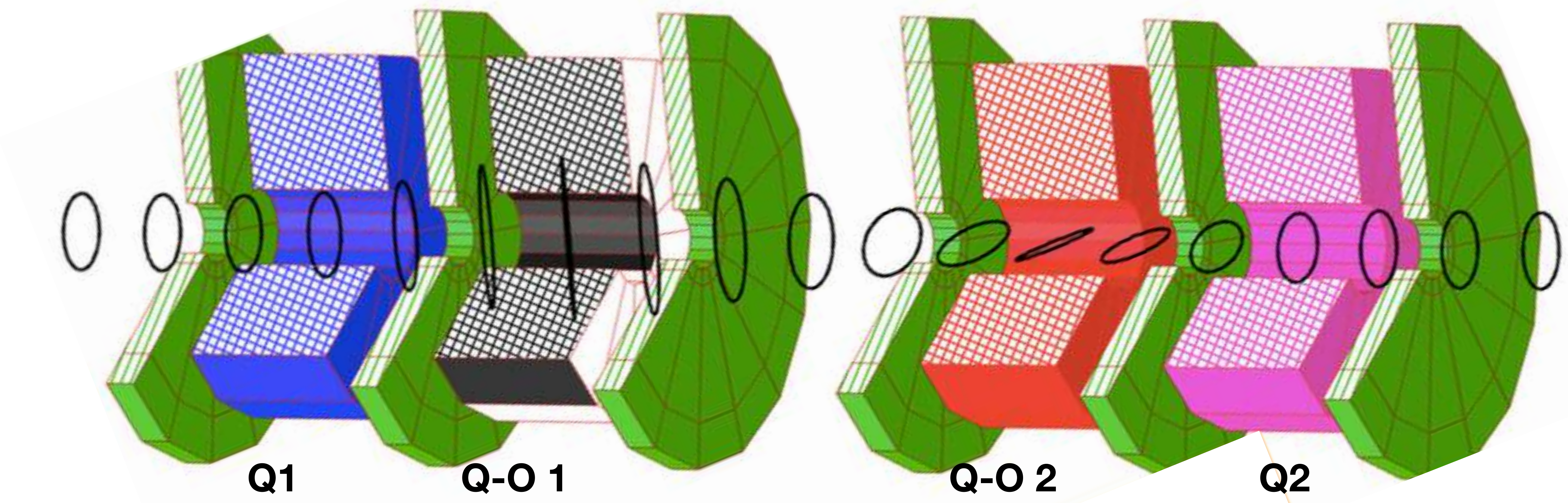

Modern Qpol/Opol corrector

Probe corrector from NION

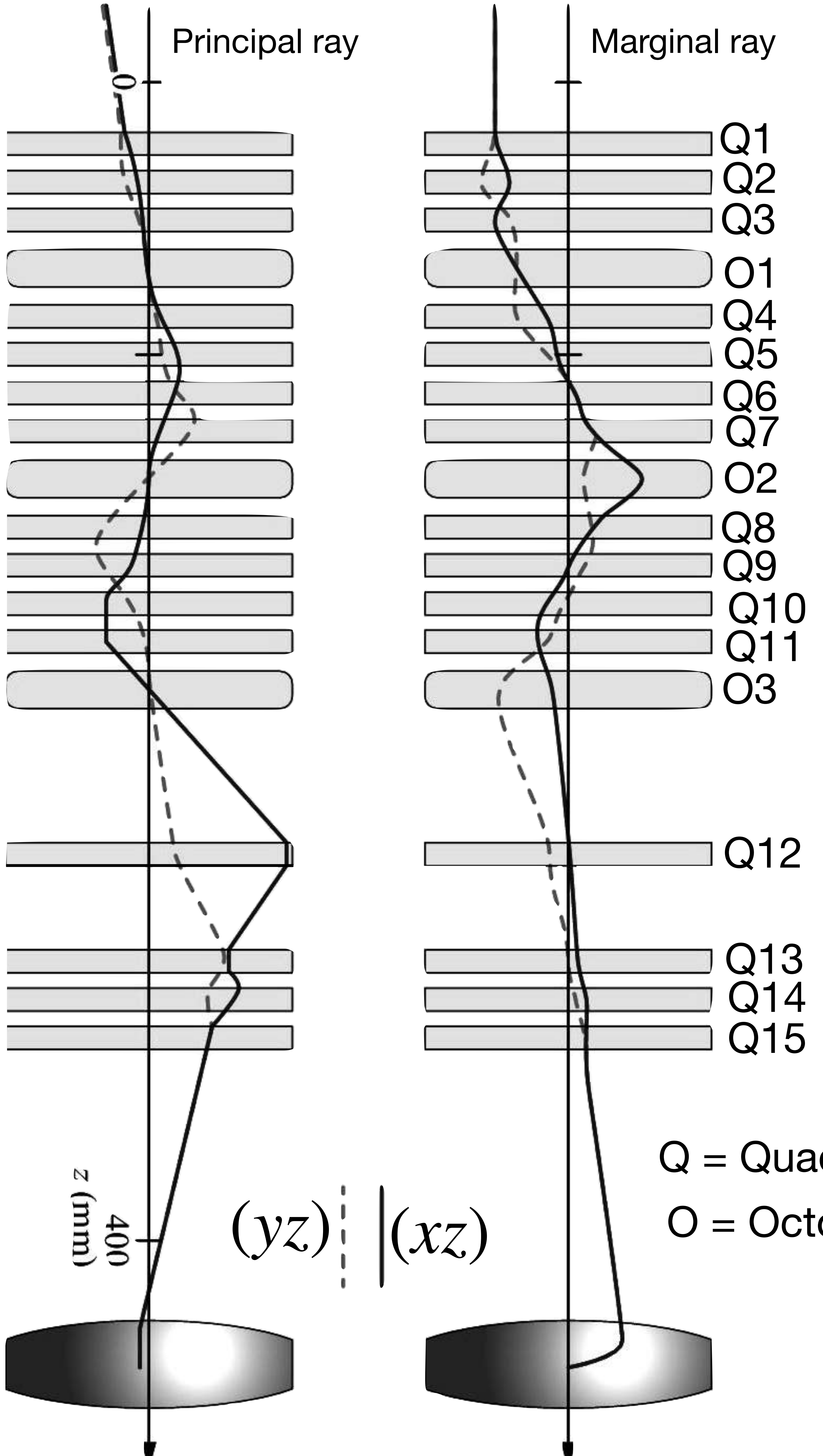

Objective lens

Q = Quadrupole

O = Octopole

STEM-HAADF corrected image

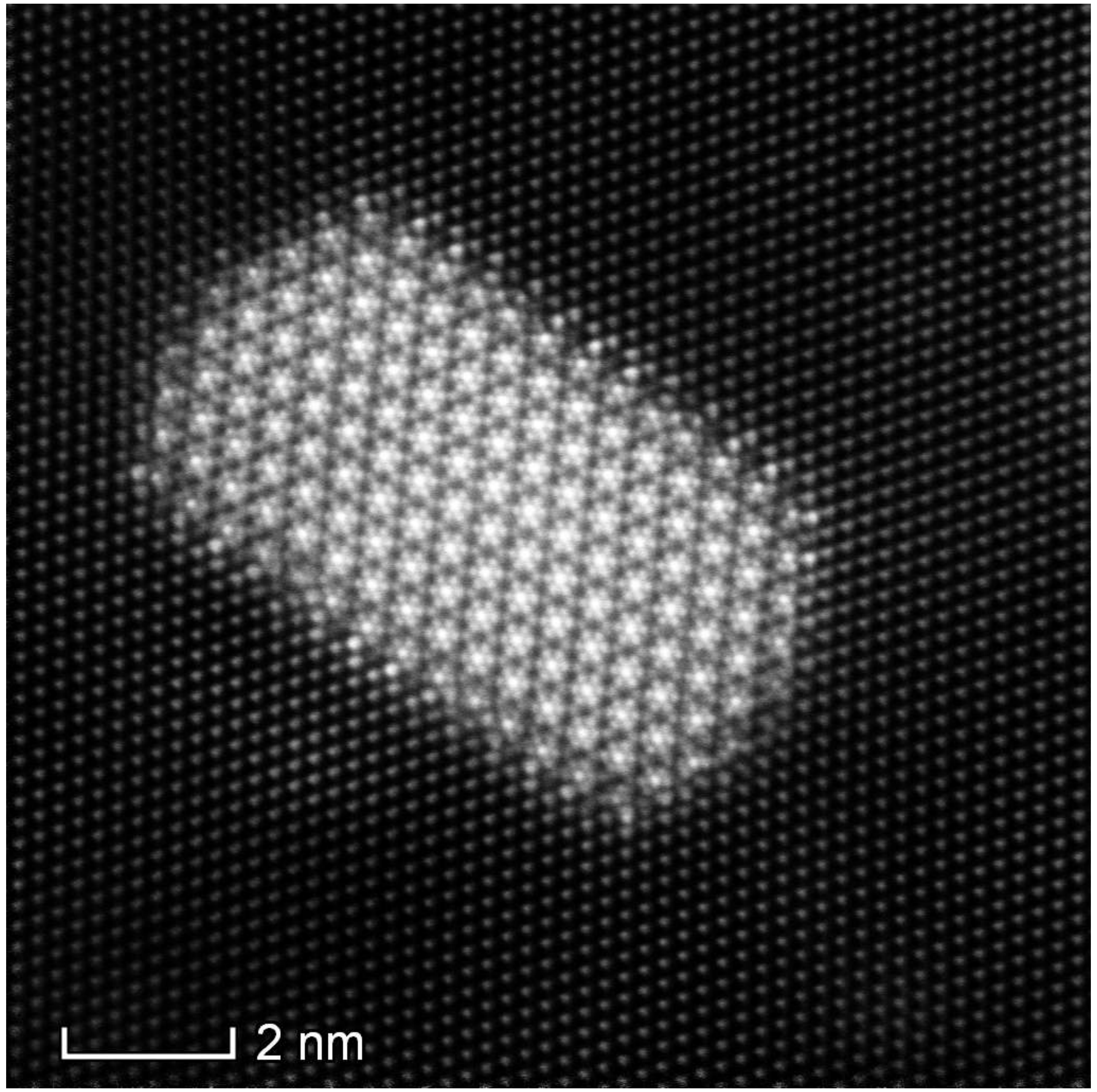

NION dedicated STEM

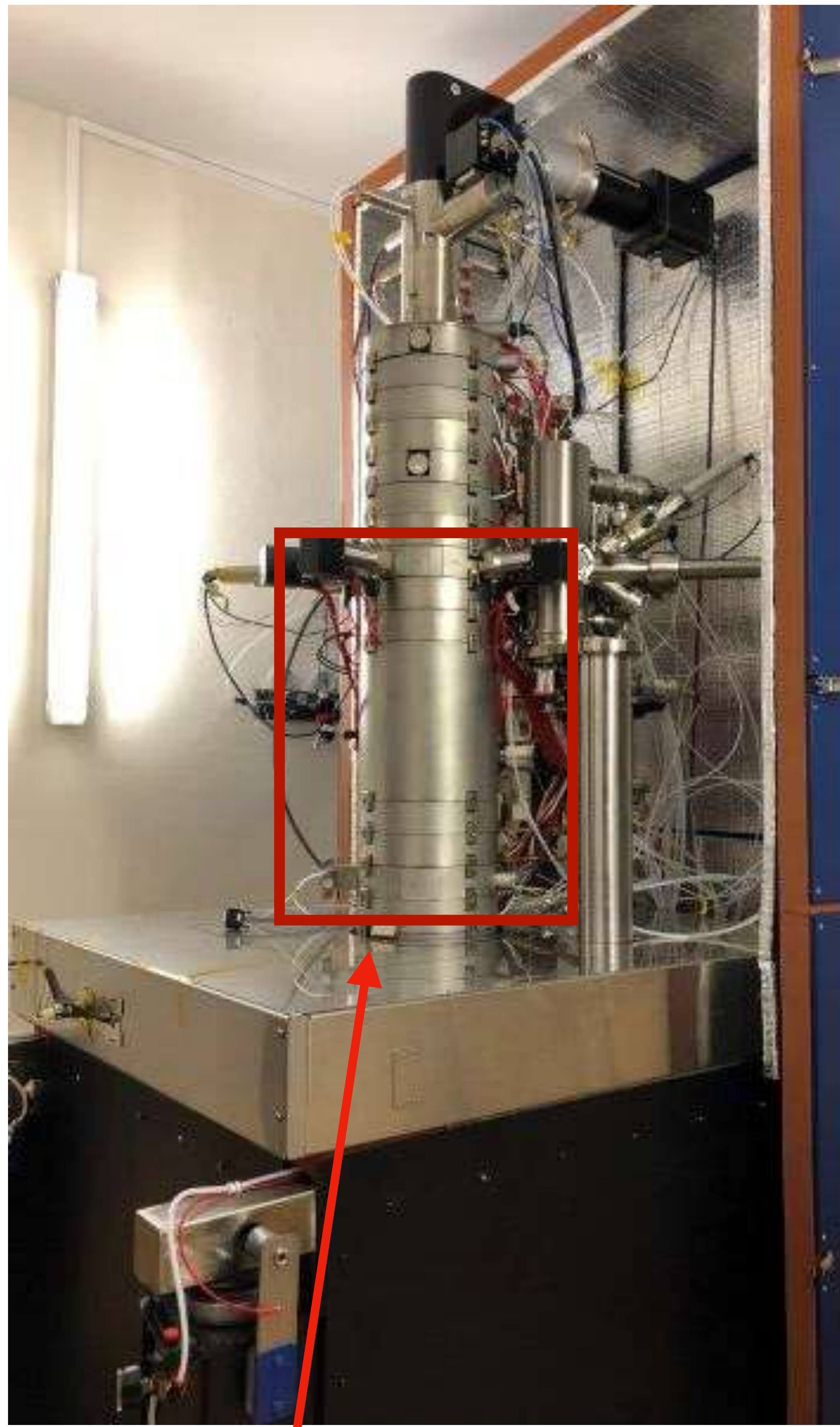

Location of the corrector

The long hexapole solution

- **Vernon D. Beck (Albert Crewe's group in Chicago)**
  « A hexapole spherical aberration corrector» (1978).

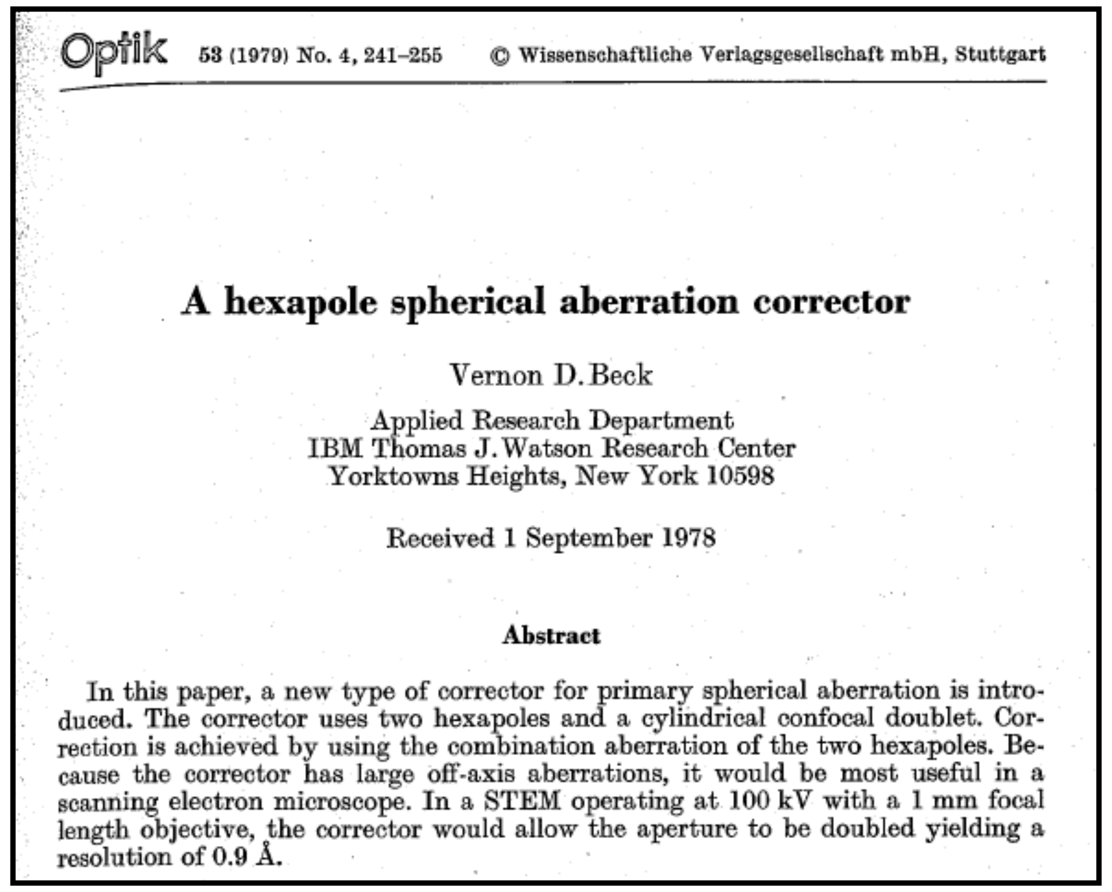

Optik 53 (1979) No. 4, 241–255 © Wissenschaftliche Verlagsgesellschaft mbH, Stuttgart

A hexapole spherical aberration corrector

Vernon D. Beck
Applied Research Department
IBM Thomas J. Watson Research Center
Yorktowns Heights, New York 10598

Received 1 September 1978

Abstract

In this paper, a new type of corrector for primary spherical aberration is introduced. The corrector uses two hexapoles and a cylindrical confocal doublet. Correction is achieved by using the combination aberration of the two hexapoles. Because the corrector has large off-axis aberrations, it would be most useful in a scanning electron microscope. In a STEM operating at 100 kV with a 1 mm focal length objective, the corrector would allow the aperture to be doubled yielding a resolution of 0.9 Å.

Hexapole action (filled circle)

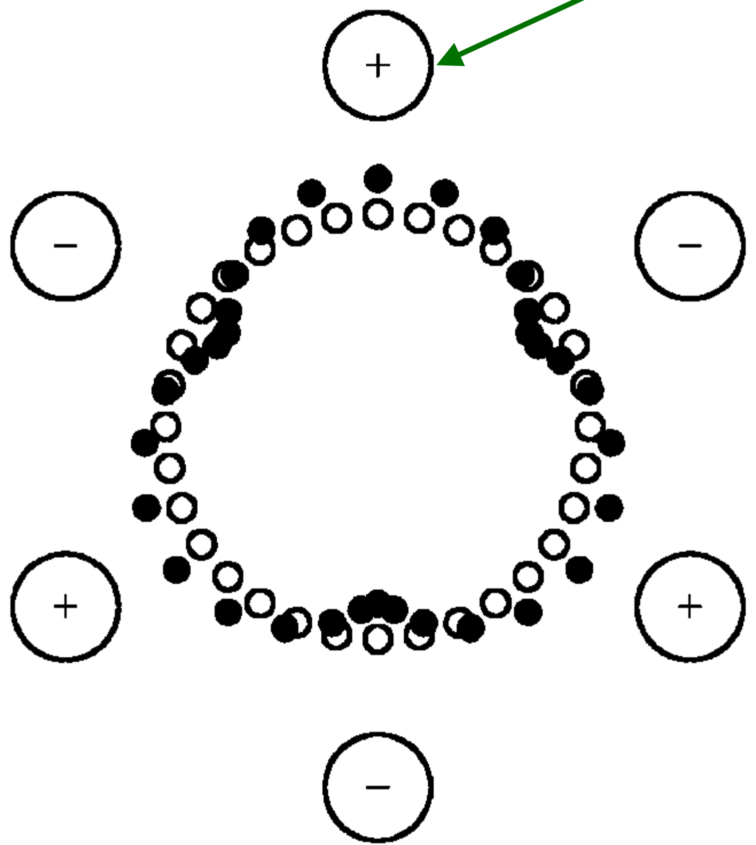

Hexapole spherical aberration

$$C_s = -6\,|\eta\Psi_3|^2 L^3 f_0^4 < 0$$

- Notation

$$\eta = \frac{\gamma_0}{\Phi_0^*}\frac{e}{2m_e}$$

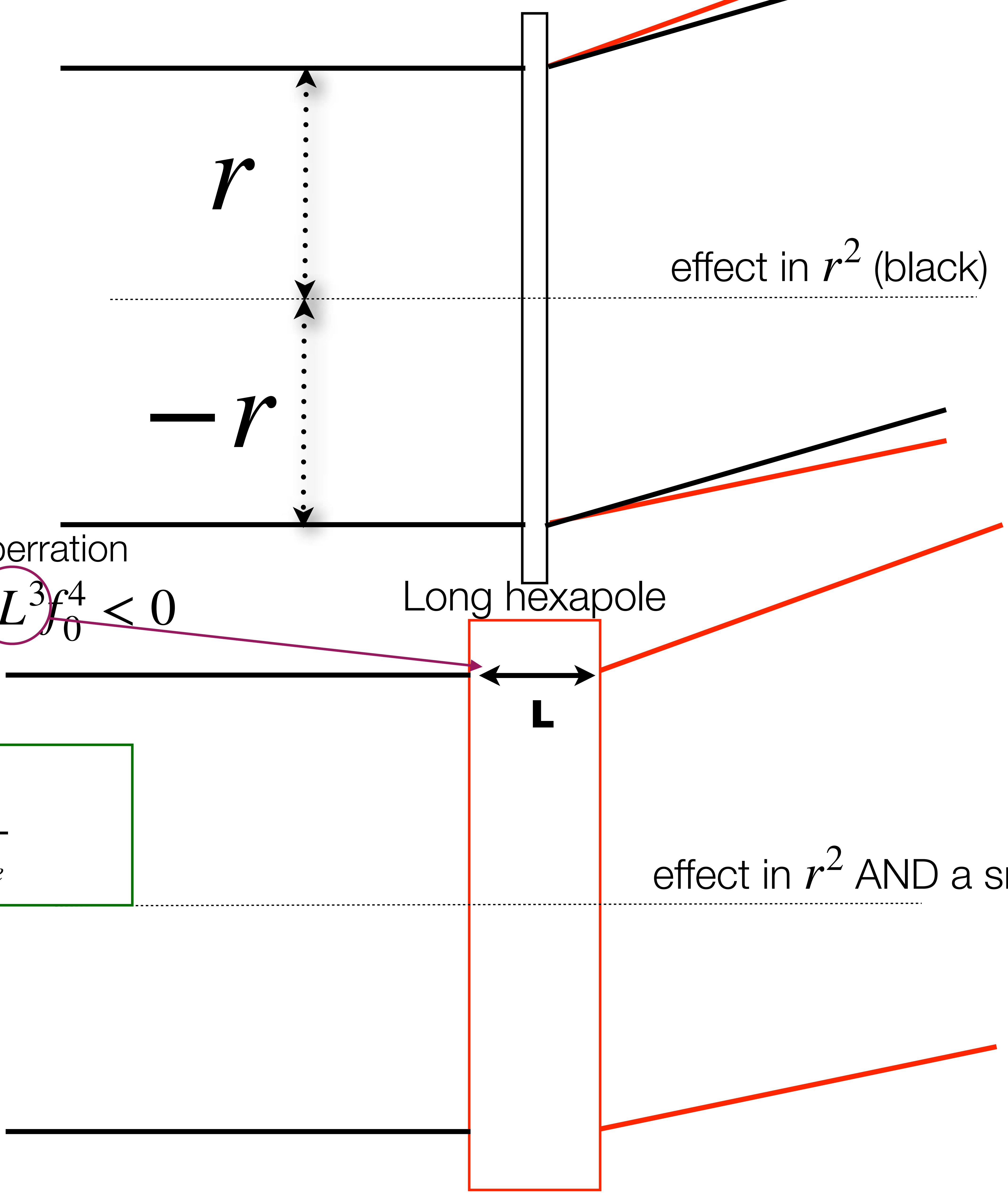

The semiaplanatic double hexapoles solution

- **Harald Rose (1935-m. ?)**
  « Outline of a spherically corrected semiaplanatic medium-voltage transmission electron microscope» (1990).

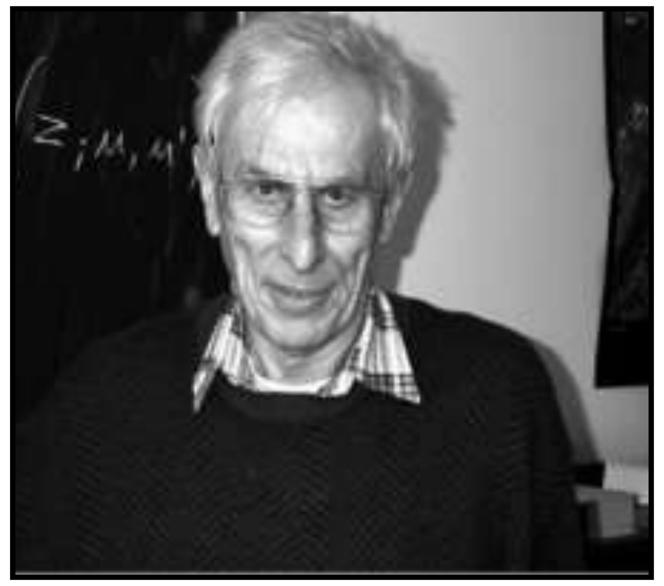

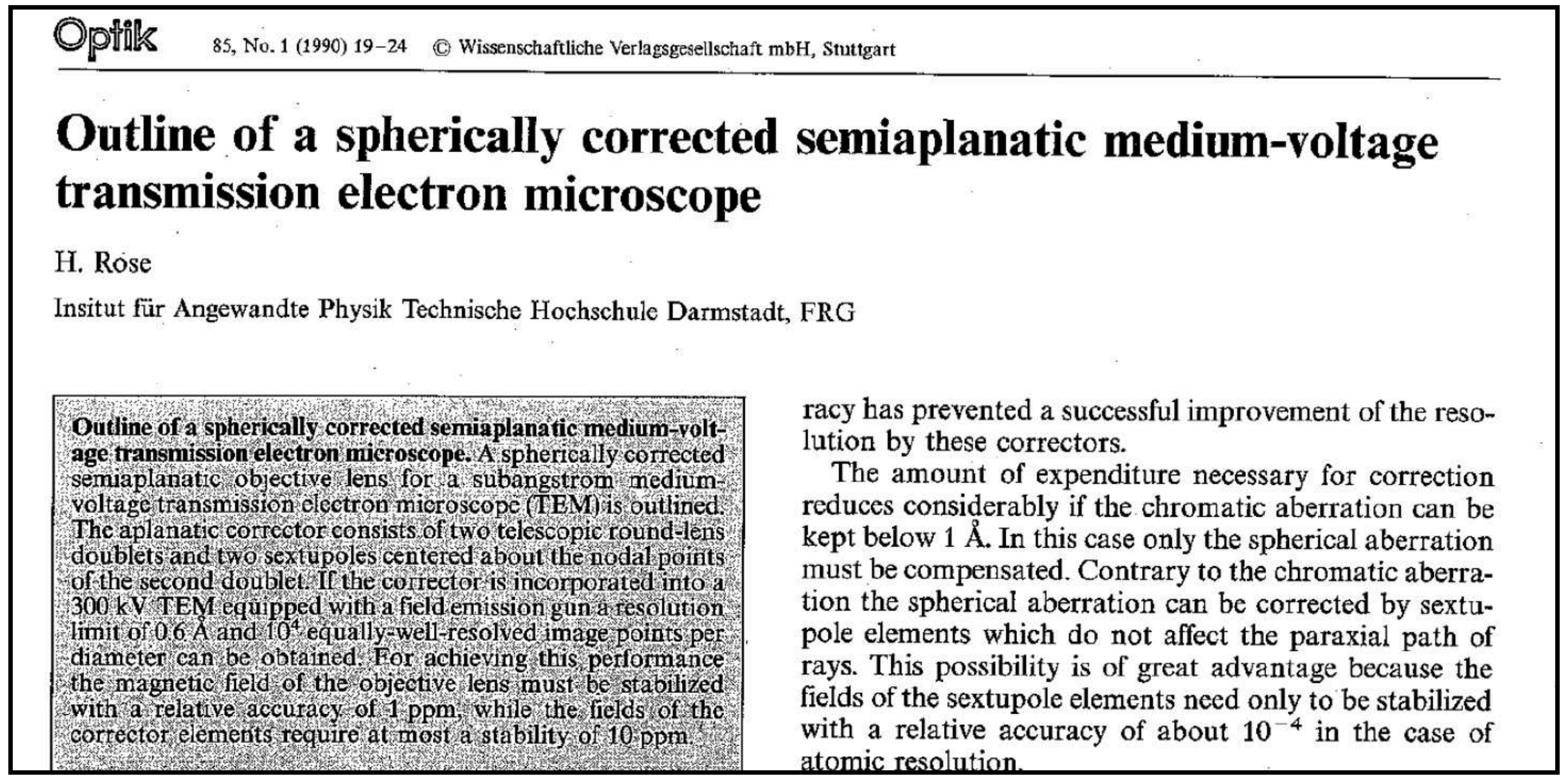

Optik 85, No. 1 (1990) 19–24 © Wissenschaftliche Verlagsgesellschaft mbH, Stuttgart

Outline of a spherically corrected semiaplanatic medium-voltage transmission electron microscope

H. Rose

Insitut für Angewandte Physik Technische Hochschule Darmstadt, FRG

Outline of a spherically corrected semiaplanatic medium-voltage transmission electron microscope. A spherically corrected semiaplanatic objective lens for a subangstrom medium-voltage transmission electron microscope (TEM) is outlined. The aplanatic corrector consists of two telescopic round-lens doublets and two sextupoles centered about the nodal points of the second doublet. If the corrector is incorporated into a 300 kV TEM equipped with a field emission gun a resolution limit of 0.6 Å and 10^4 equally-well-resolved image points per diameter can be obtained. For achieving this performance the magnetic field of the objective lens must be stabilized with a relative accuracy of 1 ppm, while the fields of the corrector elements require at most a stability of 10 ppm.

racy has prevented a successful improvement of the resolution by these correctors.

The amount of expenditure necessary for correction reduces considerably if the chromatic aberration can be kept below 1 Å. In this case only the spherical aberration must be compensated. Contrary to the chromatic aberration the spherical aberration can be corrected by sextupole elements which do not affect the paraxial path of rays. This possibility is of great advantage because the fields of the sextupole elements need only to be stabilized with a relative accuracy of about 10^{-4} in the case of atomic resolution.

Wavefront representation

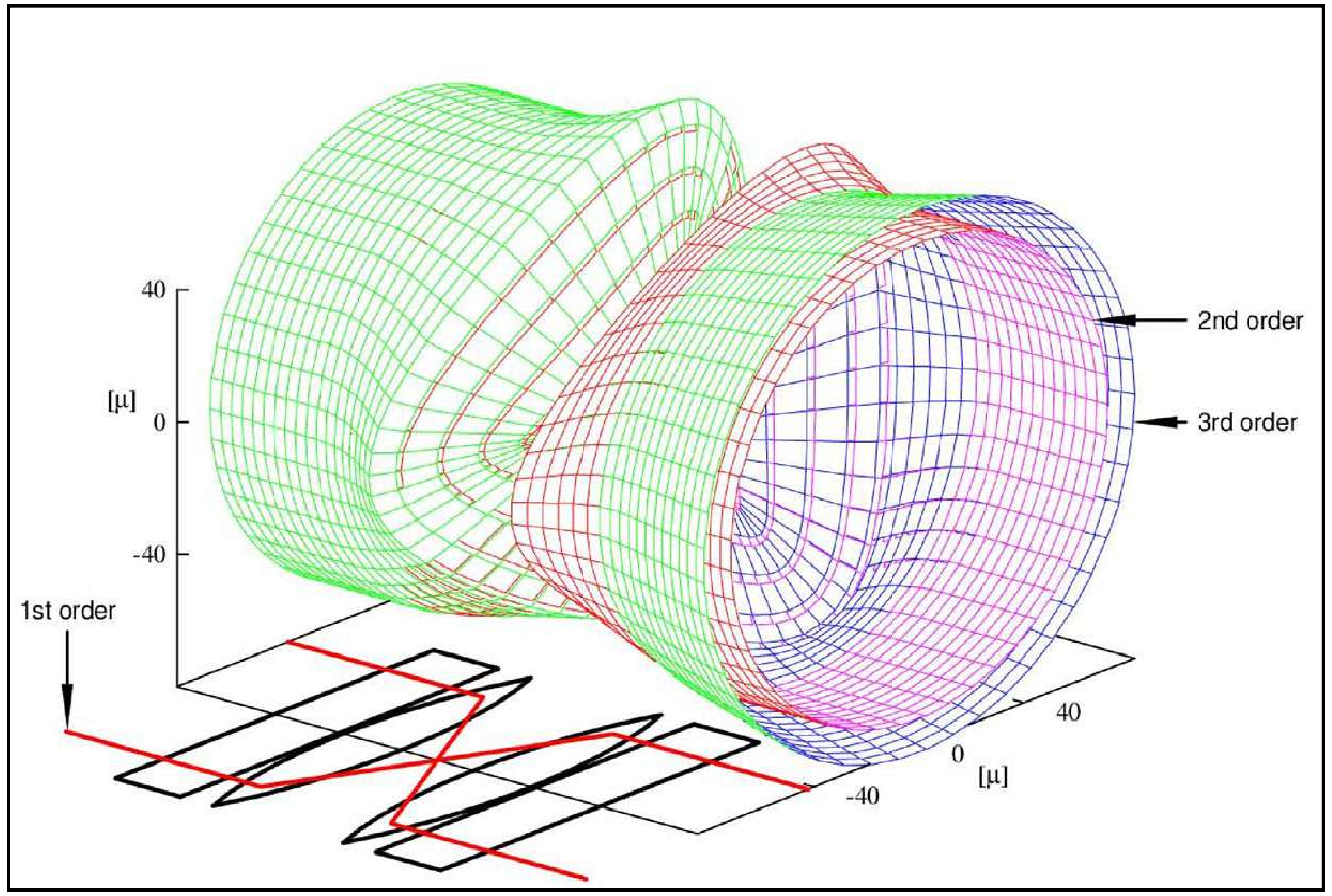

Hexapole correction

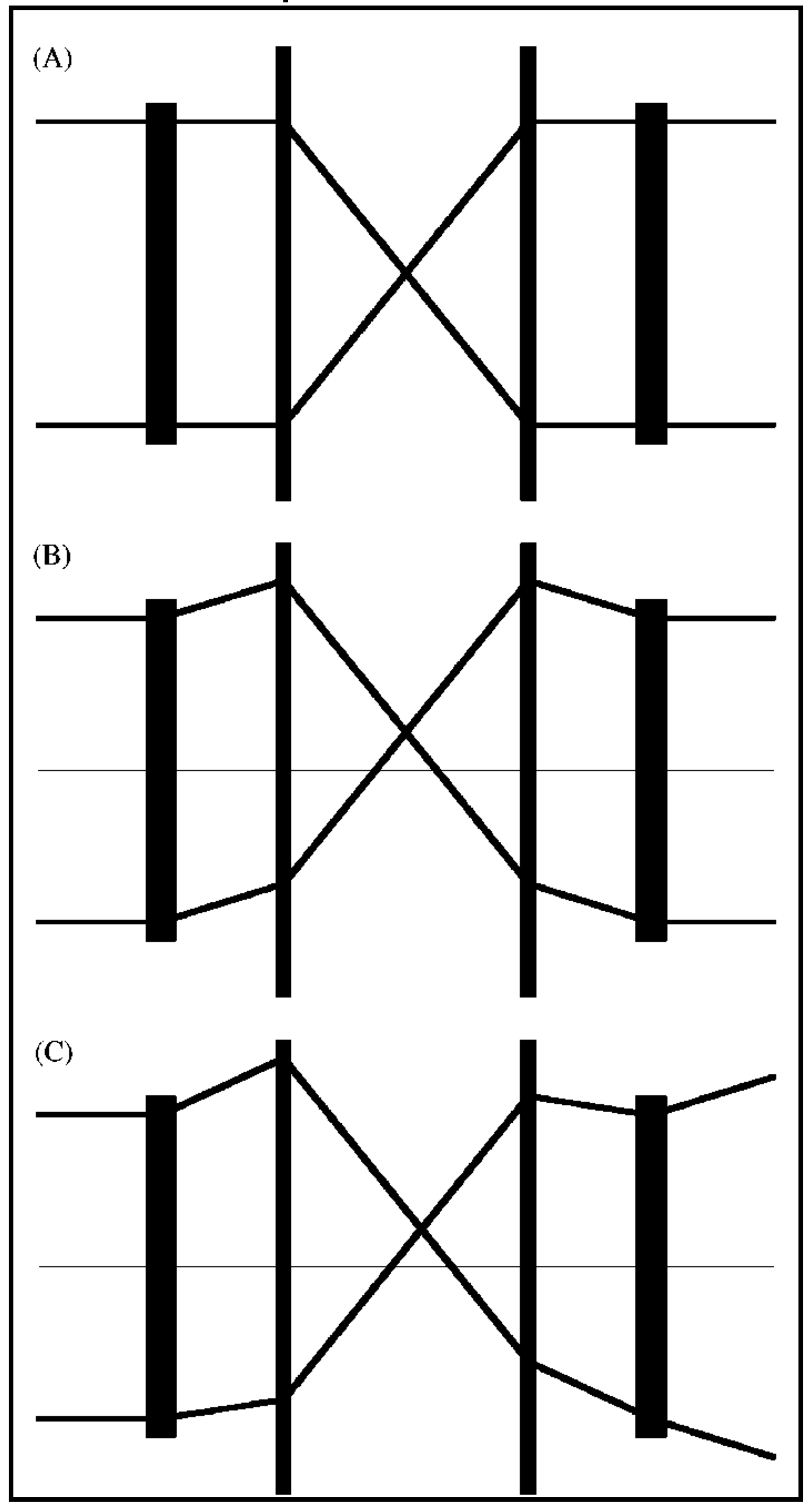

Corrector off

Short hexapoles

Long hexapoles

Adaptation to an imaging TEM objective

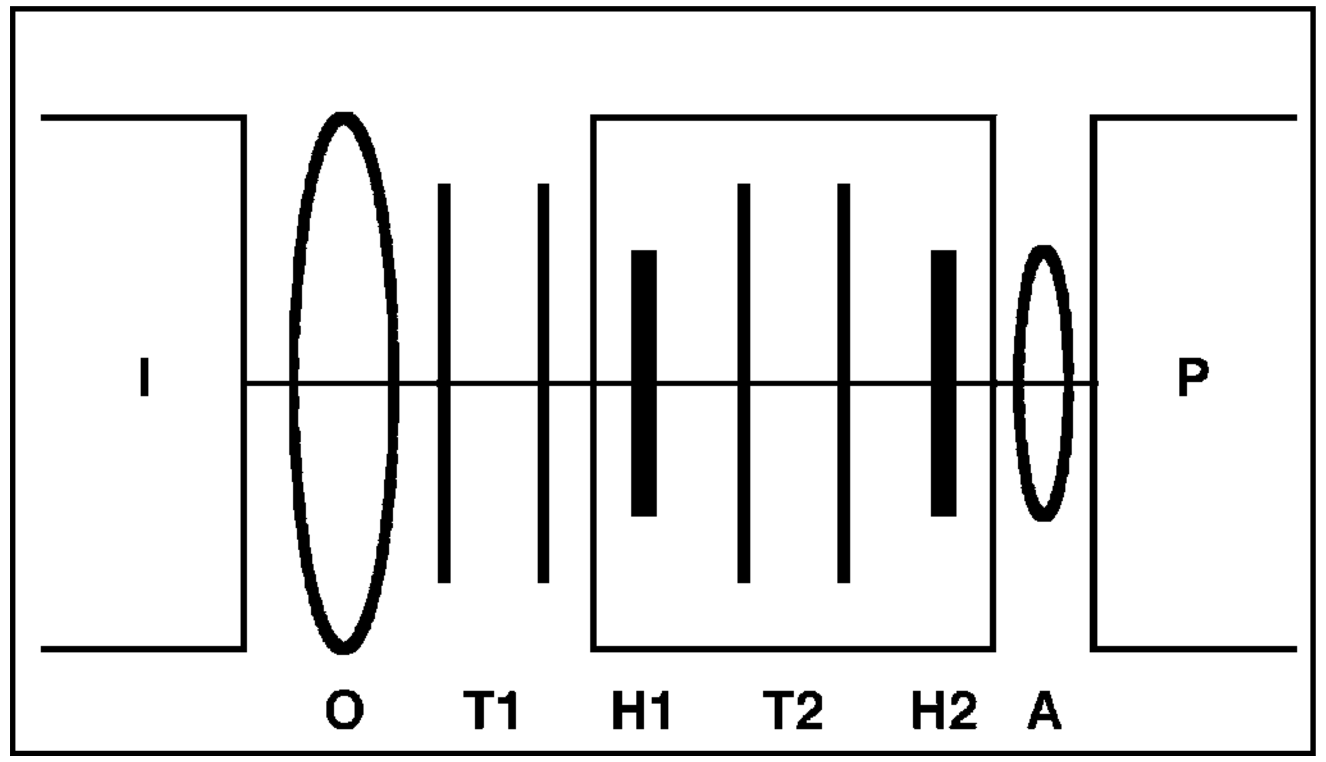

The semiaplanatic double hexapoles solution

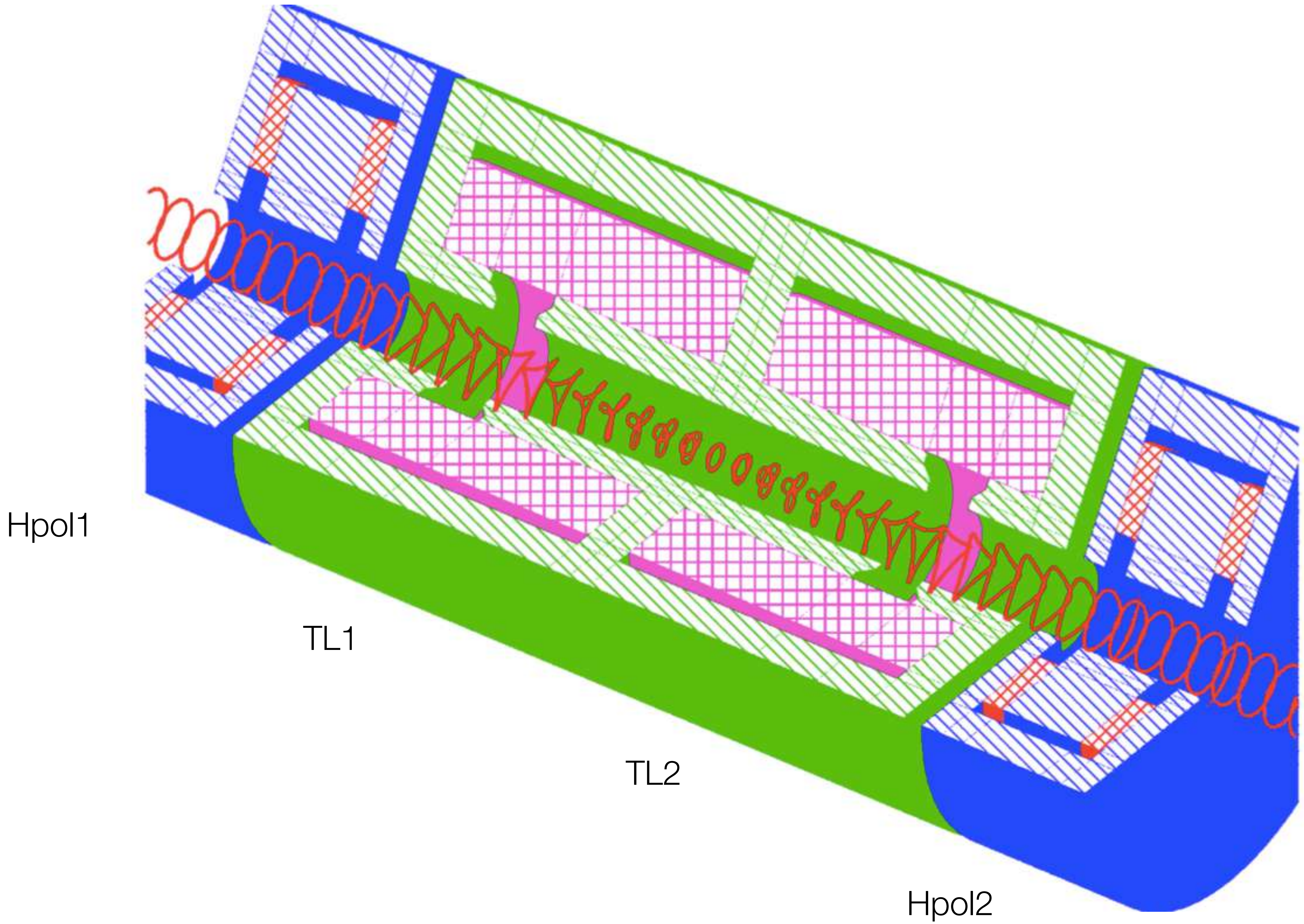

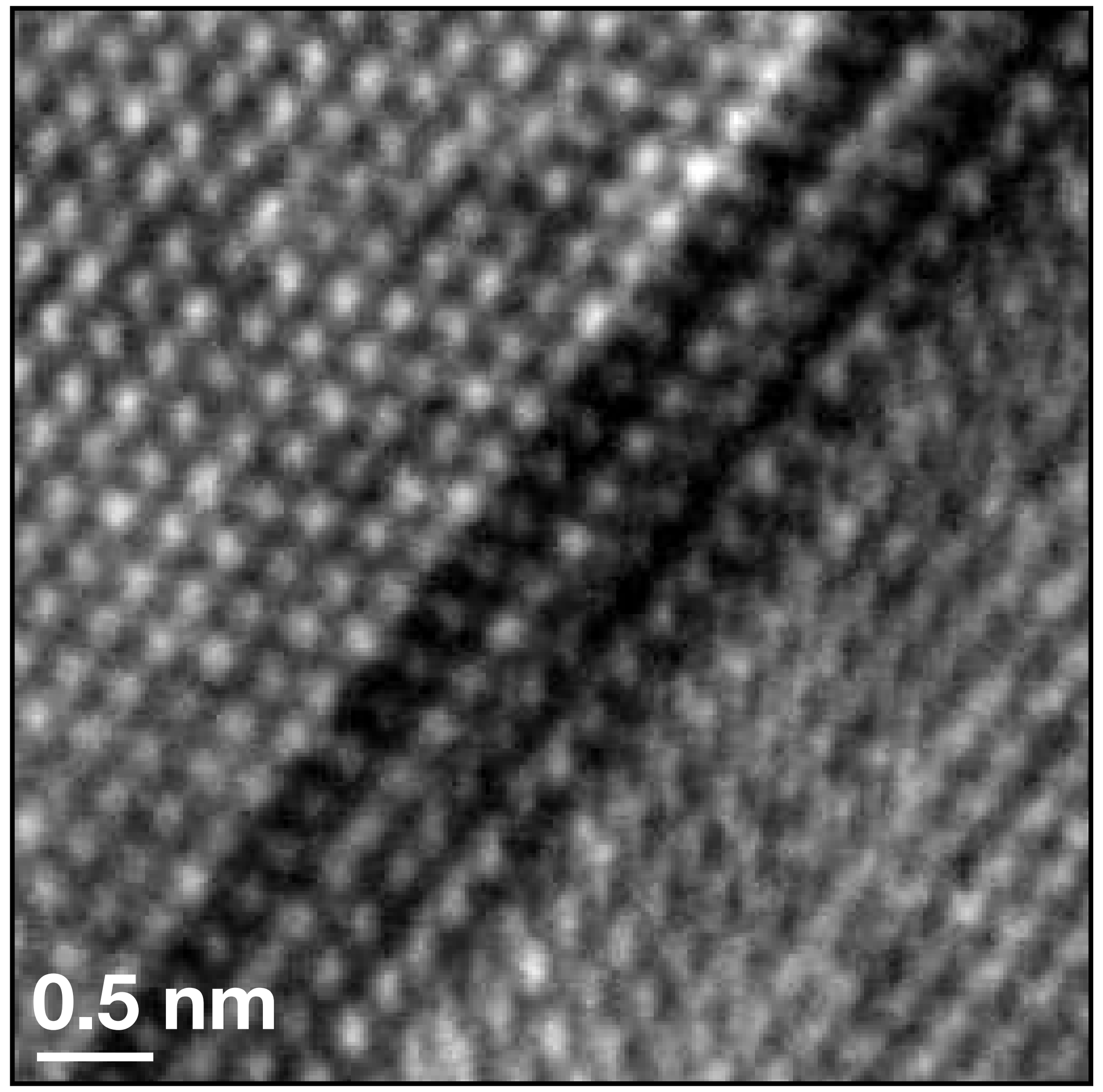

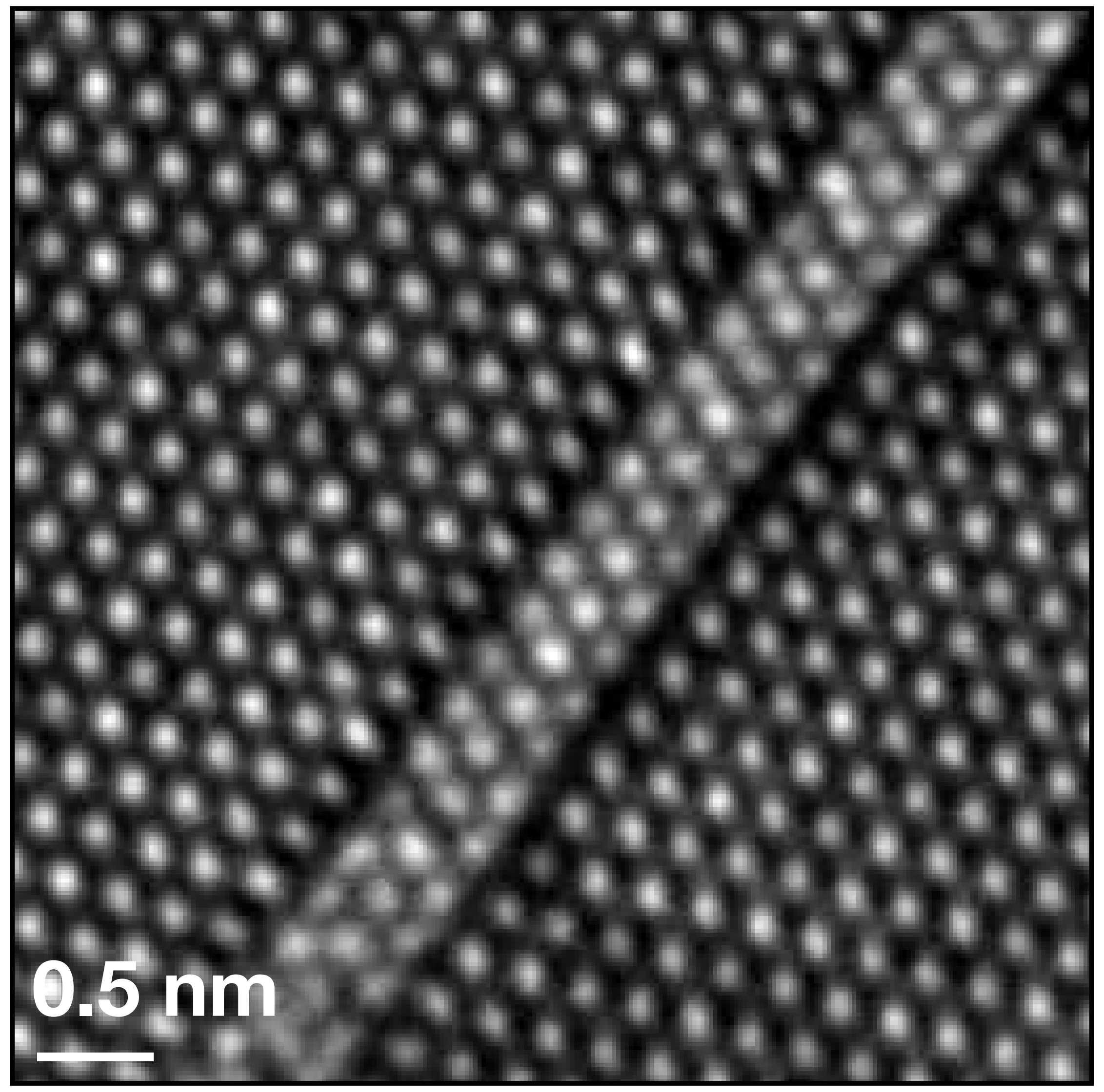

8

Introduction to symplectic relations in CPO

Canonical equations of Hamilton
Optics as a canonical transformation
Symplectic geometry and relations between coefficients due to symplecticity

INSTITUT NATIONAL DES SCIENCES APPLIQUÉES TOULOUSE

Geometrical optics as a canonical transformation

ON A GENERAL METHOD OF EXPRESSING THE PATHS OF LIGHT, AND OF THE PLANETS, BY THE COEFFICIENTS OF A CHARACTERISTIC FUNCTION

By

William Rowan Hamilton

(Dublin University Review and Quarterly Magazine, 1 (1833), pp. 795–826.)

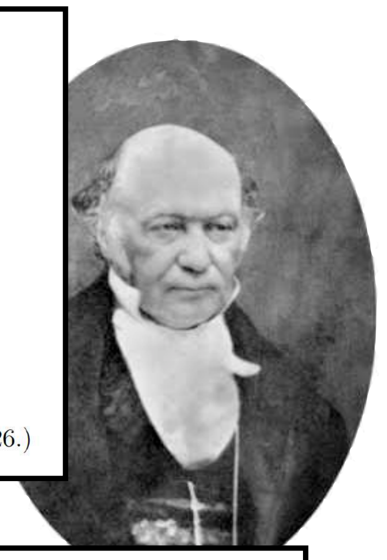

THEORY OF SYSTEMS OF RAYS

By

William Rowan Hamilton

(Transactions of the Royal Irish Academy, vol. 15 (1828), pp. 69–174.)

LAP : $\delta S = \delta \int_{t_0}^{t_1} \mathscr{L}(\vec{r}, \dot{\vec{r}}, t)dt = 0$

Canonical momentum : $\vec{p} = \dfrac{\partial \mathscr{L}}{\partial \dot{\vec{r}}}$

Hamiltonian : $H(\vec{r}, \vec{p}, t) = \vec{p}\,.\,\vec{v} - \mathscr{L}(\vec{r}, \vec{v}, t)$

The LAP can be rewritten in the Hamiltonian form :

$$\delta S = \sum_{i=1}^{n} \int_A^B \left(\delta p_i \dot{r}_i + p_i \delta \dot{r}_i - \frac{\partial H(r_i, p_i, t)}{\partial p_i}\delta p_i - \frac{\partial H(r_i, p_i, t)}{\partial r_i}\delta r_i \right) dt = 0$$

After integration by parts we find the two canonical Hamilton's equation of motion (they simply replace the Euler-Lagrange equations which are not canonical)

$$\frac{dr_i}{dt} = \frac{\partial H(r_i, p_i, t)}{\partial p_i} \;\Rightarrow\; \frac{dr_i}{dt} = \{r_i, H\}$$

$$\frac{dp_i}{dt} = -\frac{\partial H(r_i, p_i, t)}{\partial r_i} \;\Rightarrow\; \frac{dp_i}{dt} = \{p_i, H\}$$

◉ Notation

The Poisson's bracket

$$\frac{df}{dt} = \{f, H\} + \frac{\partial f}{\partial t}$$

Canonial base
In object space
(r_i, p_i)

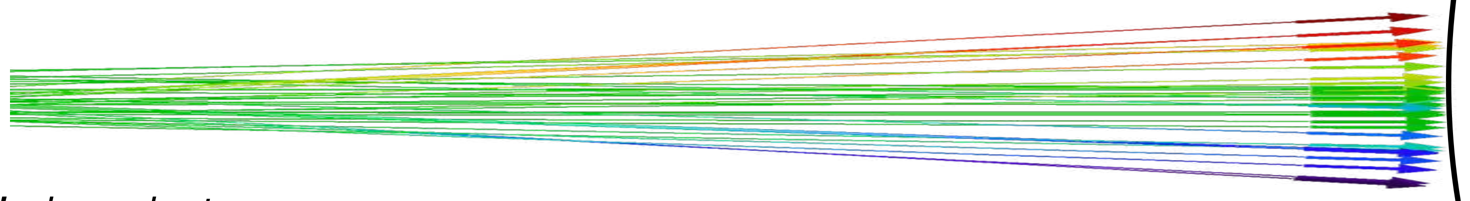

Optical system :

Canonical transformation

$(r_i, p_i) \rightarrow (R_i(r, p, t), P_i(r, p, t))$

Must conserve Poisson's brackets :

$\{f, g\}_{(r_i, p_i)} = \{f, g\}_{R_i, P_i}$

Canonial base
In image space
$(R_i(r, p, t), P_i(r, p, t))$

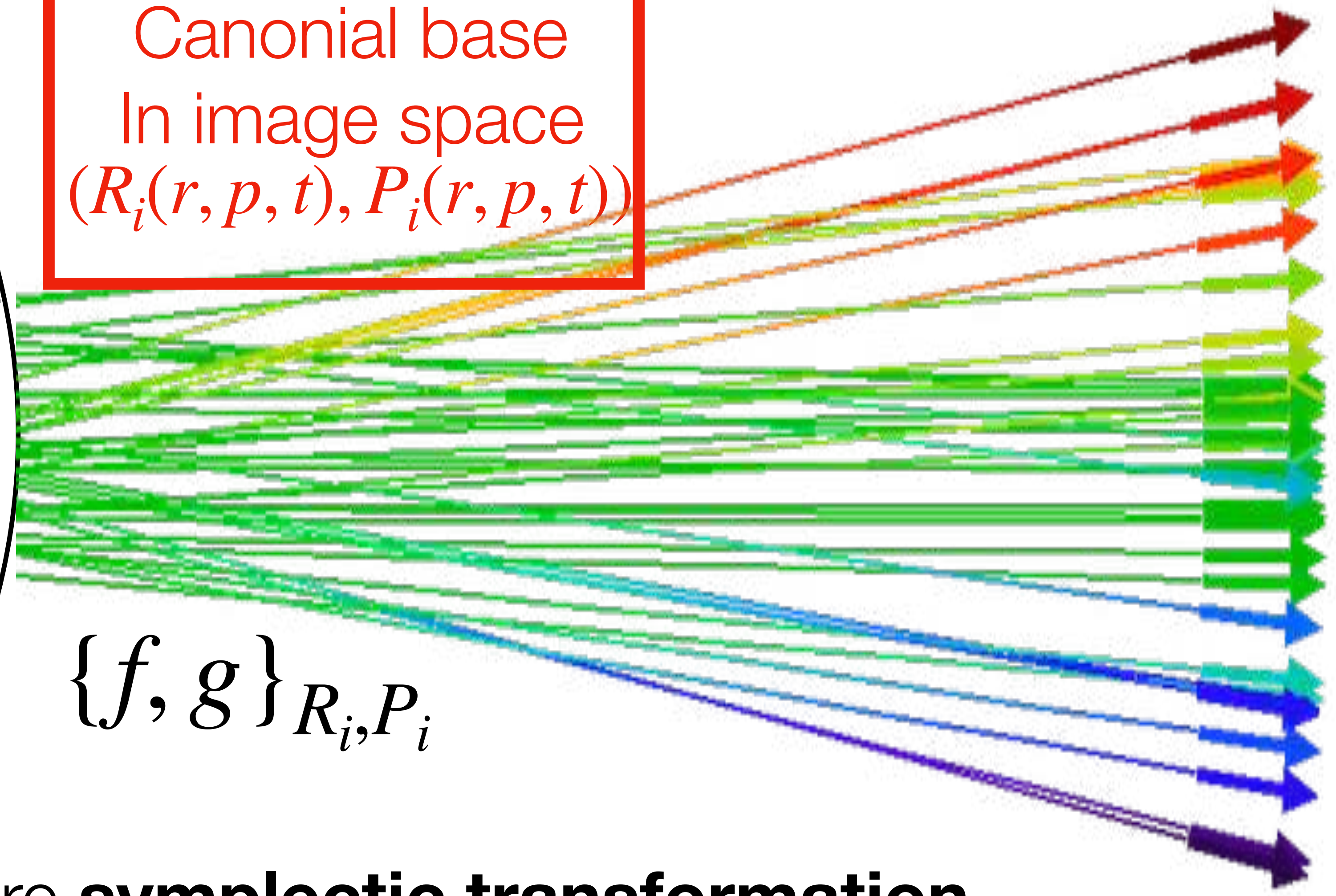

$\{f, g\}_{(r_i, p_i)}$

$\{f, g\}_{R_i, P_i}$

The Poisson's bracket rules of canonical basis

$\{r_i, p_j\} = \delta_{ij}$

$\{r_i, r_j\} = 0$

$\{p_i, p_j\} = 0$

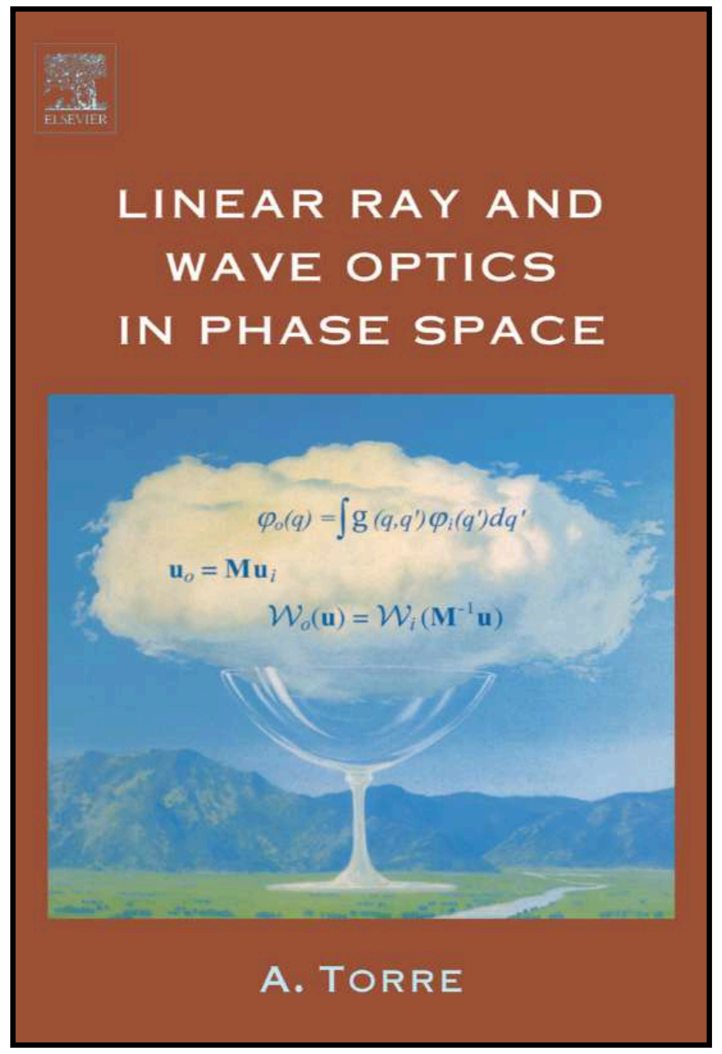

Geometric operation which conserve Poisson's bracket are **symplectic transformation**

Geometrical optics as a canonical transformation : $t \rightarrow z$

Using z as time, it's better to define the canonical transformation which transform $(x, p_x) \rightarrow (X(x, p_x, z), P_X(x, p_x, z))$ in two separate 2D planes

We define the matrix known as phase-space vector :

$$\mathbf{X}(z) = (x(z), p_x(z), y(z), p_y(z), E, t(z))$$

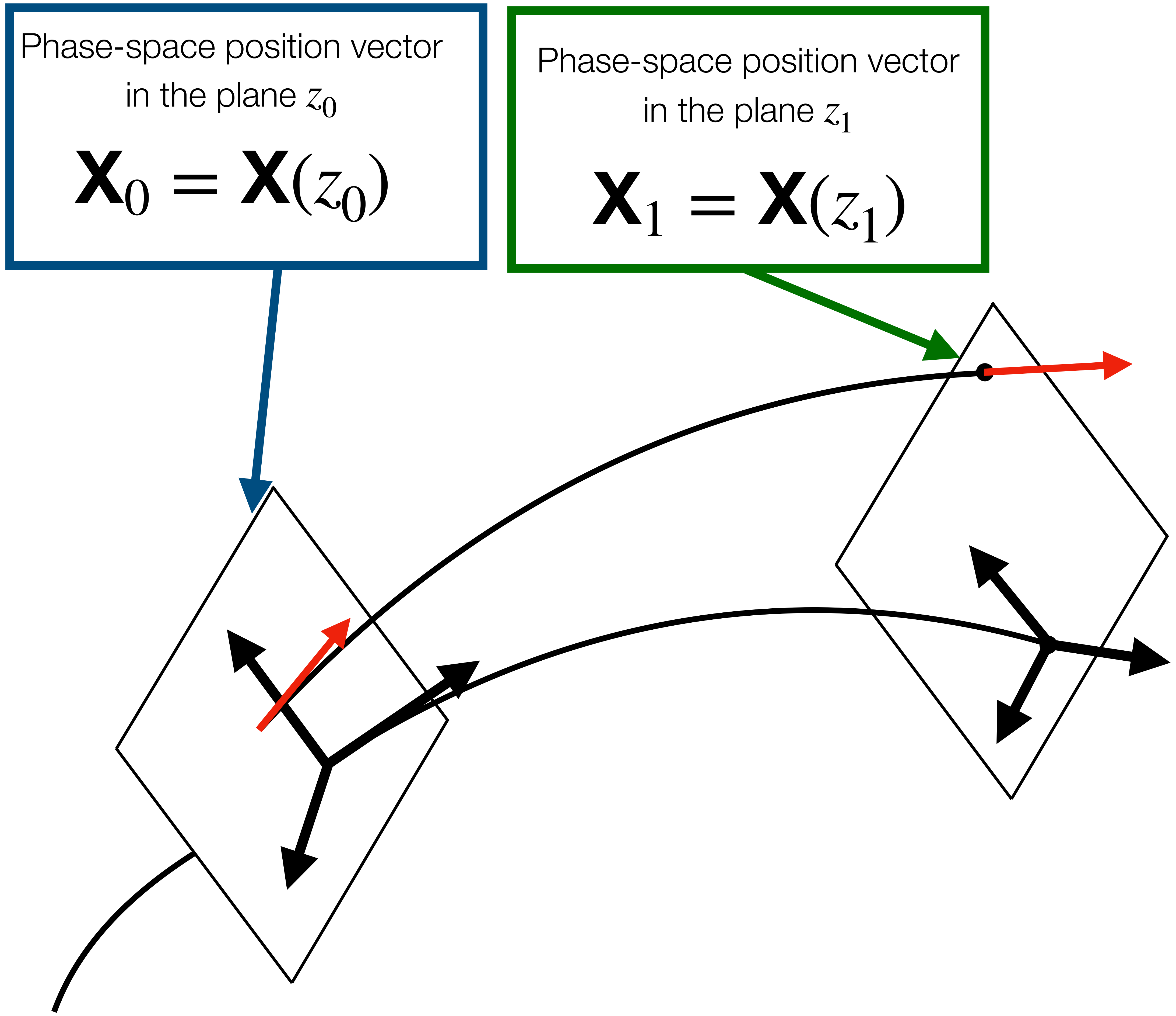

Phase-Space mapping of a beam profile : Emittance diagram

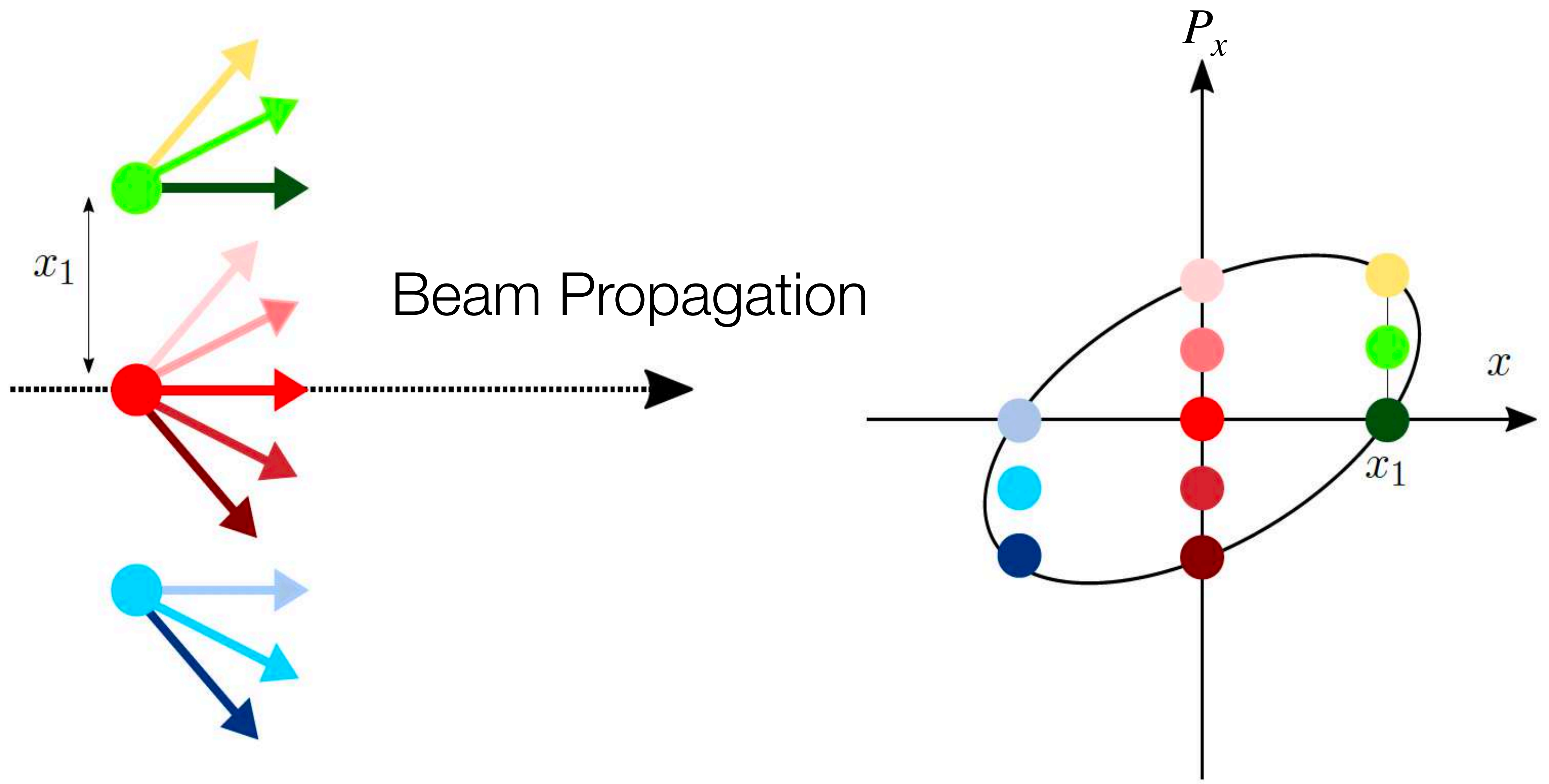

Emittance evolution in an optical system : example

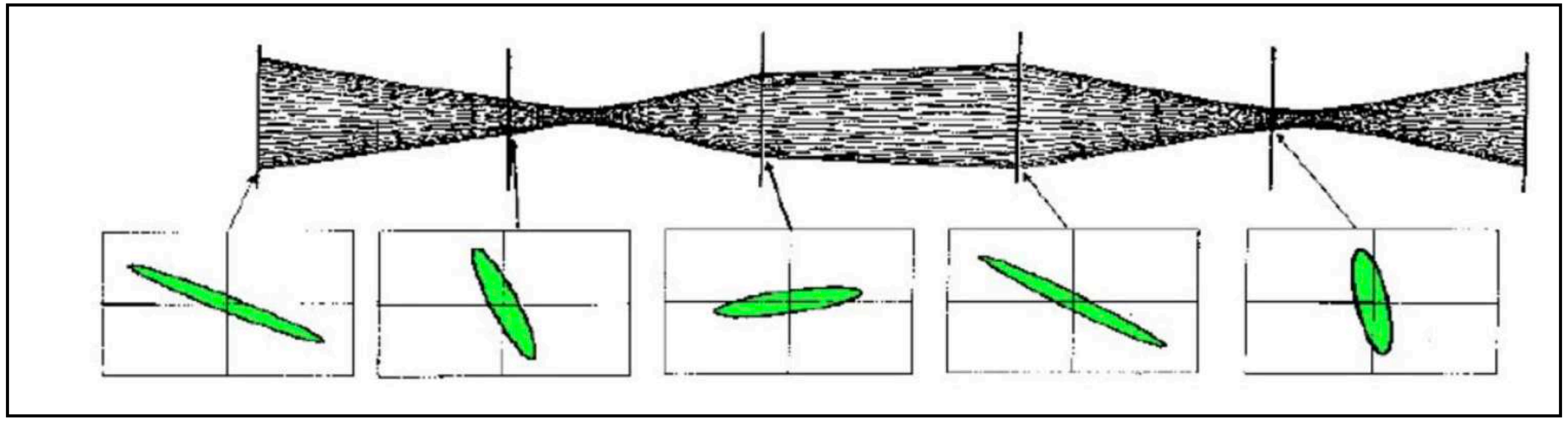

Canonical geometrical optics : the symplectic relations

Geometric operation which conserve Poisson's bracket are **symplectic transformation**

The symplectic transformation is define by the following metric relation for each phase-space vector :

$$\boxed{\tilde{J}\Gamma J = \Gamma \qquad J\Gamma\tilde{J} = \Gamma \qquad |J| = 1}$$

Aka **Symplectic relations**

Where J is the Jacobian matrix of the phase space variables
Between two phase-space « time » z_0 and z_1 (object and image)

◉ Notation

$$J = \begin{pmatrix} \partial x_1/\partial x_0 & \partial x_1/\partial p_{x0} & \partial x_1/\partial y_0 & \partial x_1/\partial p_{y0} & \partial x_1/\partial K_0 & 0 \\ \partial p_{x1}/\partial x_0 & \partial p_{x1}/\partial p_{x0} & \partial p_{x1}/\partial y_0 & \partial p_{x1}/\partial p_{y0} & \partial p_{x1}/\partial K_0 & 0 \\ \partial y_1/\partial x_0 & \partial y_1/\partial p_{x0} & \partial y_1/\partial y_0 & \partial y_1/\partial p_{y0} & \partial y_1/\partial K_0 & 0 \\ \partial p_{y1}/\partial x_0 & \partial p_{y1}/\partial p_{x0} & \partial p_{y1}/\partial y_0 & \partial p_{y1}/\partial p_{y0} & \partial p_{y1}/\partial K_0 & 0 \\ 0 & 0 & 0 & 0 & 1 & 0 \\ \partial t_1/\partial x_0 & \partial t_1/\partial p_{x0} & \partial t_1/\partial y_0 & \partial t_1/\partial p_{y0} & \partial t_1/\partial K_0 & 1 \end{pmatrix}$$

$$\Gamma = \begin{pmatrix} 0 & 1 & 0 & 0 & 0 & 0 \\ -1 & 0 & 0 & 0 & 0 & 0 \\ 0 & 0 & 0 & 1 & 0 & 0 \\ 0 & 0 & -1 & 0 & 0 & 0 \\ 0 & 0 & 0 & 0 & 0 & 1 \\ 0 & 0 & 0 & 0 & -1 & 0 \end{pmatrix}$$

This gives us the symplectic relationships ("intertwining") between the paraxial and aberrations coefficients

Example of the simplest symplectic relation :
linear magnification versus angular magnification
known as Helmholtz-Lagrange relation

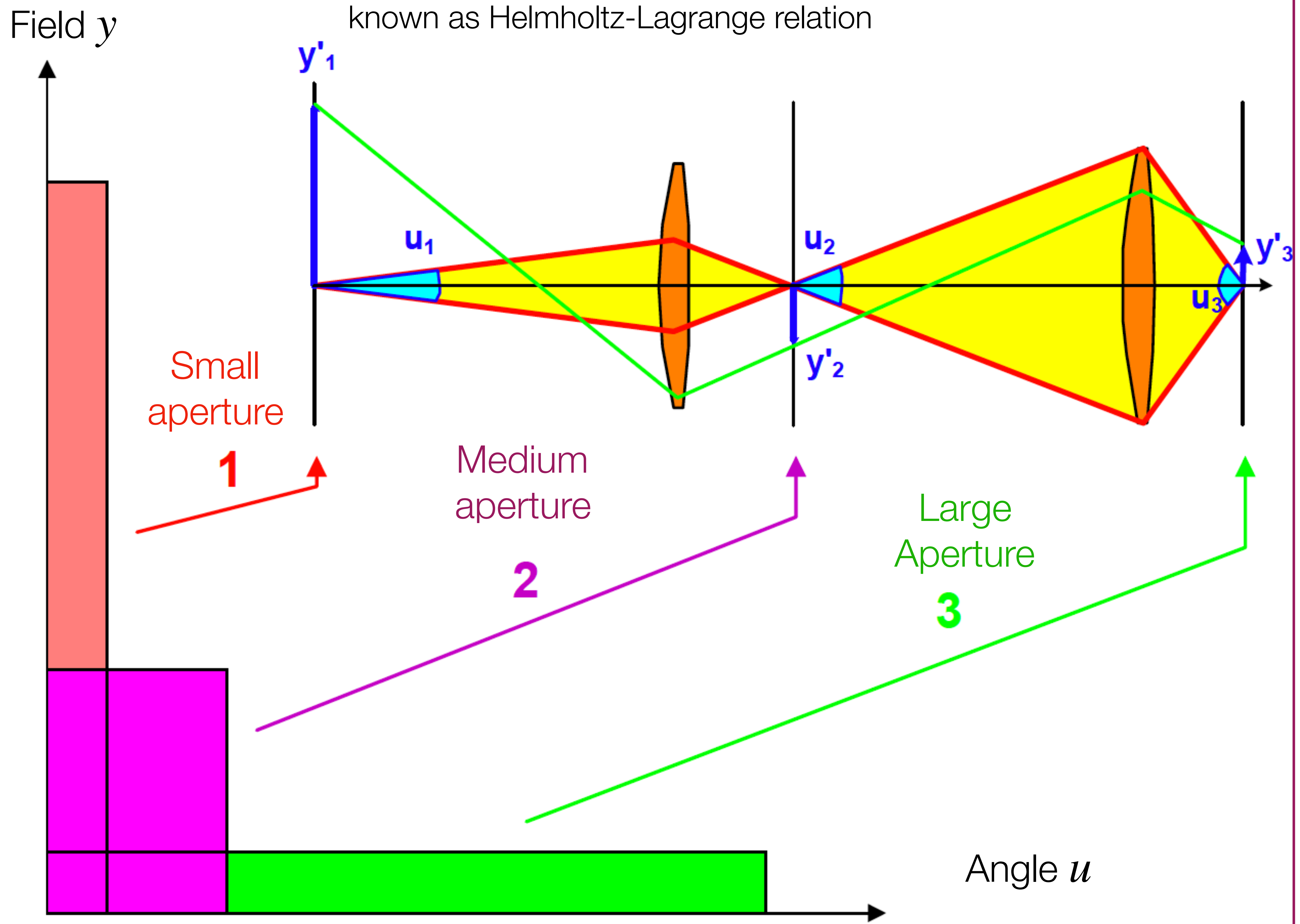

Symplectic relations taking care of non linear coefficients

Nuclear Instruments and Methods in Physics Research A238 (1985) 127–140
North-Holland, Amsterdam

RELATIONS BETWEEN ELEMENTS OF TRANSFER MATRICES DUE TO THE CONDITION OF SYMPLECTICITY

H. WOLLNIK and M. BERZ
II. Physikalisches Institut der Universität Giessen, D-6300 Giessen, Fed. Rep. Germany

Received 30 January 1985

More than 100 relations up to third order coefficients …

SYMMETRY-BASED DESIGN OF FRAGMENT SEPARATOR … Phys. Rev. ST Accel. Beams **10**, 064002 (2007)

$$-2(a|x\delta)(x|xa)+2(a|xa)(x|x\delta)+(a|xa\delta)(x|x)-(a|x)(x|xa\delta)-(a|xx\delta)(x|a)+(a|a)(x|xx\delta)=0$$

$$-2(a|x\delta)(x|aa)+2(a|aa)(x|x\delta)+(a|aa\delta)(x|x)-(a|x)(x|aa\delta)-(a|xa\delta)(x|a)+(a|a)(x|xa\delta)=0$$

$$2(a|a\delta)(x|x\delta)-2(a|x\delta)(x|a\delta)+(a|a\delta\delta)(x|x)-(a|x)(x|\delta\delta a)-(a|x\delta\delta)(x|a)+(a|a)(x|x\delta\delta)=0$$

$$2(b|ay)(y|xy)-2(b|xy)(y|ay)+(a|ayy)(x|x)-(a|x)(x|ayy)-(a|xyy)(x|a)+(a|a)(x|xyy)=0$$

$$-2(b|xy)(y|ab)+2(b|ab)(y|xy)+(a|ayb)(x|x)-(a|x)(x|ayb)-(a|xyb)(x|a)+(a|a)(x|xyb)=0$$

$$2(b|ay)(y|xb)-2(b|xb)(y|ay)-(a|x)(x|ayb)+(a|ayb)(x|x)-(a|xyb)(x|a)+(a|a)(x|xyb)=0$$

$$-2(b|xb)(y|ab)+2(b|ab)(y|xb)-(a|x)(x|abb)+(a|abb)(x|x)-(a|xbb)(x|a)+(a|a)(x|xbb)=0$$

$$-2(b|xy)(y|ay)+2(b|ay)(y|xy)-(b|y)(y|xay)+(b|xay)(y|y)-(a|xyy)(x|a)+(a|a)(x|xyy)=0$$

$$-2(b|xy)(y|ab)+2(b|ab)(y|xy)-(b|y)(y|xab)+(b|xab)(y|y)-(a|xyb)(x|a)+(a|a)(x|xyb)=0$$

$$-(b|y)(y|aay)+(b|aay)(y|y)-(a|ayy)(x|a)+(a|a)(x|ayy)=0$$

$$-2(b|ay)(y|ab)+2(b|ab)(y|ay)-(b|y)(y|aab)+(b|aab)(y|y)-(a|ayb)(x|a)+(a|a)(x|ayb)=0$$

$$-2(b|y\delta)(y|ay)+2(b|ay)(y|y\delta)+(b|ay\delta)(y|y)-(b|y)(y|ay\delta)-(a|yy\delta)(x|a)+(a|a)(x|yy\delta)=0$$

$$-2(b|y\delta)(y|ab)+2(b|ab)(y|y\delta)+(b|ab\delta)(y|y)-(b|y)(y|ab\delta)-(a|yb\delta)(x|a)+(a|a)(x|yb\delta)=0$$

$$-2(a|yy)(x|xa)+2(a|xa)(x|yy)+(b|xay)(y|y)-(b|y)(y|xay)-(a|xyy)(x|a)+(a|a)(x|xyy)=0$$

$$-2(a|yy)(x|aa)+2(a|aa)(x|yy)+(b|aay)(y|y)-(b|y)(y|aay)-(a|ayy)(x|a)+(a|a)(x|ayy)=0$$

$$2(a|a\delta)(x|yy)-2(a|yy)(x|a\delta)+(b|ay\delta)(y|y)-(b|y)(y|ay\delta)-(a|yy\delta)(x|a)+(a|a)(x|yy\delta)=0$$

$$-2(a|yb)(x|xa)+2(a|xa)(x|yb)-(b|y)(y|xab)+(b|xab)(y|y)-(a|xyb)(x|a)+(a|a)(x|xyb)=0$$

$$-2(a|yb)(x|xa)+2(a|xa)(x|yb)-(b|y)(y|xab)+(b|xab)(y|y)-(a|xyb)(x|a)+(a|a)(x|xyb)=0$$

$$-2(a|yb)(x|aa)+2(a|aa)(x|yb)-(b|y)(y|aab)+(b|aab)(y|y)-(a|ayb)(x|a)+(a|a)(x|ayb)=0$$

$$2(a|a\delta)(x|yb)-2(a|yb)(x|a\delta)-(b|y)(y|ab\delta)+(b|ab\delta)(y|y)-(a|yb\delta)(x|a)+(a|a)(x|yb\delta)=0$$

$$2(a|yy)(x|xx)-2(a|xx)(x|yy)+(a|xyy)(x|x)-(a|x)(x|xyy)+(b|y)(y|xxy)-(b|xxy)(y|y)=0$$

$$-2(a|xx)(x|yb)+2(a|yb)(x|xx)+(a|xyb)(x|x)-(a|x)(x|xyb)+(b|y)(y|xxb)-(b|xxb)(y|y)=0$$

$$2(a|yy)(x|xa)-2(a|xa)(x|yy)-(a|x)(x|ayy)+(a|ayy)(x|x)+(b|y)(y|xay)-(b|xay)(y|y)=0$$

$$-2(a|xa)(x|by)+2(a|by)(x|xa)-(a|x)(x|ayb)+(a|ayb)(x|x)+(b|y)(y|xab)-(b|xab)(y|y)=0$$

$$2(a|yy)(x|x\delta)-2(a|x\delta)(x|yy)+(a|yy\delta)(x|x)-(a|x)(x|yy\delta)+(b|y)(y|xy\delta)-(b|xy\delta)(y|y)=0$$

$$-2(a|x\delta)(x|yb)+2(a|yb)(x|x\delta)+(a|yb\delta)(x|x)-(a|x)(x|yb\delta)+(b|y)(y|xb\delta)-(b|xb\delta)(y|y)=0$$

◉ Notation

$$(x|a)=\partial x(z)/\partial a_0$$

$$(b|xx)=(1/2!)(\partial^2 b(z)/\partial x_0^2)$$

An example of useful symplectic relation in the TOF-SIMS technique

$$(T|aa)=-\frac{p_1^{ref}}{K_0^{ref}}(x|a\delta)M_a$$

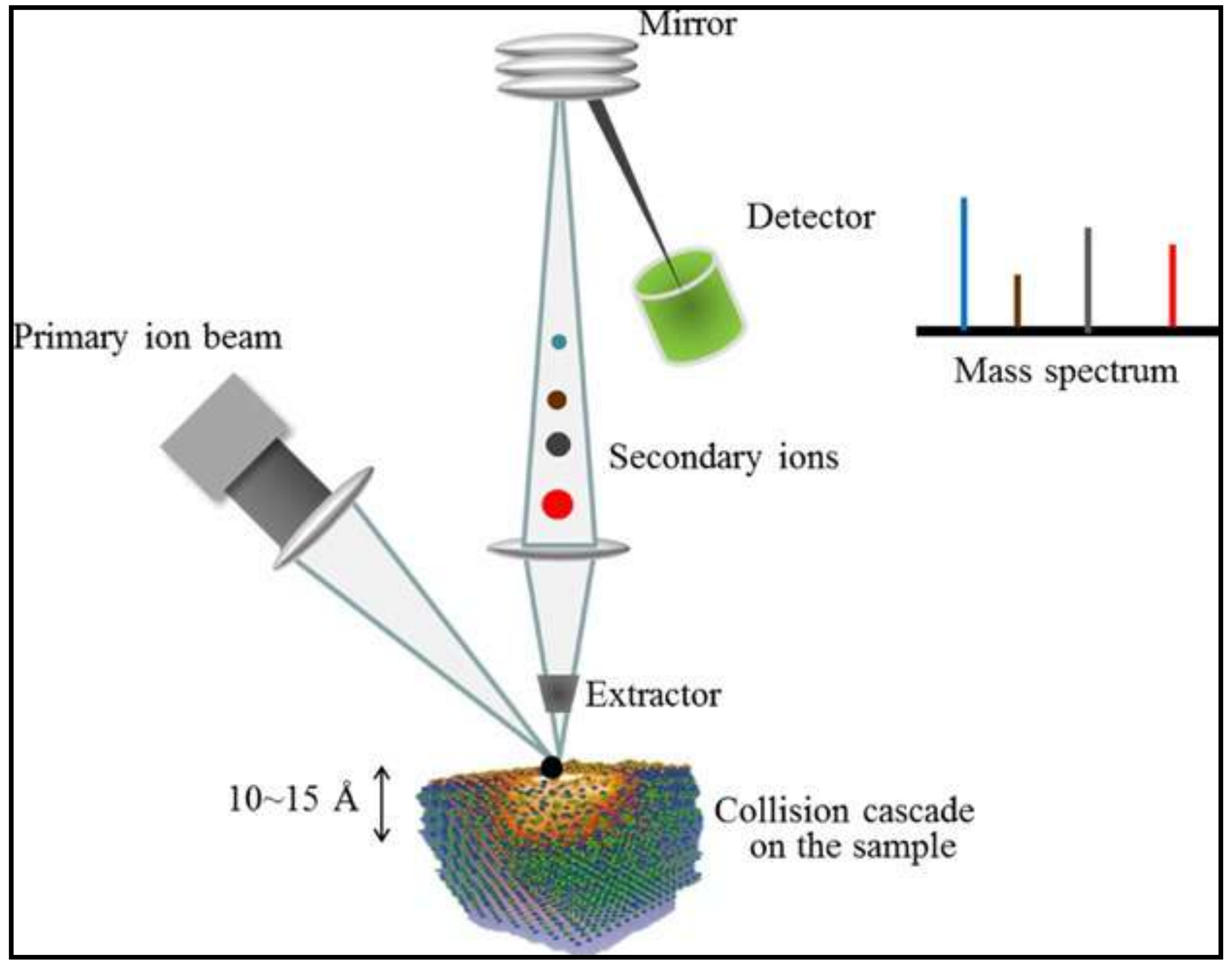

9

Some books to conclude

cnrs

INSA INSTITUT NATIONAL DES SCIENCES APPLIQUÉES TOULOUSE

Bibliotherapy

Conventional optics

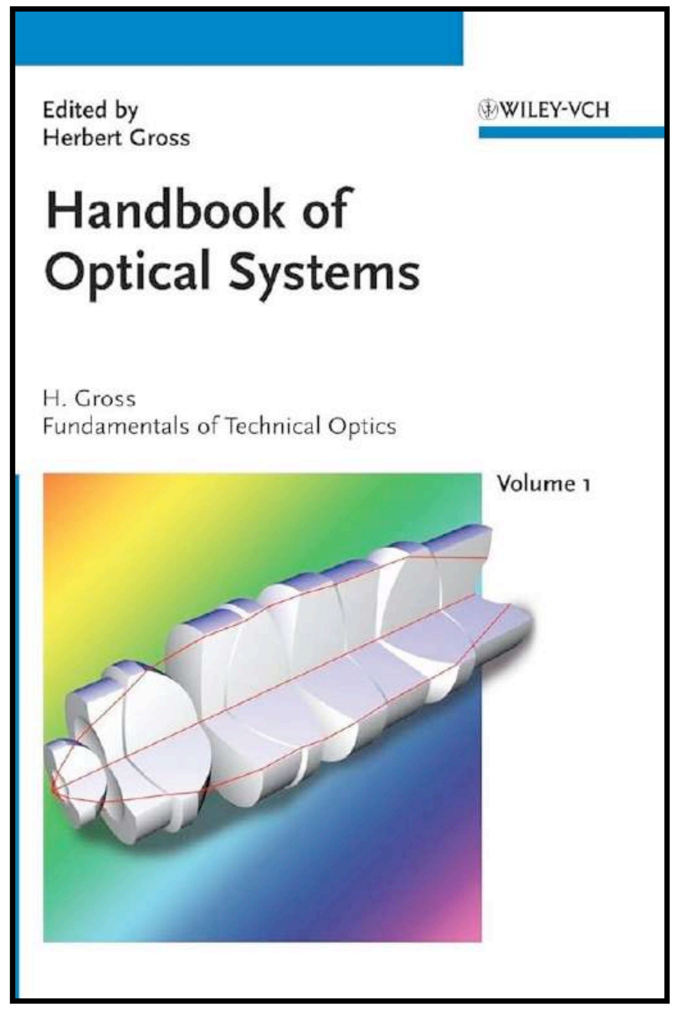

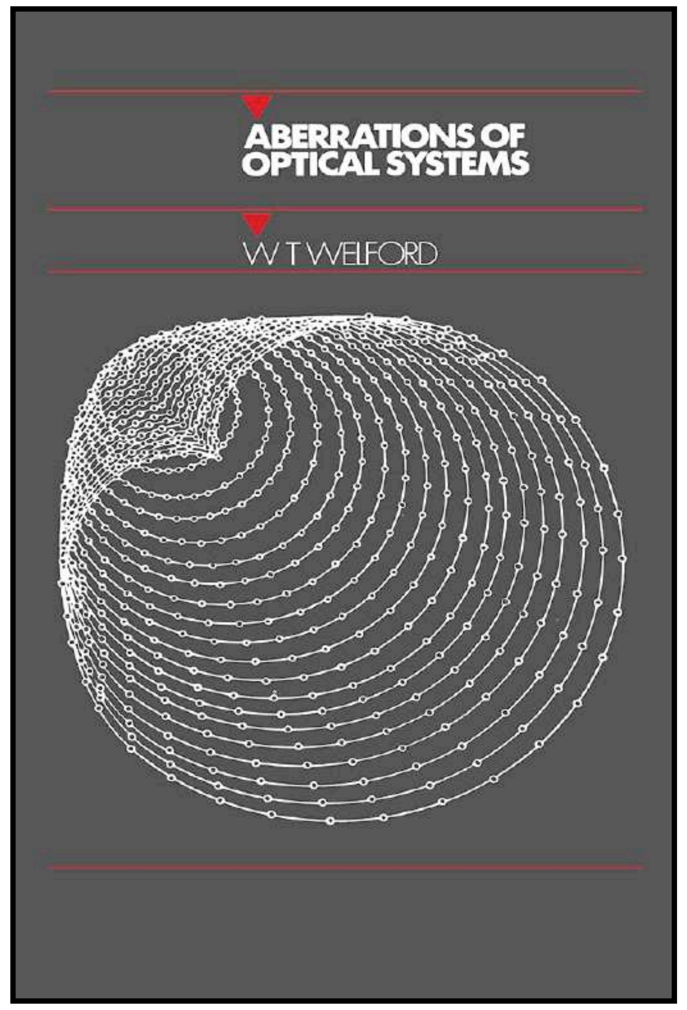

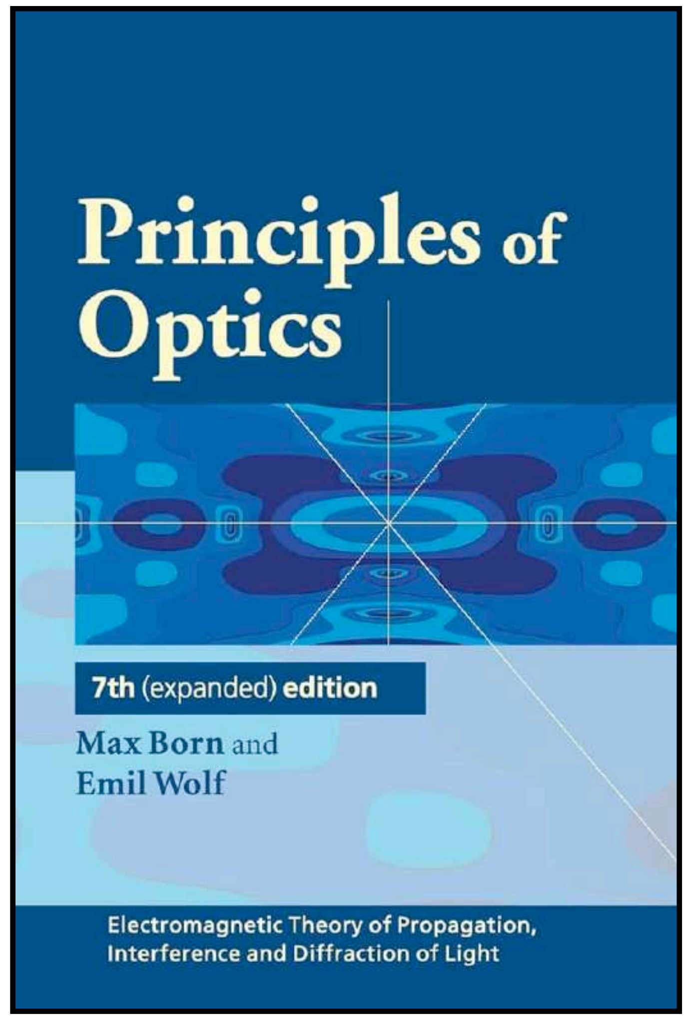

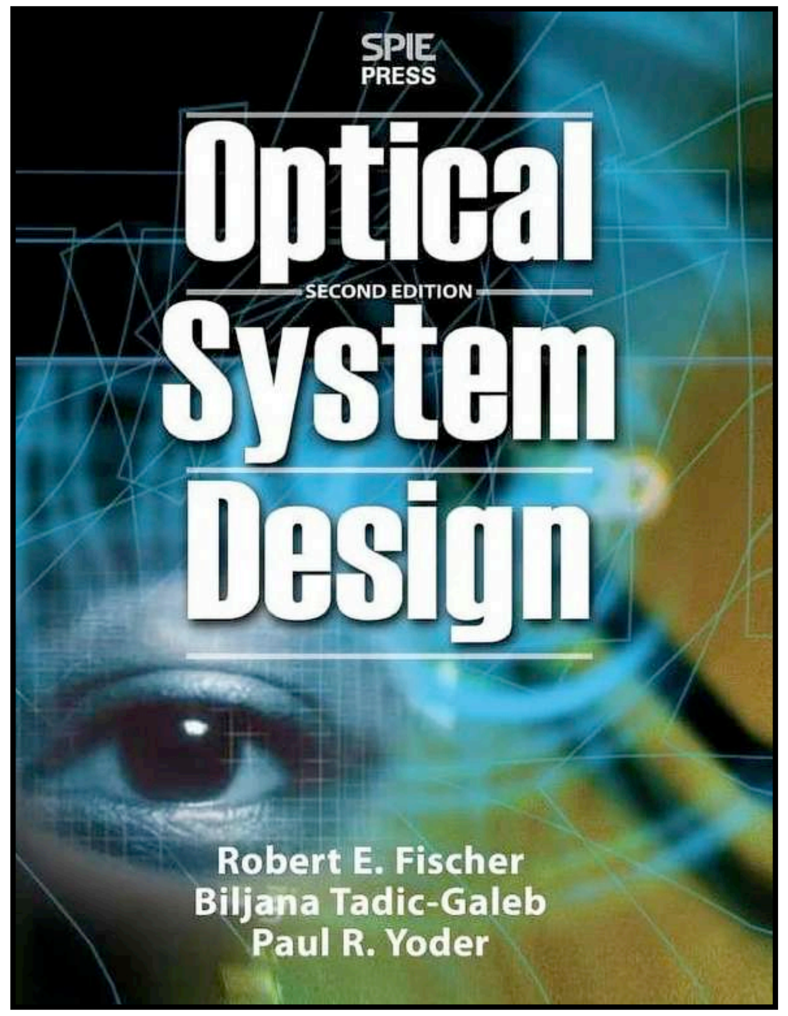

Charged particles optics

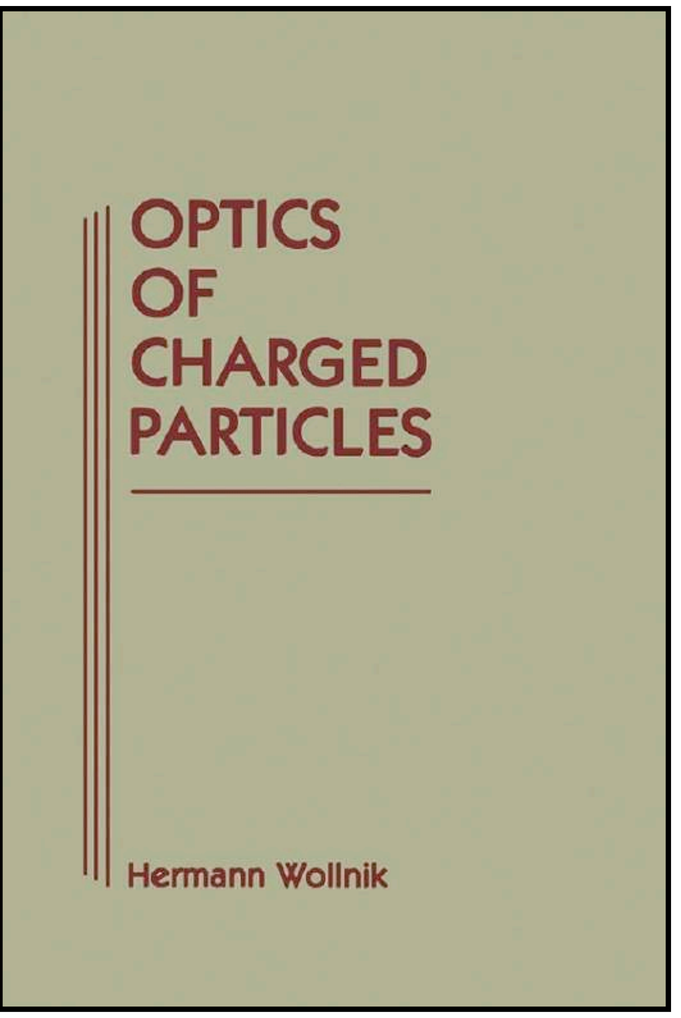

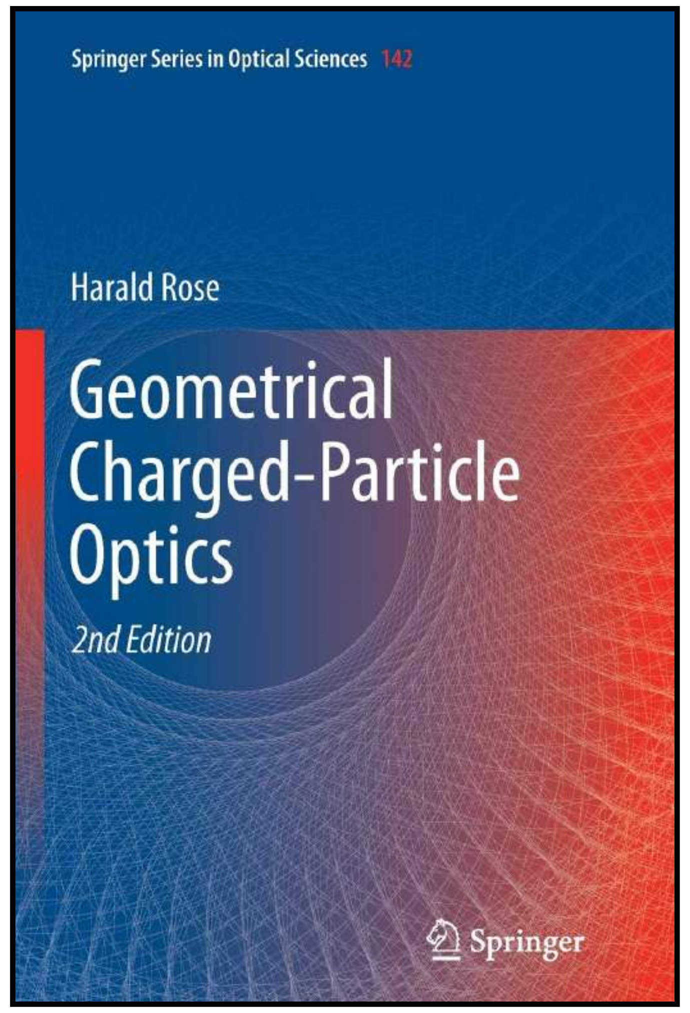

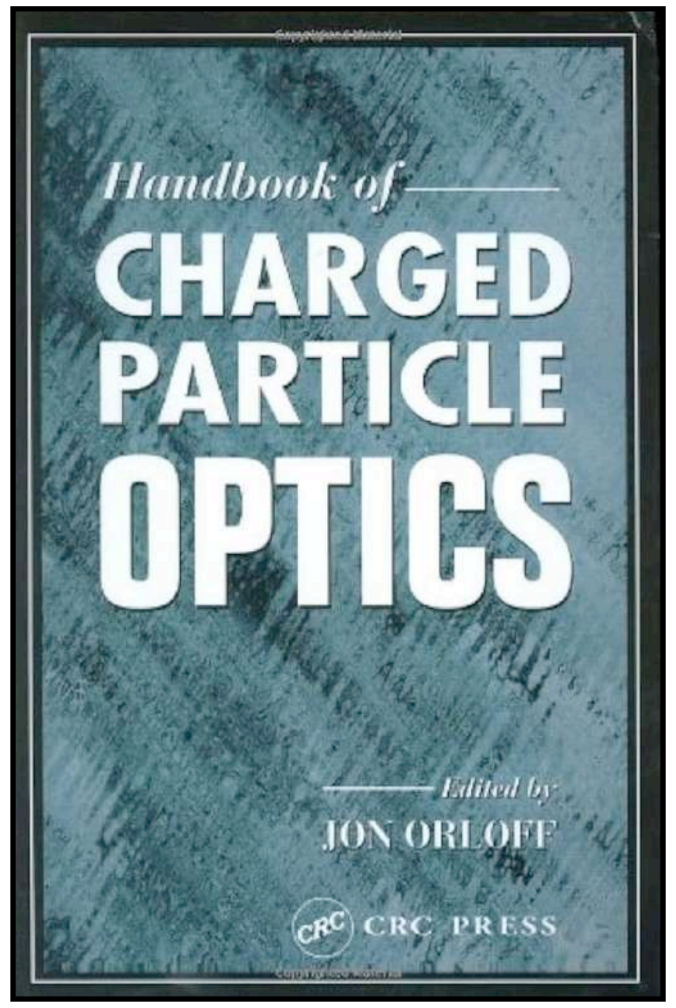

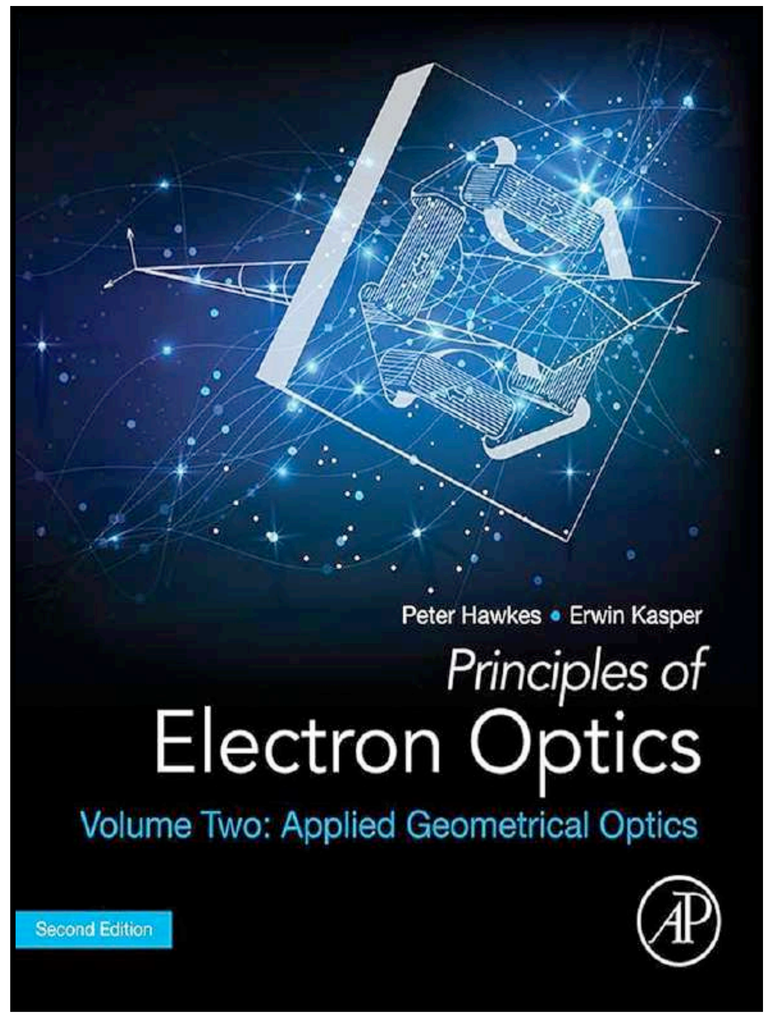

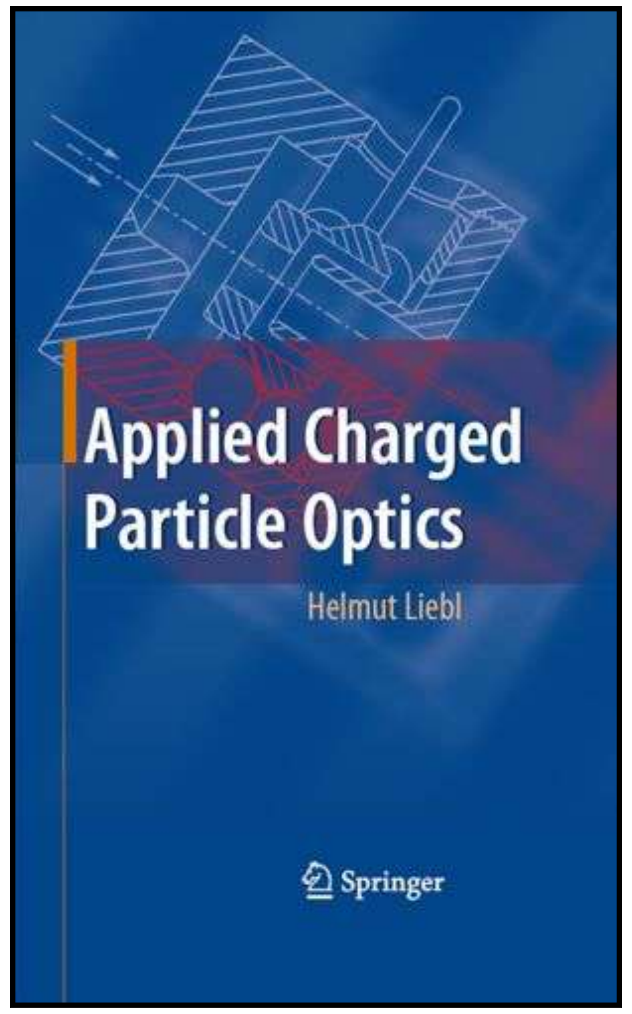

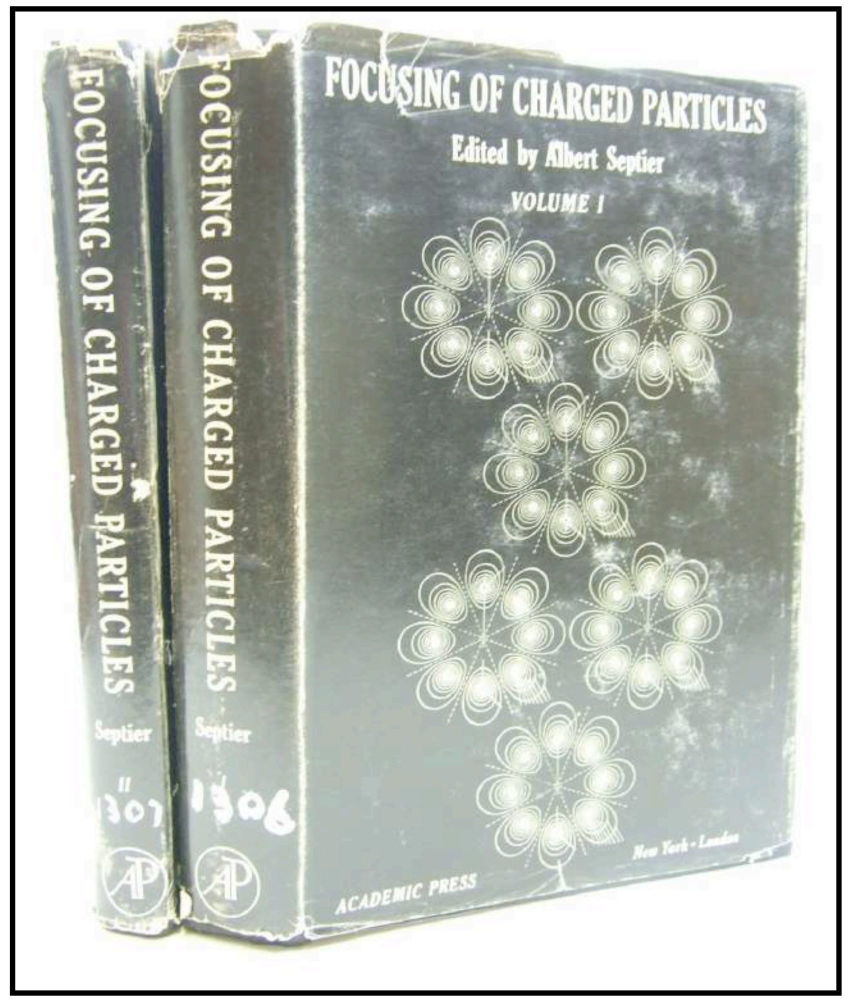

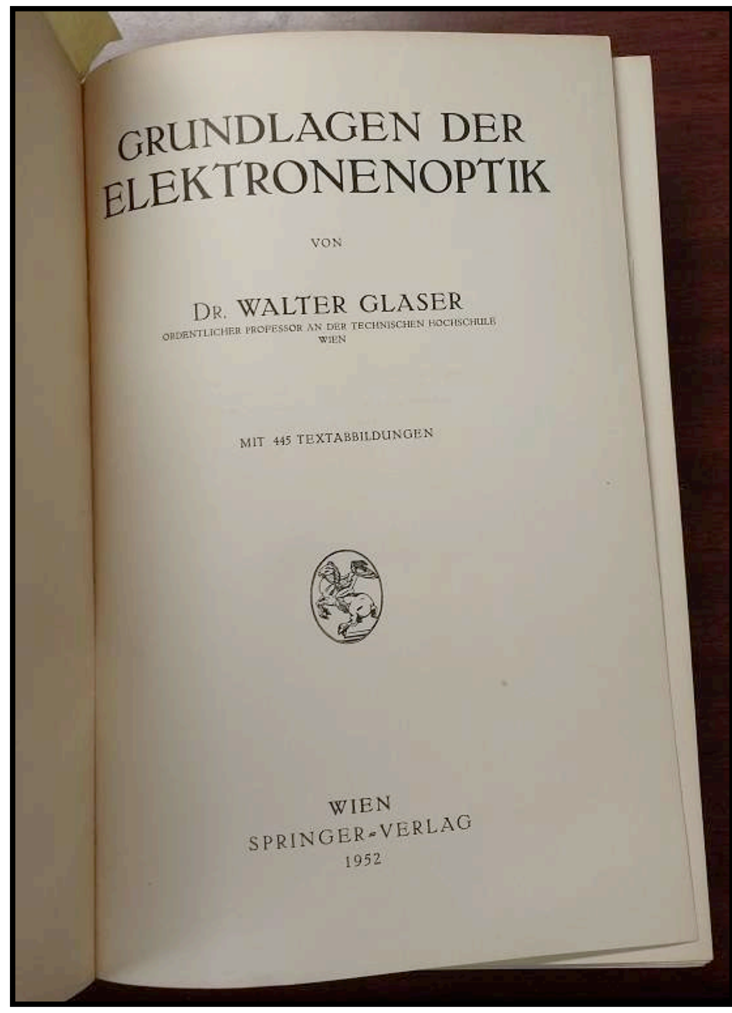

Thank you